HTRA1 as a Novel Regulator of Human Mesenchymal Stem Cell Adipogenesis

---

Dissertation

zur

Erlangung der naturwissenschaftlichen Doktorwürde
(Dr. sc. nat.)

vorgelegt der

Mathematisch-naturwissenschaftlichen Fakultät

der

Universität Zürich

von

Gregor Bahrenberg

aus
Deutschland

Promotionskomitee

Prof. Dr. François Verrey (Vorsitz)
PD Dr. Peter J. Richards (Leitung der Dissertation)
Prof. Dr. Beat Thöny
Prof. Dr. Michael Ehrmann

Zürich 2015

Summary

The serine protease HTRA1 has previously been identified as playing a role in the degradation of extracellular matrix (ECM) proteins, thus implicating it in various degenerative disorders such as intervertebral disc degeneration, arthritis and age-related macular degeneration (AMD). However, findings from previous studies performed in our laboratory investigating the role of HTRA1 in the regulation of mesenchymal stem cells (MSCs) osteogenesis, have led us to re-evaluate its biological properties with respect to mammalian tissue development and disease. In the current study, we asked whether HTRA1, in addition to its positive effects on MSC osteogenesis, could also influence the adipogenic differentiation of MSCs. In order to address this question, we investigated the effects of exogenously added recombinant HTRA1 and small interfering RNA (siRNA)-mediated depletion of HTRA1 on the development of hMSCs into mature adipocytes. The effects of HTRA1 were assessed using different techniques including qRT-PCR, intracellular and extracellular protein analyses, enzyme assays and histological analyses. We could demonstrate that HTRA1 acts to significantly suppress adipocyte development, primarily through upregulation of JNK activity and MMP production. Moreover, we were able to localize HTRA1 to sites of immune cell infiltrate within the adipose tissue of an insulin resistant obese patient, thus implicating it in adipose tissue remodeling under pathological conditions. In conclusion, our findings identify HTRA1 as a negative regulator of hMSC adipogenesis, which may be of relevance when considering its potential role in the underlying processes governing adipose tissue and adipocyte dysregulation. Moreover, the differential effects imparted by HTRA1 on hMSC adipogenic and osteogenic differentiation may also offer novel insights into its potential impact on other pathological conditions such as age-related bone loss, where its capacity to inhibit adipogenesis and stimulate osteogenesis would be deemed beneficial to the preservation of bone quality.

Zusammenfassung

Die Serinprotease HTRA1 wurde als ein Faktor beim Abbau extrazellulärer Matrix (ECM) Proteine identifiziert, wodurch sich Implikationen in verschiedenen degenerativen Erkrankungen wie Bandscheibenschäden, Arthritis und altersbedingte Makuladegeneration (AMD) ergeben. Jedoch zeigten Ergebnisse früherer Studien unseres Labors welche Rolle HTRA1 in der Regulation der Osteogenese mesenchymaler Stammzellen (MSCs) hat, was uns zu einer Neubewertung seiner biologischen Eigenschaften im Hinblick auf humane Gewebeentwicklung und Krankheiten führte. In der aktuellen Studie fragten wir, ob HTRA1, zusätzlich zu seiner positiven Auswirkungen auf die Knochenbildung in MSCs, auch die adipogene Differenzierung von MSCs beeinflussen könnte. Um diese Frage zu beantworten, untersuchten wir die Auswirkungen exogen zugegebenen rekombinanten HTRA1 Proteins, sowie die von small-interfering RNA (siRNA) vermittelte Depletion von HTRA1, hinsichtlich ihrer Auswirkungen auf die Entwicklung von hMSCs hin zu reifen Adipozyten. Diese Auswirkungen von HTRA1 wurden mittels verschiedener Techniken einschließlich qRT-PCR, intra- und extrazellulärer Proteinanalysen, Enzymassays und histologischer Analysen bewertet. Wir konnten zeigen, dass HTRA1 die Adipozytenentwicklung deutlich unterdrücken kann, in erster Linie durch das Heraufregulieren von JNK-Aktivität und MMP-Produktion. Darüber hinaus konnten wir HTRA1 im Bereich von Immunzellen, die das Fettgewebe eines insulinresistenten adipösen Patienten infiltrieren, lokalisieren, was eine Beteiligung am Umbau des Fettgewebes unter pathologischen Bedingungen nahe legt. Abschließend konnten unsere Erkenntnisse HTRA1 als negativen Regulator der hMSC Adipogenese identifizieren, was, angesichts einer möglichen Beteiligung in den zugrunde liegenden Vorgängen während Fettgewebe- und Fettzellfehlregulation, von großer Bedeutung sein kann. Darüber hinaus können die gegenteiligen Wirkungen von HTRA1 auf hMSC Adipogenese und Osteogenese auch neue Erkenntnisse über mögliche Auswirkungen auf andere pathologische Zuständen liefern, wie z.B. altersbedingten Knochenverlust, wo die Fähigkeit Adipogenese zu hemmen und Knochenbildung zu stimulieren, als vorteilhaft interpretiert würde, um so dem Prozess der Erhaltung der Knochenqualität positiv beizusteuern.

Table of contents

Abbreviations

ADAM	a disintegrin and metalloproteinase
AMD	age-related macular degeneration
AMPK	AMP-activated protein kinase
ASC	adipose-derived stromal cell
ATP	adenosine triphosphate
BAT	brown adipose tissue
BMSC	bone marrow stromal cell
CVD	cardiovascular disease
ECM	extracellular matrix
ESC	embryonic stem cell
FFA	free fatty acid
FS	follistatin
GAG	glucosaminoglycan
HSC	hematopoietic stem cell
HTRA1	high temperature requirement factor A1
IFN	interferon
IGF	insulin-like growth factor
IL	interleukin
iPS	induced pluripotent stem cell
MMP	matrix metalloproteinase
MSC	multipotent stromal cell
OA	osteoarthritis
Ppar	peroxisome proliferator-activated receptor
RANK	receptor activator of nuclear factor- κ B
RANKL	receptor activator of nuclear factor- κ B ligand
SVF	stromal vascular fraction
TGF	transforming growth factor
TNF	tumor necrosis factor
WAT	white adipose tissue

1 Introduction

1.1 Stem cells

It is well acknowledged that the main underlying prerequisite of a cell to be classified as a stem cell lies within its capability to either differentiate into one of multiple lineages of a more specialized cell type or to replicate and divide and to reside in a quiescent state [1-3]. The ability to give rise to and to fulfil any known function in a multicellular organism gives the stem cell a central role in maintaining a healthy homeostasis and balance, and is very likely to be one of the key features of general health and survival of an individual [4-6].

1.1.1 Stem cell niche

When trying to characterize a stem cell and its fate and properties, of great importance is the environment that it is exposed to. The stem cell niche describes all extrinsic factors and stimuli that interact with the stem cell to determine its cellular fate [7, 8]. The list of contributing factors is long and spreads from hormones, growth factors and other protein based compounds to proteoglycans, sugars and even inorganic factors such as pH, and extracellular matrix (ECM) architecture. All of these stimuli are generally sensed by a variety of intracellular second messenger pathways of the cell and ultimately lead to a rearrangement of the transcriptome and hence can create an entirely different type of cell. The complexity of the process of stimulation between a stem cell and its niche cannot be underestimated, as the number of potential levels to manipulate this interaction is extremely high [9]. Scientists therefore not only focus on hormonal growth factor stimulation of the stem cell, but an increasing number of laboratories around the world are now extensively studying the mere influence of the physical surrounding and environment of the cell (e.g. ECM composition), as this seems to have a direct influence on cells [10]. Indeed, via protein-protein interactions directly crossing the cell membrane barrier, the cell has found an additional way to control the dialogue with its niche [11-14]. Thus, an entirely new way of communication between the cell and its exterior is thereby created, which is closely linked to the cell´s cytoskeleton [14]. Together, all factors contribute to the specific characteristics of

what we call the stem cell niche.

1.1.2 Stem cell hierarchy

Not every stem cell is the same. In fact, a huge variety of stem cells was identified and new types are added to the list every year [9]. Different types of stem cells are classified based on their capacity to differentiate into specific cell types:

1. **Totipotency**: This status refers to cells that are able to differentiate into practically any known cell of the body, including all cells of the Endo-, Meso- and Ectoderm. These cells are therefore able to give rise to an entire organism. So far, the only known totipotent cell type is the zygote, although first breakthroughs in induced totipotent cells were made rather recently [15].
2. **Pluripotency**: The pluripotent status of a stem cell is reached when it is capable of differentiating into all cell types of the germ layers. However, the difference to totipotency lies mainly in the fact that a pluripotent cell is not self-sufficient and cannot give rise to an individual organism. The cell types that are classified as pluripotent are therefore embryonic stem cells (ESCs), as well as induced pluripotent stem cells (iPS) [16].
3. **Multipotency**: The term multipotency describes stem cells with the ability to generate cells from one germ layer. Different types of cells are known to be typically involved in the differentiation of the mesoderm, such as hematopoietic and bone marrow derived stem cells. The great variety, easy accessibility and utility, make the mesenchymal stem cell an interesting target for regenerative medicine, without the compromising ethical aspects found when dealing with ESCs [17].
4. **Oligopotency**: This newly established term defines stem cells that are already predetermined for a specific cell type, such as osteoblasts or preadipocytes and exhibit a very limited capacity to differentiate into other cell types [18].
5. **Nulipotency**: Nulipotency describes a cell that is terminally differentiated and exhibits no more differentiation potential [1].

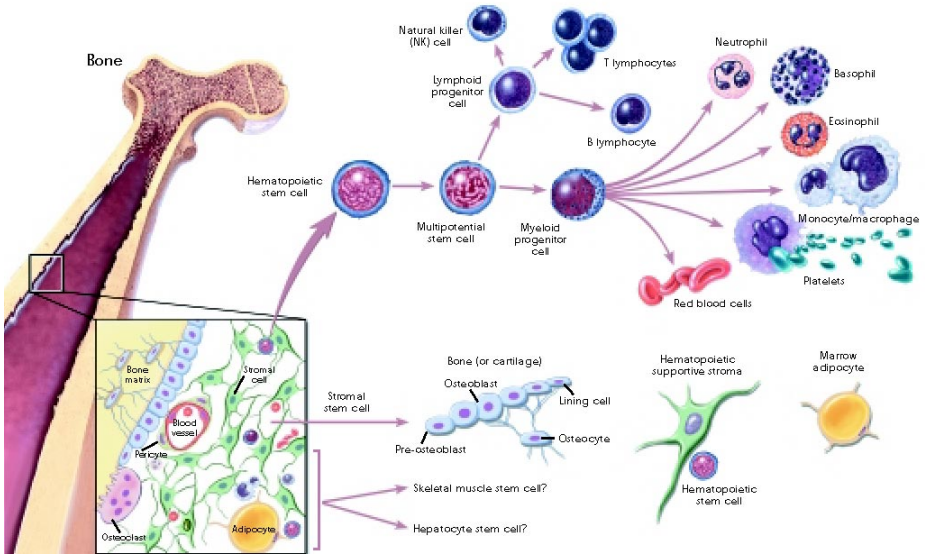

Figure 1: Schematic overview of the hematopoietic and mesenchymal stem cell differentiation. (© Terese Winslow 2008)

1.1.3 Differentiation

Stem cell differentiation is the process of an unspecified cell type converting towards a more specified cell until it is classified as a somatic, hence terminally differentiated cell. It is a complex, tightly regulated and orchestrated process which is in the focus of cell biology research for decades. Differentiation affects every aspect of the cell including the transcriptome and proteome, as well as cell morphology, cytoskeleton composition, cell membrane architecture, secretome, ECM composition, metabolic state and activity, microRNAs, epigenetics (hypermethylation), histone modifications etc. The interaction of the stem cell with its niche and vice versa is therefore likely to be one of the most complex single cell occurrences that we know [8, 19].

In general, global changes in the gene expression of the cell are the underlying force that is driving cellular differentiation [20-22]. However, the one rule that holds true for all types of differentiation for every cell type is that it is a one way route. Once a cell is terminally differentiated, the changes made are absolute and the cell will always remain in this state. There are exceptions to that rule (transdifferentiation, iPS), but they remain a rare exception [16, 23].

As a stem cell can either divide and thereby multiply, or start the process of

differentiation, two types of cell division are commonly described for a stem cell:

1. **Symmetric cell division** describes the process of a stem cell that divides and gives rise to two cells with an identical cellular fate. It is found during growth or regeneration.
2. **Asymmetric cell division** is the process where two daughter cells have a different cellular fate. While one of the two daughter cells remains identical to the parental generation, the other cell starts differentiation and thus, loses its stem cell characteristics [24].

Understanding the details of stem cell differentiation is clearly one of the major scientific challenges of our times, as it, as mentioned, comprises almost every aspect of cellular biology in a highly organized and orchestrated way and therefore holds many answers to diseases such as cancer, autoimmune disorders and other cell-based diseases [2, 6].

1.1.4 Adult vs. embryonic stem cells

As highlighted in the previous sections, stem cells possess the potential to play a major role in fighting diseases. While a cell that exhibits maximum differentiation capabilities (ESCs) is potentially of most use for basic research, this cell type clearly also exhibits the most controversially discussed ethical issues [4, 9], as the cells have to be extracted from a zygote or early embryo [15]. Especially when it comes to scenarios of human medical applications, this hurdle is likely to become unassailable. Therefore, adult stem cells that in fact do not show a totipotent differentiation potential but show pluripotent features appear to be the saviour in this debate. Adult stem cells remain in the body throughout an organism's lifetime. In fact, their permanent influence on maintenance and homeostasis of the organism appears to become more and more apparent [5, 6]. Furthermore, research is trying to put their regenerative potential to good use, as these cells can be extracted from the body and manipulated *in vitro* for further applications [2]. The following section lists some examples of the different adult stem cell sources and their implications in human medicine:

1. **Hematopoietic stem cells** derived from the mesoderm are located in the red bone marrow and give rise to all types of blood cells. Specifically, they give rise to myeloid (e.g. erythrocytes, thrombocytes, monocytes and macrophages) and lymphoid (e.g. NKCs and lymphocytes) cell types.
   Among many other research implications, these cells are broadly used for stem cell transplantation of the red bone marrow which helps to fight leukaemia. It therefore represents a well-established field of application for human stem cells [25, 26].
2. **Mammary stem cells** are a source for the cells of the mammary gland and are known to be involved in the carcinogenesis of the breast [27]. These cells have been successfully proven to be multipotent or even totipotent and are thus an interesting candidate to conduct research with in the future [28].
3. **Intestinal stem cells** are found in the epithelium of the intestines. They provide a source for the continuously regenerating epithelium of the intestines. Due to their lifelong commitment to cell division, they also represent an important contributor to the carcinogenesis of the intestinal tissue [29]. Their potential implications for research and medicine are also in the focus of regenerative research today [30].
4. **Mesenchymal stem cells** (MSCs) belong to the most studied cell type of adult stem cells. They are of a stromal origin and are therefore found in many tissues of the body. Known sources of stromal cells include the bone marrow, the placenta, adipose tissue, blood, the lung, the umbilical cord and teeth. This makes them especially interesting, as they can differentiate into a large variety of cell types including osteoblasts, chondrocytes and adipocytes [7].

As this Thesis is primarily concerned with the adipogenic potential of human MSCs (hMSCs), the following sections are dedicated to providing a more detailed description of hMSC adipogenesis and the major events governing this process.

1.2 hMSC adipogenesis

Adipogenesis describes the process of adipocyte formation. It usually involves the differentiation from a pre-adipogenic cell type towards the terminally differentiated adipocyte, which is capable to fulfil all functions characteristic for adipose tissue as a whole.

The main biological function of adipocytes and thereby fat tissue in general, is to store large quantities of energy. This energy (stored as triglycerides) is readily available for the cells in the surrounding environment and even cells at distant locations. Furthermore, hormone secretion gives it endocrine-like features (c.f. section 1.2.3). Next to its energy storage function, fat tissue is also used for insulation and protection of the body [31]. In the following sections, the adipose tissue with its cells and functions will be explained in detail.

1.2.1 Adipose tissue

Adipose tissue is a connective tissue mainly composed of adipocytes that store lipids in enormous amounts. Due to the hydrophobic properties of lipid, the energy that is kept in the form of fatty acids needs to be stored differently than that from for example ATP or NADPH, which is simply kept in solution within specialized compartments of the cell.

The adipocytes derive from adipocyte precursor cells, i.e. from the hMSC pool of the adipose tissue. They exhibit a specialized metabolism which enables efficient storage and release of this energy source, which is further highlighted in section 1.2.1.1. Adipocytes undergo a constant turnover of uptake and release of lipids (shuttled in the form of free fatty acids (FFAs)) and, depending on whether or not the uptake of lipid exceeds the release, the cells either expand in size (accumulation of lipids) or enter the so called mobilization phase (lipid release) [32].

Free fatty acids are the only fat molecule available for uptake for these cells. Since fatty acids taken up by ingestion only occur in the form of lipoproteins, it is necessary to break down these solubilized lipoproteins into free fatty acids to make them readily available for the cells. A protein called lipoprotein lipase (LPL), which is found in the ECM of adipocytes, is the limiting factor that makes this

conversion possible. Once the FFA has entered the adipocyte, it is reassembled into triglycerides and is finally stored in lipid droplets that build hydrophobic spheres in the cytoplasm of the cell. These spheres, called lipid droplets, can make up a huge percentage of the total volume of the cell [33].

The regulation of uptake and release of these FFAs and lipids is realized mostly by insulin. Stimulation of adipocytes by insulin results in an increased uptake of FFAs and thereby in the expansion of the adipocyte. On the other hand, hormones such as epinephrine, glucagon and the adrenocorticotropic hormone (ACTH) regulate lipolysis and thereby the release of FFAs from the cell [34].

Next to the adipocytes, the adipose tissue also contains a fraction (although only to a small percentage) of different cell types, summarized as stromal vascular fraction (SVF). This synonym is a broad term for all other cell types found in the adipose tissue which includes hMSCs, preadipocytes, endothelial progenitor cells, macrophages, as well as immune cells like B- and T-cells. This pool of non-lipid carrying cells plays an important role in the maintenance of the tissue by providing a source for new adipocytes, amplification for signals from other tissues as well as immunological regulation of the adipose tissue. The exact role of these cells within the adipose tissue is poorly understood, but is likely to go beyond being a mere backup for the adipocyte cell pool and towards a direct involvement in tissue health maintenance (c.f. chapter 1.1) [33, 35]. As an example, macrophages are known to be involved in the maintenance of the adipose tissue of obese individuals. The percentage of macrophages within the white adipose tissue can go up to 50%, as they help to catabolize dead adipocytes (usually due to a locally occurring inflammation reaction), surround them and form crown-like structures (CLS). Hence, they are directly involved in the depletion of defective adipocytes [36, 37] and thereby fat tissue maintenance.

1.2.1.1 Energy metabolism of fatty acids

As mentioned earlier, adipose tissue has enabled a way for the organism to make the energy stored in fatty acids readily available. To do so, a unique metabolic pathway is found in the adipocytes, which will be described in detail in this chapter. A fat molecule consists of three fatty acid chains which are connected via a glycerol backbone. Hence, a fatty acid simply is a long chain of carbon and hydrogen atoms with a lot of energy stored in the bonds [38].

Starting from the dietary ingestion of fatty acids as triglycerides, the fat is broken down in the intestines by the pancreatic lipase into monoglycerides and free fatty acids. After they are solubilized into micelles together with bile salts and certain proteins, the lipids can now be absorbed into the intestine epithelium by specialized membrane proteins. The triglycerides (in the form of chylomicrons and lipoproteins) are now rebuilt in the cells of the intestine and can enter the blood stream and thereby the circulation of the body. Three types of cells can take up the lipids to make use of their stored energy: hepatocytes (liver), myocytes (muscle) and adipocytes (fat tissue). While the liver cells are mainly involved in the processing of fat into other types of lipoproteins, such as very low density lipoprotein (VLDL) and low density lipoprotein (LDL) in order to make them usable elsewhere, muscle cells make a direct use of the energy of the fatty acids and the adipocytes are responsible for their storage and release. However, the detailed processes underlying the fatty acid metabolism of the hepatocytes and muscle cells will not be further discussed here, but instead the process of uptake and release of fatty acids by adipocytes will be in the focus.

Once lipoproteins have become bound to the extracellular portion of the adipocyte´s cell membrane (i.e. the ECM), the enzyme lipoprotein lipase (LPL) breaks them down into FFAs to enable their directed uptake into the cell by specific membrane proteins (e.g. LRP-1) [39]. In the cytoplasm of the adipocyte, these neutral fatty acids now form lipid droplets, consisting of a phospholipid layer with a core of triacylglycerols and sterol esters. A covering layer of a protein called perilipin prevents endogenous degradation by lipases. These lipid droplets can merge into bigger lipid droplets, if necessary, and can make up to 90% of the cell size [40].

When needed (for instance upon low insulin levels due to low blood sugar levels) the adipocyte can release large quantities of fatty acids into the circulation. An extracellular stimulus provokes an intracellular secondary messenger cascade which results in an activation of the hormone-sensitive lipase (HSL). The HSL breaks down the triglycerides of the lipid droplets into glycerol and free fatty acids.

The process of fatty acid release into the blood is called lipolysis. Contrary to the fatty acids bound to lipoproteins, these FFAs in the blood (bound to serum albumin to facilitate solubility) remain as FFAs which makes them easily accessible for target tissue that is in need of energy. The FFAs are now metabolically available

for muscle and cardiac tissue, whereas the glycerol is taken up by the liver for gluconeogenesis for the generation of glucose which is the only energy source for brain tissue.

Interestingly, of all the molecules, fatty acids yield the most adenosine triphosphate (ATP) (energy per gram ratio), which represents the main source of energy for cells. When the cell is in need of energy, the FFA gets broken down into Acetyl CoA by an enzyme called acetyl Coenzyme-A. The resulting Acetyl CoA molecules are then oxidized in the citric acid cycle, just like glucose in the aerobic glucose metabolism. However, for every two carbon atoms in a fatty acid, 17 ATP molecules can be generated, making fatty acid a highly energetic molecule [38, 40]. To further clarify the connection between fatty acid and glucose metabolism in the human body, a simplified overview of these two pathways can be found in figure 2.

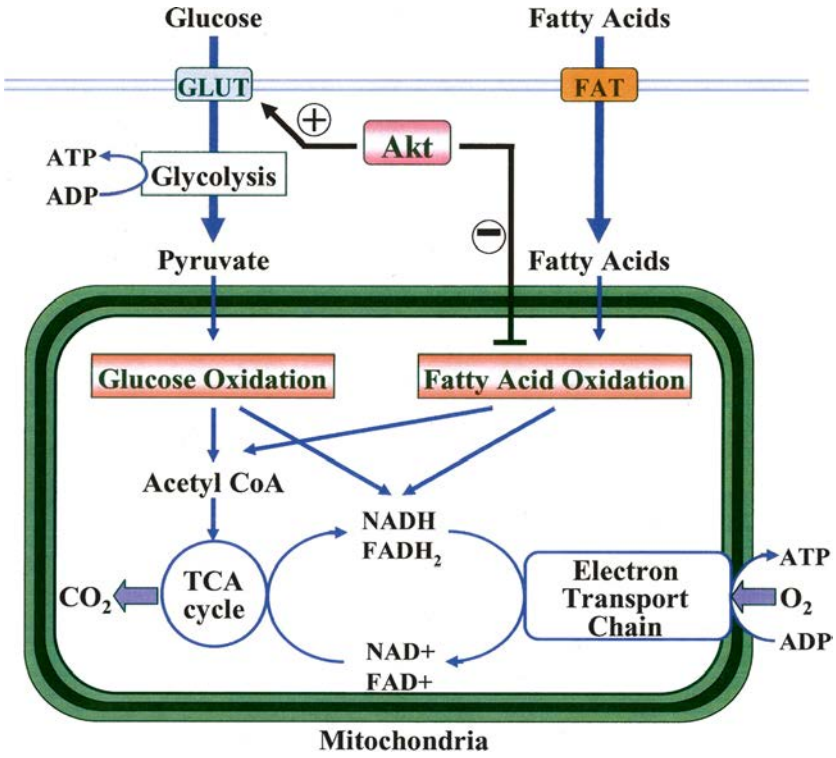

Figure 2: Schematic representation of the glucose and fatty acid catabolism [41] REMARK: please note that Glucose Oxidation as depicted in this figure is inaccurate and requires correction.

1.2.1.2 Brown vs. white adipose tissue

It is of great importance to differentiate between white and brown fat tissue (WAT and BAT) when characterizing adipose tissue. While the cells of the WAT derive from hMSCs and carry one large lipid droplet in the cytoplasm in their mature state, cells from the BAT appear to be deriving from muscle progenitor cells (they share surface markers such as Myf5, which cells from the WAT are lacking) and numerous, smaller lipid droplets can be found in these cells [42].

The main difference in function is that WAT cells store excessive lipids collected from the periphery of the body and make them available for the whole organism, while brown adipose cells are mainly responsible for body heat generation. This heat production is realized by a large number of mitochondria that are found in the cytoplasm of the BAT, which gives them their brownish appearance (c.f. figure 3). Next to producing ATP, mitochondria can also make use of the proton gradient in a different way. Instead of using the gradient for enzymatic ATP synthesis, the protons flow back into the cytoplasm via uncoupling protein 1 or thermogenin. This protein allows usage of the energy stored in the proton gradient to be released as heat [43].

Large quantities of BAT are therefore mostly found in new-borns and hibernating animals that produce body heat not by an unconscious hyperactivity of muscles (shivering under hypothermal conditions), but by the help of the BAT. Importantly, the high mitochondrial activity of BAT consumes a lot of oxygen, which is why BAT is highly vascularized compared to the WAT [44].

Overall, in adult humans BAT is only found in small quantities. However, as it was believed that this adipose tissue is exclusively found in infants and other animal species, it is important to note that BAT remains active throughout life and shares higher similarities to muscle tissue than to WAT. Therefore, BAT may have other as yet unknown implications. On the other hand, WAT usually makes up to 20% of the body weight of men and women and is directly involved in energy metabolism of the body and indirectly in body heat maintenance by insulating the body [45].

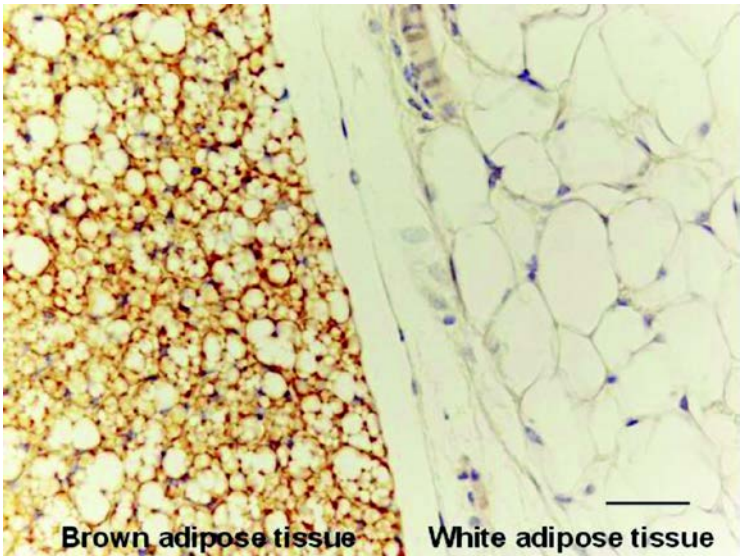

Figure 3: Light microscopy image of a histological staining of brown and white adipose tissue. (© Charmaine S. Tam et al)

1.2.2 Adipose tissue function

The main functions of adipose tissue can be summarized as follows:

1. Thermal insulation of the body (WAT)
2. Energy storage and release (WAT)
3. Storage of excessive fats, that would otherwise be harmful for the organism (WAT)
4. Body heat production (BAT)

However, next to its classical functions directly implicated to fat storage and release as well as thermal insulation, the fat tissue may hold other regulatory functions with implications for the whole organism. The discovery of so called adipokines gives us a hint as to the importance of the mutual dialogue of different compartments of the human body. Thus, the importance of an intact adipose tissue may even go beyond the diseases indirectly or directly linked to the adipose tissue (c.f. section 1.2.4) and may become of great importance in the future of medicine.

1.2.3 Adipokines

It was originally believed that cytokines, hormones and other immunologically active molecules are exclusively secreted by immune cells such as B- and T-lymphocytes, macrophages etc. It is now being appreciated that the number of cells secreting and sensing cytokines is much larger, including myocytes, adipocytes, fibroblasts and many more [46].

Since adipose tissue is closely linked to many metabolic events in the human body, it is becoming increasingly apparent that a large number of so called adipocytokines or adipokines are secreted and also sensed by adipocytes themselves. Understanding the crosstalk of adipose tissue and other endocrine organs (pancreas, liver, bone etc.) is a major task of basic research in order to understand a variety of human diseases such as obesity, type 2 diabetes, and even osteoporosis etc. [47, 48].

One of the first adipokines to be discovered was leptin, but many others have followed since. This also includes factors not exclusive to adipose tissue, but which are also released by other cell types. This includes interleukins and interferons (IL-6, RBP-4, TNF-α, IFN-γ etc.). A second prominent adipokine is adiponectin, which is known to be involved in many cellular and endocrine regulatory processes. Together, leptin and adiponectin regulate the activity of AMP-activated protein kinase (AMPK), which is known to be a major regulator of apoptosis, differentiation and the cell cycle. This highlights the central role of adipose tissue to regulate globular parameters in the human body, which can simply have an impact on appetite and glucose levels (insulin regulation), or can even extend to the regulation of stem cell differentiation [49, 50]. Their involvement in adipose tissue regulation and even disease progression has been under investigation by researchers for years and holds great potential for therapeutic applications [51].

Conclusively, due to the existence of adipokines, it is likely that the immunology of the human body extends beyond the classical immune cell types, such as lymphocytes, T-cells and macrophages, and may involve many more cell types.

1.2.4 Adipose tissue associated diseases

One of the major health risk factors of our generation is obesity. This disease, closely associated to the adipose tissue, is directly linked to the most common cause of death worldwide, which are cardiovascular diseases (CVDs). While obesity itself is not a life threatening condition, many diseases result from obesity, such as the before mentioned CVDs, as well as type 2 diabetes, cancer and osteoarthritis (OA) [47, 52]. It is generally caused by a combination of one of three factors:

a) Excessive food intake
b) Insufficient physical activity
c) Genetic predisposition

Although exceptions have been described, there is no trustworthy evidence convincing enough to show any other factor to be involved in the progression of obesity [53]. The medical classification of obesity nowadays refers to the body mass index (BMI) which was introduced by the world health organization (WHO) [54]. An overview about the indices can be found in figure 4. Many secondary effects on the organism are known to be caused by obesity. An overview about the most well-known relationships is given in the following:

1) **CVDs** are the most common, occurring as a direct result of chronic obesity. Many factors are involved in the development, including dyslipidemia (a massive increase of lipids or lipoproteins in the blood), high blood pressure, thrombosis, embolisms, etc. An increase in blood lipids contributes to plaque formation on blood vessel epithelia and thereby induces stenosis of the blood vessels. This facilitates the occurrence of ischemia, hence heart diseases such as myocardial infarctions, as well as strokes, thrombi, embolisms etc. A high blood pressure further increases the risk of cardiovascular malfunctions. Taken together, many reactions resulting from CVDs can be life threatening, which is why CVDs are a major reoccurring problem in most developed countries [55].
2) **Type 2 diabetes** is the result of insulin resistance and/ or insufficient insulin production from the beta cells of the pancreas. Insulin resistance describes

the inability of the muscle, the liver and the fat tissue to respond to insulin. In a healthy organism insulin reduces the amount of glucose being released from the liver in order not to increase blood sugar levels further. However, due to insulin resistance, the release of sugar into the blood remains at a high level and at the same time, relative to these high amounts of blood sugar, insulin levels remain low. The combination of high blood sugar levels and low insulin levels results in a very low uptake of glucose by adipose tissue and muscle cells. Also, the level of lipolysis from adipose tissue may be increased, further elevating the levels of energy molecules into the blood, as insulin normally provokes the storage of FFA´s rather than their release [56]. Thus, next to the resulting effect that the excess glucose in the blood is not available for target cells, high amounts of glucose in the blood can even be toxic, which can have drastic consequences over longer time periods [57].

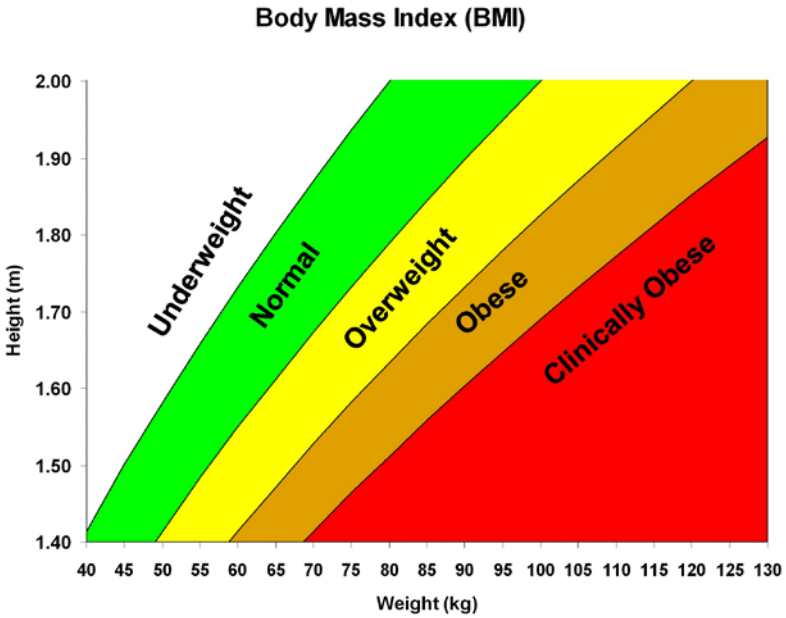

Figure 4: graphical representation of the BMI score. (© www.metric.org.uk)

1.3 The ECM as a regulator of hMSC multipotency

The ECM is a general term describing all extracellular molecules that are secreted from a cell and fulfil their function only in the extracellular space. Typically, the ECM was thought to exhibit structural and biochemical support only, but it is now becoming increasingly apparent, that the ECM is more than just filling up the extracellular space or building up connective tissue such as bone or cartilage. It is, in fact, also involved in many regulatory processes in the crosstalk between cells and tissues [11, 58, 59]. The importance of remodeling the ECM is now being appreciated as one of the major events in stem cell differentiation, tissue development and regeneration, and even cancer progression [14, 58, 60, 61].
The following chapter will therefore explain the ECM´s structure, function, key players and involvement in biological processes and disease development.

1.3.1 General set up

Although very different between different cell types, a general architecture of the ECM can be described for all types of cells. Two types of an ECM can be distinguished:

1. While the **basement membrane** serves as a barrier between any given epithelium, mesothelium and endothelium found in the body to its underlying tissue, the
2. **interstitial space** makes up all other extracellular space that is found throughout the body.

The name basement membrane is therefore misleading as it is an extracellular space, but with the specific function to separate two distinct tissue compartments from one another. The main components of every ECM usually comprises proteoglycans and other non-proteoglycan polysaccharides and a large number of different fibers. **Proteoglycans** mainly consist of heparan-, chondroitin- and keratin-sulfate. These are three different types of carbohydrate polymers of the ECM that are bound to proteins such as perlecan, agrin and collagens, but also proteins bound directly to the cell membrane. They are usually referred to as

GAGs (glucosaminoglycans), which is the same molecule without a specific protein attached to it [12]. Together they form a branched, tightly interconnected net of proteoglycans that, due to their net negative charge, attracts positively charged ions and thereby water, making it a well-hydrated environment. This guarantees a lively exchange between the cell and its surrounding environment. Furthermore, this network builds a scaffold for many regulatory molecules (like growth factors, hormones and other peptides) to bind to and even be stored in [62]. As many of the peptides associated to the carbohydrate are directly or indirectly linked to membrane proteins of the cell, these cell-cell or cell-matrix interactions can have a direct intracellular signaling event via membrane-spanning proteins like integrins or other cell surface receptors. Furthermore, the close proximity of this part of the ECM makes many substrates available for an interaction of compounds secreted by the cell (e.g. lipoprotein lipase in fatty acid uptake or alkaline phosphatase in matrix mineralization during osteogenesis) [63, 64].

Non-proteoglycan polysaccharides (mainly represented by hyaluronic acid) are not bound to any protein of the ECM or the membrane of the cell. Their specific function is to provide mechanical shock absorbance by exhibiting swelling properties of the ECM with relatively large amounts of water. They are therefore mostly found in load-bearing joints, but also make up a key component of the interstitial space. However, studies do provide evidence for hyaluronic acid directly associating with CD44, to which it exhibits regulatory functions. Thus, its implications in many processes of the body may be possible [65, 66].

The group referred to as **fibers** are the most abundant proteins found in the ECM. **Collagen** is by far largest member of this family and is found in large quantities in every ECM of any cell type. This makes it the most abundant protein of the human body, as it is the main protein component in many tissues such as bone tissue, skin, cartilage, ligaments, tendon and blood vessels. Collagen’s main function is to give stability to a connective tissue due to its remarkable tensile strength, realized by its mostly fibrous nature [67]. It is generally accepted that 80 – 90% of collagens in the human body are formed by Collagen I – III [68]. Due to the fact that collagens are secreted from the cells in a premature state (procollagen), collagenases on the outside of the cell are responsible for the maturation of the ECM by cleaving the procollagen molecules. A malfunction in the respective

collagen gene or its specific collagenase enzyme results in a number of diseases affecting connective tissues, such as osteogenesis imperfecta [69], epidermolysis bullosa etc. [70]. In order to allow for tensile strength and also three-dimensional elasticity within the tissue, a protein called **elastin** is also found in large quantities in tissues that require elasticity more than stiffness. Examples are the skin, blood vessels as well as the lungs. The elastin provides stretching properties of the tissue and is mainly secreted by fibroblasts and cells of the smooth muscle tissue, but typically found in any ECM. Since elastin is encoded by a single gene, deficiencies in elastin synthesis also result in diseases of the connective tissue such as cutis laxa or Williams syndrome which make the skin hyper flexible [71].

In addition to proteoglycans, other peptides associated to sugar residues can be found in the ECM. **Fibronectin** is a glycoprotein important for the linkage of the ECM to collagen, thereby anchoring the cell closer to its ECM. It is believed that this allows the cell to execute a certain degree of movement within the ECM by reorganizing the intracellular cytoskeleton [72]. Thus, fibronectin is an essential molecule for cell-ECM contact which allows the cell to sense the status of its ECM, thus making it a vital part of the cell-ECM dialogue. Furthermore, proteins called **laminins** are complex molecules that are also found in the ECM, mostly within the basement membrane. They can be assembled in many different oligomers [73] and represent another very important molecule of the ECM. On the one hand they facilitate the interaction of collagens and entactins by binding to them, and on the other hand they assist in the process of cell adhesion, thus supporting their capacity to form networks of molecules, rather than fibre-like structures (such as collagen). This gives the laminins the unique feature of resisting tensile forces that the cell membrane otherwise could not tolerate [74]. Furthermore, they are known to be involved in certain signaling events, thereby representing another member of the cell-ECM dialogue [75].

As mentioned earlier, bridge molecules connecting the cell´s cytoplasm and the ECM are mainly built by **integrins**. These transmembrane receptors are considered as the main player of cell-cell and cell-ECM interactions. Their ability to transduce a signal in both directions enables a cell to react to outside and inside stimuli [76]. Thus, a quick response to extracellular changes can be mediated into the cell directly via integrins (e.g. a certain ECM composition can initiate differentiation in certain cell types [77]). Integrins are also known to be associated

with and triggered by other ECM proteins such as collagen, laminin, fibronectin (introduced above), cadherin and several others. This highlights their central role in mediating a signal with regards to the ECM composition into the cell. Their intracellular functions include signal transduction by various second messenger systems, but also attachment to microfilaments has been described, thereby attaching the cytoskeleton of a cell directly to the ECM, which creates one interconnected network in- and outside of the cell [78]. All integrins consist of an α- and a β-subunit which together build a heterodimer which is biologically active. However, the variety of subunits is huge and depending on the composition of the integrin, different cellular functions can be found [79]. In conclusion, integrins nicely underline the central role of the ECM to determine a cells fate, future and status. A cell is not simply anchored to its ECM, but the crosstalk between the surroundings of the cell to the actions taken by the cell, highly depends on a tightly regulated mechanism that can lead to differentiation, apoptosis, growth, division etc. [80].

Lastly, the group of **syndecans** will be presented. They represent another important player in the cell-ECM crosstalk machinery. These proteins are single transmembrane domain molecules that can act as receptors. Importantly, upon ligand binding, they can induce a second messenger cascade in the cell which ultimately leads to transcriptional changes of the genome [81]. In contrast to other transmembrane proteins such as integrins, they are not bound to other ECM protein ligands, but they themselves are covalently bound to proteoglycans of the ECM (e.g. heparan sulfate and chondroitin sulfate). This makes them an exclusive member of the ECM itself. This feature further increases the amount of potential ligands to the syndecans, as many signaling molecules are known to be associated to proteoglycans (TGF-β, fibronectin, FGFs etc.) [82]. Cleavage of the ectodomain of a syndecan (a process called **shedding**) is an important regulatory step in signal processing of the cell towards outside stimuli. It was shown that syndecans can be specifically cleaved, thereby releasing a peptide that can in turn have stimulatory functions towards a cell [83]. Interestingly, certain diseases of the connective tissue show elevated levels of these cleaved syndecan ectodomains [84]. Very likely, syndecans are only one example for shedding with subsequent signaling events, as many ECM proteins exhibit specific extracellular cleavage sites, by for instance matrix metalloproteinases (MMPs) and the disintegrin and

metalloproteinases (ADAMs) [85, 86]. A total of four different syndecan family members have been described so far and the ratio, distribution and localization defines a cell´s specific sensitivity towards syndecan-related signals [81].

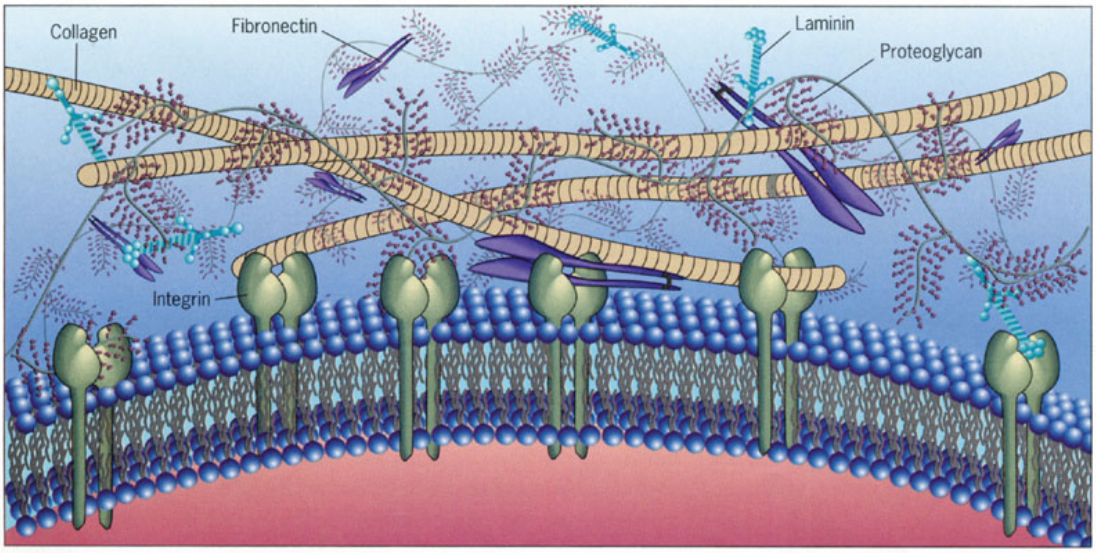

Figure 5: Schematic overview of the extracellular matrix (ECM). (© www.jonlieffmd.com)

1.3.2 Reorganization of the ECM during stem cell commitment

As mentioned previously, the crosstalk between a cell and its ECM is of great importance to determine cellular fate. As an example of this dialogue, this chapter will discuss the complexity of ECM reorganization during stem cell differentiation.
As already discussed in chapter 1.1.1, the stem cell niche defines the cells character and reactivity towards specialization and differentiation. However, a stem cell undergoing differentiation reorganizes almost every aspect of its cellular strategy. Not only is the ECM an integral component of this reorganization, evidence now hints to the fact that it might even be an essential part of stem cell commitment towards a specific lineage [11, 87]. Thus, the ECM needs to be remodelled completely during the process of stem cell differentiation. Interestingly, evidence exists to support the notion that an extracellular input on certain cell types, induces a mechanosensitive response of the cell, leading to differentiation of stem cells towards, for instance, osteogenesis (stiff environment) or adipogenesis (loose environment). This sensing of the cell´s surrounding is

executed by multiple proteins of the ECM, which were introduced above [77, 88]. While these studies clearly showed that ECM stiffness and architecture has a direct effect on stem cell differentiation, the question remains as to what happens to the ECM of a multipotent stromal cell during differentiation. It seems obvious that a breakdown and rebuilding of the ECM must take place as well.

Since it is known that many molecules such as hormones, growth factors and even molecules of the ECM itself can have an impact on cell signaling, the complexity of the ECM in a regulatory context becomes even greater. **MMPs** are prominent candidates of the ECM breakdown process [13, 14]. They are secreted from a cell when a reorganization of the ECM is needed, thereby generating a multitude of signaling peptides that are released by the ECM. These signaling molecules now can in turn have a positive or negative feedback effect on the cell. It is therefore crucial for the cell (or other cells in close proximity) to secrete the correct enzymes responsible for the breakdown of the ECM at the right time. It could otherwise have detrimental effects, resulting in a waste of energy and resources of the cell. A long list of specialized extracellular enzymes is necessary to guarantee successful ECM reorganization [11, 14, 89, 90].

While it is known that ectodomain shedding of several components of the ECM is regulated by MMPs and other extracellular proteases [85, 91-93], some MMPs themselves are subject to cleavage, which activates the enzyme and results in its maturation [94]. Furthermore, it is known that MMPs are involved in the acute inflammatory process of the connective tissue [95]. However, the detailed regulation of MMPs, their substrates and inhibitors, as well as MMP activation remains largely unknown, and it seems likely that they are involved in many more processes together with other proteases of the ECM. An overview about the best characterized MMPs, their function and inhibitors can be seen in figure 6.

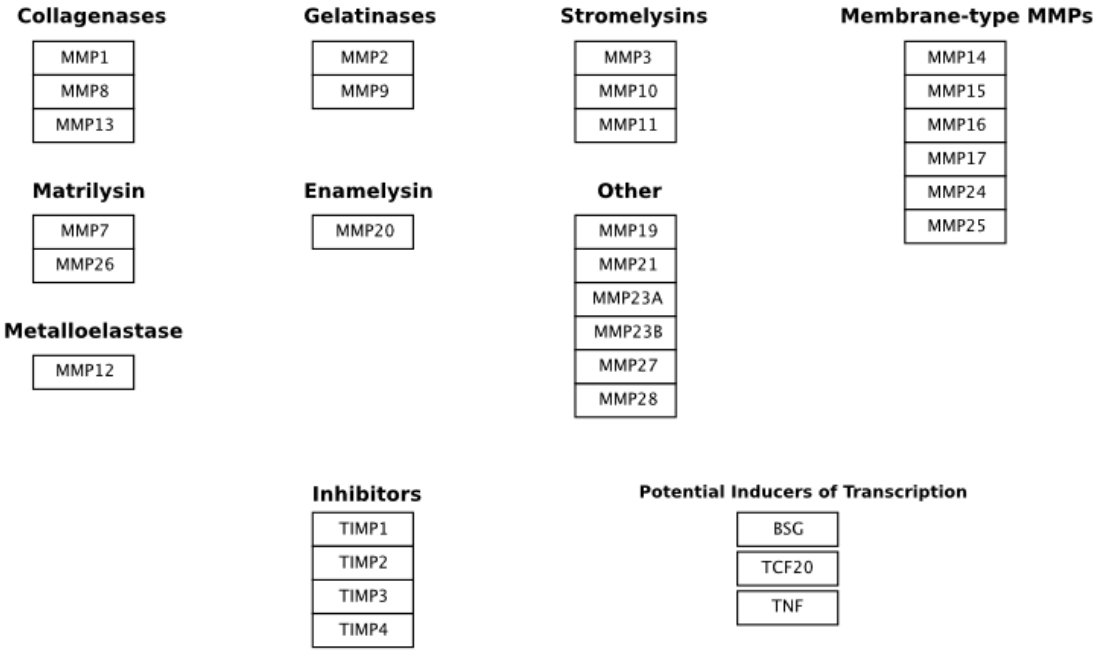

Figure 6: An overview of MMP proteins, together with their function. (© Kdahlquist, Martin van Iersel 2008)

The ADAMs metalloproteinase family is another example of a protein involved in ECM reorganization in multiple ways. Not only does it have a direct effect on the cells to stimulate MMP secretion, it also creates substrate breakdown products itself, which in turn activate different factors known to be involved in tumor progression [96]. A novel protease, called high temperature requirement serine protease A1 (HTRA1), was also found to be involved in ECM reorganization [97, 98]. Although they are not members of the MMP family, which is the most prominent participant in ECM reorganization, both ADAMs and HTRA1 represent two examples of recently discovered proteases involved in ECM reorganization [86, 97]. This highlights the fact that ECM reorganization complexity has not yet been fully realized and it is likely that increasingly more candidates will be identified.

Importantly, a naturally occurring equilibrium between proteases and their broad or specific inhibitors exists [99]. Hence, another regulatory level for substrate-enzyme reactivity is thereby created. Enzymatic activity on a certain substrate is therefore highly dependent on many factors involving both, enzyme and substrate. Here, events such as transcription, post-translational modification, molecular stoichiometry, protein inhibition/ activation etc. are important. This is why inhibitors

of certain extracellular proteases can have a positive or negative impact on disease progression or cell integrity [100]. For instance, the serpin peptide family represents a family of well-known inhibitors. They are capable of potently inhibiting a wide range of serine proteases and are known to be involved in a quick deactivation of many serine proteases, thereby regulating many extracellular processes, as for instance blood coagulation [101]. In conclusion, this highlights their potential involvement in reorganization of the ECM, making the tightly orchestrated machinery for ECM content homeostasis even more complex.

1.4 HTRA1

HTRA1 is a secreted peptidase involved in numerous intracellular and extracellular processes [102, 103]. HTRA1 is a protein found ubiquitously in almost every tissue of the human body [104] and is one of four so far described HTRA's that together build a highly conserved family. The HTRA family members share several common domains including a protease domain and at least one PDZ domain [105, 106]. A schematic overview of HTRA1 with its subdomains can be seen in figure 7. It is believed that alterations in HTRA1 activity are involved in the onset and progression of many diseases such as cancer, CARASIL, rheumatic disorders, and intervertebral disc (IVD) degeneration [107-109]. Still, its detailed mode of action remains largely unknown. However, many features have been well described and will therefore be highlighted here.

1.4.1 Structural properties

With the help of state-of-the-art techniques such as crystallography and stopped flow, it was possible to determine the exact architecture of HTRA1 either in the absence or presence of a substrate. We can therefore now distinguish between five distinct domains within the primary structure of the HTRA1 molecule:

1.4.1.1 Signal sequence

The N-terminal signal sequence is a feature found in mammalian HTRA1, -3 and -4. These three members of the HTRA family are all known to be secreted from the cell and hence, have to carry a signal sequence for the initiation of the protein´s

secretion. Thus, the signal sequence is very likely crucial to the directed secretion of HTRA1 from the cell. However, the detailed mechanism of the secretion pathway of HTRA1 remains largely unknown [110].

1.4.1.2 IGFBP/Mac25 domain

This domain is termed the Mac25 domain due to structural similarities to IGFBP (insulin-like growth factor-binding protein) domains. Surprisingly, no direct interaction of this domain to IGFs has so far been shown, suggesting that the domain may have an entirely different mode of action. Similarly, the term Mac25-domain remains misleading, as also the similarity to the Mac25 protein (a follistatin (FS)-like protein) did not show any functional similarities to FS-like proteins at all [110]. Thus, the function of this domain remains largely unknown, as it does not seem to have any impact on proteolytic activity either [111, 112]. However, it was proposed that HTRA1 may have two different ways of identifying its potential substrates. The most prominent one being a direct recognition of the substrate with the help of the PDZ domain (c.f. 1.4.1.5) in order to allow for proteolysis to occur. The other one is the IGFBP/Mac25 domain which potentially helps to bind and cleave, for example, IGFBP-5 and thereby to regulate IGF signaling [113]. Furthermore, it was also shown that the alteration of the TGF-β pathway by HTRA1 is dependent on both proteolytic activity and the presence of the preceding region to the protease domain [114], thereby strengthening the importance of this sequence with regards to HTRA1's substrate specificity. Nevertheless, the details about this domains' importance have yet to be elucidated.

1.4.1.3 Kazal-type serine protease inhibitor domain

Interestingly, upstream of the protease domain, a Kazal-type serine protease inhibitor domain (Kazal domain) can be found. This domain is known to inhibit serine proteases specifically by binding to the proteolytically active domain and thereby inhibiting substrate binding. It is often found next to the IGFBP-like domain described above. Due to its close proximity to the HTRA1 protease domain, it is likely to be inhibitory during the resting state of HTRA1 in the absence of any substrate, although its inhibitory effect could so far not be shown [112, 115, 116]. However, the combination of the IGFBP/Mac25 and Kazal domain is found in many proteins, although their functional implications remain unknown [117].

Hence, it could be part of the zymogen status of the non-active enzyme, which prevents it from premature activation and hints to the idea of maturation induced by cleavage by other proteases or auto-cleavage.

1.4.1.4 Protease domain

HTRA1 exhibits the classical composition of a trypsin-like serine endopeptidase. The term trypsin-like refers to a subset of serine proteases that cleave peptide bonds following a positively charged amino acid (a lysine or arginine) in the target protein, which gives them their specific nomenclature. The specificity of the protease domain to its substrates is given by the composition of the catalytic triad, the secondary structure of the enzyme´s proteolytic pocket and its amino acid residues, as well as by other domains of the enzyme (e.g. a PDZ domain) [102]. As in most serine proteases, the catalytically active region consists of a highly conserved domain where the proteolytic activity of the enzyme takes place. Proteolytic activity refers to the process of the enzymes ability to cleave peptide bonds within a protein, making it an endopeptidase. The name serine protease derives from the fact that a serine residue within the catalytic triad of the protease domain is responsible for the nucleophilic attack of the carbonyl group of the peptide bond, thereby erasing a covalent bond which results in the separation into two individual peptides [118].

1.4.1.5 PDZ domain

The C-terminus of HTRA1 carries a post-synaptic density protein (PSD95), Drosophila disc large tumor suppressor (Dlg1), and zonula occludens-1 protein (zo-1) domain (PDZ-domain). Generally, its function is to provide substrate specificity towards many different proteins. This is accomplished in a very directed manner, which is why the PDZ domain also represents a highly conserved domain, being similar in many PDZ-domain carrying proteins, but highly specific for a group of target proteins [119]. This is brought about via a distinct sequence specificity of the PDZ domain towards its targets [120]. Thousands of proteins with many different functions are known to carry a PDZ-domain whenever substrate specificity is needed [121]. Due to their complexity, PDZ-substrate interactions are a critical factor in many processes and diseases of the cell and even the body as a whole. Predicting potential targets of a known PDZ-domain sequence could

therefore help to understand many processes in- and outside of the cell [121]. The PDZ domain of HTRA1 and its specificity is well described by Truebestein et al [111]. However, other HTRA proteins may carry one or multiple PDZ domains of different specificities. Furthermore, the PDZ domain is described to represent a bottleneck of enzymatic activity, as the binding of the substrate to the PDZ-domain induces a conformational change of the whole HTRA1 enzyme, which allows the protease domain to execute its function, which would otherwise be sterically blocked [110, 122]. However, recent findings indicate that PDZ-domain lacking mutants of HTRA1 only show a marginal decrease in enzymatic activity (c.f. section 4).

As HTRA1 is also known to be secreted from certain cell types, it may seem surprising to find a PDZ domain on the C-terminus of HTRA1, as PDZ-domain have mostly been described intracellularly [119]. In conclusion, the PDZ domain of HTRA1 provides substrate specificity and induces a conformational change upon substrate binding, thereby allowing enzymatic activity to occur [111, 123].

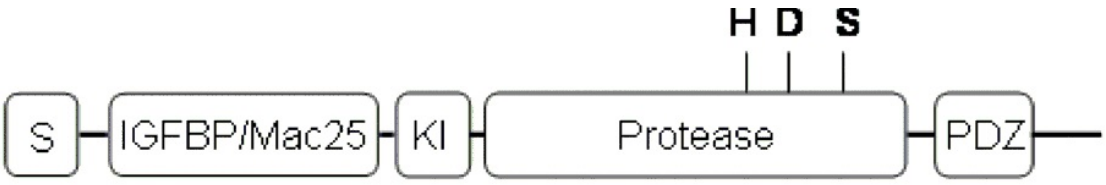

Figure 7: Overview about the functional domains of human HTRA1 [124].

1.4.1.6 Oligomerization

Although a single molecule of HTRA1 is soluble and stable, higher hierarchies of HTRA1 oligomerization have been described and are likely to coexist upon different environmental conditions [111]. Especially homotrimers appear to be the most abundant form of HTRA1 protein, although *in vitro* tests indicate even higher oligomeric states (c.f. section 4). This oligomeric state was found to be increased drastically in the bacterial homologues of HTRA1 (DegP [125]), but is also found in mammalian HTRA1 and is thought to be a key feature of activation and deactivation of HTRA1 proteolysis [126]. While usually three protease domains are capable of forming a trimer, higher assembly hierarchies are also facilitated by

PDZ-PDZ interactions. It is believed that the homotrimer state corresponds to a resting state of HTRA1, whereas 12- and 24-mers are believed to be involved in the functions of HTRA1 with regards to protein quality control and stress response of the cell [126]. Findings of Truebestein et al (2011) also suggest that the protease domain of several HTRA1 molecules assemble, thereby creating a barrel-like structure which exhibits an increased enzymatic activity [111]. However, it is questionable if this oligomeric state is of a high physiological relevance, as most other HTRA proteins and their homologues exhibit a higher activity at higher oligomeric states, thereby creating huge barrel-like structures which are believed to facilitate the chaperone and proteolytic activity of the protease [123, 127]. Thus, the oligomeric status of HTRA1 and other HTRA family members is likely to be an additional layer of regulating protease activity and helps to discriminate between the mere proteolysis and its involvement in acute protein quality control.

1.4.2 Functional implications

The mode of action of HTRA1 can be divided into two main categories:

1. **Binding** to a substrate in- or outside of the cell and thereby stabilizing, destabilizing (microtubule association) [128], inhibiting or activating certain factors [107, 114].
2. **Degradation** of target molecules by its enzymatic activity and thereby creating signaling molecules (e.g. syndecan shedding) or physically breaking down molecules (e.g. fibronectin in the ECM) [129].

Found as a heat shock induced chaperone in bacteria [130], the chaperone function (stabilization of otherwise non-stable and insoluble peptides) remains to be demonstrated in mammalian cells. Despite this, HTRA1's involvement in numerous mammalian cell processes has been well described, and range from intracellular functions [105] to extracellular secretion from the cells where it might fulfil different tasks. This clearly highlights its various functions and implications in- and outside of the cell with many potential involvements in diseases [117]. However, details on its role in the stress response of the mammalian cell appears to be less well understood, as HTRA1 secretion is increased as a response to heat

shock conditions [102]. Under these conditions it can efficiently degrade heat-sensitive proteins that could otherwise be a threat to the survival of the cell. Still, recent studies highlight the importance of HTRA1 in developing tissues, which would confirm its importance in the process of ECM reorganization [104].
It is therefore important to distinguish between HTRA1´s basic functions intra- and extracellularly, as these very different compartments vary in the protein quality control machinery and many other aspects.

1.4.3 Involvement in developing tissues

Expression profile studies of the *HTRA1* gene revealed an upregulation in developing tissues and organs [131]. Especially the placenta (an area of high proliferation rates and stem cell activity) shows a significant upregulation of *HTRA1* and a loss of *HTRA1* in this tissue was shown to have a negative impact on tissue development [131-133]. Hence, it appears that HTRA1 is necessary in regions that require highly dynamic cellular restructuring processes. Indeed, it has been shown that a lack of HTRA1 results in an abnormal development of the placenta in mice [133]. In conclusion, the developing placenta is likely to be a prominent example of the necessity of HTRA1 and other proteases to be directly involved in the development of a tissue.

1.4.4 Intracellular function

1.4.4.1 Association to tubulin

Intracellularly, HTRA1 is highly localized to microtubules in mammalian cells [128]. Although it is not clear what function this may serve, it was demonstrated that HTRA1 overexpression resulted in inhibition of cell migration, which would indicate a tumor suppressor-like function of HTRA1 [134]. However, while low concentrations of HTRA1 are able to stabilize microtubule polymerization *in vitro*, higher concentrations seem to have no effect on stability. Furthermore, HTRA1 was found to degrade tubulin *in vitro* [135].

1.4.4.2 TSC2

Moreover, other intracellular components were found as direct targets of HTRA1. The protein tuberous sclerosis complex 2 (TSC2) is known to be a negative regulator of the mTOR pathway, is involved in embryogenesis and was shown to be a direct target of HTRA1. Upon degradation by HTRA1, downstream targets of the TSC2 pathway are effectively inhibited. Since it is known that HTRA1 is upregulated in developing tissues of the embryo, TSC2 could be an example of one of many potential HTRA1 targets inside of the cell during development [136].

1.4.4.3 XIAP

The X-linked inhibitor of apoptosis protein (XIAP) is an important inhibitor of apoptosis. It was recently shown that HTRA1 may be directly involved in regulating the intracellular amounts of this factor by degrading it, thereby actively down-regulating apoptosis [137, 138]. Thus, a direct involvement in cancer progression and chemotherapy resistance is postulated.

1.4.5 Extracellular function

As mentioned earlier, HTRA1 is known to be secreted in various conditions, be it stress-response, inflammation and disease or the differentiation of stem cells [109, 139, 140]. Therefore, it was not surprising to find it involved in the regulation of several processes, including joint degeneration [107], cancer progression and several others [141, 142]. Due to its ability to potentially cleave several components of the ECM [143], it appears obvious that a tight regulation of HTRA1 during development and rearrangement of a tissue is needed in order to maintain tissue integrity and health. HTRA1 can therefore potentially be seen as an essential developmental factor during many transition conditions of a cell or even tissue. However, its detailed mode of action remains largely unknown, as well as its regulatory pathways of expression and secretion. Known substrates for extracellular HTRA1 are, amongst others, fibronectin [129], aggrecan [144], type II collagen [145], elastin, biglycan, syndecan-4, nidogen [146], glypican-4 [97], all of which are important for specific ECM integrity (c.f. section 1.3). Potentially, the list of substrates for HTRA1 is even greater [143]. However, next to its proteolytic activity, HTRA1 was also shown to have signaling effects on cells, resulting in an

upregulation of MMPs, independent of HTRA1 proteolytic activity [107].

Transforming growth factor-beta (TGF-β) signaling is inhibited by HTRA1. This cytokine is secreted by various cell types and controls many cellular processes such as differentiation and proliferation [147]. Due to its possible association to HTRA1, TGF-β signaling can be inhibited, thus inhibiting receptor activation of various TGF-β ligands, as described by Oka et al [114]. This represents an example of how HTRA1´s extracellular presence can affect an intracellular pathway of a developing cell, thereby connecting the in- and outside functions of HTRA1 on the cell. However, recent reports identified HTRA1 as being a stimulatory factor towards TGF-β signalling under certain conditions, by the degradation of latent TGF-β binding protein 1 (LTBP1) [148].

1.4.6 HTRA1 in disease

To further highlight the importance of HTRA1 in heath and disease, some of the best studied human diseases in which HTRA1 is implicated as being an underlying cause are described in the following chapter.

1.4.6.1 AMD

The disease age-related macular degeneration (AMD) is a medical condition of the eye, which results in blindness. It occurs in a dry and wet (also referred to as neovascular AMD) state in which the retina loses its function over the progression of the disease. It was found that genetic variants, leading to loss-of-function mutations of HTRA1 protein, could be the underlying cause in the onset of this disease. Here, HTRA1´s ability to act on TGF-β signaling due to the degradation of TGF-β pathway members seems to be the mechanism of action [149-151]. On the other hand, it was shown that mutations in the promoter region of HTRA1 (as well as ARMS2) can lead to an upregulation of HTRA1 expression, which ultimately leads to an increased proteolytic activity in the ECM of the affected tissue. This can therefore lead to structural changes of the ECM, which results in AMD progression [146].

1.4.6.2 Cancer

Several studies have investigated the influence of HTRA1 on cancer progression. Increasing awareness towards an involvement of the ECM in cancer and other cellular processes acknowledges the fact that the rearrangement of the ECM can have a major impact on cancer progression. It is generally accepted that HTRA1 levels in cancerous tissue are significantly down regulated, thereby suggestive of HTRA1´s role as a tumor suppressor [141]. However, the influence of HTRA1 on cancer progression goes beyond its activity on ECM components and includes intracellular cytoskeletal deficiencies [134], as well as chemotherapy resistance [138]. Generally, it appears that the expression levels of HTRA1 in certain cancer types are dysregulated, more than the activity of HTRA1 itself [152, 153]. However, more functional analyses are needed to fully investigate this. Thus, the mutual crosstalk between HTRA1 and its many substrates and binding partners can result in a diverse range of conditions, in which the cell tends to further progress in its malign status. Furthermore, expression levels of certain inhibitory molecules can have an important role as recent studies have shown. One example is given by serpin alpha-1 antitrypsin (A1AD), which was found to be a target of HTRA1 [100].

1.4.6.3 CARASIL

Next to AMD and different types of cancer, loss-of-function mutations in the *HTRA1* gene were also found to be the underlying cause of certain neurological disorders, such as Cerebral Autosomal-recessive Arteriopathy with Subcortical Infarcts and Leukoencephalopathy (CARASIL). In this rare disease, mutations in the *HTRA1* gene lead to errors in the TGF-β signaling cascade, which ultimately leads to dysfunctional arterioles of the brain resulting in reoccurring strokes of the brain tissue. Although the disease was described in only a small group of patients, it stresses the diverse impact that dysfunctional HTRA1 protein can have in different types of tissues throughout the body [154, 155].

1.4.6.4 Alzheimer's disease

There is conflicting data concerning the involvement of HTRA1 in Alzheimer's disease. While a study by Grau et al (2006) confirmed HTRA1 to be involved in the processing of the amyloid precursor [156], another study found no association between *HTRA1* gene polymorphism and Alzheimer's [157]. Hence, if HTRA1 is involved in the progression of this particular disease, this involvement is, contrary to many other disease conditions as for instance cancer, not based on a genetic variant of HTRA1 itself but could involve many other candidates (e.g. enzyme-to-substrate ratio, enzyme inhibition etc.). However, the involvement of HTRA1 in Alzheimer´s disease is likely when considering the characteristics of the disease to be caused by protein aggregates, called plaques. A dysregulation of HTRA1 activity could therefore facilitate plaque formation and hence, disease progression. Thus, further investigations are needed.

1.4.6.5 Musculoskeletal Diseases

The term musculoskeletal disease (MSD) comprises muscle and bone tissue, as well as connective tissue associated to it in the human body. Together they make up a wide variety of tissues, including joints, bones, muscles, cartilage, tendon and ligaments. Diseases in any of these tissues can drastically affect the mobility of an individual and is known to affect millions of people worldwide. Contrary to cancer, many diseases of the connective tissue are caused by increased levels of secreted HTRA1 by the surrounding cells [109, 158] as is the case in OA and IVD disease [107, 129, 159, 160].

With regards to its role in MSD, HTRA1 was initially identified as having a potential role in Duchenne muscular dystrophy (DMD). This disease results in muscle degeneration and can even lead to a premature death. Although no functional studies about HTRA1 activity have yet been performed, a study exists in which *HTRA1* expression levels were significantly increased in the muscle tissue of a patient with DMD. It was speculated that HTRA1 could act on insulin-growth factor binding protein 5 (IGFBP5), which it can deactivate by degradation. A lack of IGFBP5 in the muscle is known to be an underlying cause of DMD, which is needed for proper muscle development and maintenance by insulin-growth factor-1 (IGF-1) augmentation [113, 161].

It is of note that the involvement of HTRA1 in bone development has been under investigation for several years now [124, 162, 163]. It still remains controversial as to how it may potentially influence bone formation due to several studies reporting both positive and negative effects of HTRA1 on osteogenesis [163, 164]. An early *in vitro* study performed by Hadfield et al [179] resulted in HTRA1 being labeled as an inhibitor of osteoblast differentiation. However, the detailed mechanism underlying this regulatory process of HTRA1 on bone formation remains an open question. Somewhat in contrast to these findings, molecular- and histological-based studies in mice have demonstrated high levels of HTRA1 to be present in osteoid and newly formed bone [114, 162]. Furthermore, HTRA1 loss-of-function studies in hMSCs undergoing osteogenic differentiation resulted in impaired osteoblast-derived mineral formation [165]. However, a more recent study by Graham et al [163] demonstrated an anti-osteogenic effect of HTRA1 *in vitro* and *in vivo*, and this was considered to be primarily due to its ability to cleave TGF-β receptors thereby disrupting TGF signaling pathways. However, more studies confirming this effect need to be conducted.

It should be mentioned that most of the studies described above were conducted in immortalized cell lines and may not be representative of primary bone-forming cells, as is the case in the study performed by Tiaden et al [165]. In addition, findings by Oka et al (2004) identified a number of HTRA1 substrates both *in vitro* and *in vivo*, the most important ones being members of the TGF-β family [114], with implications for the bone development process [163, 166]. Interestingly, the TGF-β signaling cascade is also known to be involved in adipogenesis, although its detailed mode of action remains largely unknown [167], thus implying a potential role for HTRA1 in differentiation pathways other than osteogenesis. This assumption is further highlighted by the fact that the secretion of proteases, such as HTRA1, can restructure the ECM and thereby have an impact on stem cell commitment towards osteogenesis or adipogenesis [168-170]. In conclusion, HTRA1 protein and gene expression have successfully been shown to be the underlying cause of many different diseases affecting the connective tissue, as well as in the process of cellular maturation and differentiation [109, 124, 162, 164, 171]. This is most likely due to a combination of both HTRA1´s proteolytic activity and its ability to bind and thereby disrupt critical signaling events (a central one being TGF-β) [124, 148, 166].

Thus, despite the fact that HTRA1 was long seen as a factor contributing to certain MSDs, it is important to understand that other conditions may require a fully functional protease like HTRA1 to be active in the ECM in order to allow for healthy tissue development and maintenance [109]. In conclusion, many MSDs in which a turnover of the ECM has an effect on disease onset or progression rely on the absence or presence of HTRA1 and other proteases (e.g. MMPs). Undoubtedly, the number of MSDs involving HTRA1 as being a positive or negative regulator will therefore increase over the next years.

1.5 Conclusion

Stem cells hold great promise as future therapeutic strategies in regenerative and preventive medicine. The fact that stem cells can themselves differentiate into any known cell type and thereby even allow the development of an entire organ in an autologous manner, makes them an attractive target for medical research in many given areas. As such, a full understanding of stem cell differentiation is an absolute requirement and would undoubtedly allow for the optimized use of stem cells in biomedical and therapeutic applications of many different kinds. It is now well acknowledged that osteogenesis and adipogenesis are regulated reciprocally on many levels [19, 172-175] and that imbalances in these two processes can contribute to the development of debilitating disorders such as osteoporosis. Identifying these factors could therefore represent a major breakthrough in fighting these diseases, as well as in understanding the fundamental stem cell differentiation process in more detail. HTRA1 may represent one such factor, based on its ability to regulate osteogenesis [124, 164], although its impact on other lineage pathways has not yet been fully investigated.

Therefore, in the realms of this thesis, the influence of extracellular HTRA1 on hMSC lineage commitment is addressed, with a predominant focus on its role in hMSC adipogenesis.

2 Hypothesis and aims of the thesis

The primary premise of the current study is that HTRA1 acts as a negative regulator of adipocyte development in differentiating human MSCs, and that these effects can help establish its potential role in fat homeostasis in both health and disease. This hypothesis is tested by fulfilling the following aims:

Aim 1: Express and purify active and inactive forms of recombinant human HTRA1 using an E.coli expression system.
Aim 2: Examine the effects of exogenous HTRA1 and siRNA-mediated HTRA1 silencing on human MSC adipogenesis
Aim 3: Established a mechanism of action for HTRA1 with regards to its ability to influence human MSC adipocyte development
Aim 4: Validate the relevance of HTRA1's involvement in regulating human MSC adipogenesis in health and disease

It is envisaged that the results generated from this study will enhance our understanding of the role played by the serine protease HTRA1 in the adipogenic differentiation of human MSCs and subsequently allow us further insight into the intricacies governing this process. Furthermore, our findings may have significant relevance with regards to fat homeostasis, whereby dysregulation of adipocyte formation and function are considered to be key events in the development of various disorders including diabetes type II and osteoporosis.

3 Results

3.1 Overview of published and submitted manuscripts

3.1.1 Novel function of serine protease HTRA1 in inhibiting adipogenic differentiation of human mesenchymal stem cells via MAP kinase-mediated MMP upregulation.

Authors: Tiaden AN*, **Bahrenberg G***, Mirsaidi A, Glanz S, Blüher M, Richards PJ.
*authors contributed equally

Journal: under review by *Stem Cells (August 2015)*

Contribution: Execution of recombinant HTRA1 protein production and *in vitro* test (Fig. S1B+C, S3), ELISA (Fig. 2G, 3E+F, 5C+D), qPCR (Fig. 3 A-D, 6B+C, S4C-E), FACS (Fig. 2A-F, S2), oil red staining and quantification (Fig. 1B-D, 5E+F, 6D, S4F), FN *in vitro* studies (Fig. S4A+B, S5C+D), Western blots (Fig. 6A). Planning, evaluation of the study. Writing of materials and methods and discussion section.

3.1.2 Use of biomimetic microtissue spheroids and specific growth factor supplementation to improve tenocyte differentiation and adaptation to a collagen-based scaffold *in vitro.*

Authors: Theiss F, Mirsaidi A, Mhanna R, Glanz S, **Bahrenberg G**, Tiaden AN, Richards PJ.

Journal: *Biomaterials 2015 Aug 10;69:99-109*

Contribution: Planning, execution and evaluation of the cell culture and molecular biology aspects, i.e. cell culture work, qPCR (Fig. 4+5). Contribution to writing of discussion section.

3.1.3 Human serine protease HTRA1 positively regulates osteogenesis of human bone marrow-derived mesenchymal stem cells and mineralization of differentiating bone-forming cells through the modulation of extracellular matrix protein.

Authors: Tiaden AN, Breiden M, Mirsaidi A, Weber FA, **Bahrenberg G**, Glanz S, Cinelli P, Ehrmann M, Richards PJ.

Journal: *Stem Cells. 2012 Oct;30(10):2271-82.*

Contribution: Execution of recombinant HTRA1 protein production, qPCR (Fig. 1A), oil red staining (Fig. 1B, 2D+E, 3C, Fig. 4A-D). Planning, evaluation of the study.

3.1.4 Detrimental role for human high temperature requirement serine protease A1 (HTRA1) in the pathogenesis of intervertebral disc (IVD) degeneration.

Authors: Tiaden AN, Klawitter M, Lux V, Mirsaidi A, **Bahrenberg G**, Glanz S, Quero L, Liebscher T, Wuertz K, Ehrmann M, Richards PJ.

Journal: *J Biol Chem. 2012 Jun 15;287(25):21335-45.*

Contribution: Execution of recombinant HTRA1 protein production and *in vitro* studies (Fig. 2A+B). qPCR (Fig. 2C-F, 3D), Western blots (Fig.4 A-C). Planning, evaluation of the study.

3.1.5 Assessment of the Matrix Degenerative Effects of MMP-3, ADAMTS-4 and HTRA1 injected into a bovine Intervertebral Disc Organ Culture Model.

Authors: Furtwängler T, Chan SC, **Bahrenberg G**, Richards PJ, Gantenbein-Ritter B.

Journal: *Spine (Phila Pa 1976). 2013 Oct 15;38(22):E1377-87.*

Contribution: Execution of recombinant HTRA1 protein production.

Novel function of serine protease HTRA1 in inhibiting adipogenic differentiation of human mesenchymal stem cells via MAP kinase-mediated MMP upregulation

André N. Tiaden[1*], Gregor Bahrenberg[1,2*], Ali Mirsaidi[1,2], Stephan Glanz[1,2], Matthias Blüher[3], Peter J. Richards[1,2*]

[1]Bone and Stem Cell Research Group, CABMM, University of Zurich, 8057 Zurich, Switzerland. [2]Zurich Center for Integrative Human Physiology (ZIHP), University of Zurich, 8057 Zurich Switzerland. [3]Department of Medicine, Dermatology und Neurology, Department of Endocrinology und Nephrology, University of Leipzig, Leipzig, Germany.

*authors contributed equally

Author contributions

André N Tiaden: Collection and/or assembly of data, Data analysis and interpretation

Gregor Bahrenberg: Collection and/or assembly of data, Data analysis and interpretation

Ali Mirsaidi: Collection and/or assembly of data, Data analysis and interpretation

Stephan Glanz: Collection and/or assembly of data

Matthias Blüher: Provision of study material or patients, Collection and/or assembly of data, Data analysis and interpretation

Peter J Richards: Conception and design, Financial support, Collection and/or assembly of data, Data analysis and interpretation, Manuscript writing, Final approval of manuscript

***Correspondence:** Dr. Peter J. Richards, Bone and Stem Cell Research Group, Competence Center for Applied Biotechnology and Molecular Medicine, Room 13-L-86, University of Zurich, Winterthurerstrasse 190, CH-8057 Zurich, Switzerland, Telephone: +41-44-635-3800; E-mail: peter.richards@cabmm.uzh.ch

SG and GB were supported by SNSF grants 31003A_134935 and 31003A_156313. AM and NAT were supported by the Uniscientia Foundation and the Forschungskredit University of Zurich.

Running Head: HTRA1 inhibits mesenchymal stem cell adipogenesis

Keywords: Adipogenesis; adult stem cells; cell signaling; diabetes; differentiation

ABSTRACT

Adipogenesis is the process by which mesenchymal stem cells (MSCs) develop into lipid-laden adipocytes. Due to their high prevalence within adipose tissue, adipocytes play a central role in regulating circulating fatty acid levels, which is considered to be of critical importance in maintaining insulin sensitivity. High temperature requirement protease A1 (HTRA1) is a newly recognized regulator of MSC differentiation, although its role as a mediator of adipogenesis has not yet been defined. The aim of this work was therefore to evaluate HTRA1's influence on hMSC adipogenesis and to establish a potential mode of action. We report that the addition of exogenous HTRA1 to adipogenic human MSCs suppressed their ability to develop into lipid laden adipocytes. These effects were demonstrated as being reliant on both its protease and PDZ domain, and were mediated through the actions of c-Jun N-terminal kinase (JNK) and matrix metalloproteinases (MMPs). The relevance of such findings with regards to HTRA1's potential influence on adipocyte function *in vivo*, is made evident by the fact that HTRA1 and MMP-13 were readily identifiable within inflammatory infiltrate present in visceral adipose tissue samples from insulin resistant obese human subjects. These data therefore implicate HTRA1 as a negative regulator of MSC adipogenesis and are suggestive of its potential involvement in adipose tissue remodeling under pathological conditions.

INTRODUCTION

Adipogenesis is a complex developmental process in which mesenchymal stem cells (MSCs) first become committed adipo-precursor cells and then undergo a tightly regulated differentiation program to generate mature adipocytes [1, 2]. Of critical importance in the body's ability to adapt to energy requirements, is the capacity for pre-adipocytes to develop into adipocytes and for them to be able to acquire more fat. Both these conditions require alterations in cell shape and volume, and are heavily reliant on the versatility and integrity of the adipocyte extracellular matrix (ECM), termed basal lamina [3]. The basal lamina is composed of numerous core proteins, including type IV collagen [4, 5], various laminin isoforms [5], and heparan sulfate proteoglycan (HSPG) [6] to name but a few, and is subject to continual turnover mediated by a wide variety of matrix metalloproteinases (MMPs) [7, 8]. Interference with basal lamina dynamics may therefore have significant consequences to adipogenesis and subsequent adipocyte stability.

Dysregulation of adipogenesis and adipose tissue remodeling has been linked to several human disorders, most notably of which is obesity-induced insulin resistance [9, 10]. A characteristic feature of obese adipose tissue is the presence of an inflammatory infiltrate consisting mainly of macrophages, thought to be instigated by elevated levels of adipocyte-derived cytokines as well as an increased incidence of adipocyte cell death [11]. Exposure to such an environment not only impairs adipocyte responsiveness to insulin, but can also lead to deviations in the differentiation status of pre-adipocytes [9]. As such, there is currently a strong focus on the identification of key factors involved in the regulation of adipogenic commitment.

HTRA1 has been newly identified as a modulator of human MSC (hMSC) differentiation, whereby it acts to enhance osteoblast formation most likely through proteolytic modification of the ECM, and its expression levels in bone tissue coincide with the appearance of new bone formation during fracture repair in mice [12]. Furthermore, preliminary findings from loss of function studies have suggested that HTRA1's ability to influence hMSC lineage commitment may extend to adipogenic differentiation [12]. However, the extent to which these effects are mediated by secreted HTRA1 and the possible mechanisms underlining its mode of action remain to be determined. Certainly, the growing number of reports pertaining to HTRA1's ability to modulate the ECM both under normal physiological conditions and in disease, may provide some basis for how it could potentially interact with and regulate adipocyte formation [13-15].

To define HTRA1's role in adipogenesis and its potential physiological relevance, we investigated the effects of exogenously added recombinant HTRA1 on the development of hMSCs into mature adipocytes and further analysed its expression levels in visceral adipose tissue from obese patients. We demonstrate that HTRA1 acts to significantly suppress adipocyte development, primarily through upregulation of JNK activity and MMP production. We further localized HTRA1 and MMP-13 to sites of immune cell infiltrate within the adipose tissue of an insulin resistant obese patient. This work thus identifies HTRA1 as being a potentially novel mediator of adipose tissue homeostasis.

MATERIALS AND METHODS

Materials

Anti-ERK1/2, anti-phospho-ERK1/2 (Thr202/Tyr204), anti-SAPK/JNK, anti-phospho-SAPK/JNK (Thr183/Tyr185), anti-p38, anti-phospho-p38 (Thr180/Tyr182) were all purchased from Cell signaling Technology (Leiden, The Netherlands). Anti-tubulin was from Sigma-Aldrich. Anti-type IV collagen (M3F7) and anti-laminin γ-1 (2E8) were from the Developmental Studies Hybridoma Bank (University of Iowa). Anti-fibronectin (MAB1936) was from Merck Millipore (Schaffhausen, Switzerland). Monoclonal anti-human HTRA1 was generously supplied by Prof. Michael Ehrmann (University Duisburg-Essen, Germany) and generated as previously described [16]. Rabbit anti-MMP-13 was purchased from Abcam (Cambridge, UK). Mouse IgG, HRP- or Cy3-labeled secondary antibodies specific for mouse or rabbit IgG were purchased from Jackson ImmunoResearch (Suffolk, UK), and biotin-labeled goat anti-mouse IgG and Vectastain ABC system used in immunohistochemical staining studies was from Reactolab SA (Servion, Switzerland). Biotinylated swine anti-rabbit IgG was from Dako (Baar, Switzerland). Histidine-labeled HTRA1 proteins were overexpressed in *E. coli* and purified using previously described methodologies [16].

hMSC Culture

The hMSCs employed in this work were provided by the Texas A&M Health Science Center College of Medicine Institute for Regenerative Medicine at Scott & White through a grant from NCRR of the NIH, Grant # P40RR017447. hMSCs were isolated from bone

marrow aspirates and multipotency fully defined in accordance with the minimal criteria outlined by International Society for Cellular Therapy [17]. hMSCs were maintained at 37°C, in 5% CO_2 and 98% humidity in normal growth medium consisting of Dulbecco's modified eagle medium (DMEM-low glucose, with GlutaMAX) (Life Technologies, Zug, Switzerland), supplemented with 10% fetal bovine serum (FBS, BioWest), penicillin/streptomycin (50 units/ml; 50 µg/ml), and used between passage 5 and 8 unless otherwise stated.

Adipogenic differentiation of hMSCs

The adipogenic differentiation of hMSCs was performed using a protocol previously established in our laboratory [12]. Briefly, hMSCs seeded in cell culture plates at 10'000 cells/cm^2 were incubated for 3 days with adipogenic induction medium consisting of normal growth medium (DMEM-high glucose, GlutaMAX) supplemented with 1 µM dexamethasone, 10 µg/ml insulin, 0.1 mM Indomethacin, and 0.5 mM isobutylmethylxanthine (IBMX) (all from Sigma-Aldrich). Cells were subsequently cultured in adipogenic maintenance medium consisting of IBMX-free adipogenic medium, and replenished with fresh medium every 72 h for up to 14-24 days unless otherwise stated. Adipocyte formation was confirmed by positive staining of lipid droplets by Oil Red O (Sigma-Aldrich). Oil Red O staining was quantified by extraction with isopropanol absorption measured at 510 nm using a Multiplate reader (Infinite M200, Tecan). Values were normalized to cell number assessed by DAPI staining as described below. For recombinant HTRA1 addition studies, hMSCs undergoing adipogenic differentiation were treated with recombinant HTRA1 starting at day 3 after adipogenic induction. For

inhibition studies, cells were treated with recombinant HTRA1 in the presence of MMP-3 inhibitor NNGH, MMP-13 inhibitor CL-82198, or MAP Kinase inhibitors PD98059, SP600125 and SB239063 (all from Enzo Life Science, Lausen, Switzerland). DMSO (0.05%) was added as vehicle control and was equivalent to highest concentration of inhibitor used.

RT-qPCR

Gene expression levels were quantified by reverse-transcription quantitative PCR (RT-qPCR) using TaqMan Gene Expression Assays (Life Technologies) (Supporting Information Table S1) as previously described [12]. Total RNA was harvested from cells at selected time points during differentiation and 0.5µg of total RNA reverse-transcribed using Superscript II (Life Technologies). An equivalent of 10ng total RNA was applied as cDNA template in the successive qRT-PCR reaction using the StepOnePlus (Life Technologies). Values were normalized to *GUSB* mRNA levels and presented as fold change as compared to control cells or cells treated with vehicle alone (value = 1) according to the $2^{-\Delta\Delta CT}$ method.

siRNA Assays

Silencing of *HTRA1* and *MMP13* gene expression was performed with Silencer Select siRNA oligos (Life Technologies) according to the manufacturer's protocol as previously described [12]. For *HTRA1* knockdown, hMSCs (1 x10^5) were transfected with 40 nM *HTRA1*-specific (s11279, s11280) or negative control siRNA (Negative Control-1) using the NEON Transfection System (Life Technologies). Transfected cells were immediately

seeded in cell culture plates with fresh growth medium (without antibiotics) and incubated for 24 h at 37°C, 5% CO2. Medium was then replaced with either fresh growth medium or adipogenic differentiation and total RNA and supernatants harvested at selected time points for further analysis. For *MMP13* knockdown, adherent hMSCs were initially seeded in cell culture plates and cultured in induction medium for 3 days. Thereafter, hMSCs were transfected for 24 h with 40 nM *MMP13*-specific (11496, 104024) or negative control siRNA (Negative Control-1) using Lipofectamine RNAiMAX (Life Technologies). Supernatants were subsequently replaced with adipogenic maintenance medium and total RNA and supernatants harvested at selected time points for further analysis. The effect of *HTRA1* and *MMP13* gene silencing on lipid droplet formation was evaluated by Oil Red O staining as described above.

Proteolysis Assays

HTRA1 mediated digestion of BODIPY-FL-labeled DQ-elastin or DQ-type IV collagen was performed using EnzChek assay kits (Life Technologies) as previously described [18].

ELISAs

Extracellular protein levels of HTRA1, MMP-3, MMP-13, syndecan-1 and -4 were measured in the supernatants of hMSCs at selected time points by ELISA. The HTRA1 ELISA was performed as previously described [19]. The MMP-3, MMP-13, Syndecan-1 and -4 specific ELISAs were performed using Duo-Set ELISA Development Systems according to the manufacturer's instructions (R & D Systems, Abingdon, UK).

FACS Analysis

Subconfluent adherent hMSCs were detached using Accutase (Life Technologies) and resuspended in ice cold FACS buffer (PBS/BSA 0.1%) in round bottom 96-well plates to 2 x10^6/ml. Cells were incubated on ice for 1 h with equimolar concentrations of his-labeled recombinant HTRA1 either alone, or in combination with heparin, heparanase, chondroitinase (all from Sigma-Aldrich), collagenase (Roche), or peptide competitors of integrin binding CS1 and GRGDSP (from ANAWA Trading SA, Zurich, Switzerland). Cells were then washed in cold FACS buffer and incubated with a FITC conjugated rabbit anti-6xHis tag antibody (Lucerna-Chem, Luzern, Switzerland) on ice for 1 h. Bound HTRA1 was detected by FACS analysis using a FACS-Canto II (BD Biosciences) and quantified using FlowJo 10 software.

Protein Electrophoresis and Immunoblotting

Whole cell extracts from untreated or HTRA1 treated hMSCs were harvested using CelLytic M (Sigma Aldrich) supplemented with protease and phosphatase inhibitor cocktails (Sigma Aldrich) and 1mM PMSF at 2 weeks post adipogenic induction. Protein concentrations were determined by Bradford-based protein assay (Bio-Rad). Protein samples were boiled for 5 min in loading buffer (50 mM Tris-HCl, pH 6.8, 2% (v/v) SDS, 10% (v/v) glycerol, 100 mM DTT, 0.002% (w/v) bromophenol blue) and equal amounts of protein analyzed by SDS-PAGE using or 10% or 4-15% precast Tris-HCl gels (BioRad) under reducing conditions and electroblotted onto PVDF membranes using the Trans-Blot Turbo blotting system (BioRad). Membranes were then blocked with 5% (w/v) skim milk in TBST (50mM Tris-HCl, pH 7.6, 150mM NaCl, 0.05% (v/v) Tween 20) for 1 h at room

temperature and then incubated with specific antibodies overnight at 4°C at recommended dilutions in blocking buffer. Antibody binding was detected using HRP-conjugated secondary antibodies followed by incubation in Super Signal West Pico or West Dura Chemiluminescent Substrate (Life Technologies) and exposed to x-ray film.

Preparation and identification of Fnfs

For the identification of native Fnfs in supernatants, hMSCs undergoing adipogenic differentiation for 14 days were treated for a further 24 h with HTRA1 (45 nM) in fresh growth medium without FCS. Where indicated, HTRA1 was also added in combination with CL-82198 (20 nM). Supernatants were then harvested and immediately placed on ice. Cellular debris was removed by centrifugation and the remaining supernatant concentrated 40-fold by centrifugation at 3000G for 30 min in Amicon Ultra columns (10 kDa size exclusion, Millipore). Concentrated protein solutions were then supplemented with protease inhibitor cocktail (1:100, Sigma Aldrich) and 1mM PMSF and separated on a 4-12% SDS-PAGE pre-cast gel (BioRad). Methods for preparing purified Fnfs generated from HTRA1-digested plasma fibronectin were carried out as previously described [18]. Fnfs were visualized by immunoblotting using a specific antibody against the N-terminus of fibronectin and detected using an HRP-conjugated secondary antibody as described above.

VLDL uptake

Lipid uptake by adipogenic hMSCs was performed using DiI-labeled human VLDL (KALEN Biomedical) at late time points of adipogenesis between days 18-24. Cultured

hMSCs were rinsed once with PBS and then incubated for 3 h under standard culture conditions in assay buffer supplemented with DiI-labeled VLDL (4 μg/ml) and carrier protein ApoE2 (3 μg/ml, PeproTech, UK). Following incubation, cells were washed 3 times with PBS and fixed with PBS-buffered formaldehyde (4%) for 30 min. Nuclei were stained with DAPI (1:10'000) in PBS for 10 min and mounted in Mowiol containing 2.5% (w/v) DABCO. Images were captured using a Leica DMI6000B automated inverted research microscope system (Leica Microsystems). Relative linear median fluorescence intensity (RMFI) was quantified using NIH ImageJ software as described previously with some modifications [20]. Briefly, images were processed using identical image acquisition settings and exposure times. TIFF files were converted to 8-bit gray-scale mode and inverted onto a white background. Negative and positive staining controls were used to set measurable limits and threshold levels, and were then applied to all samples. Finally, RMFI was calculated as mean grey value per area and normalized to the number of cells per image as assessed by automated counting of DAPI-positive nuclei staining using the ImageJ software.

Immunofluorescence staining

hMSCs undergoing adipogenesis were fixed with PBS-buffered formaldehyde (4%) for 30 min, washed 3 times with PBS and then blocked for 30 min in 2% BSA and 5% normal goat serum in PBS. Cells were incubated overnight at 4°C with a monoclonal mouse anti-type IV collagen or monoclonal mouse anti-Laminin γ-1 antibodies, or an isotype control at an equivalent concentration. Antibody binding was detected using a Cy3-conjugated secondary antibody and nuclei stained with DAPI. Cells were mounted with Mowiol

containing 2.5% DABCO and images captured using a Leica DMI6000B automated inverted research microscope system (Leica Microsystems). Positive staining was quantified as described above. Relative mean fluorescence intensity (RMIF) was quantified using NIH ImageJ software as described above.

Immunohistochemical staining

Dewaxed paraffin sections of adipose tissue were rehydrated and blocked in normal serum (Jackson ImmunoResearch) for 30 min. Sections were then incubated for 1 h at 37°C with monoclonal mouse anti-HTRA1 (2.5 μg/ml) or rabbit anti-MMP-13 (5 μg/ml), and staining specificity controlled for using either mouse or rabbit IgG at equivalent concentrations. Sections were then washed in PBS and incubated with biotinylated goat anti-mouse IgG (1:200) or swine anti-rabbit IgG (1:400) for 1 h at 37°C followed by washing and a further incubation for 30 min with Vectastain. Sections were then developed using 3,3' diaminobenzidine tetrahydrochloride (DAB), counterstained with Harris' Hematoxylin and mounted in Mowiol.

Human Patients

Visceral tissue was obtained during bariatric surgery from morbidly obese, non-diabetic patients (Supporting Information Table S2). All adipose tissue donors gave written informed consent before the study, which had been approved by the Ethics Committee of the Medical Faculty, University of Leipzig. Insulin sensitivity was defined by the glucose infusion rate (GIR) during the steady state of an euglycemic hyperinsulinemic clamp as previously described [21].

Statistical Analysis

Two-tailed unpaired Student's *t*-test for comparison of two groups or one-way analysis of variance (ANOVA) with Tukey's post hoc test for multiple group comparisons were used. In all cases, a *P*-value of < 0.05 was considered statistically significant, and all data were expressed as mean ± standard deviation (S.D).

RESULTS

HTRA1 suppresses lipid uptake and droplet formation in adipogenic hMSCs

Preliminary studies utilizing an HTRA1-specific ELISA were conducted to investigate HTRA1 production by hMSCs. In undifferentiated control hMSCs, secreted HTRA1 levels increased over culture time, reaching a maximum level of 9.6 ± 0.5 ng/ml after 10 days of culture (Fig. 1A). HTRA1 production also increased over time in hMSC cultures undergoing adipogenesis, although levels were significantly reduced as compared to the undifferentiated control hMSCs throughout the 2 week culture period. Interestingly, these observations are in direct contrast to the stimulatory effects of osteogenic induction on HTRA1 production by hMSCs [12]. These data therefore suggest that reductions in HTRA1 might be a necessary requirement for hMSC adipogenesis. To address this model, we effectively eliminated endogenous HTRA1 from the culture system through the use of small interfering RNA (siRNA) (Supporting Information Fig. S1A) and assessed the ability of hMSCs to undergo adipogenesis using Oil Red O staining. Indeed, hMSCs deficient in HTRA1 produced significantly more lipid droplets than those treated with control siRNA,

thereby indicating that loss of HTRA1 had an overall positive influence on adipocyte formation (Fig. 1B). Furthermore, stimulation of HTRA1 deficient hMSCs with functional HTRA1 could reduce Oil Red O staining to a level comparable to that observed in control cultures (Fig. 1C). These studies also provided the first evidence that the addition of exogenous HTRA1 acts to suppress lipid droplet formation in developing adipocytes. Note that an HTRA1 variant (ΔMac) was used that is lacking its N-terminal Mac domain, for which no function is known to date [22] (Supporting Information Fig. S1B). Furthermore, N-terminal truncation does not affect HTRA1 function (Supporting Information Fig. S1C) and therefore this variant is termed HTRA1 throughout.

As HTRA1 contains both a C-terminal PDZ domain and a functional serine protease domain, we asked whether either domain was required for determining HTRA1's inhibitory influence over hMSC adipogenesis. Therefore, we generated several different proteolytically active and inactive recombinant HTRA1 proteins (Supporting Information Fig. S1B and S1C) and assessed their ability to influence oil droplet formation in adipogenic hMSCs. Indeed, inactivation of HTRA1's proteolytic activity through replacement of residue Ser328 with Ala (HTRA1 S328A), significantly impaired it's ability to inhibit lipid droplet formation in adipogenic hMSCs (Fig. 1D). Similarly, deletion of the PDZ domain in proteolytically active HTRA1 (HTRA1ΔPDZ) also abolished its inhibitory action on hMSC adipogenesis. These findings led us to conclude that HTRA1's inhibitory influence over hMSC adipogenesis most likely involves its binding to one or more substrates essentially involved in the development of lipid laden adipocytes, possibly via its PDZ domain. When considering potential substrate candidates, we became aware of a previous study in which HTRA1 was shown to cleave Xenopus

syndecan-4 [23]. Syndecans are cell surface HSPGs and represent a predominant feature of developing adipocytes, in which they play a central role in mediating lipid uptake [6]. In order to investigate this, we assessed the potential for various recombinant HTRA1 proteins to bind to hMSCs using fluorescence activated cell sorting (FACS) analysis. We could demonstrate that intact, but proteolytically inactive HTRA1 S328A was able to bind to hMSCs in a PDZ-dependent manner (Fig. 2A). The involvement of the PDZ domain in cellular binding of HTRA1 was further substantiated through the use of a recombinant HTRA1 containing the PDZ domain only (HTRA1Δprotease) (Fig. 2B). We next investigated whether removal of heparan sulfate (HS) using heparanase or competition with heparin could reduce cellular binding of HTRA1, and thereby provide support for an HTRA1-HSPG interaction. Indeed, the ability of HTRA1 S328A (Fig. 2C) and HTRA1Δprotease (Fig. 2D) to bind to hMSCs was markedly reduced by pre-treatment with heparanase. Similarly, pre-treatment of cells with heparin could also dramatically reduce cellular binding of both HTRA1 S328A (Fig. 2E) and HTRA1Δprotease (Fig. 2F). By contrast, replacement of heparanase with collagenase (Supporting Information Fig. S2A) or chondroitinase (Supporting Information Fig. S2B), and heparin with integrin-binding competitor peptides CS-1 (Supporting Information Fig. S2C) or GRGDSP (Supporting Information Fig. S2D), had little or no effect on the cellular binding capacity of HTRA1's PDZ domain.

Although these data demonstrated HTRA1's ability to bind to HSPG, they fell short of confirming whether HSPG was a proteolytic substrate of HTRA1. To address this question, we used an ELISA to determine levels of cleaved soluble syndecan-4 in supernatants from hMSCs at various stages of adipogenesis. Low levels of soluble

syndecan-4 were observed at day 10 (4.2 pg/ml ± 1.5) and day 21 (16.4 pg/ml ± 1.9) in normally differentiating adipogenic hMSCs (Fig. 2G). By contrast, significantly higher soluble syndecan-4 levels were measured in hMSCs treated with HTRA1 at day 10 (44.8 pg/ml ± 3.5; $P < 0.001$) and day 21 (84 pg/ml ± 7.7; $P < 0.001$). Again, these effects were determined as being dependent on HTRA1 possessing an intact PDZ domain, and were therefore in accordance with the findings from our binding studies. Studies were also undertaken to examine soluble syndecan-1. However, protein levels remained below detection limits in all treatment groups (data not shown). Based on syndecan-4 being a prominent regulator of lipid uptake by differentiating adipocytes [6], we surmised that HTRA1-induced syndecan-4 shedding would result in significant impairment of this process. Studies to investigate activate lipid uptake in adipogenic hMSCs were therefore undertaken using fluorescently labeled VLDL (VLDL-DiI). The uptake and accrual of high levels of VLDL-DiI in normally differentiating cells was apparent after a 3 h incubation period (Fig. 2H). However, VLDL-DiI levels were significantly diminished in hMSCs that had previously been treated with HTRA1. Furthermore, the inability of HTRA1 to exert a significant influence over VLDL-DiI uptake in the absence of either a protease or PDZ domain, convincingly supports a causal relationship between HTRA1's ability to impair lipid accrual in adipogenic hMSCs and its propensity to interact with and cleave HSPG from the cell surface.

Induction of MMPs by HTRA1

Although HTRA1 has the potential to directly interact with and cleave HSPG, it is also possible that the observed effects are indirect e.g. via other proteases. Our previous studies

utilizing synovial fibroblasts and intervertebral disc cells have identified MMPs to be strongly upregulated in response to HTRA1 stimulation, being mediated through the production of reactive fibronectin species [18, 19]. In addition to their ability to induce HSPG cleavage and shedding [24], MMPs are also potent regulators of adipogenesis, having both inhibitory and stimulatory effects [7, 8, 25]. This led us to investigate the possibility that MMP production by adipogenic hMSCs might be regulated by HTRA1. Indeed, treatment of adipogenic hMSCs with HTRA1 resulted in significant increases in the mRNA expression levels of *MMP1* (Fig. 3A), *MMP3* (Fig. 3B), *MMP9* (Fig. 3C), and *MMP13* (Fig. 3D). Additionally, ELISA measurements of supernatants revealed significant increases in MMP-3 (Fig. 3E) and MMP-13 (Fig. 3F) protein levels. Small, but significant increases in *MMP9* and *MMP13* mRNA expression, along with MMP-3 and -13 protein production, were also observed in hMSCs treated with HTRA1 S328A, although to a significantly lesser degree as compared to HTRA1. In order to ascertain whether the observed increases in MMP production were associated with increases in MMP activity, we undertook immunofluorescence studies to assess the levels of major MMP substrates present within cultures of differentiating hMSCs. The basal lamina of adipogenic hMSCs stained positive for both laminin (Fig. 4A) and type IV collagen (Fig. 4B) at day 22 after adipogenic induction. Based on HTRA1's ability to upregulate MMP production, we additionally examined whether it could also induce alterations in type IV collagen and laminin in adipogenic hMSC cultures. Indeed, treatment with HTRA1 resulted in a significant reduction in the levels of both laminin (Fig. 4A) and type IV collagen (Fig. 4B). Furthermore, the effects of HTRA1 were significantly more pronounced than either HTRA1 S328A or HTRA1ΔPDZ, and were therefore in accordance with HTRA1's ability

to regulate MMP production. Although it's possible that changes in the basal lamina were additionally due to factors other than MMPs, we are confident that they were not the direct result of HTRA1's actions based on the findings from previous studies in which HTRA1 failed to degrade either type IV collagen or laminin [13]. Indeed, we were only able to observe partial degradation of type IV collagen by HTRA1 at concentrations starting from 0.86 μM, 20-fold higher than that used in our culture system (Supporting Information Fig. S3).

As HTRA1-generated fibronectin fragments (Fnfs) are known to be potent stimulators of MMP production [18, 19], we additionally investigated whether such fragments could be identified within adipogenic hMSC cultures. Protein analysis of supernatants from hMSCs identified several Fnf species, including the well described 29 kDa Fnf (Supporting Information Fig. S4A) [18, 19]. Interestingly, levels of this particular fragment decreased upon adipogenic induction of control cultures, but was still present in the supernatants of adipogenic hMSCs treated with HTRA1. Furthermore, proteolytic inactive HTRA1 S328A failed to generate such Fnfs, thereby confirming it to be dependent on HTRA1's protease activity. In order to investigate whether the 29 kDa Fnf had the same capabilities as HTRA1 in terms of stimulating MMP production by adipogenic hMSCs, we purified HTRA1-generated Fnfs (Supporting Information Fig. S4B) and assessed their ability to influence MMP expression in comparison to HTRA1. Although Fnfs at a final concentration of up to 40 μg/ml were able to stimulate *MMP1* (Supporting Information Fig. S4C), *MMP3* (Supporting Information Fig. S4D) and *MMP13* (Supporting Information Fig. S4E) expression in adipogenic hMSCs, levels were significantly reduced as compared to HTRA1 treatment. Moreover, the addition of Fnfs failed to have any significant impact on

the level of oil droplet formation in adipogenic hMSCs (Supporting Information Fig. S4F). It therefore seems unlikely than Fnfs are the major instigators of MMP production and adipogenic suppression in hMSCs in response to HTRA1 addition.

The inhibitory effects of HTRA1 are dependent on MMP and MAP kinase activation

Having established MMP overproduction as being a predominant feature in HTRA1 stimulated hMSCs, we sought to determine whether they had any significant relevance in defining HTRA1's influence over hMSC adipogenesis. In order to investigate this, we utilized MMP inhibitors NNGH and CL-82198 at concentrations deemed to be selective for the inhibition of MMP-3 and MMP-13 respectively [26, 27], as well as siRNA targeted knockdown of *MMP13* gene expression. Initial immunofluorescence studies confirmed that type IV collagen levels were significantly elevated in HTRA1-treated cultures when exposed to NNGH (Fig. 5A) or CL-82198 (Fig. 5B) as compared to hMSCs treated with HTRA1 alone. Similarly, both NNGH (Fig. 5C) and CL-82198 (Fig. 5D) significantly reduced HTRA1's ability to generate cleaved soluble syndecan-4 in adipogenic hMSC cultures in a concentration dependent manner. Based on our assumption that alterations in basal lamina composition are the predominant driving force behind HTRA1's anti-adipogenic effects, we anticipated that the inhibition of either MMP-3 or MMP-13 in HTRA1-treated cultures should preserve adipocyte development as compared to hMSCs treated with HTRA1 alone. In order to investigate this, we quantified Oil Red O staining in adipogenic HTRA1-treated hMSCs cultured in the presence or absence of either MMP inhibitor. Our findings confirmed that inhibition of either MMP-3 (Fig. 5E) or MMP-13 (Fig. 5F) could significantly restore oil droplet formation in HTRA1-treated adipogenic

hMSCs to levels similar to those observed in adipogenic hMSCs cultured in the absence of HTRA1. These observations were additionally supported when *MMP13* gene expression was silenced in adipogenic hMSCs. *MMP13* expression could be effectively suppressed in both HTRA1-treated and untreated adipogenic hMSCs (Supporting Information Fig. S5A), and was shown to significantly impair HTRA1's ability to inhibit oil droplet formation as determined by quantitative analysis of Oil Red O staining (Supporting Information Fig. S5B). Furthermore, when analyzing the supernatants of HTRA1-treated adipogenic hMSCs in which the MMP-13 inhibitor had been added, we observed a clear decrease in the amount of the HTRA1-generated 29 kDa Fnf (Supporting Information Fig. S5C and S5D). This finding therefore lends additional support to the theory that in this culture system at least, HTRA1's capacity to induce MMP expression and impair adipogenesis in hMSCs is primarily mediated through mechanisms unrelated to Fnfs, and that at least in the case of MMP-13, Fnf generation in cultured hMSCs is actually dependent on the actions of MMPs rather than HTRA1 proteolysis directly.

Having therefore confirmed the central importance of MMPs in mediating HTRA1's effects on adipogenic hMSCs, we explored potential mechanisms through which HTRA1 could induce MMP production. Our previous findings from studies utilizing primary cultures of IVD cells have hinted towards the MAP kinase signaling pathway as playing a significant role in mediating the upregulation of MMPs in response to HTRA1 [18]. Moreover, alterations in MAP kinase activation are known to have a profound influence on both adipogenesis and adipose tissue function [28]. Based on this, we investigated the role of MAP kinase signaling in adipogenesis and evaluated its involvement in mediating HTRA1's effects on adipogenic hMSCs. Initial Western blot

analysis of adipogenic hMSCs revealed minimal levels of activated ERK, JNK and p38 at day 14 post induction (Fig. 6A). By contrast, phosphorylated levels of both ERK, JNK and p38 were noticeably increased in HTRA1-treated hMSCs in both a protease and PDZ dependent manner. In order to further investigate the involvement of MAP kinase signaling in MMP expression in adipogenic hMSCs, we utilized MAP kinase inhibitors PD98059, SP600125 and SB239063 at concentrations deemed to be selective for the inhibition of ERK, JNK and p38 respectively [29, 30]. Treatment of adipogenic hMSCs with MAP kinase inhibitors significantly reduced the basal expression of *MMP3* at day 17 post induction (Fig. 6B). The enhanced *MMP3* expression observed in HTRA1-treated adipogenic hMSCs was similarly reduced following the addition of MAP kinase inhibitors. By contrast, no significant changes in *MMP13* expression levels were observed in adipogenic hMSCs treated with PD98059, and HTRA1's ability to upregulate *MMP13* expression was not significantly affected (Fig. 6C). However, inhibition of JNK or p38 activity had a profound effect on both basal *MMP13* levels, as well as on HTRA1 - mediated upregulation of *MMP13* expression. In order to assess the possible consequence of such changes in MMP expression on hMSC adipogenesis, we investigated the effects of MAP kinase inhibitors on oil droplet formation in hMSCs undergoing adipogenesis. Neither PD98059 or SP600125 had any significant effect on oil droplet formation in normally differentiating hMSCs (Fig. 6D). By contrast, basal levels of oil droplet formation were dramatically reduced in control cultures treated with SB239063. The addition of either PD98059 or SP600125 to HTRA1-treated adipogenic hMSCs resulted in significant increases in Oil Red O staining, and in the case of SP600125, fully restored oil droplet formation to levels comparable to those observed in cultures undergoing

adipogenesis in the absence of HTRA1. However, the addition of SB239063 failed to alleviate the inhibitory effects of HTRA1, and instead led to a significant reduction in Oil Red O staining as compared to hMSCs treated with HTRA1 alone.

Detection of HTRA1 in visceral fat from obese patients

In order to validate the relevance of these findings with regards to HTRA1's potential role in mediating adipogenesis *in vivo*, immunohistochemical analysis was performed on visceral adipose tissue taken from obese patients (Supporting Information Table S2) that were diagnosed as being either insulin sensitive (IS) or insulin resistant (IR) as described previously in detail [21]. Analysis of visceral fat from either IS (Supporting Information Fig. S6A) or IR (Supporting Information Fig. S6B) obese patients revealed HTRA1 primarily localized to large blood vessels found throughout the tissue. HTRA1 was also identified in areas of macrophage infiltrate detected as crown-like structures in both IS (Fig. 7A) and IR (Fig. 7B) obese patients, although the level of staining at these sites was markedly enhanced in IR adipose tissue in accordance with increases in infiltrate. Furthermore, immune cell infiltrate expressing HTRA1 also showed positive staining for MMP-13 (Fig. 7C), thus re-enforcing the concept of there being a close working relationship between these two proteases. In all cases, specificity of immunostaining was confirmed using relevant IgG isotype controls (Fig. 7D-F).

DISCUSSION

In the current study, we have identified HTRA1 as a potent inducer of MAP kinase-dependent MMP production in adipogenic hMSC cultures, the result of which leads to

modulation of ECM components and impaired lipid droplet accrual in differentiating cells. Furthermore, the observation that HTRA1 is present at high levels in visceral adipose tissue at sites of increased inflammatory cell infiltration is suggestive of its active involvement in mediating adipose tissue function under pathological conditions.

HTRA1 is now well established as a key regulator of ECM turnover, having been linked to various diseases in which the breakdown of normal ECM is a prominent pathological feature [13-16, 18]. Findings from our own studies into the role of HTRA1 in joint and IVD degeneration have led to the suggestion that HTRA1 may instigate tissue breakdown through an upregulation in MMP production, most likely via the action of reactive Fnf species [18, 19]. In the context of adipose tissue, MMP-mediated ECM remodelling and reorganization forms an integral part of normal tissue homeostasis, being required for adipocyte differentiation and function [7, 8]. Abnormal fluctuations in MMP levels within adipose tissue may therefore represent an important factor in determining adipocyte health and subsequent risk of disease. This is supported by our current findings where increased production of MMPs by adipogenic hMSCs in response to HTRA1 led to a loss of vital ECM components and impaired lipid accrual. Such observations are therefore suggestive of HTRA1 as having a detrimental role in hMSC adipogenesis and that these effects are related to the actions of MMPs. However, in contrast to previous studies [18, 19], these effects do not appear to be reliant on the generation of Fnfs. In fact, we provide evidence to suggest that MMP-13 itself may be responsible for the appearance of such fragments in response to HTRA1. As such, alternative mechanisms must exist through which HTRA1 can instigate changes in hMSC MMP production and adipogenic potential.

Some insights into HTRA1's mode of action could be gleaned through manipulation of its trypsin-like serine protease domain and its protein-binding PDZ domain. Certainly, both domains were of critical importance in determining HTRA1's inhibitory influence over hMSC adipogenesis, being required for both efficient MMP production as well as for the observed decreases in type IV collagen, laminin and lipid uptake in adipogenic hMSCs. Of particular interest was the novel finding that HTRA1 could interact with surface bound HS in a PDZ-dependent manner. It is possible therefore that sequestration of HTRA1 to the cell surface by HS would allow for close interactions to form between HTRA1 and HS-containing glycoproteins. This concept is supported by the finding that increased levels of soluble syndecan-4 could be detected in adipogenic hMSC cultures treated with structurally intact HTRA1. Syndecans are important regulators of lipid uptake in differentiating adipocytes [6, 31] and their liberation from the cell surface by proteolytic cleavage may constitute a potential cause of diminished lipid accrual in adipogenic hMSCs following HTRA1 treatment. In addition to syndecans, numerous other glycoproteins also exist within the adipocyte ECM, including the previously identified HTRA1 substrate nidogen [13]. Nidogen represents an important stabilizing component of the adipocyte basal lamina through its binding to type IV collagen and laminin [32]. The possible targeting of nidogen by HTRA1 may therefore represent an alternative means through which the ECM could be affected by HTRA1, and adipogenesis inhibited. Interestingly, nidogen cleavage by HTRA1 also has the potential to generate various fragment species *in vitro*, although their influence on MMP production and adipogenesis remains to be determined.

HTRA1's ability to both induce MMP production and inhibit hMSC adipogenesis was additionally identified as being dependent on the activities of JNK, and to a lesser extent, ERK. Interpretation of the data concerning the involvement of p38 were hampered by the fact that inhibition of p38 activation resulted in a significant reduction in oil droplet formation in adipogenic hMSCs regardless of treatment conditions. The regulation of MMP expression by MAP kinases is well documented [reviewed in 33], and several studies have now identified ERK and JNK as potent negative regulators of MSC adipogenesis [34-36]. Despite having demonstrated the importance of MAP kinase activation in mediating the effects of HTRA1 during hMSC adipogenesis, we were unable to ascertain the cause for such signaling events. Certainly, both the proteolytic activity and PDZ domain of HTRA1 were essential requirements for efficient MAP kinase activation, thereby inferring substrate binding and degradation were necessary. One potential means by which HTRA1 could invoke MAP kinase activation in the context of the current study, is through syndecan-4 shedding, whereby disruption of the syndecan-4 to MAP kinase signaling cascade may have contributed to increases in JNK activity levels [37].

The relevance of such findings is made apparent by the fact that both MAP kinases and MMPs are centrally linked to the pathophysiology of adipose tissue, being implicated in the development of insulin resistance in obese mice and humans [28, 38, 39]. Adipocyte dysfunction clearly plays a major role in determining the severity of insulin resistance among obese patients and as such, factors which negatively influence adipocyte development are likely to contribute to and potentially exacerbate the disease state [9]. In this regard, inappropriately high levels of HTRA1 in the adipose tissue of obese individuals may be viewed as being potentially harmful and an indication of deficiencies in

adipocyte development and function. The significance of this is made evident by the fact that HTRA1 could be detected in the visceral fat from obese patients, and that levels were greatest at sites where cellular infiltration was most apparent, encompassing adipocytes in typical crown like structures. This, together with the fact that MMP-13 was also localized to these same regions, lends further support to the concept of HTRA1 representing a novel mediator of adipogenesis and fat turnover. Furthermore, based on the fact that macrophages are considered to represent the predominant cell type within crown-like structures [11, 40], and are potent inducers of MMPs in adipocytes [41], these findings may also offer a potential source from which HTRA1 may be introduced into adipose tissue.

CONCLUSIONS

In conclusion, our findings identify HTRA1 as a negative regulator of hMSC adipogenesis, which may be of relevance when considering its potential role in the underlying processes governing adipose tissue and adipocyte dysregulation. Moreover, the differential effects imparted by HTRA1 on hMSC adipogenic and osteogenic differentiation may also offer novel insights into its potential impact on other pathological conditions such as age-related bone loss, where its capacity to inhibit adipogenesis and stimulate osteogenesis would be deemed beneficial to the preservation of bone quality [42].

ACKNOWLEDGEMENTS

SG and GB were supported by SNSF grants 31003A_134935 and 31003A_156313. AM and NAT were supported by the Uniscientia Foundation. The authors would like to express their gratitude to Daniela Kern for preparing the patient tissue sections.

DISCLOSURE OF POTENTIAL CONFLICTS OF INTEREST

The authors indicate no potential conflicts of interest.

REFERENCES

1. Rosen ED, MacDougald OA.Adipocyte differentiation from the inside out. Nat Rev Mol Cell Biol 2006;7:885–896.
2. Christodoulides C, Lagathu C, Sethi JK et al. Adipogenesis and WNT signalling. Trends Endocrinol Metab 2009;20:16-24.
3. Mariman EC, Wang P. Adipocyte extracellular matrix composition, dynamics and role in obesity. Cell Mol Life Sci 2010;67:1277-92.
4. Sillat T, Saat R, Pöllänen R et al. Basement membrane collagen type IV expression by human mesenchymal stem cells during adipogenic differentiation. J Cell Mol Med 2012;16:1485-95.
5. Noro A, Sillat T, Virtanen I et al. Laminin production and basement membrane deposition by mesenchymal stem cells upon adipogenic differentiation. J Histochem Cytochem 2013;61:719-30.
6. Wilsie LC, Chanchani S, Navaratna D et al. Cell surface heparan sulfate proteoglycans contribute to intracellular lipid accumulation in adipocytes. Lipids Health Dis 2005;4:2.

7. Maquoi E, Munaut C, Colige A et al. Modulation of adipose tissue expression of murine matrix metalloproteinases and their tissue inhibitors with obesity. Diabetes 2002;51:1093-101.
8. Chavey C, Mari B, Monthouel MN et al. Matrix metalloproteinases are differentially expressed in adipose tissue during obesity and modulate adipocyte differentiation. J Biol Chem 2003;278:11888-96.
9. Guilherme A, Virbasius JV, Puri V et al. Adipocyte dysfunctions linking obesity to insulin resistance and type 2 diabetes. Nat Rev Mol Cell Biol 2008;9:367-77.
10. Lee MJ, Wu Y, Fried SK. Adipose tissue remodeling in pathophysiology of obesity. Curr Opin Clin Nutr Metab Care 2010;13:371-6.
11. Cinti S, Mitchell G, Barbatelli G et al. Adipocyte death defines macrophage localization and function in adipose tissue of obese mice and humans. J Lipid Res 2005;46:2347-55.
12. Tiaden AN, Breiden M, Mirsaidi A et al. Human serine protease HTRA1 positively regulates osteogenesis of human bone marrow-derived mesenchymal stem cells and mineralization of differentiating bone-forming cells through the modulation of extracellular matrix protein. Stem Cells 2013;30:2271-2282.
13. Vierkotten S, Muether PS, Fauser S. Overexpression of HTRA1 leads to ultrastructural changes in the elastic layer of Bruch's membrane via cleavage of extracellular matrix components. PLoS One 2011;6:e22959.
14. Tiaden AN, Richards PJ. The emerging roles of HTRA1 in musculoskeletal disease. Am J Pathol 2013;182:1482–1488.

15. Beaufort N, Scharrer E, Kremmer E et al. Cerebral small vessel disease-related protease HtrA1 processes latent TGF-β binding protein 1 and facilitates TGF-β signaling. Proc Natl Acad Sci U S A 2014;111:16496-501.

16. Grau S, Baldi A, Bussani R et al. Implications of the serine protease HtrA1 in amyloid precursor protein processing. Proc Natl Acad Sci U S A 2005;102:6021-6.

17. Dominici M, Le Blanc K, Mueller I, et al. Minimal criteria for defining multipotent mesenchymal stromal cells. The International Society for Cellular Therapy position statement. Cytotherapy 2006;8:315-7.

18. Tiaden AN, Klawitter M, Lux V et al. Detrimental role for human high temperature requirement serine protease A1 (HTRA1) in the pathogenesis of intervertebral disc (IVD) degeneration. J Biol Chem 2012;287:21335-45.

19. Grau S, Richards PJ, Kerr B et al. The role of human HtrA1 in arthritic disease. J Biol Chem 2006;281:6124-9.

20. Burgess A, Vigneron S, Brioudes E et al. A Loss of human Greatwall results in G2 arrest and multiple mitotic defects due to deregulation of the cyclin B-Cdc2/PP2A balance. Proc Natl Acad Sci U S A 2010;107:12564-9.

21. Klöting N, Fasshauer M, Dietrich A et al. Insulin-sensitive obesity. Am J Physiol Endocrinol Metab 2010;299:E506-15.

22. Eigenbrot C, Ultsch M, Lipari MT et al. Structural and functional analysis of HtrA1 and its subdomains. Structure 2012;20:1040-50.

23. Hou S, Maccarana M, Min TH et al.The secreted serine protease xHtrA1 stimulates long-range FGF signaling in the early Xenopus embryo. Dev Cell 2007;13:226-41.

24. Manon-Jensen T, Multhaupt HA, Couchman JR. Mapping of matrix metalloproteinase cleavage sites on syndecan-1 and syndecan-4 ectodomains. FEBS J 2013;280:2320-31.

25. Shih CL, Ajuwon KM. Inhibition of MMP-13 prevents diet-induced obesity in mice and suppresses adipogenesis in 3T3-L1 preadipocytes. Mol Biol Rep 2015;42:1225-32.

26. Kim EM, Shin EJ, Choi JH et al. Matrix metalloproteinase-3 is increased and participates in neuronal apoptotic signaling downstream of caspase-12 during endoplasmic reticulum stress. J Biol Chem 2010;285:16444-52.

27. Rath T, Stöckle J, Roderfeld M et al. Matrix metalloproteinase-13 is regulated by toll-like receptor-9 in colorectal cancer cells and mediates cellular migration. Oncol Lett 2011:2:483-488.

28. Bost F, Aouadi M, Caron L et al. The role of MAPKs in adipocyte differentiation and obesity. Biochimie 2005;87:51-6.

29. Ando C, Takahashi N, Hirai S et al. Luteolin, a food-derived flavonoid, suppresses adipocyte-dependent activation of macrophages by inhibiting JNK activation. FEBS Lett 2009:583:3649-54.

30. Vallet S, Mukherjee S, Vaghela N et al. Activin A promotes multiple myeloma-induced osteolysis and is a promising target for myeloma bone disease. Proc Natl Acad Sci U S A 2010;107:5124-9.

31. Kasza I, Suh Y, Wollny D et al. Syndecan-1 is required to maintain intradermal fat and prevent cold stress. PLoS Genet 2014;10:e1004514.

32. Yurchenco PD. Basement membranes: cell scaffoldings and signaling platforms. Cold Spring Harb Perspect Biol 2011;3:a004911.

33. Reuben PM, Cheung HS. Regulation of matrix metalloproteinase (MMP) gene expression by protein kinases. Front Biosci 2006;11:1199-215.

34. Tominaga S, Yamaguchi T, Takahashi S et al. Negative regulation of adipogenesis from human mesenchymal stem cells by Jun N-terminal kinase. Biochem Biophys Res Commun 2005;326:499-504.

35. Chiu LH, Yeh TS, Huang HM et al. Diverse effects of type II collagen on osteogenic and adipogenic differentiation of mesenchymal stem cells. J Cell Physiol 2012;227:2412-20.

36. Fu L, Tang T, Miao Y et al. Stimulation of osteogenic differentiation and inhibition of adipogenic differentiation in bone marrow stromal cells by alendronate via ERK and JNK activation. Bone 2008;43:40-7.

37. Saoncella S, Calautti E, Neveu W et al. Syndecan-4 regulates ATF-2 transcriptional activity in a Rac1-dependent manner. J Biol Chem 2004;279:47172-6.

38. Unoki H, Bujo H, Shibasaki M et al. Increased matrix metalloproteinase-3 mRNA expression in visceral fat in mice implanted with cultured preadipocytes. Biochem Biophys Res Commun 2006;350:392-8.

39. Meissburger B, Ukropec J, Roeder E et al. Adipogenesis and insulin sensitivity in obesity are regulated by retinoid-related orphan receptor gamma. EMBO Mol Med 2011;3:637-51.

40. Murano I, Barbatelli G, Parisani V et al. Dead adipocytes, detected as crown-like structures, are prevalent in visceral fat depots of genetically obese mice. J Lipid Res 2008;49:1562-8.

41. Gao D, Bing C. Macrophage-induced expression and release of matrix metalloproteinase 1 and 3 by human preadipocytes is mediated by IL-1β via activation of MAPK signaling. J Cell Physiol 2011;226:2869-80.

42. Rosen CJ, Bouxsein ML. Mechanisms of disease: is osteoporosis the obesity of bone? Nat Clin Pract Rheumatol 2006;2:35-43.

Figure 1. HTRA1 suppresses lipid uptake and droplet formation in adipogenic hMSCs. **(A):** ELISA measurement of HTRA1 secretion in supernatants from undifferentiated (control) and differentiated (adipogenic) hMSCs. *$p < 0.001$ as compared to adipogenic hMSCs. **(B):** Quantification of Oil Red O staining in adipogenic hMSCs treated with scrambled siRNA (scr) or siRNAs specific for HTRA1 (H1 and H2) at day 14 post induction. Scale bar = 1 mm. **(C):** Quantification of Oil Red O staining in hMSCs treated with siRNA specific for HTRA1 (H2), HTRA1 (45 nM) or a combination of both H2 and HTRA1. *$p < 0.01$ as compared to siRNA (scr) treated cells. **(D):** Quantification of Oil Red O staining in hMSCs at day 14 post adipogenic induction cultured in the absence (untreated) or presence of recombinant HTRA1 (45 nM). *$p < 0.001$ as compared to untreated. Scale bar = 1 mm. Data are representative of at least 2 separate experiments performed in triplicate. Abbreviations: hMSC, human mesenchymal stem cells; ELISA, enzyme-linked immunosorbent assay; HTRA1, high temperature requirement protease A1; siRNA, small interfering RNA.

Figure 2. HTRA1 interacts with surface bound HSPG. **(A-F):** hMSC binding of PDZ domain-containing HTRA1 S328A (0.45 μM) **(A)** or HTRA1Δprotease (0.45 μM) **(B)** as compared to HTRA1ΔPDZ (0.45 μM) was determined by FACS analysis using a FITC labeled anti-histidine antibody. The involvement of HSPG in the binding of HTRA1 S328A **(C, E)** and HTRA1Δprotease **(D, F)** was assessed using either heparanase (10 U/ml) **(C, D)** or heparin (10 μg/ml) **(E, F)**. **(G):** ELISA measurement of soluble syndecan-4 levels in the supernatants of untreated or HTRA1 (45 nM) treated hMSCs at day 10 and 21 post adipogenic induction. **(H):** Quantification of VLDL-DiI (red) uptake in untreated

or HTRA1 (45 nM) treated hMSCs at day 24 post adipogenic induction. Nuclei were stained with DAPI (blue). Scale bar = 75 μm. *$p < 0.001$ as compared to untreated hMSCs. Data are representative of at least 2 separate experiments performed in triplicate. Abbreviations: hMSC, human mesenchymal stem cells; HTRA1, high temperature requirement protease A1; HSPG, heparan sulfate proteoglycan; ELISA, enzyme-linked immunosorbent assay; FITC, Fluorescein isothiocyanate; VLDL-DiI, very low density lipoprotein- dialkylcarbocyanine.

Figure 3. HTRA1 upregulates MMP production by adipogenic hMSCs. RT-qPCR analysis of *MMP1* **(A)**, *MMP3* **(B)**, *MMP9* **(C)** and *MMP13* **(D)** gene expression in untreated or HTRA1 (45 nM) treated hMSCs at day 21 post adipogenic induction. Data was normalized to *GUSB* and expressed as fold change as compared to untreated hMSCs (value = 1) using the comparative C_T method. **(E, F):** ELISA measurements of MMP-3 **(E)** and -13 **(F)** protein in supernatants from untreated or HTRA1 (45 nM) treated hMSCs at day 21 post adipogenic induction. *$p < 0.05$, **$p < 0.001$ as compared to untreated hMSCs. Data are representative of at least 2 separate experiments performed in triplicate. Abbreviations: hMSC, human mesenchymal stem cells; HTRA1, high temperature requirement protease A1; MMP, matrix metalloproteinase; RT-qPCR, reverse transcription-quantitative polymerase chain reaction; ELISA, enzyme-linked immunosorbent assay.

Figure 4. (A, B): Immunofluorescence staining of laminin (red) **(A)** and type IV collagen (red) **(B)** in untreated or HTRA1 (45 nM) treated hMSCs at day 24 post adipogenic induction. Nuclei were stained with DAPI (blue). Scale bar = 100 μm. *$p < 0.01$ as

compared to untreated hMSCs. Data is representative of at least 2 separate experiments performed in triplicate. Abbreviations: hMSC, human mesenchymal stem cells; HTRA1, high temperature requirement protease A1.

Figure 5. HTRA1's effects are mediated through MMP activities. **(A, B):** Quantification of type IV collagen staining in untreated or HTRA1 (45 nM) treated hMSCs at day 22 post adipogenic induction following pre-treatment with either vehicle control or with 10 μM of NNGH **(A)** or 20 μM of CL-82198 **(B)**. **(C, D):** ELISA measurement of soluble syndecan-4 levels in the supernatants of untreated or HTRA1 (45 nM) treated hMSCs at day 17 post adipogenic induction following pre-treatment with either vehicle control or with varying concentrations of NNGH **(C)** or CL-82198 **(D)**. **(E, F)**: Quantification of Oil Red O staining in untreated or HTRA1 (45 nM) treated hMSCs at day 18 post adipogenic induction following pre-treatment with either vehicle control or with varying concentrations of NNGH **(E)** or CL-82198 **(F)**. $*p < 0.05$, $**p < 0.01$, $***p < 0.001$ as compared to controls from untreated or HTRA1-treated groups respectively. Data are representative of at least 2 separate experiments performed in triplicate. Abbreviations: hMSC, human mesenchymal stem cells; HTRA1, high temperature requirement protease A1; MMP, matrix metalloproteinase; ELISA, enzyme-linked immunosorbent assay.

Figure 6. HTRA1's effects are mediated through MAP kinase activities. **(A):** Effect of recombinant HTRA1 on MAP kinase activation in adipogenic hMSCs at day 14 as determined by Western blot analysis of protein lysates using specific antibodies against JNK, p38 and ERK. An anti-tubulin monoclonal was used to confirm equal loading. **(B-**

D): Quantitative analysis of *MMP3* expression **(B)**, *MMP13* expression **(C)** and Oil Red O staining **(D)** in untreated or HTRA1 (45 nM) treated hMSCs at day 17 post adipogenic induction following pre-treatment with either vehicle control or with PD98059 (10 μM), SP600125 (20 μM) or SB239063 (10 μM). RT-qPCR data was normalized to *GUSB* and expressed as fold change relative to untreated, control hMSCs (value = 1) using the comparative C_T method. *$p < 0.05$, **$p < 0.01$, ***$p < 0.001$ as compared to controls from untreated or HTRA1-treated groups respectively. Data are representative of at least 2 separate experiments performed in triplicate. Abbreviations: hMSC, human mesenchymal stem cells; HTRA1, high temperature requirement protease A1; MMP, matrix metalloproteinase; MAP, mitogen-activated protein; RT-qPCR, reverse transcription-quantitative polymerase chain reaction; GUSB, Glucuronidase, beta.

Figure 7. Identification of HTRA1 in adipose tissue. Paraffin wax sections of human visceral (omental) adipose tissue from insulin sensitive (IS) or insulin resistant (IR) obese patients were incubated with an anti-HTRA1 antibody **(A, B)**, anti-MMP-13 antibody **(C)** or relevant IgG controls **(D-F)**, and positive staining identified using an appropriate HRP-labeled polyclonal antibody with subsequent development using 3,3'-diaminobenzidine (brown). *Arrow heads*, HTRA1 or MMP-13 present in immune cell infiltrate in crown-like structures. Scale bar = 200 μm. Abbreviations: HTRA1, high temperature requirement protease A1; MMP, matrix metalloproteinase; HRP, horseradish peroxidase.

Supplementary Fig. 1. (A): ELISA measurement of HTRA1 in supernatants from adipogenic hMSCs (Adipo) treated with scrambled siRNA (scr) or siRNA specific for

HTRA1 (H1 and H2). *$p < 0.001$ as compared to siRNA (scr) treated cells. **(B):** Schematic of recombinant human HTRA1 proteins; active HTRA1 (ΔMac), inactive HTRA1 (HTRA1 S328A), active HTRA1 without PDZ domain (HTRA1ΔPDZ), inactive HTRA1 without PDZ domain (HTRA1 S328AΔPDZ), HTRA1 without protease domain (HTRA1ΔProtease). The purified recombinant histidine-labeled human HTRA1 proteins were also visualized on a Coomassie blue-stained SDS-PAGE gel. *M*, protein marker; *lane 1*, HTRA1; *lane 2*, HTRA1 S328A; *lane 3*, HTRA1ΔPDZ; *lane 4*, HTRA1 S328AΔPDZ; *lane 5*, HTRA1ΔProtease. **(C):** Proteolytic activity of recombinant HTRA1 proteins (45 nM) towards BODIPY-FL-labeled DQ elastin (25 μg/ml) at 37°C as determined using a Multiplate reader. Abbreviations: hMSC, human mesenchymal stem cells; HTRA1, high temperature requirement protease A1; ELISA, enzyme-linked immunosorbent assay; siRNA, small interfering RNA; SDS-PAGE, sodium dodecyl sulfate polyacrylamide gel electrophoresis.

Supplementary Fig. 2. Fluorescence activated cell sorting (FACS) analysis of recombinant HTRA1 binding to non-differentiated hMSCs. HTRA1Δprotease (0.45 μM) was incubated with hMSCs for 1 h at 4°C and cell-bound HTRA1 protein detected using a FITC labeled anti-his antibody. The influence of pre-incubating cells with collagenase (1 mg/ml) **(A)**, chondroitinase (10 U/ml) **(B)**, CS1 (50 μM) (**C**) or GRGDSP (50 μM) **(D)** on the percentage of cell-bound HTRA1Δprotease was calculated using FlowJo 10 software. Data are representative of least two individual experiments performed in duplicate. Abbreviations: hMSC, human mesenchymal stem cells; HTRA1, high temperature requirement protease A1; FACS, fluorescence activated cells sorting.

Supplementary Fig. 3. Capacity for HTRA1 to degrade type IV collagen. Varying concentrations of HTRA1 or HTRA1 S328A were incubated with DQ-type IV collagen (25 μg/ml) at 37°C and the relative fluorescence units (RFU) generated after 24 h determined using a Multiplate reader. Abbreviations: HTRA1, high temperature requirement protease A1.

Supplementary Fig. 4. (A): Western blot analysis of native Fnfs in concentrated supernatants harvested from 14 day old undifferentiated hMSCs (control), untreated adipogenic hMSCs, or adipogenic hMSCs treated with HTRA1 (45 nM) for a further 24 h. Protein was subjected to immunoblotting using antibody Mab 1936 specific for the fibronectin amino-terminal fibrin- and heparin-binding domain. *Arrow head* indicates the HTRA1-cleaved 29 kDa Fnf. **(B):** An equimolar ratio of human plasma-derived Fn and HTRA1 were incubated in TBS, pH 8.5, for 16 h at 37°C and Fnfs purified by affinity chromatography and analysed on a Coomassie Blue stained 4-15% gradient SDS-PAGE gel. Fn and HTRA1 alone were also loaded and served as controls. *Arrow head* indicates the purified 29 kDa Fnf due to HTRA1-mediated cleavage. **(C-E):** RT-qPCR analysis of *MMP1* **(C)**, *MMP3* **(D)** and *MMP13* **(E)** in adipogenic hMSCs at day 11 following treatment with HTRA1 (45 nM), purified HTRA1-digested Fn (40 μg/ml) (Fn+HTRA1) or TBS, pH 7.6, eluate from the affinity purification reaction using HTRA1 alone (TBS+HTRA1). Data was normalized to *GUSB* and expressed as fold change as compared to untreated hMSCs (value = 1) using the comparative C_T method. **(F):** Oil Red O staining of adipogenic hMSCs at day 14 following treatment with HTRA1 (45 nM), Fn+HTRA1 or

TBS+HTRA1. *$p < 0.05$, **$p < 0.01$, ***$p < 0.001$ as compared to untreated cells. Scale bar = 2 mm. Data are representative of least two individual experiments performed in triplicate. Abbreviations: hMSC, human mesenchymal stem cells; HTRA1, high temperature requirement protease A1; Fnf, fibronectin fragments; SDS-PAGE, sodium dodecyl sulfate polyacrylamide gel electrophoresis; RT-qPCR, reverse transcription-quantitative polymerase chain reaction; GUSB, Glucuronidase, beta; MMP, matrix metalloproteinase; TBS, Tris-buffered saline.

Supplementary Fig. 5. (A): RT-qPCR analysis of *MMP13* gene expression in untreated or HTRA1 (45 nM) treated adipogenic hMSCs at day 3 following pre-treatment with scrambled control siRNA (scr) or siRNAs specific for *MMP13* (M1 and M2). Data was normalized to *GUSB* and expressed as fold change relative to untreated siRNA (scr) hMSCs (value = 1) using the comparative C_T method. **(B):** Quantification of Oil Red O staining in adipogenic hMSCs at day 22 following treatment with either a scrambled control siRNA (scr), siRNAs specific for *MMP13* (M1 and M2), or a combination of both siRNAs and HTRA1 (45 nM). *$p < 0.05$, **$p < 0.01$, ***$p < 0.001$ as compared to siRNA (scr) controls from untreated or HTRA1 -treated groups respectively. Data are representative of least two individual experiments performed in triplicate. **(C):** Western blot analysis of native Fnfs in concentrated supernatants harvested from 14-day-old adipogenic hMSCs treated for 24 h without (untreated) or with CL-82198 (20 μM), HTRA1 (45 nM) or HTRA1 and CL-82198. Protein was subjected to immunoblotting using Mab 1936 specific for the Fn amino-terminal fibrin- and heparin-binding domain. *Arrow heads* indicate the 29 kDa Fnf due to HTRA1 treatment. **(D):** Coomassie stained gel

of total protein from supernatant to control for equal loading. Data are representative of least two individual experiments. Abbreviations: hMSC, human mesenchymal stem cells; HTRA1, high temperature requirement protease A1; RT-qPCR, reverse transcription-quantitative polymerase chain reaction; GUSB, Glucuronidase, beta; MMP, matrix metalloproteinase; siRNA, small interfering RNA; Fnf, fibronectin fragments.

Supplementary Fig. 6. Identification of HTRA1 in adipose tissue. Paraffin wax sections of human visceral (omental) adipose tissue from IS or IR obese patients were incubated with an anti-HTRA1 antibody **(A, B)** or relevant IgG controls **(C, D)**, and positive staining identified using an appropriate HRP-labeled polyclonal antibody with subsequent development using 3,3'-diaminobenzidine (*brown*). *Asterisks*, HTRA1-positive blood vessels; Scale bar = 200 μm. Insulin sensitivity was defined as glucose infusion rate (GIR) during the steady state of an euglycemic-hyperinsulinemic clamp > 70 μmol/kg/min, insulin resistance as GIR < 50 μmol/kg/min. Abbreviations: HTRA1, high temperature requirement protease A1; IS, insulin sensitive; IR, insulin resistant; HRP, horseradish peroxidase.

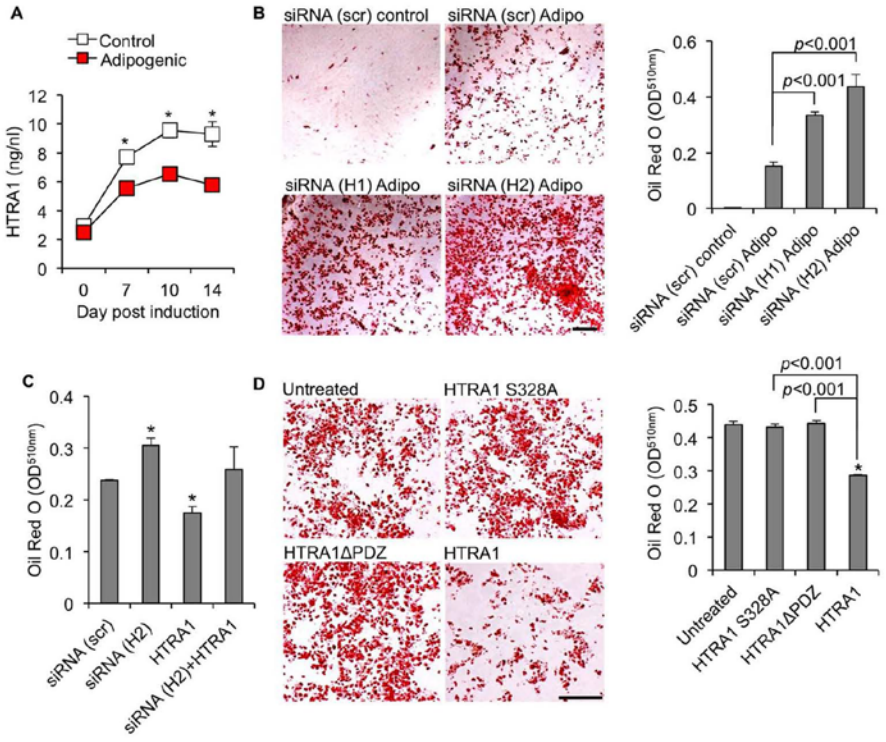

Figure 1. HTRA1 suppresses lipid uptake and droplet formation in adipogenic hMSCs. **(A):** ELISA measurement of HTRA1 secretion in supernatants from undifferentiated (control) and differentiated (adipogenic) hMSCs. *$p < 0.001$ as compared to adipogenic hMSCs. **(B):** Quantification of Oil Red O staining in adipogenic hMSCs treated with scrambled siRNA (scr) or siRNAs specific for HTRA1 (H1 and H2) at day 14 post induction. Scale bar = 1 mm. **(C):** Quantification of Oil Red O staining in hMSCs treated with siRNA specific for HTRA1 (H2), HTRA1 (45 nM) or a combination of both H2 and HTRA1. *$p < 0.01$ as compared to siRNA (scr) treated cells. **(D):** Quantification of Oil Red O staining in hMSCs at day 14 post adipogenic induction cultured in the absence (untreated) or presence of recombinant HTRA1 (45 nM). *$p < 0.001$ as compared to untreated. Scale bar = 1 mm. Data are representative of at least 2 separate experiments performed in triplicate. Abbreviations: hMSC, human mesenchymal stem cells; ELISA, enzyme-linked immunosorbent assay; HTRA1, high temperature requirement protease A1; siRNA, small interfering RNA.
68x57mm (600 x 600 DPI)

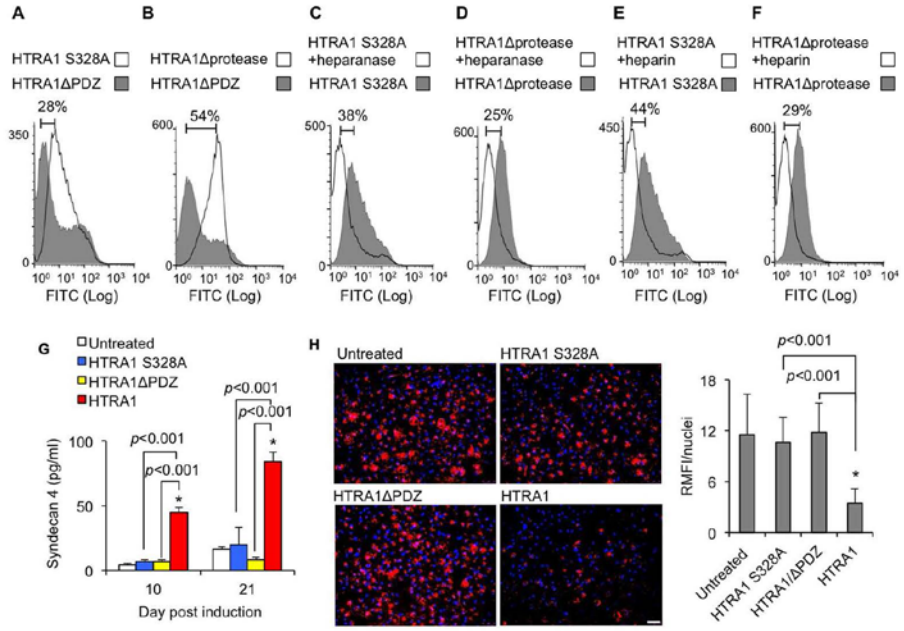

Figure 2. HTRA1 interacts with surface bound HSPG. **(A-F):** hMSC binding of PDZ domain-containing HTRA1 S328A (0.45 µM) **(A)** or HTRA1Δprotease (0.45 µM) **(B)** as compared to HTRA1ΔPDZ (0.45 µM) was determined by FACS analysis using a FITC labeled anti-histidine antibody. The involvement of HSPG in the binding of HTRA1 S328A **(C, E)** and HTRA1Δprotease **(D, F)** was assessed using either heparanase (10 U/ml) **(C, D)** or heparin (10 µg/ml) **(E, F)**. **(G):** ELISA measurement of soluble syndecan-4 levels in the supernatants of untreated or HTRA1 (45 nM) treated hMSCs at day 10 and 21 post adipogenic induction. **(H):** Quantification of VLDL-DiI (red) uptake in untreated or HTRA1 (45 nM) treated hMSCs at day 24 post adipogenic induction. Nuclei were stained with DAPI (blue). Scale bar = 75 µm. *p < 0.001 as compared to untreated hMSCs. Data are representative of at least 2 separate experiments performed in triplicate. Abbreviations: hMSC, human mesenchymal stem cells; HTRA1, high temperature requirement protease A1; HSPG, heparan sulfate proteoglycan; ELISA, enzyme-linked immunosorbent assay; FITC, Fluorescein isothiocyanate; VLDL-DiI, very low density lipoprotein- dialkylcarbocyanine.
85x64mm (600 x 600 DPI)

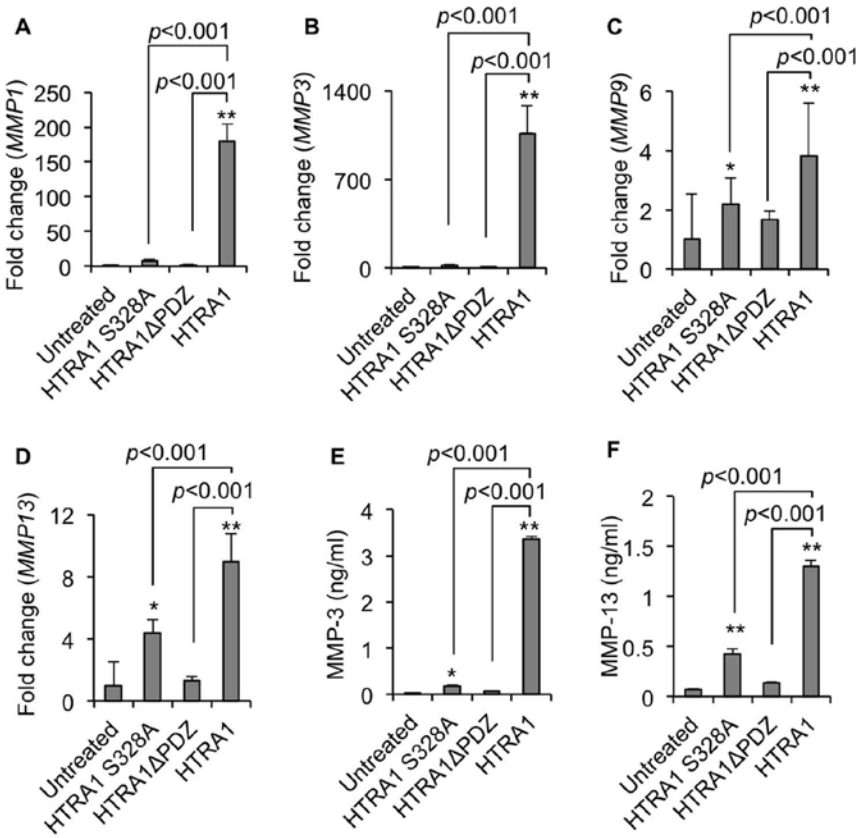

Figure 3. HTRA1 upregulates MMP production by adipogenic hMSCs. RT-qPCR analysis of *MMP1* **(A)**, *MMP3* **(B)**, *MMP9* **(C)** and *MMP13* **(D)** gene expression in untreated or HTRA1 (45 nM) treated hMSCs at day 21 post adipogenic induction. Data was normalized to *GUSB* and expressed as fold change as compared to untreated hMSCs (value = 1) using the comparative CT method. **(E, F):** ELISA measurements of MMP-3 **(E)** and -13 **(F)** protein in supernatants from untreated or HTRA1 (45 nM) treated hMSCs at day 21 post adipogenic induction. *$p < 0.05$, **$p < 0.001$ as compared to untreated hMSCs. Data are representative of at least 2 separate experiments performed in triplicate. Abbreviations: hMSC, human mesenchymal stem cells; HTRA1, high temperature requirement protease A1; MMP, matrix metalloproteinase; RT-qPCR, reverse transcription-quantitative polymerase chain reaction; ELISA, enzyme-linked immunosorbent assay.
80x78mm (600 x 600 DPI)

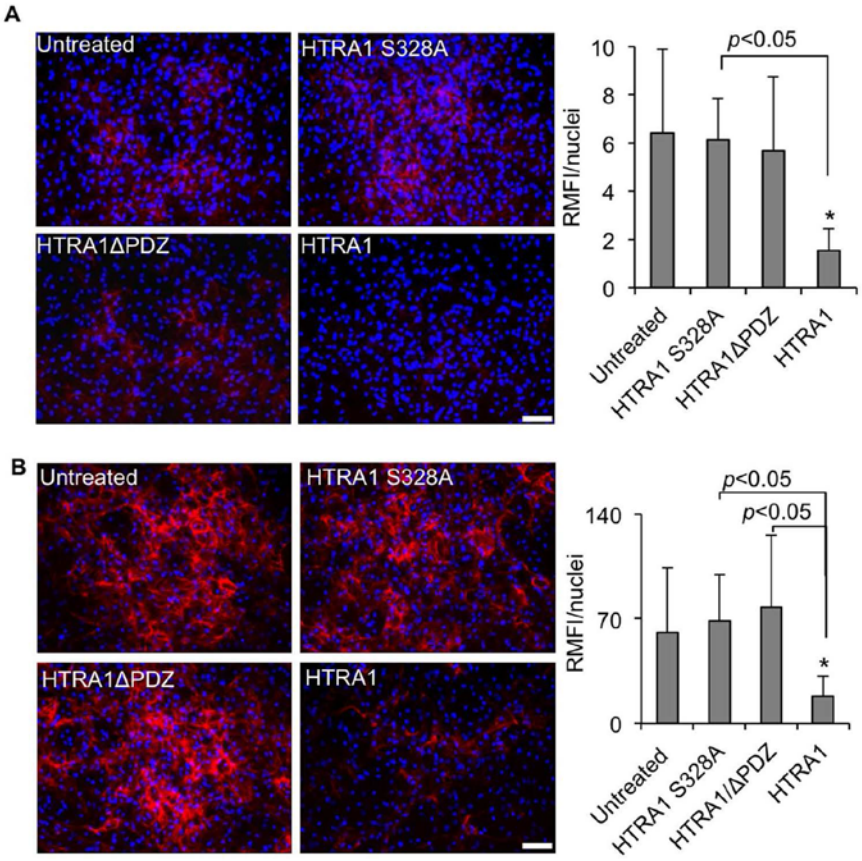

Figure 4. (A, B): Immunofluorescence staining of laminin (red) **(A)** and type IV collagen (red) **(B)** in untreated or HTRA1 (45 nM) treated hMSCs at day 24 post adipogenic induction. Nuclei were stained with DAPI (blue). Scale bar = 100 µm. *p < 0.01 as compared to untreated hMSCs. Data is representative of at least 2 separate experiments performed in triplicate. Abbreviations: hMSC, human mesenchymal stem cells; HTRA1, high temperature requirement protease A1.
81x81mm (600 x 600 DPI)

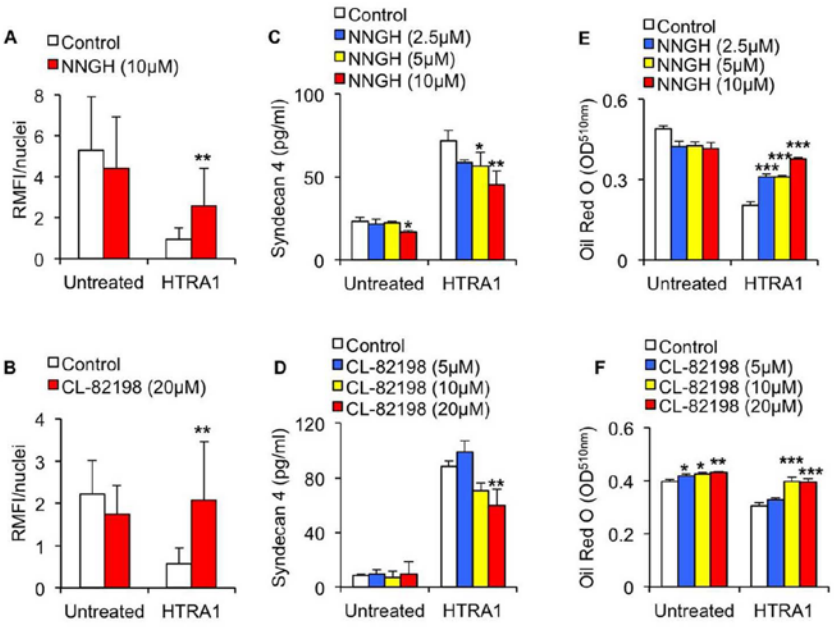

Figure 5. HTRA1's effects are mediated through MMP activities. **(A, B):** Quantification of type IV collagen staining in untreated or HTRA1 (45 nM) treated hMSCs at day 22 post adipogenic induction following pre-treatment with either vehicle control or with 10 μM of NNGH **(A)** or 20 μM of CL-82198 **(B)**. **(C, D):** ELISA measurement of soluble syndecan-4 levels in the supernatants of untreated or HTRA1 (45 nM) treated hMSCs at day 17 post adipogenic induction following pre-treatment with either vehicle control or with varying concentrations of NNGH **(C)** or CL-82198 **(D)**. **(E, F):** Quantification of Oil Red O staining in untreated or HTRA1 (45 nM) treated hMSCs at day 18 post adipogenic induction following pre-treatment with either vehicle control or with varying concentrations of NNGH **(E)** or CL-82198 **(F)**. $*p < 0.05$, $**p < 0.01$, $***p < 0.001$ as compared to controls from untreated or HTRA1-treated groups respectively. Data are representative of at least 2 separate experiments performed in triplicate. Abbreviations: hMSC, human mesenchymal stem cells; HTRA1, high temperature requirement protease A1; MMP, matrix metalloproteinase; ELISA, enzyme-linked immunosorbent assay.
65x51mm (600 x 600 DPI)

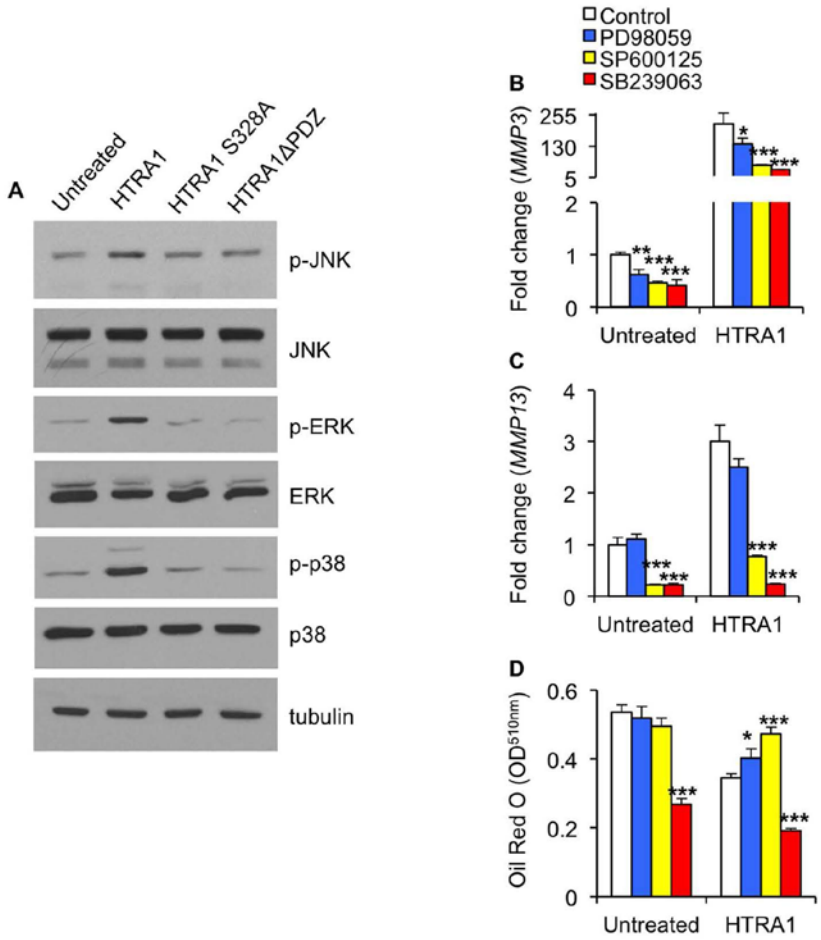

Figure 6. HTRA1's effects are mediated through MAP kinase activities. **(A):** Effect of recombinant HTRA1 on MAP kinase activation in adipogenic hMSCs at day 14 as determined by Western blot analysis of protein lysates using specific antibodies against JNK, p38 and ERK. An anti-tubulin monoclonal was used to confirm equal loading. **(B-D):** Quantitative analysis of *MMP3* expression **(B)** *MMP13* expression **(C)** and Oil Red O staining **(D)** in untreated or HTRA1 (45 nM) treated hMSCs at day 17 post adipogenic induction following pre-treatment with either vehicle control or with PD98059 (10 μM), SP600125 (20 μM) or SB239063 (10 μM). RT-qPCR data was normalized to *GUSB* and expressed as fold change relative to untreated, control hMSCs (value = 1) using the comparative CT method. *$p < 0.05$, **$p < 0.01$, ***$p < 0.001$ as compared to controls from untreated or HTRA1-treated groups respectively. Data are representative of at least 2 separate experiments performed in triplicate. Abbreviations: hMSC, human mesenchymal stem cells; HTRA1, high temperature requirement protease A1; MMP, matrix metalloproteinase; MAP, mitogen-activated protein; RT-qPCR, reverse transcription-quantitative polymerase chain reaction; GUSB, Glucuronidase, beta.
90x97mm (600 x 600 DPI)

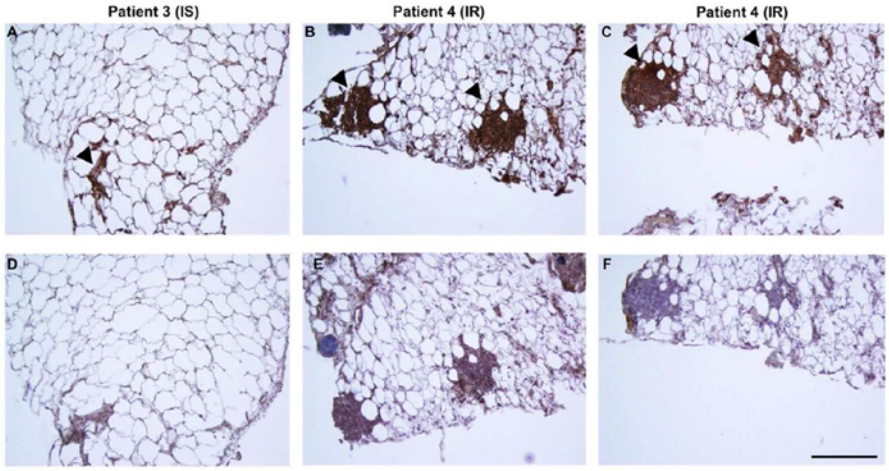

Figure 7. Identification of HTRA1 in adipose tissue. Paraffin wax sections of human visceral (omental) adipose tissue from insulin sensitive (IS) or insulin resistant (IR) obese patients were incubated with an anti-HTRA1 antibody **(A, B)**, anti-MMP-13 antibody **(C)** or relevant IgG controls **(D-F)**, and positive staining identified using an appropriate HRP-labeled polyclonal antibody with subsequent development using 3,3'-diaminobenzidine (*brown*). *Arrow heads*, HTRA1 or MMP-13 present in immune cell infiltrate in crown-like structures. Scale bar = 200 µm. Abbreviations: HTRA1, high temperature requirement protease A1; MMP, matrix metalloproteinase; HRP, horseradish peroxidase.
43x23mm (600 x 600 DPI)

Supplemental Table S1. List of Gene Expression Assays used in RT-qPCR analysis.

Gene	Protein Product	Assay ID [a]
HTRA1	High-Temperature Requirement Protease A1	Hs01016151_m1
MMP1	Matrix metalloproteinase 1 / Interstitial Collagenase	Hs00899658_m1
MMP3	Matrix metalloproteinase 3 / Stromelysin-1	Hs00968305_m1
MMP9	Matrix metalloproteinase 9 / gelatinase B	Hs00234579_m1
MMP13	Matrix metalloproteinase 13 / Collagenase-3	Hs00233992_m1
GUSB	Glucuronidase, beta	Hs99999908_m1

[a] TaqMan Expression Assay identity code according to supplier (Life Technologies, Zug, Switzerland).

Supplemental Table S2. Human patient information.

Patient	Sex	Age (yrs)	BMI (kg/m^3)	Insulin sensitivity group [a]
1	F	43	40.4	Insulin sensitive
2	F	42	49.1	Insulin resistant
3	M	43	50.7	Insulin sensitive
4	F	56	30.9	Insulin resistant

[a] Defined by the glucose infusion rate (GIR) during the steady state of an euglycemic hyperinsulinemic clamp as previously described [21].

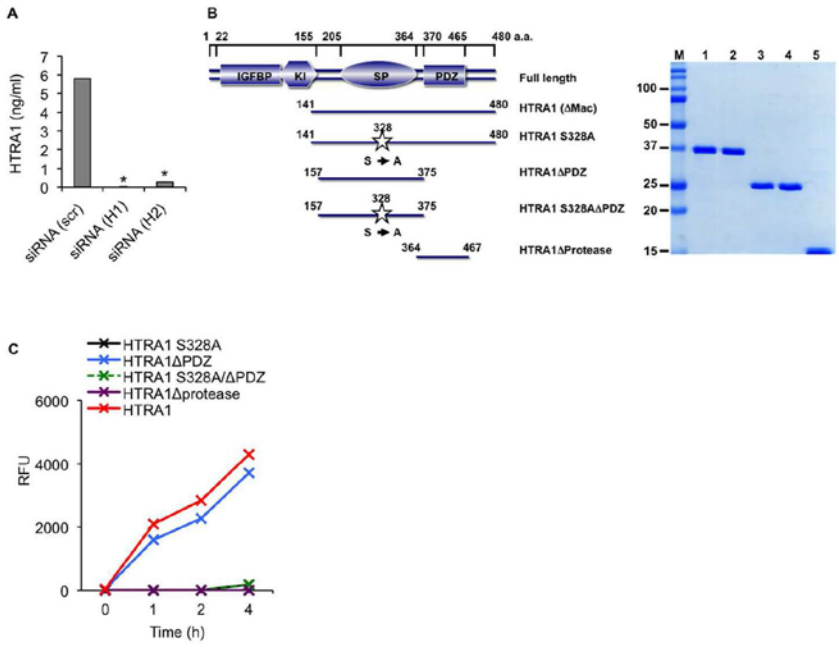

Supplementary Fig. 1. (A): ELISA measurement of HTRA1 in supernatants from adipogenic hMSCs (Adipo) treated with scrambled siRNA (scr) or siRNA specific for HTRA1 (H1 and H2). *$p < 0.001$ as compared to siRNA (scr) treated cells. **(B):** Schematic of recombinant human HTRA1 proteins; active HTRA1 (ΔMac), inactive HTRA1 (HTRA1 S328A), active HTRA1 without PDZ domain (HTRA1ΔPDZ), inactive HTRA1 without PDZ domain (HTRA1 S328AΔPDZ), HTRA1 without protease domain (HTRA1ΔProtease). The purified recombinant histidine-labeled human HTRA1 proteins were also visualized on a Coomassie blue-stained SDS-PAGE gel. *M*, protein marker; *lane 1*, HTRA1; *lane 2*, HTRA1 S328A; *lane 3*, HTRA1ΔPDZ; *lane 4*, HTRA1 S328AΔPDZ; *lane 5*, HTRA1ΔProtease. **(C):** Proteolytic activity of recombinant HTRA1 proteins (45 nM) towards BODIPY-FL-labeled DQ elastin (25 µg/ml) at 37°C as determined using a Multiplate reader. Abbreviations: hMSC, human mesenchymal stem cells; HTRA1, high temperature requirement protease A1; ELISA, enzyme-linked immunosorbent assay; siRNA, small interfering RNA; SDS-PAGE, sodium dodecyl sulfate polyacrylamide gel electrophoresis.
61x46mm (600 x 600 DPI)

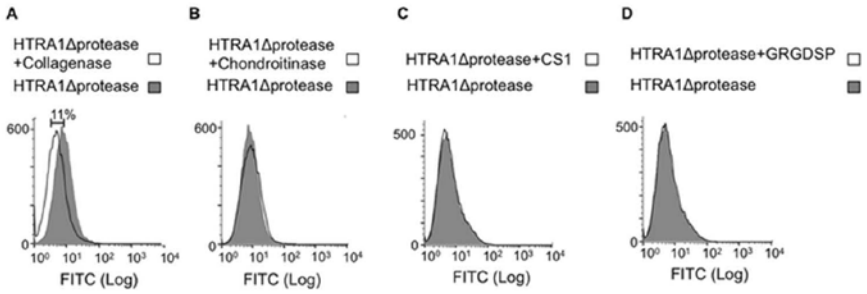

Supplementary Fig. 2. Fluorescence activated cell sorting (FACS) analysis of recombinant HTRA1 binding to non-differentiated hMSCs. HTRA1Δprotease (0.45 μM) was incubated with hMSCs for 1 h at 4°C and cell-bound HTRA1 protein detected using a FITC labeled anti-his antibody. The influence of pre-incubating cells with collagenase (1 mg/ml) **(A)**, chondroitinase (10 U/ml) **(B)**, CS1 (50 μM) **(C)** or GRGDSP (50 μM) **(D)** on the percentage of cell-bound HTRA1Δprotease was calculated using FlowJo 10 software. Data are representative of least two individual experiments performed in duplicate. Abbreviations: hMSC, human mesenchymal stem cells; HTRA1, high temperature requirement protease A1; FACS, fluorescence activated cells sorting.
29x10mm (600 x 600 DPI)

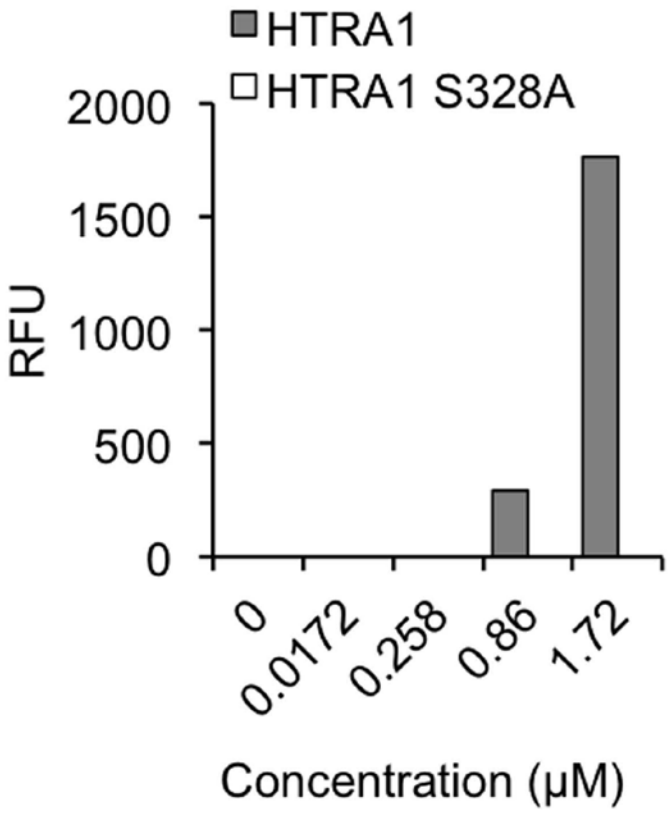

Supplementary Fig. 3. Capacity for HTRA1 to degrade type IV collagen. Varying concentrations of HTRA1 or HTRA1 S328A were incubated with DQ-type IV collagen (25 μg/ml) at 37°C and the relative fluorescence units (RFU) generated after 24 h determined using a Multiplate reader. Abbreviations: HTRA1, high temperature requirement protease A1.
96x113mm (600 x 600 DPI)

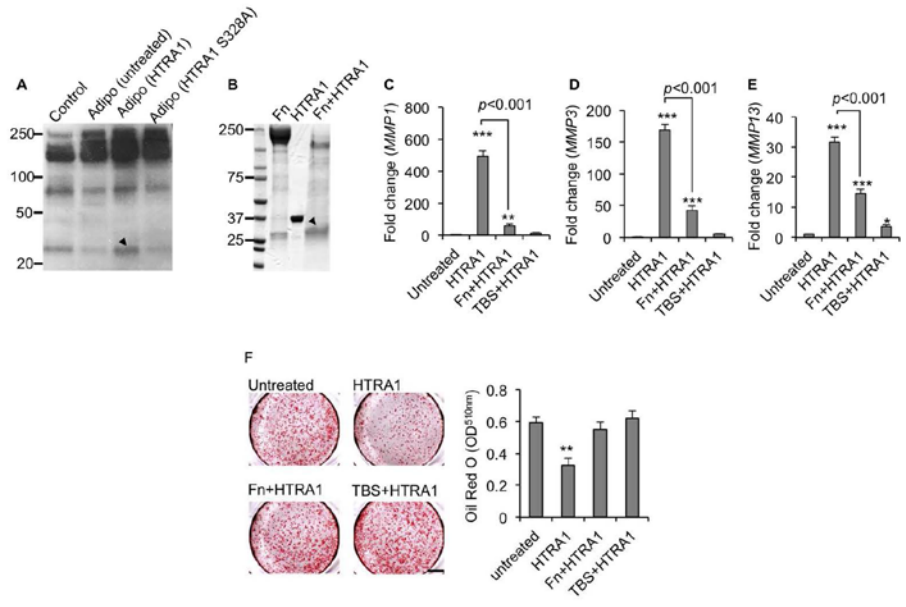

Supplementary Fig. 4. (A): Western blot analysis of native Fnfs in concentrated supernatants harvested from 14 day old undifferentiated hMSCs (control), untreated adipogenic hMSCs, or adipogenic hMSCs treated with HTRA1 (45 nM) for a further 24 h. Protein was subjected to immunoblotting using antibody Mab 1936 specific for the fibronectin amino-terminal fibrin- and heparin-binding domain. *Arrow head* indicates the HTRA1-cleaved 29 kDa Fnf. **(B):** An equimolar ratio of human plasma-derived Fn and HTRA1 were incubated in TBS, pH 8.5, for 16 h at 37°C and Fnfs purified by affinity chromatography and analysed on a Coomassie Blue stained 4-15% gradient SDS-PAGE gel. Fn and HTRA1 alone were also loaded and served as controls. *Arrow head* indicates the purified 29 kDa Fnf due to HTRA1-mediated cleavage. **(C-E):** RT-qPCR analysis of *MMP1* **(C)**, *MMP3* **(D)** and *MMP13* **(E)** in adipogenic hMSCs at day 11 following treatment with HTRA1 (45 nM), purified HTRA1-digested Fn (40 µg/ml) (Fn+HTRA1) or TBS, pH 7.6, eluate from the affinity purification reaction using HTRA1 alone (TBS+HTRA1). Data was normalized to *GUSB* and expressed as fold change as compared to untreated hMSCs (value = 1) using the comparative CT method. **(F):** Oil Red O staining of adipogenic hMSCs at day 14 following treatment with HTRA1 (45 nM), Fn+HTRA1 or TBS+HTRA1. $*p < 0.05$, $**p < 0.01$, $***p < 0.001$ as compared to untreated cells. Scale bar = 2 mm. Data are representative of least two individual experiments performed in triplicate. Abbreviations: hMSC, human mesenchymal stem cells; HTRA1, high temperature requirement protease A1; Fnf, fibronectin fragments; SDS-PAGE, sodium dodecyl sulfate polyacrylamide gel electrophoresis; RT-qPCR, reverse transcription-quantitative polymerase chain reaction; GUSB, Glucuronidase, beta; MMP, matrix metalloproteinase; TBS, Tris-buffered saline.
85x64mm (600 x 600 DPI)

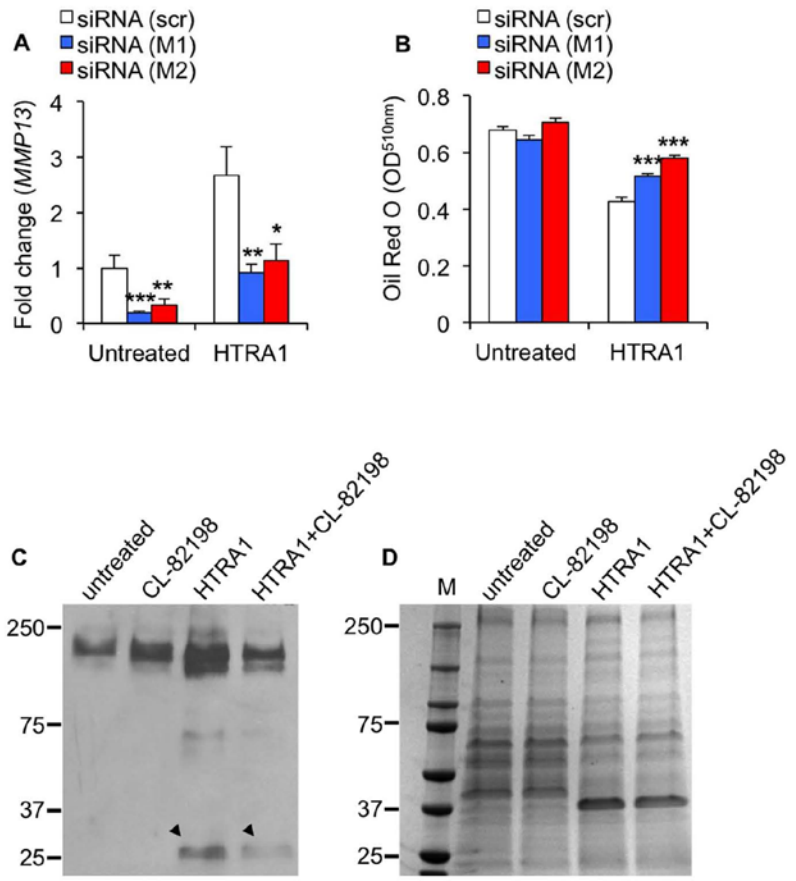

Supplementary Fig. 5. (A): RT-qPCR analysis of *MMP13* gene expression in untreated or HTRA1 (45 nM) treated adipogenic hMSCs at day 3 following pre-treatment with scrambled control siRNA (scr) or siRNAs specific for *MMP13* (M1 and M2). Data was normalized to *GUSB* and expressed as fold change relative to untreated siRNA (scr) hMSCs (value = 1) using the comparative CT method. **(B):** Quantification of Oil Red O staining in adipogenic hMSCs at day 22 following treatment with either a scrambled control siRNA (scr), siRNAs specific for *MMP13* (M1 and M2), or a combination of both siRNAs and HTRA1 (45 nM). *$p < 0.05$, **$p < 0.01$, ***$p < 0.001$ as compared to siRNA (scr) controls from untreated or HTRA1 -treated groups respectively. Data are representative of least two individual experiments performed in triplicate. **(C):** Western blot analysis of native Fnfs in concentrated supernatants harvested from 14-day-old adipogenic hMSCs treated for 24 h without (untreated) or with CL-82198 (20 μM), HTRA1 (45 nM) or HTRA1 and CL-82198. Protein was subjected to immunoblotting using Mab 1936 specific for the Fn amino-terminal fibrin- and heparin-binding domain. *Arrow heads* indicate the 29 kDa Fnf due to HTRA1 treatment. **(D):** Coomassie stained gel of total protein from supernatant to control for equal loading. Data are representative of least two individual experiments. Abbreviations: hMSC, human mesenchymal stem cells; HTRA1, high temperature requirement protease A1; RT-qPCR, reverse transcription-quantitative polymerase chain reaction; GUSB, Glucuronidase, beta; MMP, matrix metalloproteinase; siRNA, small interfering RNA; Fnf, fibronectin fragments.
88x92mm (600 x 600 DPI)

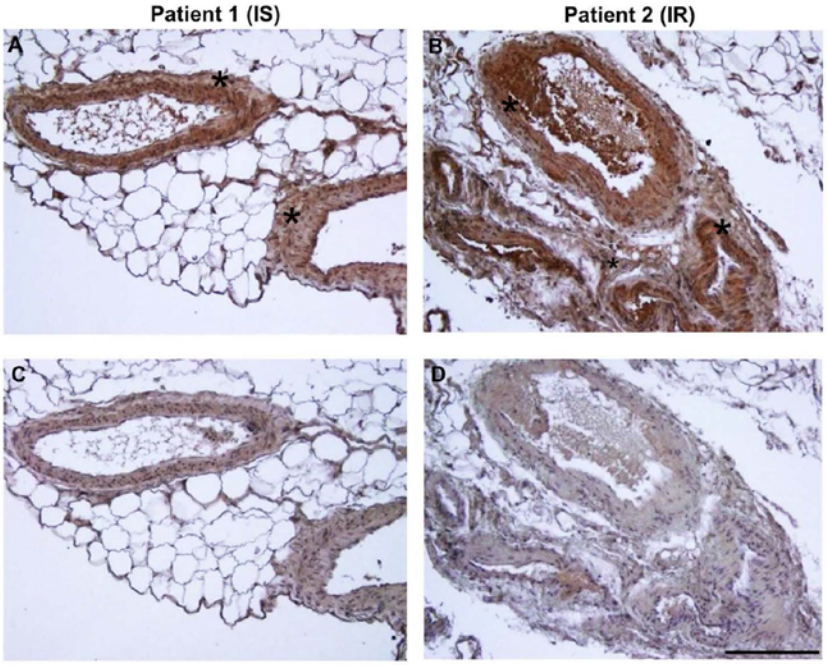

Supplementary Fig. 6. Identification of HTRA1 in adipose tissue. Paraffin wax sections of human visceral (omental) adipose tissue from IS or IR obese patients were incubated with an anti-HTRA1 antibody **(A, B)** or relevant IgG controls **(C, D)**, and positive staining identified using an appropriate HRP-labeled polyclonal antibody with subsequent development using 3,3'-diaminobenzidine (*brown*). *Asterisks*, HTRA1-positive blood vessels; Scale bar = 200 µm. Insulin sensitivity was defined as glucose infusion rate (GIR) during the steady state of an euglycemic-hyperinsulinemic clamp > 70 µmol/kg/min, insulin resistance as GIR < 50 µmol/kg/min. Abbreviations: HTRA1, high temperature requirement protease A1; IS, insulin sensitive; IR, insulin resistant; HRP, horseradish peroxidase.
65x53mm (600 x 600 DPI)

Use of biomimetic microtissue spheroids and specific growth factor supplementation to improve tenocyte differentiation and adaptation to a collagen-based scaffold *in vitro*

Felix Theiss, ECVS, DVM[1,2,3], Ali Mirsaidi, PhD[1,4], Rami Mhanna, PhD[5,6], Stephan Glanz[1,4], Gregor Bahrenberg[1,4], André N. Tiaden, PhD[1], Peter J. Richards, PhD[1,4*]

[1]Center for Applied Biotechnology and Molecular Medicine (CABMM), University of Zurich, Winterthurerstrasse 190, 8057 Zurich, Switzerland. [2]Equine Department, Vetsuisse-Faculty, University of Zurich, Winterthurerstrasse 260, 8057 Zurich, Switzerland. [3]Graduate School for Cellular and Biomedical Sciences, University of Bern, 3012 Bern, Switzerland. [4]Zurich Center for Integrative Human Physiology (ZIHP), University of Zurich, 8057 Zurich, Switzerland. [5]Cartilage Engineering and Regeneration, ETH Zurich, 8093 Zurich, Switzerland. [6]American University of Beirut, Faculty of Engineering and Architecture, Riad El Solh 1107 2020, Beirut, Lebanon.

Running head: Improved cultivation of equine tenocytes

* **Correspondence:** Dr. Peter J. Richards, Bone and Stem Cell Research Group, Competence Center for Applied Biotechnology and Molecular Medicine, Room 13-L-86, University of Zürich, Winterthurerstrasse 190, CH-8057 Zürich, Switzerland, Tel: +41446353800; e-mail: peter.richards@cabmm.uzh.ch

Abstract

Tenocytes represent a valuable source of cells for the purposes of tendon tissue engineering and regenerative medicine and as such, should possess a high degree of tenogenic differentiation prior to their use *in vivo* in order to achieve maximal efficacy. In the current report, we identify an efficient means by which to maintain differentiated tenocytes *in vitro* by employing the hanging drop technique in combination with defined growth media supplements. Equine tenocytes retained a more differentiated state when cultured as scaffold-free microtissue spheroids in low serum-containing medium supplemented with L-ascorbic acid 2-phosphate, insulin and transforming growth factor (TGF)-β1. This was made evident by significant increases in the expression levels of pro-tenogenic markers collagen type I (*COL1A1*), collagen type III (*COL3A1*), scleraxis (*SCX*) and tenomodulin (*TNMD*), as well as by enhanced levels of collagen type I and tenomodulin protein. Furthermore, tenocytes cultured under these conditions demonstrated a typical spindle-like morphology and when embedded in collagen gels, became highly aligned with respect to the orientation of the collagen structure following their migration out from the microtissue spheroids. Our findings therefore provide evidence to support the use of a biomimetic microtissue approach to culturing tenocytes and that in combination with the defined growth media described, can improve their differentiation status and functional repopulation of collagen matrix.

Keywords: Tendon; Growth factors; TGF (transforming growth factor); Microsphere; In vitro test

1. Introduction

Tendon lesions in equine and human athletes are mainly the result of overstrain injury rather than percutaneous trauma, where the athletic discipline generally predisposes specific tendons to injuries. In the racehorse and event horses, injuries occur most frequently in the suspensory ligament and the superficial digital flexor tendon (SDFT) [1]. In humans, tendinopathy is most commonly diagnosed in the Achilles, patellar, rotator cuff and medial/lateral elbow tendons and accounts for 30 – 50% of all sports-related injuries [2]. As such, there is an ever growing need for more effective therapies with which to combat tendon injuries and the ensuing degeneration associated with such trauma. The use of cell-based tissue engineering approaches are fast emerging as alternative therapeutic strategies for the management of tendon injury both in humans and animals [3]. Indeed, a growing number of reports now exist in which multipotent stromal cells (MSCs) isolated from various sources have been successfully implemented in the treatment of both experimentally induced tendon defects [4-7], as well as in clinical cases of tendinopathy [8,9]. The use of MSCs primarily relies on their ability to differentiate into fully functional tendon cells, termed tenocytes. As such, investigators have also sought to utilize mature tenocytes directly as an additional means by which to regenerate tendon tissue as evidenced by the initiation of human clinical trials [source: ClinicalTrials.gov, Trial Number: NCT01343836 and source: ClinicalTrialsRegister.eu, Trial Number:2010-021869-73] with the aim to evaluate the efficacy of autologous tenocytes in treating chronic tendinopathy.

Tenocytes are fibroblast-like cells derived from embryonic mesenchyme and form a three dimensional network of cell processes throughout the extracellular matrix linked by

gap junctions [10]. These cell processes not only connect tenocytes with each other, but also enclose the collagen bundles. It is thought that this close relationship between tenocytes and collagen fibril bundles enables cellular load sensing and coordination of response to load. Characterization of tenocyte gene expression has revealed several markers considered to be essential for their development into fully functional tendon-forming cells, of which tenomodulin (TNMD) may be considered one of the most important and well studied [11-13]. TNMD is a type II transmembrane protein that is mainly expressed in dense connective tissues, and is generally regarded as being a late marker of tendon development [14]. *TNMD* gene expression is positively regulated during tendon development by scleraxis (SCX) [14, 15], a transcription factor considered essential for efficient tendon differentiation [16]. However, both TNMD and SCX have also been detected in tissues form sources other than tendon, thereby bringing into question their reliability as specific markers of tendon [17]. Despite this fact, both TNMD and SCX still serve as a means by which to gauge the differentiation status of tenocytes isolated from tendon tissue.

It has previously been reported that *in vitro,* mature tenocytes have a reduced tendency to express *TNMD*, as well as collagen type 1 (*COL1*), and lose their elongated morphology when cultured for extended periods [18-20]. This so called dedifferentiation of cultured tenocytes is not only considered to be potentially detrimental to their efficiency as a cell-based therapy in tendon repair, but also to their usefulness as an *in vitro* cell system for developing and testing alternative treatments. In this regard, various studies have been undertaken with an aim to improving the genotype and phenotype of isolated tenocytes. Of critical importance in this regard, is the growth medium and its components

used to maintain tenocytes in culture. Several investigators have identified transforming growth factor (TGF)-β and insulin-like growth factor (IGF)-1 as being potent inducers of tenogenic differentiation in both MSCs and tenocytes [21-26], allowing cells to maintain a tenogenic genotype and phenotype *in vitro*. Furthermore, the transfer of cultured tenocytes to high density, three-dimensional (3D) growth environments also appears to stimulate differentiation and prevent cellular dedifferentiation to some degree [21, 25-27].

In the present study, we set out to examine the effects of culturing equine tenocytes with different combinations of TGF-β- or IGF-1-containing culture media under 2D or 3D conditions, with an aim to improving the differentiation status of cultured tenocytes. A detailed examination was undertaken with regards to tenocyte microtissue spheroid formation using the hanging drop culture system, and their tenogenic potential compared to monolayer cultures through the use of genetic- and protein-based assays.

2. Materials and methods

2.1. Animals

Tenocytes were isolated from the superficial digital flexor tendon of Warm blood horses, aged between 2 and 4 years, which were naturally destroyed for clinical reasons other than orthopaedic disease and where owner consent was obtained.

2.2. Isolation and culture of equine tenocytes

The mid-metacarpal region of the superficial digital flexor tendon was harvested under sterile conditions. All tendons were free of pathology on clinical and post mortem examination. After removal of the peritendineum, tendon sections of approximately 1 cm in length were cut into 2 mm^3 pieces and subjected to 0.2% collagenase NB4 (Roche Diagnostics, Rotkreuz, Switzerland) and 0.3% dispase II (Roche Diagnostics) digestion overnight in phosphate-buffered saline (Life Technologies, Zug, Switzerland) containing 5% penicillin/streptomycin (Life Technologies) on an orbital shaker at 37° C. Digested tissue was filtered through a 70 µm cell strainer, centrifuged and cells re-suspended in normal growth medium (GM) consisting of Dulbecco's modified eagle medium (DMEM-high glucose) supplemented with 10% fetal bovine serum (FBS) and penicillin/streptomycin (all from Life Technologies). Supernatant was replaced after 1 day and thereafter every 3 to 4 days with fresh GM and cells were used between passage 4 and 7 unless otherwise stated. Equine fetal tendon cells were obtained from the Laboratory of Cellular Therapy, Department of Musculoskeletal Medicine, University Hospital of Lausanne or were isolated as described above from unborn foals where the mare had to be euthanized during gestation and where owner consent was present.

2.3. Stimulation of equine tenocytes

For 2D monolayer cultures, equine tenocytes seeded at 6 x10^4 cells/cm^2 and stimulated with GM, or DMEM-high glucose supplemented with either 1% FBS, TGFβ1 (10 ng/ml; Peprotech, London, UK) and IGF-1 (50 ng/ml; Peprotech, London, UK) (termed tenogenic differentiation medium-I; TDM-I) or with 1% FBS, 50 μM L-ascorbic acid 2-phosphate sesquimagnesium salt hydrate, 0.5 μg/ml insulin (all from Sigma-Aldrich, Buchs, Switzerland) and 10 ng/ml human TGF-β1 (termed tenogenic differentiation medium-II; TDM-II). In order to generate tenocyte (TC)-microtissue spheroids, cells were seeded as hanging drops in Terasaki plates (VWR International, Dietikon, Switzerland) at 1 x10^3 to 5 x10^3 cells/well in GM, TDM-I or TDM-II according to previously published methodologies [28]. Cells grown as either monolayers or as microtissue spheroids were then harvested at selected time points for further analysis.

2.4. Tenocyte outgrowth studies

The potential for tenocytes to grow out from microtissue spheroids structures was examined using both 2D and 3D culture systems. TC-microtissues were initially cultured for 6 days in hanging drops using either GM or TDM-II. In the case of 2D outgrowth studies, TC-microtissues were transferred to 48-well plates at 60 spheroids/well for up to 3 days, and cell outgrowth visualized at selected time points by phase contrast microscopy. For analysis of cell outgrowth under 3D culture conditions, TC-microtissues consisting of 5 x10^3 cells were mixed with 0.8% bovine collagen (Koken Co., Tokyo, Japan) at 800 microtissues/ml and transferred to silicon molds containing support ridges in order to allow for effective anchoring of the collagen gel [29]. Collagen gels cultured with either GM or

TDM-II were harvested at selected time points, fixed in 4% paraformaldehyde for 12 h and then embedded in paraffin wax and sections stained using hematoxylin and eosin.

2.5. Quantitative Reverse-Transcription Polymerase Chain Reaction (qRT-PCR)

Total RNA was isolated and purified using TRIzol reagent (Life Technologies) according to the manufacture's instructions. RNA (0.5 μg) was reverse transcribed to cDNA using superscript II (Life Technologies) and random hexanucleotide primers (Promega AG, Dübendorf, Switzerland). Quantification of mRNA expression was performed with TaqMan Gene Expression Assays (Life Technologies) specific for *COL1A1* (Ec03469522_m1), *COL2A1* (Ec03467390_m1), *COL3A1* (Ec03469743_m1), *SCX* (Ec03818452_s1), *TNMD* (Ec03467883_m1) and *SOX9* (Ec03469763_s1) using the StepOnePlus Real-Time PCR System (Life Technologies) and values normalized to *GAPDH* (Ec03210916_gH) and presented as $2^{-\Delta CT}$. Each 10 μl reaction consisted of 1x TaqMan Fast Universal PCR Master Mix (Life Technologies), 1x TaqMan Gene Expression Assay and 10 ng cDNA. All reactions were performed in fast optical 96-well reaction plates (Life Technologies) at 95°C for 20 seconds and 40 cycles of 95°C for 1 second and 60°C for 20 seconds.

2.6. Histology

For hematoxylin and eosin staining, dewaxed paraffin sections (5 μm) were rehydrated and stained with Harris' hematoxylin (Sigma-Aldrich, Buchs, Switzerland) for 2 min, rinsed in tap water, and treated with Scott's tap water for a further 2 min. Following washing in tap water, sections were stained with eosin Y (Sigma-Aldrich) for 3 min, rinsed quickly in tap

water, dehydrated and mounted in DPX (Sigma-Aldrich). For immunohistochemical analysis, rehydrated tissue sections were blocked with normal 10% rabbit serum for 30 min and then incubated with polyclonal goat anti-collagen type I (1:100; LabForce, Muttenz, Switzerland) for 1 h at 37°C. Sections were then washed in PBS and incubated with biotinylated rabbit anti-goat IgG (1:200; Reactolab SA, Servion, Switzerland) for 1 h at 37°C followed by washing and a further incubation for 30 min with Vectastain (Reactolab SA). Sections were then developed using 3,3' diaminobenzidine tetrahydrochloride (DAB), counterstained with Harris' Hematoxylin and mounted in DPX.

For active caspase-3 staining of TC-microtissue spheroids, paraffin wax tissue sections were initially microwaved in Target Retrieval Solution (Dako, Zug, Switzerland) for a total of 20 minutes at 750W and then counterstained with Hemalaun for 2 minutes. Endogenous peroxidase activity was quenched using 3% H_2O_2 and sections blocked for 10 min using Protein Block Serum-Free (Dako). Slides were then incubated with rabbit anti-human/mouse active caspase-3 (1:50; R&D Systems, Abingdon, UK) overnight at 4°C. Staining was detected using the Envision System (Dako) and developed using 3-amino-9-ethylcarbazole (AEC) (Life Technologies). Sections were subsequently mounted in Kaiser's gelatin glycerin (Fluka, Buchs, Switzerland) and visualized by light microscopy.

2.7. Immunoblotting

Protein was analyzed by SDS-PAGE using 4-15% precast Tris-HCl gels (Bio-Rad Laboratories AG, Cressier, Switzerland) under reducing conditions, and electroblotted onto PVDF membranes using the Trans-Blot Turbo blotting system (Bio-Rad Laboratories AG). After blocking in 5% fat-free milk, 50 mM Tris-HCl, pH 7.6, 150mM NaCl, 0.1% Tween

20 (TBS-T) for 1 h at room temperature, membranes were incubated overnight at 4°C with rabbit anti-tenomodulin (1:1000; Abcam, Cambridge, UK) or mouse anti-tubulin (1:10'000; Sigma-Aldrich). After washing in TBS-T, membranes were incubated for 1 h at room temperature with HRP-conjugated goat anti-rabbit (1:10'000; LabForce) followed by incubation in SuperSignal West Pico Chemiluminescent Substrate (Thermo Fisher Scientific, Reinach, Switzerland) and exposure to x-ray film.

2.8. Statistical Analysis

All statistical analyses were carried out using SPSS19.0 (SPSS Inc., Chicago, IL). Parametric analysis of normally distributed data was performed using one-way analysis of variance (ANOVA) with Tukey's post hoc test for multiple group comparisons. In all cases, a p-value of <0.05 was considered statistically significant, and all data were expressed as mean ± standard deviation (S.D.).

3. Results

3.1. Equine tenocytes form microtissue spheroids in hanging drop cultures

The equine tenocytes utilized in the current study typically demonstrated a fibroblast-like morphology when cultured in 2D monolayers as determined by phase contrast microscopy (Fig. 1a and b). The randomness of their orientation became apparent as cells approached confluency (Fig. 1b). Following their incorporation into hanging drop cultures, equine tenocytes readily self-assembled into microtissue spheroids after 60 h of incubation (Fig. 1 c-h). The capacity for equine tenocytes to form microtissue spheroids was largely dependent on the initial cell seeding density, where 2500 (Fig. 1 e and f) to 5000 (Fig. 1 g

and h) cells was considered to be the optimal cell number for efficient microtissue formation in the given time frame. During the first 4 days of hanging drop culture, cells were found randomly dispersed throughout the microtissue spheroids and lacked the characteristic fibroblast-like appearance of cells grown in 2D cultures (Fig. 2a and b). However, by day 6, the majority of cells within the microtissue spheroids displayed an elongated phenotype and had become more ordered in appearance (Fig. 2c). The capacity for equine tenocytes to tolerate the hanging drop 3D culture environment was made evident by the lack of caspase-3 activity in the microtissue spheroids at any of the time points tested (Fig. 2e-g). By contrast, high levels of caspase-3 activity were found to be a predominant feature of fetal equine TC-microtissues (Fig. 2d and h).

3.2. Variations in culture media composition significantly influence TC-microtissue phenotype and genotype

We next evaluated the effects of different growth media on the capacity of equine tenocytes to form microtissue spheroids over a 6 day period. In comparison to equine tenocytes cultured as hanging drops in the presence of GM alone (Fig. 3a *top panel*), there was a clear delay in the formation of single microtissue spheroids by cells grown in TDM-I (Fig. 3a *middle panel*) or TDM-II (Fig. 3a *lower panel*). In contrast to GM-treated cells, both TDM-I- and TDM-II-treated cells initially formed numerous smaller spheroids during the first 4 days of culture, but had generally coalesced by day 6 to form a single microtissue spheroid (Fig. 3b). Furthermore, in the case of cells cultured in TDM-II, there was also an appreciable accumulation of extracellular material surrounding the spheroid culture at days 4 and 6. In order to ascertain the influence of culture conditions on the

tenocyte genotype, we analysed the expression levels of several tenogenic markers including *COL1A*, *COL3A1*, *SCX*, and *TNMD*, as well as the chondrogenic markers *COL2A1* and *SOX9*. Comparisons were made between equine tenocytes that had been grown under 2D- or 3D-culture conditions with GM, TDM-I or TDM-II.

2D cultures: Cells cultured for 2 days in either TDM-I or TDM-II showed significant increases in *COL1A1*, *COL3A1*, *SCX* and *SOX9* expression levels as compared to cells in GM alone (Fig. 4a). However, expression levels of *TNMD* remained undetectable in all treatment groups. By day 6, cells cultured in TDM-II showed the greatest increases in gene expression for all makers tested, and represented the only culture condition in which *TNMD* expression could be detected. These results were therefore already suggestive of TDM-II as being a potential alternative to conventional growth medium for the maintenance of equine tenocytes in a more tenogenic-like state.

3D cultures: Treatment of TC-microtissue spheroids for 2 days with either TDM-I or TDM-II induced significant increases in *SCX* expression as compared to cultures receiving GM alone (Fig. 4b). TDM-II additionally induced significant increases in *COL3A1* and *SOX9* at this early time point. Expression levels of *COL1A1*, *COL3A1*, *SCX* and *TNMD* remained significantly elevated at day 6 in cultures treated with either TDM-I or TDM-II, with the greatest effects being observed in TDM-II-treated microtissues. In the case of *SOX9* expression, although TDM-I and TDM-II treatments resulted in significantly more gene expression in comparison to GM alone, *SOX9* mRNA levels were significantly reduced in all treatment groups at day 6 as compared to day 2 measurements. Therefore, in

addition to its beneficial effects on tenogenic gene expression in tenocyte monolayers, TDM-II also appeared to have a pro-tenogenic effect when used to culture tenocytes in 3D microtissue spheroids.

2D vs. 3D cultures: Comparisons in gene expression were also made between tenocytes grown in 2D or 3D culture systems. Microtissues cultured in GM alone for 2 days showed significant increases in *COL1A1*, *COL3A1*, *SCX* and *SOX9* expression levels when compared to tenocytes grown in monolayers (Fig. 5a). Similarly, microtissues stimulated with TDM-I or TDM-II demonstrated significant increases in *COL3A1*, *SCX* and *SOX9* expression as compared to their 2D counter parts. However, incorporation of tenocytes into 3D microtissues did not significantly enhance their capacity to express *COL1A1* in response to TDM-I or TDM-II. By contrast, *TNMD* mRNA was only detected in TC-microtissues, with the greatest levels being observed following TDM-II treatment. At day 6, overall gene expression was either unchanged or significantly reduced in GM-treated TC-microtissues as compared to tenocyte monolayers (Fig. 5b). Conversely, TC-microtissues cultured in TDM-I expressed greater levels of *COL1A1*, *COL3A1* and *TNMD* as compared to tenocytes in monolayers. Similarly, TDM-II induced significant increases in *COL3A1*, *SCX* and *TNMD*, whilst significantly reducing the expression of the chondrogenic marker *SOX9*. The chondrogenic marker *COL2A1* was not detected in any of the culture conditions at either the 2 or 6 day time points. Taken together, these results demonstrate the effectiveness of culturing equine tenocytes as hanging drops in the presence of TDM-II for the purpose of maintaining cells in a more tenogenic-like state.

3.3. Collagen type I production by TC-microtissues

Immunohistochemical analysis of TC-microtissue spheroids was undertaken to assess the impact of TDM-II on collagen type I protein expression. A noticeable increase in collagen type I was evident in equine TC-microtissue spheroids cultured in TDM-II for 6 days as compared to those cultured in GM alone (Fig. 6). In both cases, the majority of positive staining was observed at the periphery of the microtissue structures. These observations are in accordance with the differences observed in *COL1A1* gene expression between GM-treated and TDM-II-treated TC-microtissues, and thus supports the use of TDM-II as an efficient means by which to maintain equine tenocytes in 3D cultures. It should be noted that the agarose used to embed the microtissues for the purposes of histological processing also interacted non-specifically with the anti-COL1A antibody at the concentrations tested thereby generating a diffuse background stain.

3.4. Tenomodulin production by TC-microtissues

In an attempt to further confirm the pro-tenogenic effects of the hanging drop culture and TDM-II stimulation, we analysed protein extracts for the presence of tenomodulin using Western blot. Although tenomodulin is predicted to have a molecular weight of 37 kDa, numerous sized bands ranging from 20 to 250 kDa were identified in TC-microtissue protein samples (Fig. 7). Similarly, numerous different sized protein bands were also detected in protein extracts from native equine tendon, with the most prominent bands being observed at 28, 34, 40, 65 and 250 kDa. Although it remains unclear as to the identity and specificity of these protein products, the 250 kDa protein band was only

detected in samples taken from native equine tendon or equine TC-microtissues cultured in TDM-II.

3.5. Equine tenocyte outgrowth from microtissue spheroids

In order to assess the proliferative status of tenocytes cultured as hanging drops in GM or TDM-II, 6-day-old TC-microtissues were transferred to tissue culture plates and visualized by phase contrast microscopy over the course of 3 days (Fig. 8). During the first 24 h of culture, cells were observed to migrate out from the microtissues onto the plastic surface of the tissue culture plate (Fig. 8A and B). Furthermore, cells previously cultured as TC-microtissues in the presence of TDM-II (Fig. 8B) appeared to have a more spindle shaped, tenocyte-like appearance as compared to those cultured in GM alone (Fig. 8A). By day 3, the number of cells populating the tissue culture surface had noticeably increased in both GM- and TDM-II-treated TC-microtissue cultures (Fig. 8C and D). Cells emanating from the TDM-II-treated TC-microtissues continued to demonstrate morphology reminiscent of tenocytes (Fig. 8D) in comparison to the rounded cell appearance of the GM-treated TC-microtissues (Fig. 8C). The ability of tenocytes to migrate out from the microtissue spheroids was further examined using collagen gels as a means by which to simulate a more physiologically relevant 3D environment. Macroscopic observations of TC-microtissue seeded collagen gels revealed noticeable amounts of matrix contraction in gels containing the TDM-II-treated microtissues (Supp. Fig. 1). Gel contraction was already evident after 2 days of TC-microtissue seeding and continued to increase over the next 3 days. By contrast, no such contraction was seen in gels seeded with GM-treated microtissues at any of the time points tested. Similarly to the 2D culture system, migration

of tenocytes out from the microtissues was observed for both GM- and TDM-II-treated cells within the first 24 h (Supp. Fig. 2) and continued to increase over the next 4 days in association with a gradual reduction in microtissue structure (Fig. 9). However, in contrast to collagen gels containing GM-treated microtissues, gels seeded with TDM-II-treated microtissues contained numerous, well-orientated cells aligned in the direction of the contracted collagen matrix (Fig. 9B, D and F). Moreover, by day 5 after the initial TC-microtissue seeding, collagen gels containing TDM-II-treated microtissues started to take on a more native tendon-like appearance, with cells displaying the characteristic spindle-like morphology dispersed throughout the matrix (Fig. 9F) (Supp. Fig. 3).

4. Discussion

Tendons are highly specialized structures composed mainly of collagen type I, whose principal function is to transmit muscular forces to bone and thereby enable stabilization and movement of joints. Furthermore, in horses, specific tendons can function as elastic energy storage structures, allowing for an athletic and energy efficient gait [30]. Repetitive overloading of tendons can result in cumulative micro-damage with degenerative changes of the ECM [31,32], and these alterations are invariably associated with physical disruption of fibres, cross-links and matrix proteins [33], being secondary to impaired tenocyte metabolism possibly also due to hyperthermic insults [34] or hypoxic cell injury [35]. In all cases, the resident cell population of the tendon fails to repair this cumulative micro-damage. As such, efforts are now being made to utilize various cell-based tissue engineering approaches to treat tendon injuries, with an aim to restoring tissue function as well as preventing associated degenerative changes.

As the primary source of collagen production in tendons, tenocytes have long been considered as a potential tissue engineering strategy to facilitate tendon repair and regeneration. Indeed, several studies now exist in which tenocytes have been successfully used for the purpose of augmenting tendon repair in both animal and human subjects [36-39]. However, in order to generate sufficient numbers of tenocytes for use *in vivo*, cells must first be expanded in culture. Although the isolation and expansion of tenocytes is nowadays a relatively standardized procedure, the choice of growth conditions under which tenocytes are cultivated can have a significant impact on their differentiation status and hence their functional capacity to repair tendon tissue. This has been highlighted in several studies in which the expression of tendon-associated markers, including *COL1*,

COL3, *SCX* and *TNMD*, were shown to be downregulated in tenocytes cultured for extended periods [19, 20]. These limitations however, could be overcome to some degree by incorporation of tenocytes into 3D culture systems [25, 27, 40] or though the addition of specific growth factors [22, 24, 25]. In the current report, we initially investigated the effectiveness of culturing equine tenocytes as hanging drops as a means by which to generate scaffold-free 3D microtissue spheroids. Tenocytes readily aggregated together and formed well-organized, viable microtissue spheroid structures within 6 days of culture. Furthermore, cells within these late stage cultures appeared to have an elongated fibroblast-like morphology and demonstrated a basic cell alignment growth pattern. However, despite tenocyte-derived microtissue spheroids demonstrating early significant increases in tendon-associated markers such as *COL1A1*, *COL3A1* and *SCX* when compared to tenocyte monolayers, they were unable to maintain these elevated levels after prolonged culture times. Interestingly, the pro-chondrogenic marker *SOX9* was significantly reduced in these late-stage 3D cultures as compared to cells grown in monolayers. Moreover, in neither case were tenocytes observed to express *TNMD* or the chondrogenic-associated marker *COL2A1* at any of the time points tested. Taken together, these initial observations suggested that scaffold-free microtissue spheroid cultures may indeed have some immediate beneficial impact on tenocyte differentiation, although lacked the ability to maintain this effect over extended periods in culture.

In order to better optimize the tenogenic status of tenocytes cultured under either 2D or 3D conditions, we next focused our attention on the growth media used in each system. Findings from recent studies have strongly hinted at the use of TGF-β and IGF-1, or combinations thereof, to enhance and possibly even maintain tenocyte differentiation

during extended periods of cultivation. Caliari *et al.* [22] demonstrated that IGF-1 at concentrations ranging from 10 to 200 ng/ml was capable of significantly enhancing *COL1A2*, *COL3A1* and decorin (*DCN*) gene expression in equine tenocytes cultured in collagen scaffolds in the absence of serum for 7 days. By contrast, a study performed by Qiu *et al.* [24] demonstrated that IGF-I (50 ng/ml) alone was unable to significantly influence *COL1*, *SCX* or *TNMD* expression in human tenocytes. However, incubation of cells with TGF-β3 (10 ng/ml), or TGF-β3 and IGF-1 together, significantly enhanced gene expression above that of control cultures incubated in the presence of serum-supplemented growth medium. In support of this, studies investigating the tenogenic potential of primary canine MSCs revealed that combinations of TGF-β1 and IGF-1 (5 ng/ml of each) were sufficient to induce the expression of *COL1*, *COL3*, *DCN*, *SCX* and *TNMD* after 7 and 14 days in combination with high density 3D culture conditions [26]. Similarly, a more recent report by Barsby *et al.* [21] has confirmed a synergistic effect between 3D growth environments and the addition of TGF-β3 (20 ng/ml) in the tenogenic differentiation of equine embryonic stem cells (ESCs). Therefore, based on these previous findings, we elected to assess the effects of low-serum media containing human TGF-β1 (10 ng/ml) in combination with either human IGF-1 (50 ng/ml) (termed TDM-I), or human insulin and L-ascorbic acid 2-phosphate (termed TDM-II) on tenocyte differentiation in either 2D or 3D culture systems. Treatment of tenocytes in 2D with TDM-I had a moderate effect on most of the genetic markers tested, with the majority of genes being significantly increased within the first 2 days of culture as compared to cells cultured in growth medium alone. However, induction of *TNMD* expression was not observed at any time point, and *COL1A1* and *COL3A1* expression levels were reduced by day 6. With regards to 3D cultures, early

significant increases in gene expression were limited to *SCX* only, but at later stages included increases in *COL1A1*, *COL3A1*, *SCX*, *TNMD* and *SOX9*. In comparison to 2D cultures, late stage 3D cultures demonstrated modest benefits in terms of *COL1A1*, *COL3A1* and *TNMD* expression, with similar levels of *SOX9* being observed. These observations therefore go someway to supporting the concept of culturing tenocytes under 3D conditions in the presence of TGF-β and IGF-1 in order to enhance and maintain a tendon like genotype. However, the most pronounced effects were observed in culture medium where IGF-1 had been replaced by insulin and L-ascorbic acid 2-phosphate (TDM-II). Regardless of which system was used, cultivation in TDM-II resulted in marked increases in the expression of all tenogenic gene markers in late stage cultures. Furthermore, in comparison to 2D cultures, TC-microtissue spheroids examined at day 6 demonstrated significantly enhanced expression levels of *COL3A1*, *SCX* and *TNMD*, with a noticeable decrease in the expression of the chondrogenic marker *SOX9*, and a complete absence of *COL2A1*. Moreover, not only were the expression levels of tenogenic markers maintained in this medium, but were also in some cases enhanced at the later stages. Clearly therefore, the combination of TGF-β1, insulin and ascorbic acid appears to represent a novel supplement for the purpose of enhancing and maintaining a tendon-like genotype in 3D tenocyte cultures, without inducing chondrocyte-associated gene expression.

In accordance with these findings, we could demonstrate that collagen type I was also increased at the protein level in TC-microtissue spheroids cultured in the presence of TDM-II. Furthermore, when assessing protein lysates for the presence of TNMD, we detected an additional, high molecular weight protein not observed in TC-microtissue

spheroids treated with growth medium alone. It is unclear as to why TNMD was detected in tenocyte cultures treated with growth medium at all, as qRT-PCR analysis failed to detect any *TNMD* mRNA transcript. However, a similar finding was also reported by Barsby *et al.* [41] in which TNMD protein was observed in TGF-β-treated equine ESC cultures in the absence of any detectable levels of *TNMD* mRNA. The cause for such inconsistencies was accredited to disparities between TNMD protein turnover and mRNA degradation rates. Therefore, it seems plausible that the 250 kDa band observed in the current study represents a high molecular weight variant of TNMD, being present in native tendon tissue, as well as being induced in TC-microtissue spheroids following stimulation with TDM-II. However, the relevance of this particular protein species with regards to the normal functioning of tendons remains to be determined. In a final series of experiments, we assessed the potential of tenocytes within microtissue spheroids to migrate out from the tissue structures and to re-populate 2D or 3D culture environments. This was based on the assumption that should such tissue constructs be considered as a viable *in vivo* treatment strategy, then the cells contained within the tissue spheroids would be required to grow out and invade the surrounding host tissue in order to mediate their therapeutic effects. Indeed, we could demonstrate that TC-microtissue spheroids treated with TDM-II were capable of growing out from the tissues and could proliferate on a 2D culture surface whilst maintaining a tenocyte-like morphology. Moreover, when transferred to collagen gels, microtissue-derived cells treated with TDM-II also had the capacity to promote contraction of the collagen matrix and were observed to independently align with respect to the orientation of the collagen structure following microtissue outgrowth.

5. Conclusions

Taken together, our findings demonstrate the beneficial effects of culturing tenocytes as gravity-enforced microtissue spheroids and supports the use of low-serum containing growth medium in combination with TGF-β1, insulin and ascorbic acid as an effective means by which to maintain the tenogenic differentiation status of cultured tenocytes. This therefore raises the interesting possibility of whether such a system could be directly incorporated into future *in vivo* tissue engineering strategies for the purpose of more effectively treating tendon disorders.

Acknowledgements

This study was funded in part by the Stiftung Forschung für das Pferd. SG and GB were supported by SNSF grants 31003A_134935 and 31003A_156313. AM and NAT were supported by the Uniscientia Foundation. The authors would like to thank Prof. Dr. Brigitte von Rechenberg (Musculoskeletal Research Unit, Equine Department, Vetsuisse-Faculty, University of Zurich) and Dr. Silke Kalchofner-Mark (CABMM, University of Zurich) for their scientific input and support, Prof. Lee Ann Laurent-Applegate (Laboratory of Cellular Therapy, Department of Musculoskeletal Medicine, University Hospital Lausanne) for supplying equine fetal tenocytes and Katalin Zlinszky (Musculoskeletal Research Unit, Equine Department, Vetsuisse-Faculty, University of Zurich) for performing the caspase activity assay.

References

1. Williams RB, Harkins LS, Hammond CJ, Wood JL. Racehorse injuries, clinical problems and fatalities recorded on British racecourses from flat racing and National Hunt racing during 1996, 1997 and 1998. Equine Vet J 2001;33:478-86.
2. Lui PP, Maffulli N, Rolf C, Smith RK. What are the validated animal models for tendinopathy? Scand J Med Sci Sports 2011;21:3-17.
3. Gaspar D, Spanoudes K, Holladay C, Pandit A, Zeugolis D. Progress in cell-based therapies for tendon repair. Adv Drug Deliv Rev. 2014 (Ahead of print).
4. Deng D, Wang W, Wang B, Zhang P, Zhou G, Zhang WJ, Cao Y, Liu W. Repair of Achilles tendon defect with autologous ASCs engineered tendon in a rabbit model. Biomaterials 2014;35:8801-9.
5. Zhang J, Li B, Wang, J.H. The role of engineered tendon matrix in the stemness of tendon stem cells in vitro and the promotion of tendon-like tissue formation in vivo. Biomaterials 2011;32:6972-81.
6. Lee JY, Zhou Z, Taub PJ, Ramcharan M, Li Y, Akinbiyi T, Maharam ER, *et al.* BMP-12 treatment of adult mesenchymal stem cells in vitro augments tendon-like tissue formation and defect repair in vivo. PLoS One 2011;6:e17531.
7. Chen JL, Yin Z, Shen WL, Chen X, Heng BC, Zou XH, Ouyang HW. Efficacy of hESC-MSCs in knitted silk-collagen scaffold for tendon tissue engineering and their roles. Biomaterials 2010;31:9438-51.
8. Smith RK, Werling NJ, Dakin SG, Alam R, Goodship AE, Dudhia J. Beneficial effects of autologous bone marrow-derived mesenchymal stem cells in naturally occurring tendinopathy. PLoS One 2013;8:e75697.

9. Albano JJ, Alexander RW. Autologous fat grafting as a mesenchymal stem cell source and living bioscaffold in a patellar tendon tear. Clin J Sport Med 2011;21:359-61.
10. McNeilly CM, Banes AJ, Benjamin M, Ralphs JR. Tendon cells in vivo form a three dimensional network of cell processes linked by gap junctions. J Anat 1996;189:593-600.
11. Qi J, Dmochowski JM, Banes AN, Tsuzaki M, Bynum D, Patterson M, Creighton A, *et al.* Differential expression and cellular localization of novel isoforms of the tendon biomarker tenomodulin. J Appl Physiol 2012;113:861-71.
12. Docheva D, Hunziker EB, Fässler R, Brandau O. Tenomodulin is necessary for tenocyte proliferation and tendon maturation. Mol Cell Biol 2005;25:699-705.
13. Alberton P, Dex S, Popov C, Shukunami C, Schieker M, Docheva D. Loss of Tenomodulin Results in Reduced Self-Renewal and Augmented Senescence of Tendon Stem/Progenitor Cells. Stem Cells Dev 2015;42:597-609.
14. Shukunami C, Takimoto A, Oro M, Hiraki Y. Scleraxis positively regulates the expression of tenomodulin, a differentiation marker of tenocytes. Dev Biol 2006;298:234-47.
15. Schweitzer R, Zelzer E, Volk T. Connecting muscles to tendons: tendons and musculoskeletal development in flies and vertebrates. Development 2010;137:2807-17.
16. Murchison ND, Price BA, Conner DA, Keene DR, Olson EN, Tabin CJ, Schweitzer R. Regulation of tendon differentiation by scleraxis distinguishes force-transmitting tendons from muscle-anchoring tendons. Development 2007;134:2697-708.
17. Taylor SE, Vaughan-Thomas A, Clements DN, Pinchbeck G, Macrory LC, Smith RK, Clegg PD. Gene expression markers of tendon fibroblasts in normal and diseased tissue

compared to monolayer and three dimensional culture systems. BMC Musculoskelet Disord 2009;10:27.

18. Yao L, Bestwick CS, Bestwick LA. Phenotypic drift in human tenocyte culture. Tissue Eng 2006;12:1843-9.
19. Mazzocca AD, Chowaniec D, McCarthy MB, Beitzel K, Cote MP, McKinnon W, Arciero R. In vitro changes in human tenocyte cultures obtained from proximal biceps tendon: multiple passages result in changes in routine cell markers. Knee Surg Sports Traumatol Arthrosc. 2012;20:1666-72.
20. Zhu J, Li J, Wang B, Zhang WJ, Zhou G, Cao Y, Liu W. The regulation of phenotype of cultured tenocytes by microgrooved surface structure. Biomaterials 2010;31:6952-58.
21. Barsby T, Bavin EP, Guest DJ. Three-dimensional culture and transforming growth factor beta3 synergistically promote tenogenic differentiation of equine embryo-derived stem cells. Tissue Eng Part A 2014;20:2604-13.
22. Caliari SR, Harley BA. Composite growth factor supplementation strategies to enhance tenocyte bioactivity in aligned collagen-GAG scaffolds. Tissue Eng Part A 2013;19:1100-12.
23. Costa MA, Wu C, Pham BV, Chong AK, Pham HM, Chang J. Tissue engineering of flexor tendons: optimization of tenocyte proliferation using growth factor supplementation. Tissue Eng 2006;12:1937-43.
24. Qiu Y, Wang X, Zhang Y, Carr A.J, Zhu L, Xia Z, Sabokbar A. Development of a refined tenocyte differentiation culture technique for tendon tissue engineering. Cells Tissues Organs 2013;197, 27-36.

25. Qiu Y, Wang X, Zhang Y, Carr AJ, Zhu L, Xia Z, Sabokbar A. In vitro two-dimensional and three-dimensional tenocyte culture for tendon tissue engineering. J Tissue Eng Regen Med. 2013 (Ahead of print).

26. Schneider PR, Buhrmann C, Mobasheri A, Matis U, Shakibaei M. Three-dimensional high-density co-culture with primary tenocytes induces tenogenic differentiation in mesenchymal stem cells. J Orthop Res 2011;29:1351-60.

27. Schulze-Tanzil G, Mobasheri A, Clegg PD, Sendzik J, John T, Shakibaei M. Cultivation of human tenocytes in high-density culture. Histochem Cell Biol 2004;122:219-28.

28. Mirsaidi A, Tiaden AN, Richards PJ. Preparation and osteogenic differentiation of scaffold-free mouse adipose-derived stromal cell microtissue spheroids (ASC-MT). Curr Protoc Stem Cell Biol 2013;27:Unit 2B.5.

29. Mhanna R, Öztürk E, Schlink P, Zenobi-Wong M. Probing the microenvironmental conditions for induction of superficial zone protein expression. Osteoarthritis Cartilage 2013;**21:**1924-32.

30. Smith RK. Mesenchymal stem cell therapy for equine tendinopathy. Disabil Rehabil 2008;30:1752-8.

31. Smith R, McIlwraith W, Schweitzer R, Kadler K, Cook J, Caterson B, Dakin S, *et al.* Advances in the understanding of tendinopathies: a report on the Second Havemeyer Workshop on equine tendon disease. Equine Vet J 2014;46:4-9.

32. Shepherd JH, Riley GP, Screen HR. Early stage fatigue damage occurs in bovine tendon fascicles in the absence of changes in mechanics at either the gross or micro-structural level. J Mech Behav Biomed Mater 2014;38:163-72.

33. Avella CS, Smith RKW. Diagnosis and management of tendon and ligament disorders. In: Auer, J.A., and Stick, J.A., eds. Equine Surgery. 4 ed. St. Louis, MO, USA: Elsevier Saunders. 2012, pp. 1157-79.

34. Birch HL, Wilson AM, Goodship AE. The effect of exercise-induced localised hyperthermia on tendon cell survival. J Exp Biol 1997;200:1703-8.

35. Millar NL, Reilly JH, Kerr SC, Campbell AL, Little KJ, Leach WJ, Rooney BP, *et al.* Hypoxia: a critical regulator of early human tendinopathy. Ann Rheum Dis 2012;71:302-10.

36. Liang JI, Lin PC, Chen MY, Hsieh TH, Chen JJ, Yeh ML. The effect of tenocyte/hyaluronic acid therapy on the early recovery of healing Achilles tendon in rats. J Mater Sci Mater Med 2014;25:217-27.

37. Wang A, Breidahl W, Mackie KE, Lin Z, Qin A, Chen J, Zheng MH. Autologous tenocyte injection for the treatment of severe, chronic resistant lateral epicondylitis: a pilot study. Am J Sports Med 2013;41:2925-32.

38. Chen J, Yu Q, Wu B, Lin Z, Pavlos NJ, Xu J, Ouyang H, *et al.* Autologous tenocyte therapy for experimental Achilles tendinopathy in a rabbit model. Tissue Eng Part A 2011;17:2037-48.

39. Stoll C, John T, Conrad C, Lohan A, Hondke S, Ertel W, Kaps C, *et al.* Healing parameters in a rabbit partial tendon defect following tenocyte/biomaterial implantation. Biomaterials 2011;32:4806-15.

40. Stoll C, John T, Endres M, Rosen C, Kaps C, Kohl B, Sittinger M, *et al.* Extracellular matrix expression of human tenocytes in three-dimensional air-liquid and PLGA

cultures compared with tendon tissue: implications for tendon tissue engineering. J Orthop Res 2010;28:1170-7.

41. Barsby T, Guest D. Transforming growth factor beta3 promotes tendon differentiation of equine embryo-derived stem cells. Tissue Eng Part A. 2013;19:2156-65.

Figure 1. Representative phase contrast images of sub-confluent (A) (magnification 20x) and confluent (B) (magnification 10x) equine tenocytes grown as 2D monolayer cultures. Representative images of hematoxylin and eosin stained paraffin wax sections of equine TC-microtissue spheroids after 60 h of culture using 1000 (C), 2500 (E) or 5000 (G) equine tenocytes. Phase contrast images of single hanging drops 60 h following seeding with 1000 (D), 2500 (F) or 5000 (H) equine tenocytes. Scale bar = 75μm.

Figure 2. Representative hematoxylin and eosin stained paraffin wax sections of equine TC-microtissue spheroids cultured for 2 days (A), 4 days (B) and 6 days (C) in GM and equine fetal tenocytes cultured for 6 days (D) in GM. Scale bar = 50 μm. Representative images of active caspase-3 staining (brown) in paraffin wax sections of equine TC-microtissue spheroids cultured for 2 (E), 4 (F) and 6 days (G) in GM. Equine fetal tenocytes cultured for 6 days (H) in GM were used as positive controls. Scale bar = 25 μm.

Figure 3. (A) Representative phase contrast images of microtissue spheroid formation in single hanging drops of tenocyte cultures treated for up to 6 days with either growth medium (GM) alone, tenogenic differentiation medium I (TDM-I) or tenogenic differentiation medium II (TDM-II). Scale bar = 75 μm. (B) Representative images of hematoxylin stained paraffin wax sections of TC-microtissue spheroids at day 6 following treatment with GM, TDM-I or TDM-II. Scale bar = 50 μm.

Figure 4. qRT-PCR analysis of *COL1A1*, *COL3A1*, *SCX*, *TNMD* and *SOX9* in equine tenocytes cultured in 2D monolayers (A) or 3D microtissue spheroids (B) for 2 and 6 days.

In each case, gene expression in equine tenocytes cultured in growth medium (GM) alone was compared to cells cultured in either tenogenic differentiation medium I (TDM-I) or tenogenic differentiation medium II (TDM-II) at each of the time points tested. Data was normalized to *GAPDH* and is presented as $2^{-\Delta CT}$. * $p < 0.05$, ** $p < 0.01$ as compared to tenocytes cultured in GM. Significance was determined by one-way ANOVA and Tukey's post-hoc test. (± S.D. triplicates).

Figure 5. qRT-PCR analysis of *COL1A1*, *COL3A1*, *SCX*, *TNMD* and *SOX9* in 2D or 3D equine tenocyte cultures at 2 (A) and 6 days (B) after seeding. Comparisons were made between tenocyte monolayers (2D) and microtissue spheroids (3D) when cultured in either growth medium (GM), tenogenic differentiation medium I (TDM-I) or tenogenic differentiation medium II (TDM-II). In each case, gene expression in equine tenocytes cultured in 2D was compared to those cultured in 3D, and data normalized to *GAPDH* and presented as $2^{-\Delta CT}$. * $p < 0.05$, ** $p < 0.01$ as compared to tenocytes cultured in 2D monolayers. Significance was determined by one-way ANOVA and Tukey's post-hoc test. (±S.D. triplicates).

Figure 6. Representative micrographs of anti-collagen type I stained paraffin wax sections of equine tenocytes cultured in hanging drops for 6 days in either GM (A) or TDM-II (B). Collagen type I was visualized using horseradish peroxidase-diaminodenzidine (dark brown) and sections counterstained with hematoxylin (blue). Examples of positive staining for collagen type I are indicated by arrowheads. (C-D) Representative micrographs of control paraffin wax sections in which the anti-COL1A1 primary antibody was replaced

with normal IgG. *Asterisks*, agarose in which microtissues were embedded. Scale bar = 100μm.

Figure 7. Western blot analysis of protein lysates (40 μg) from equine TC-microtissues treated with GM (GM) or TDM-II (TDM-II). Protein (10 μg) from native equine tendon (NT) was used as positive control. Protein samples were loaded onto an SDS-PAGE gel and tenomodulin detected using a specific antibody targeting the N-terminus of human tenomodulin. A monoclonal tubulin antibody was used as a loading control.

Figure 8. Phase contrast micrographs demonstrating tenocyte outgrowth from microtissue spheroids under 2D culture conditions. Equine tenocytes were cultured as hanging drops for 6 days in GM or TDM-II and transferred to 48-well plates at 60 spheroids/well for 1 (A, B) and 3 (C, D) days. Magnification = 20x

Figure 9. Outgrowth of equine tenocytes from TC-microtissue and their alignment in static 3D collagen constructs. TC-microtissues were prepared in hanging drops for 6 days in either GM or TDM-II and then embedded in 0.8% collagen matrix. Representative micrographs of hematoxylin and eosin stained paraffin wax sections of gel constructs at 2 (A, B), 4 (C, D) and 5 (E, F) days after TC-microtissue seeding of GM (A, C, E) or TDM-II (B, D, F) treated cultures. Scale bar = 100 μm. *Inset*, scale bar = 20 μm. *Arrow*, orientation of collagen gels based on their positioning in anchored silicon molds.

Supplementary Figure 1. Macroscopic images of collagen gel constructs anchored in silicon molds at 2, 3, 4 and 5 days after TC-microtissue seeding of GM or TDM-II treated cultures. Scale bar = 1 cm.

Supplementary Figure 2. Representative images of collagen gel-embedded GM- and TDM-II-treated TC-microtissues *in situ* at 12 and 24 h after seeding. Scale bar = 100 μm.

Supplementary Figure 3. Visualization of tenocyte and collagen fibre alignment in hematoxylin and eosin stained paraffin wax sections of 3D collagen constructs 5 days after seeding with TDM-II-treated TC-microtissues. (A) Scale bar = 50 μm. (B) Scale bar = 20 μm. *Arrow*, orientation of collagen gels based on their positioning in anchored silicon molds.

Figure 1

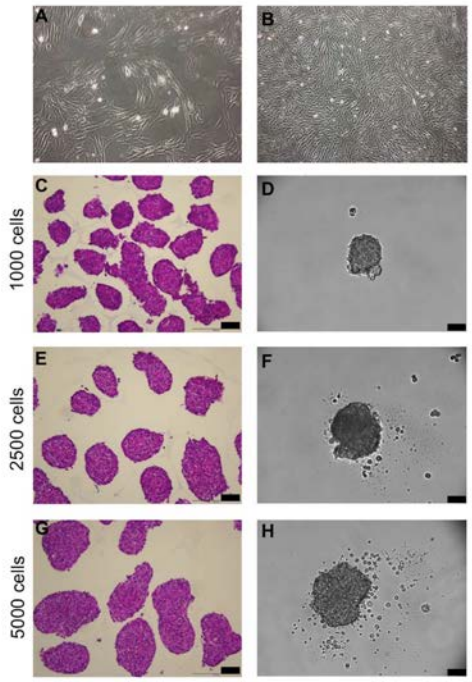

Figure 2

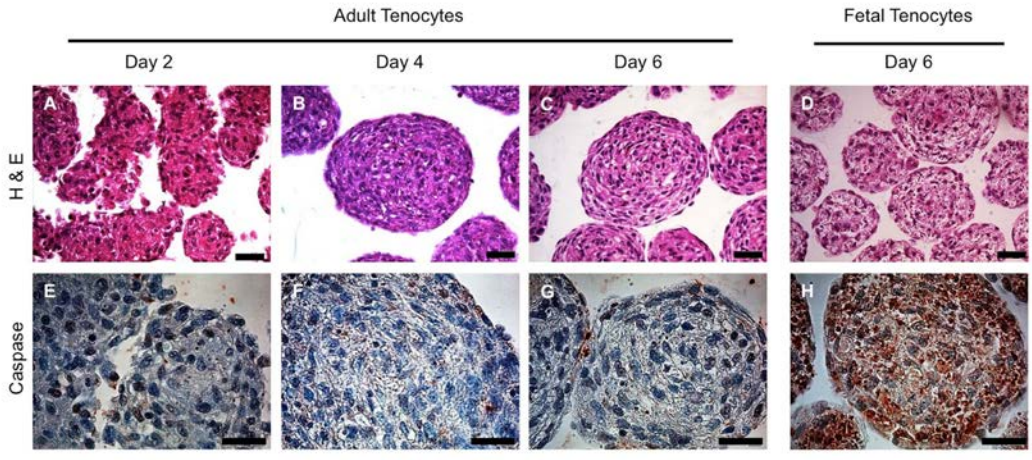

Figure 3

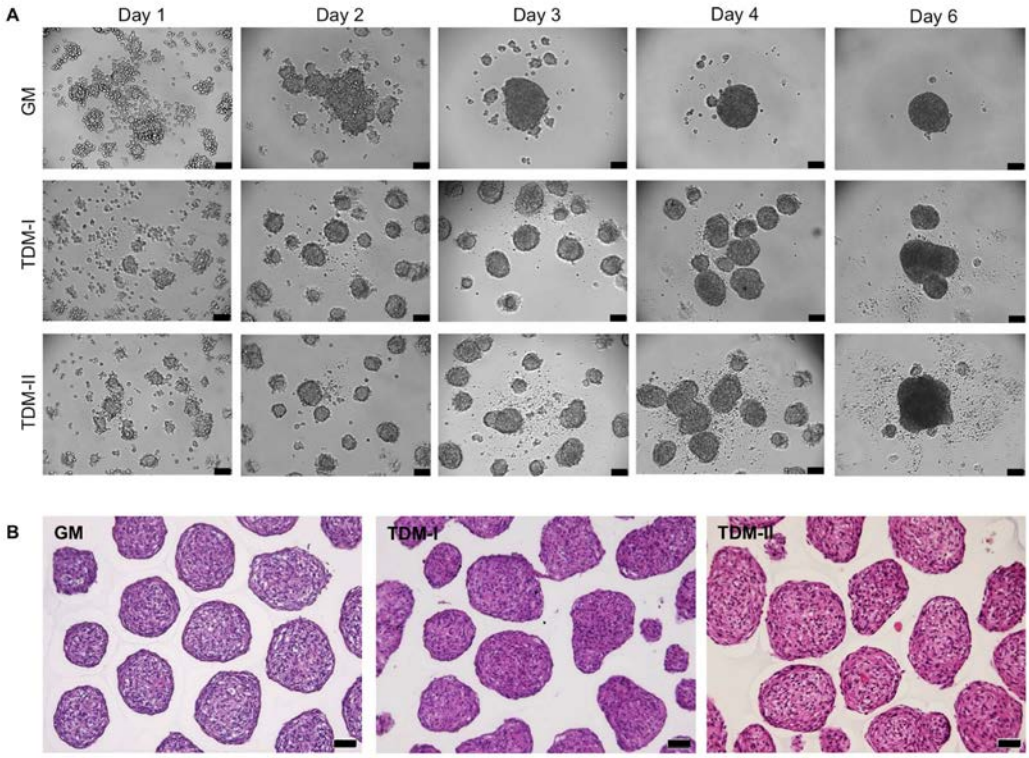

Figure 4

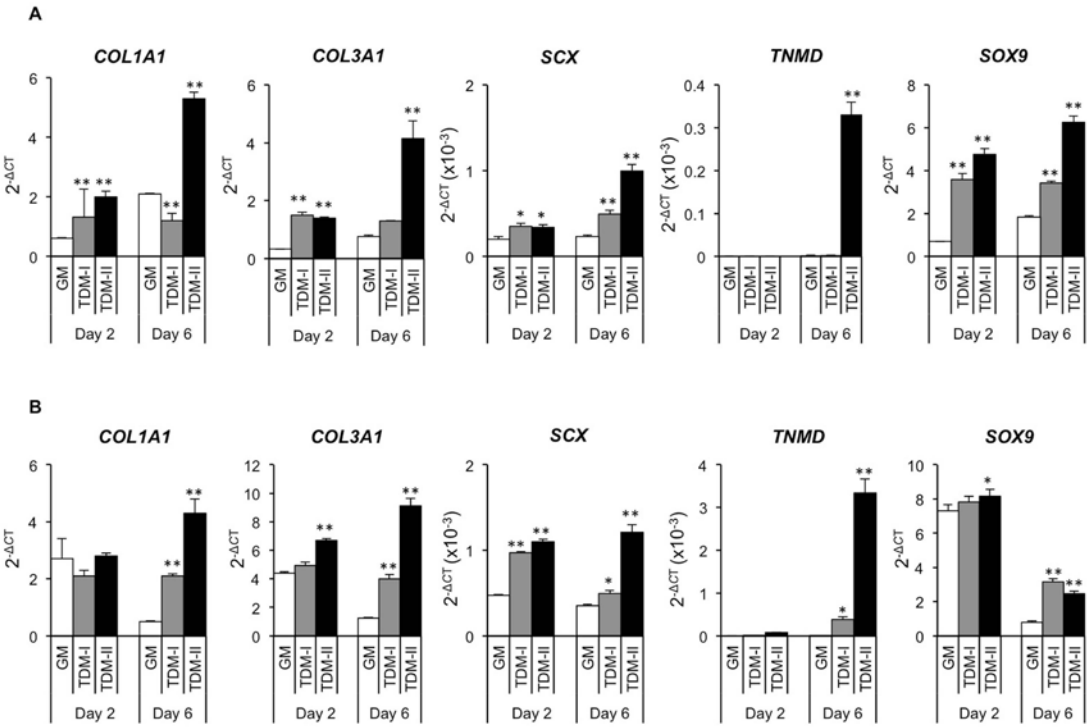

Figure 5

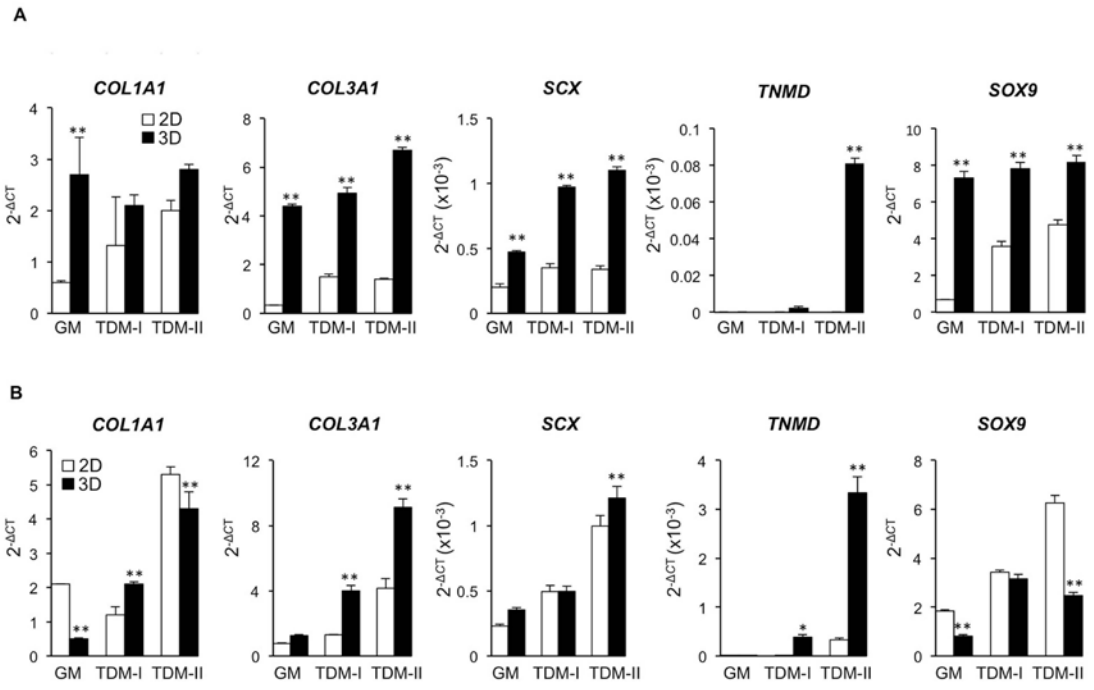

Figure 6

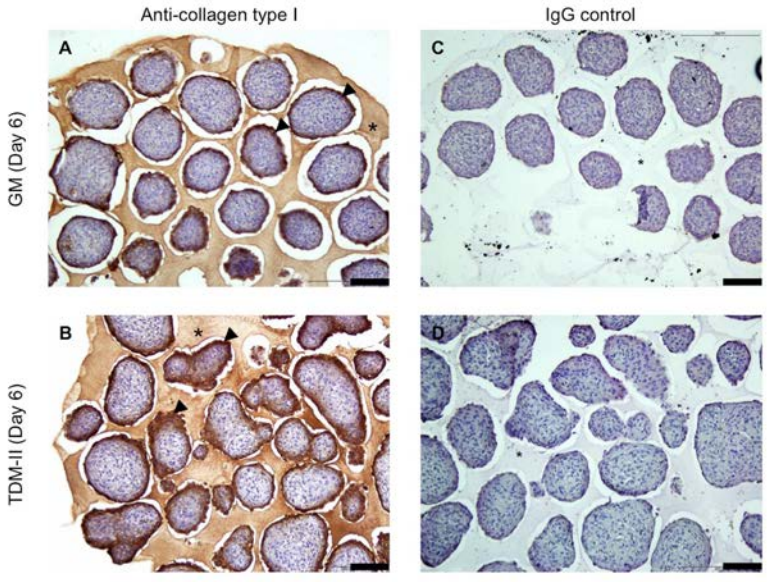

Figure 7

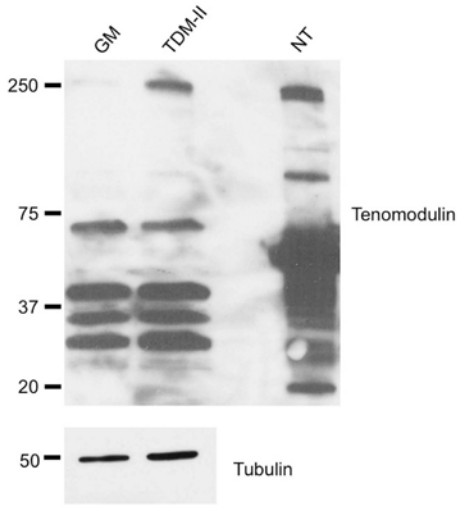

Figure 8

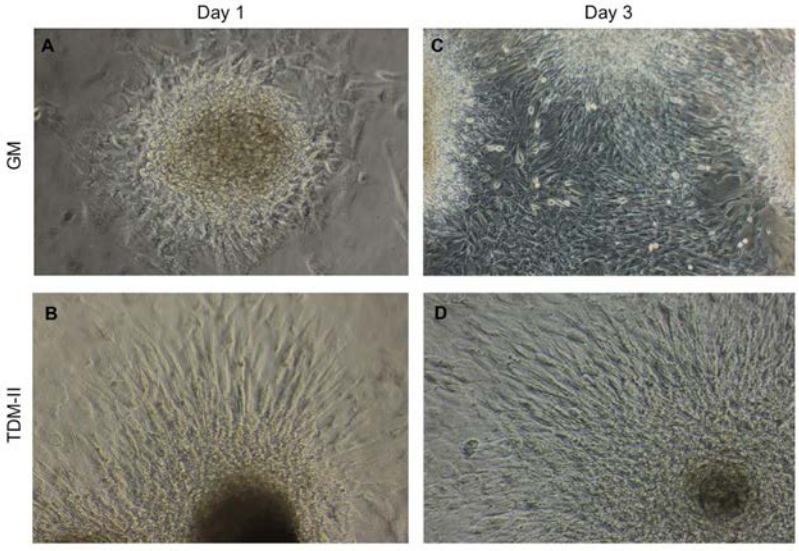

Figure 9

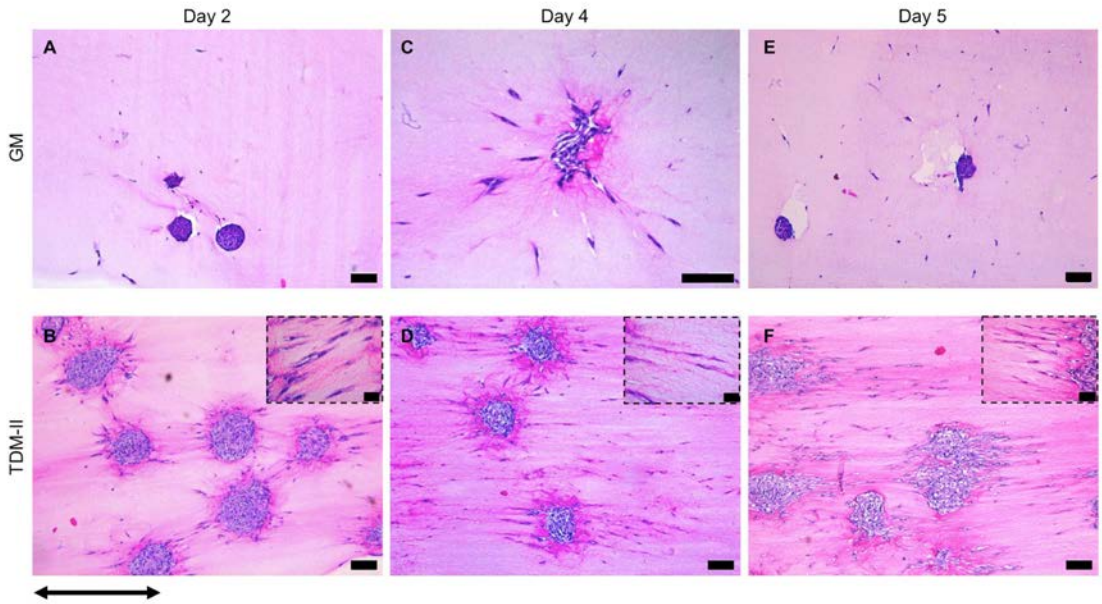

Supplementary Fig. 1

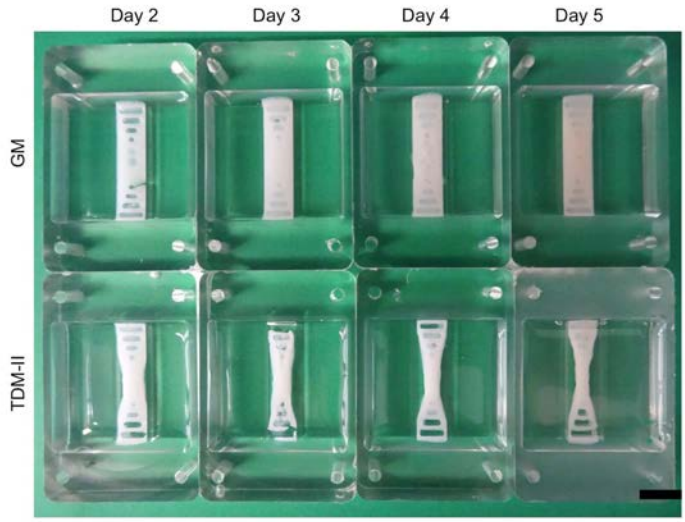

Supplementary Fig. 2

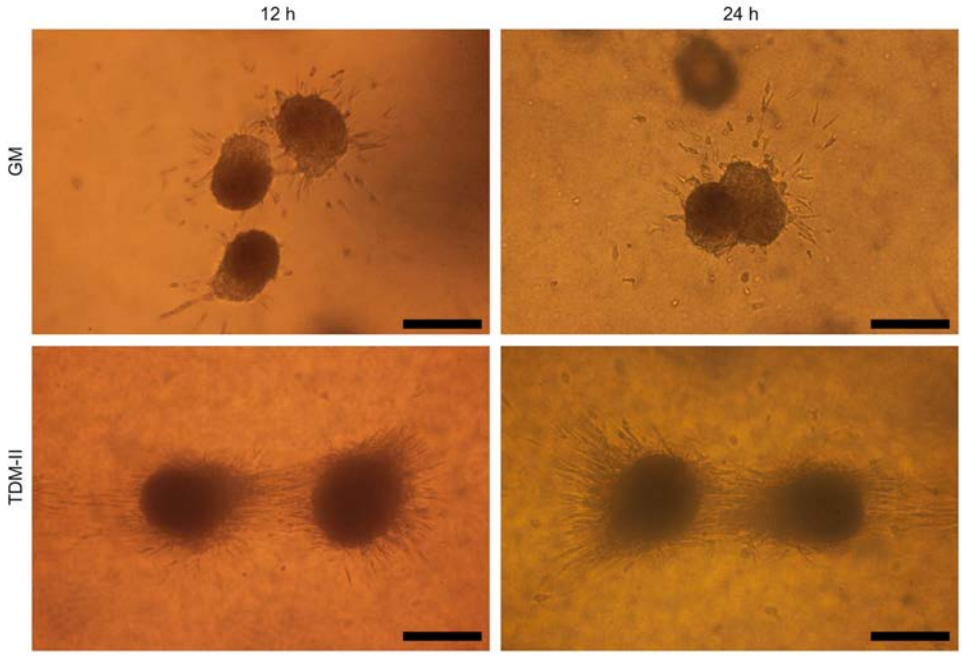

Supplementary Fig. 3

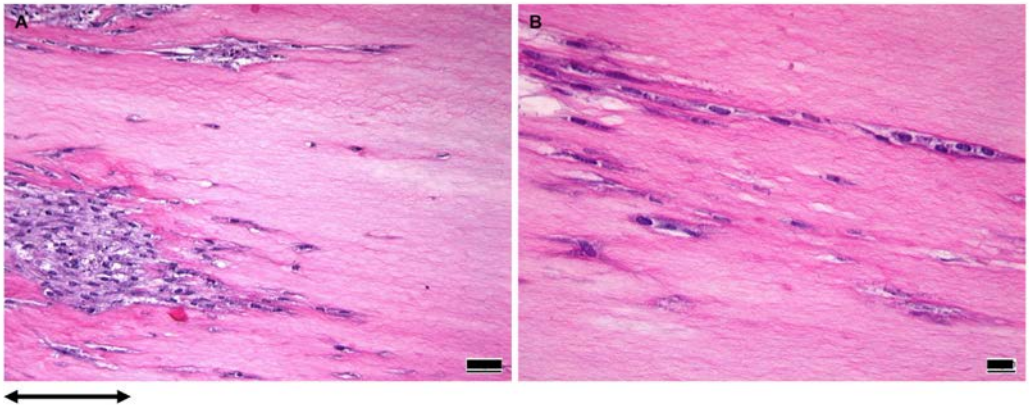

STEM CELLS®
TISSUE-SPECIFIC STEM CELLS

Human Serine Protease HTRA1 Positively Regulates Osteogenesis of Human Bone Marrow-Derived Mesenchymal Stem Cells and Mineralization of Differentiating Bone-Forming Cells Through the Modulation of Extracellular Matrix Protein

ANDRÉ N. TIADEN,[a] MAIKE BREIDEN,[b] ALI MIRSAIDI,[a,c] FABIENNE A. WEBER,[d] GREGOR BAHRENBERG,[a,c] STEPHAN GLANZ,[a,c] PAOLO CINELLI,[d] MICHAEL EHRMANN,[b] PETER J. RICHARDS[a,c]

[a]Bone and Stem Cell Research Group, CABMM, Zurich, [c]Zurich Center for Integrative Human Physiology (ZIHP), Zurich, and [d]Institute of Laboratory Animal Science, University of Zurich, Zurich, Switzerland; [b]Centre for Medical Biotechnology, Faculty of Biology and Geography, University Duisburg-Essen, Essen, Germany

Key Words. HTRA1 protein • Mesenchymal stem cell • Differentiation • Bone mineralization

ABSTRACT

Mammalian high-temperature requirement serine protease A1 (HTRA1) is a secreted member of the trypsin family of serine proteases which can degrade a variety of bone matrix proteins and as such has been implicated in musculoskeletal development. In this study, we have investigated the role of HTRA1 in mesenchymal stem cell (MSC) osteogenesis and suggest a potential mechanism through which it controls matrix mineralization by differentiating bone-forming cells. Osteogenic induction resulted in a significant elevation in the expression and secretion of HTRA1 in MSCs isolated from human bone marrow-derived MSCs (hBMSCs), mouse adipose-derived stromal cells (mASCs), and mouse embryonic stem cells. Recombinant HTRA1 enhanced the osteogenesis of hBMSCs as evidenced by significant changes in several osteogenic markers including integrin-binding sialoprotein (*IBSP*), bone morphogenetic protein 5 (*BMP5*), and sclerostin, and promoted matrix mineralization in differentiating bone-forming osteoblasts. These stimulatory effects were not observed with proteolytically inactive HTRA1 and were abolished by small interfering RNA against *HTRA1*. Moreover, loss of HTRA1 function resulted in enhanced adipogenesis of hBMSCs. HTRA1 Immunofluorescence studies showed colocalization of HTRA1 with IBSP protein in osteogenic mASC spheroid cultures and was confirmed as being a newly identified HTRA1 substrate in cell cultures and in proteolytic enzyme assays. A role for HTRA1 in bone regeneration in vivo was also alluded to in bone fracture repair studies where HTRA1 was found localized predominantly to areas of new bone formation in association with IBSP. These data therefore implicate HTRA1 as having a central role in osteogenesis through modification of proteins within the extracellular matrix. STEM CELLS *2012;30:2271–2282*

Disclosure of potential conflicts of interest is found at the end of this article.

INTRODUCTION

Mammalian high-temperature requirement serine protease A1 (HTRA1) belongs to a well-defined group of serine proteases originally identified in bacteria [1, 2]. They share many common features including a highly conserved trypsin-like serine protease domain and at least one Post synaptic density protein, Drosophila disc large tumor suppressor, and Zonula occludens-1 protein domain at the C terminus. To date, four HTRA1 family members have been identified and are termed HTRA1, HTRA2, HTRA3, and HTRA4. HTRA2 is the best characterized of the four and exists as a membrane protein primarily involved in mitochondrial quality control [2, 3]. Both HTRA1 and HTRA2 are primarily regarded as being key regulators of tumor development and subsequent malignancies [4–6], although a growing body of evidence now exists to suggest that HTRA1 may also play a central role in musculoskeletal development and disease through its proteolytic actions on proteins within the extracellular matrix (ECM) [7–10].

The skeletal ECM is a structurally dynamic scaffold that provides a well-organized framework for mineralization and orchestrates many of the cellular processes required for maintaining bone integrity. The bone tissue ECM comprises 70%–90% mineral and 10%–30% protein, the major proportion of which being glycoproteins such as collagen, fibronectin, and noncollagenous small integrin-binding ligand, N-linked

Author contributions: A.N.T.: collection and/or assembly of data, data analysis and interpretation, and manuscript writing; M.B., A.M., F.W., G.B., and S.G.: collection and/or assembly of data; P.C.: data analysis and interpretation; M.E.: data analysis and interpretation and manuscript writing; P.J.R.: conception and design, financial support, collection and/or assembly of data, data analysis and interpretation, and manuscript writing.

Correspondence: Peter J. Richards, Ph.D., CABMM, University of Zurich, Winterthurerstrasse 190, CH-8057 Zürich, Switzerland. Telephone: +41-44-635-3801; Fax: +41-44-635-6840; e-mail: peter.richards@cabmm.uzh.ch Received May 4, 2012; accepted for publication July 21, 2012; first published online in STEM CELLS *EXPRESS* August 3, 2012. 1066-5099/2012/$30.00/0 doi: 10.1002/stem.1190

glycoproteins (SIBLINGs) [11]. A direct interaction between these proteins and bone progenitor cells is essential for the development of a mineralized matrix [12–14]. Furthermore, degradation of specific glycoproteins within the ECM by serine proteases is also thought to play a central role in controlling mineral deposition by osteoblasts [15].

Bone remodeling and regeneration is a strictly regulated process, being reliant on the activities of resident osteoblasts originating from bone marrow-derived mesenchymal stem cells (BMSCs) through the process of osteogenic differentiation [16]. Osteogenesis is governed by a complex series of well-orchestrated events involving numerous different transcription factors, signaling pathways, and growth factors [17, 18]. The potential involvement of HTRA1 in osteogenesis and bone development has already been alluded to in studies examining the expression profile of *HTRA1* in developing mouse embryos and adult mouse bone where it was identified in osteocytes and osteoblasts within the bone matrix [10, 19]. More recently, it was suggested that HTRA1 may actually play a negative role in bone and mineral development through its ability to inhibit osteoblastic differentiation in the mouse 2T3 cell line [20]. However, no studies have yet sought to determine the influence of HTRA1 on the osteogenic differentiation potential of MSCs.

In this study, we examined the effects of recombinant HTRA1 on the osteogenesis of human BMSCs (hBMSCs) and matrix mineralization by differentiating bone-forming cells with an aim to establish a role for HTRA1 in bone formation. Our results demonstrate that HTRA1 is an essential requirement for osteogenesis and that its effects are mediated primarily through its proteolytic actions on ECM proteins.

Materials and Methods

Materials

4-(2-Aminoethyl) benzenesulfonyl fluoride hydrochloride (AEBSF) was from Sigma-Aldrich (Buchs, Switzerland, http://www.sigmaaldrich.com/). Recombinant integrin-binding sialoprotein (IBSP) was purchased from R&D Systems (Abingdon, U.K., http://www.rndsystems.com/). Monoclonal mouse anti-IBSP, C-terminal region (clone ID1.2) and polyclonal donkey anti-collagen type 1 were from LabForce (Nunningen, Switzerland, http://www.labforce.ch/site/site.asp), polyclonal rabbit anti-IBSP, N-terminal region was from Enzo Life Sciences (Lausen, Switzerland, http://www.enzolifesciences.com/), and polyclonal rabbit anti-HTRA1 was generated as previously described [9]. The biotinylated polyclonal swine anti-rabbit IgG was from DAKO (Baar, Switzerland http://www.dako.com/ch/). All anti-IgG horseradish peroxidase (HRP)-conjugated and fluorescence-conjugated secondary antibodies were from Jackson ImmunoResearch (Suffolk, U.K., http://www.jireurope.com/).

Animals

Experiments were performed using 5-month-old senescence-accelerated resistant mice (SAMR1) ($n = 27$) (Harlan, Netherlands, http://www.harlan.com/). All animal research procedures were approved by the Animal Experimentation Committee of the Veterinary Office of the Canton of Zürich, Switzerland (Project License 140/2005 and 151/2010), and followed the guidelines of the Swiss Federal Veterinary Office for the use and care of laboratory animals.

Cell Culture

Mouse adipose-derived stromal cells (mASCs) were isolated from the inguinal fat pads of SAMR1 mice ($n = 4$) and purity confirmed by fluorescence-activated cell sorting (Sca1, 98%; CD29, 100%; CD105, 42%; CD34, 5%; CD45, 0.5%) as previously reported [21]. Mouse embryonic stem cells (mESCs) (E14 129/Ola) are a well-established cell line and were maintained as previously described [22, 23]. hBMSCs were obtained from Lonza (Verviers, Belgium, http://www.lonza.com/) and were confirmed as being positive for CD105, CD166, CD44, and CD26, and negative for CD14, CD34, and CD45 as stated by the manufacturer. Cells were maintained in normal growth medium consisting of Dulbecco's modified Eagle's medium-low glucose (with Glutamax) (Life Technologies, Zug, Switzerland, http://www.lifetechnologies.com/), supplemented with 10% fetal bovine serum (Invitrogen AG), penicillin (50 units/ml), and streptomycin (50 μg/ml) (Life Technologies, Zug, Switzerland, http://www.lifetechnologies.com/). Cells were used between passages 2 and 6 unless otherwise stated. In some cases, hBMSCs undergoing osteogenic differentiation were treated with recombinant active or inactive HTRA1 (5 μg/ml) for up to 18 days. For protease inhibition studies, AEBSF (20 μg/ml) was also included where indicated. For three-dimensional (3D)-spheroids, mASCs were cultured in 25 μl hanging drops in normal growth medium as described above, using Terasaki plates (VWR, Dietikon, Switzerland, https://ch.vwr.com/) at 2,500 cells per drop.

Induction and Analysis of Differentiation

Well-established differentiation protocols were used to induce and analyze either osteogenesis or adipogenesis in mASCs and E14 129/Ola cells [21] and hBMSCs [24]. For differentiation assays, a starting density of 5,000 and 10,000 cells per square centimeter was used for human and mouse cells, respectively. For osteogenic 3D-spheroid preparations, mASCs were predifferentiated in two-dimensional (2D) cultures for 3 days and cultured in hanging drops containing osteogenic culture medium for a further 2, 4, or 6 days, after which time they were harvested and processed for histological analysis using previously described techniques [25]. Mineralization induced by osteogenic differentiation was identified using Alizarin Red S (Sigma-Aldrich, Buchs, Switzerland, http://www.sigmaaldrich.com/). Adipocyte formation was confirmed by positive staining for oil red O (Sigma-Aldrich, Buchs, Switzerland, http://www.sigmaaldrich.com/). Differentiation markers specific to either osteogenesis or adipogenesis were also quantified by reverse-transcription polymerase chain reaction (qRT-PCR) using TaqMan Gene Expression Assays (Life Technologies, Zug, Switzerland, http://www.lifetechnologies.com/) (Supporting Information Table S1). Total RNA was harvested from cells at given time points during differentiation, 0.5 μg total RNA was reverse-transcribed using Superscript II (Life Technologies, Zug, Switzerland, http://www.lifetechnologies.com/), and an equivalent of 10 ng total RNA was applied as cDNA template in the successive qRT-PCR reaction using the StepOnePlus (LifeTechnologies, Zug, Switzerland, http://www.lifetechnologies.com/).

Recombinant HTRA1 Production

Purified recombinant active HTRA1 (HTRA1Δmac) and inactive HTRA1 (HTRA1ΔmacSA) were produced in *Escherichia coli* and purified using metal-affinity chromatography as previously described [26].

SDS-PAGE and Western Blotting

Protein was analyzed by SDS-PAGE using 4%–15% precast Tris-HCl gels (BioRad, Reinach, Switzerland, http://www3.bio-rad.com/) under reducing conditions and electroblotted onto PVDF membranes using the Trans-Blot Turbo blotting system (BioRad, Reinach, Switzerland, http://www3.bio-rad.com/). IBSP was identified using antibodies raised against either the N-terminal (1:800) or C-terminal (1:500) regions of human IBSP and detected using HRP-conjugated secondary antibodies (1:10,000) followed by incubation in SuperSignal West Pico Chemiluminescent Substrate (Thermo Fisher Scientific, Lausanne, Switzerland, http://www.piercenet.com/) and exposure to x-ray film.

Immunofluorescence

Cells in either 2D or 3D cultures were fixed in phosphate buffered saline (PBS) buffered formaldehyde (4%) or ice-cold methanol, blocked with normal goat serum (1:10) and incubated with polyclonal rabbit anti-HTRA1 (1:50), polyclonal donkey anti-collagen type 1 (1:50), or monoclonal mouse anti-IBSP (1:50) in PBS containing 1% bovine serum albumin (BSA) overnight at 4°C. For paraffin wax sections, staining reactions were performed at 37°C for 1 hour. In the case of double immunostaining procedures, samples were incubated with both polyclonal rabbit anti-HTRA1 (1:50) and monoclonal mouse anti-IBSP (1:50) using the conditions described above. Samples were then washed and incubated with either goat anti-rabbit-Cy3 (1:400), goat anti-donkey-Cy3 (1:400), or goat anti-mouse-Cy5 (1:400) for 1 hour and mounted in 4,6-diamidino-2-phenylindole containing mounting solution and images captured using the Leica DMI6000B automated inverted research microscope system (Leica Microsystems, Heerbrugg, Switzerland, http://www.leica-microsystems.com/).

Immunohistochemistry. Dewaxed paraffin sections (8 μm) were rehydrated and blocked with normal swine serum (Dako Baar, Switzerland, http://www.dako.com/ch/) for 30 minutes. Sections were then incubated with polyclonal rabbit anti-HTRA1 (1:50) for 1 hour at 37°C. Sections were then washed in PBS and incubated with biotinylated swine anti-rabbit IgG (1:500) for 1 hour at room temperature followed by washing and a further incubation for 30 minutes with Vectastain (Reactolab, Servion, Switzerland, http://www.vectorlabs.com/). Sections were then developed using 3,3′ diaminobenzidine tetrahydrochloride, counterstained with Harris' Hematoxylin and mounted in dibutylphthalate polystyrene xylene (DPX).

Proteolytic Enzyme Assays

Degradation of IBSP by HTRA1 was determined using methods previously described [9]. Briefly, HTRA1 (45 nM) and IBSP (476 nM) were incubated in 50 mM Tris-HCl, pH 8.5, and 150 mM NaCl for up to 24 hours at 37°C. In some reactions, active HTRA1 was replaced by proteolytically inactive HTRA1. Proteins were separated on a 4%–15% SDS-PAGE gel and analyzed by Western blot as described above. The proteolytic activity of HTRA1 was also investigated in hBMSC cultures using immunofluorescence staining. Cells were incubated in osteogenic induction medium either without or with active or inactive HTRA1 (5 μg/ml), fixed in methanol and IBSP or collagen type 1 detected with specific antibodies using methods as described above.

HTRA1 Enzyme-Linked Immunosorbent Assay

The HTRA1 enzyme-linked immunosorbent assay (ELISA) was performed using HTRA1 specific monoclonal and polyclonal antibodies as previously described [9].

HTRA1 Small Interfering RNA

Specific knockdown of *HTRA1* expression was performed with Silencer Select small interfering RNA (siRNA) oligos (Life Technologies, Zug, Switzerland, http://www.lifetechnologies.com/), according to the manufacturer's protocol. hBMSCs (1×10^5 cells) were transfected with 100 nM *HTRA1*-specific (s11279, s11280) or negative control siRNA (Negative Control-1) using the NEON Transfection System (Life Technologies, Zug, Switzerland, http://www.lifetechnologies.com/). Following transfection, cells were seeded in cell culture plates with fresh growth medium (without antibiotics) and incubated for 24 hours at 37°C, 5% CO_2. Medium was then replaced with either fresh growth medium or differentiation medium and total RNA and supernatants were harvested at selected time points for further analysis.

Fracture Model

A rigidly stabilized, unilateral mid-diaphyseal osteotomy gap was created in the femurs of SAMR1 mice ($n = 5$–6 per time point) using a 0.22 mm gigli saw as previously described [24]. The immunohistochemical and immunofluorescence techniques described above were used to detect both HTRA1 and IBSP protein in decalcified paraffin wax sections (8 μm) from mouse femora at various stages of repair ($n = 3$ per time point).

Statistical Analysis

All statistical analyses were carried out using SPSS18.0 (SPSS Inc., Chicago, IL). Parametric analysis of normally distributed data was performed using the two-tailed unpaired Student's t test for comparison of two groups or one-way analysis of variance followed by Tukey's post hoc test for multiple group comparisons. The sample size used in each study was based upon the observed level of variation between individual experiments and the need for sufficient sample numbers to allow for accurate statistical analyses. In all cases, a p-value of $<.05$ was considered statistically significant, and all data were expressed as mean ± SD.

Results

HTRA1 Production Is Upregulated During Osteogenic Induction of MSCs

Differentiation studies conducted using hBMSCs demonstrated a small but significant increase in the expression of *HTRA1* during the early phases of osteogenic induction with a greater than 1.5-fold ($p < .01$) increase in gene expression being attained by day 14 (Fig. 1A). However, unlike *HTRA1*, expression levels of the closely related HTRA family member, *HTRA3*, decreased during osteogenesis and remained significantly downregulated throughout the course of the study. The early induction of *HTRA1* gene expression was accompanied by significant increases in the expression of the well-known osteogenic markers runt-related transcription factor 2 (*RUNX2*), alkaline phosphatase (*ALP*), *IBSP*, and Collagen type 1A1 (Fig. 1A). The expression level of the late osteogenic marker secreted phosphoprotein 1/osteopontin (*SPP1*) was actually downregulated during early osteogenesis but became significantly increased during the late phase of osteogenesis at day 21, along with noticeable increases in mineralized matrix deposition beginning at day 10 as determined by Alizarin red staining (Fig. 1B). As HTRA1 functions primarily as a secreted protease, we also investigated the effect of osteogenic differentiation on HTRA1 protein secretion from hBMSCs using an HTRA1-specific ELISA and immunofluorescence staining. In accordance with increases in its gene expression, secreted HTRA1 protein levels were also elevated in both the supernatant (Fig. 1C) and in the cell matrices (Fig. 1D) of hBMSC cultures undergoing osteogenic differentiation. Clearly, therefore, induction of osteogenesis in hBMSCs has a major stimulatory effect on HTRA1 production resulting in both enhanced gene expression as well as protein secretion.

In order to investigate whether such effects were limited to adult human stem cells only, we extended these studies to include both mESCs and mASCs. *HtrA1* expression was also significantly upregulated in a time-dependent manner in mESCs (Fig. 2A) and mASCs grown in either 2D- (Fig. 2B) or 3D- (Fig. 2C) culture systems in response to osteogenic stimuli. These increases in *HtrA1* expression were associated with mineralization of differentiating bone-forming cells derived from 2D-culutres of either mESCs

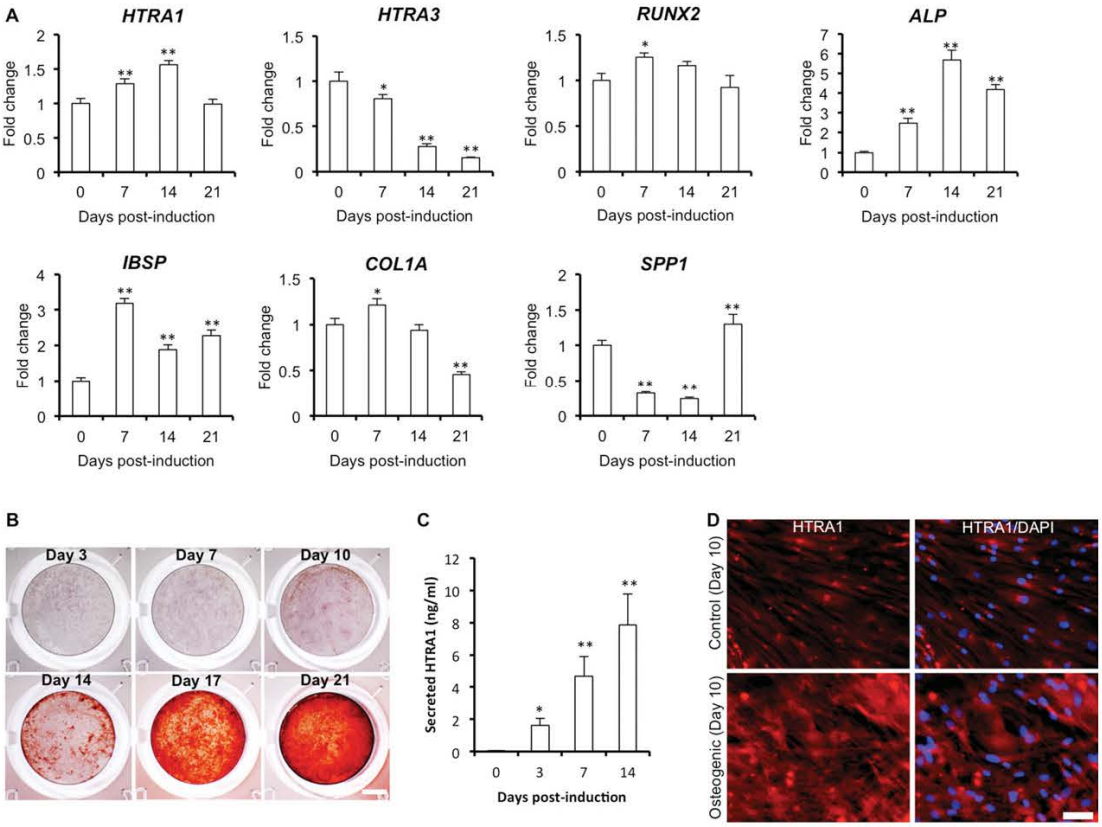

Figure 1. The expression and secretion of HTRA1 is significantly enhanced in human bone marrow-derived MSCs (hBMSCs) undergoing osteogenic differentiation. (**A**): Quantitative polymerase chain reaction analysis of genes regulated during osteogenic differentiation of hBMSCs. Data were normalized to beta glucuronidase and expressed as fold change as compared to noninduced controls at day 0 (value 1) using the comparative C_T method. Data are representative of two independent experiments performed in triplicate ± SD. *, $p < .05$; **, $p < .01$ as determined by one-way analysis of variance (ANOVA). (**B**): Representative images of Alizarin red-stained hBMSC cultures at various time points following osteogenic induction. Scale bar = 2 mm. (**C**): Secretion of HTRA1 by hBMSCs during osteogenic differentiation as determined by HTRA1-specific ELISA ($n = 4$). *, $p < .05$; **, $p < .01$ as determined by one-way ANOVA. (**D**): Representative fluorescence images of anti-HTRA1 (red) and DAPI (blue)-stained hBMSCs undergoing osteogenic differentiation. Scale bar = 25 μm. Abbreviations: ALP, alkaline phosphatase; COL1A, collagen type 1A1; DAPI, 4,6-diamidino-2-phenylindole; HTRA1, high-temperature requirement protease A1; IBSP, integrin-binding sialoprotein; RUNX2, runt-related transcription factor 2; SPP1, secreted phosphoprotein 1.

(Fig. 2D) or mASCs (Fig. 2E) as well as 3D-cultures composed of osteogenic mASCs (Fig. 2F). Furthermore, immunofluorescence staining of paraffin wax sections from mASC 3D-spheroids identified HtrA1 protein in tissues undergoing mineralization, but not in uninduced controls (Fig. 2G), thus giving a first hint as to its role in stem cell osteogenesis.

Silencing of the *HTRA1* Gene Impairs hBMSC Osteogenesis and Enhances Adipogenesis

In order to investigate the role of *HTRA1* gene expression in the regulation of osteogenesis, we next performed loss of function studies by means of RNA interference in hBMSC cultures. The transfection of hBMSCs with siRNA specific for *HTRA1* prior to osteogenic induction resulted in a significant downregulation of *HTRA1* gene expression (Fig. 3A) and HTRA1 protein secretion (Fig. 3B) that was sustained throughout the first 2 weeks of osteogenic differentiation. HTRA1 protein levels both within cells and the ECM were also markedly reduced (Supporting Information Fig. S1). This was accompanied by a noticeable reduction in Alizarin red staining at day 14, indicative of reduced mineral deposition in differentiating bone-forming cells (Fig. 3C). Biochemical analysis using the ALP activity assay revealed that these deficits in mineralization were accompanied by significant reductions in ALP protein activity, which were maintained for up to 14 days (Fig. 3D). Furthermore, *ALP* expression was also significantly downregulated in these cells at an early time point, although expression levels of the osteogenic markers *SPP1* and *RUNX2* were not significantly affected by *HTRA1* silencing (Fig. 3E).

Through the course of our studies, it became apparent that not only was osteogenesis reduced in hBMSCs following *HTRA1* gene silencing but also that the adipogenesis appeared to actually be increased. Evidence of this was first realized in late-stage osteogenic cultures of hBMSC treated with *HTRA1* siRNA, where phase-contrast microscopy revealed more cells containing lipid droplets, reminiscent of mature adipocytes although control siRNA cultures continued to demonstrate matrix mineralization (Fig. 3F). In order to confirm this finding, hBMSCs transfected with

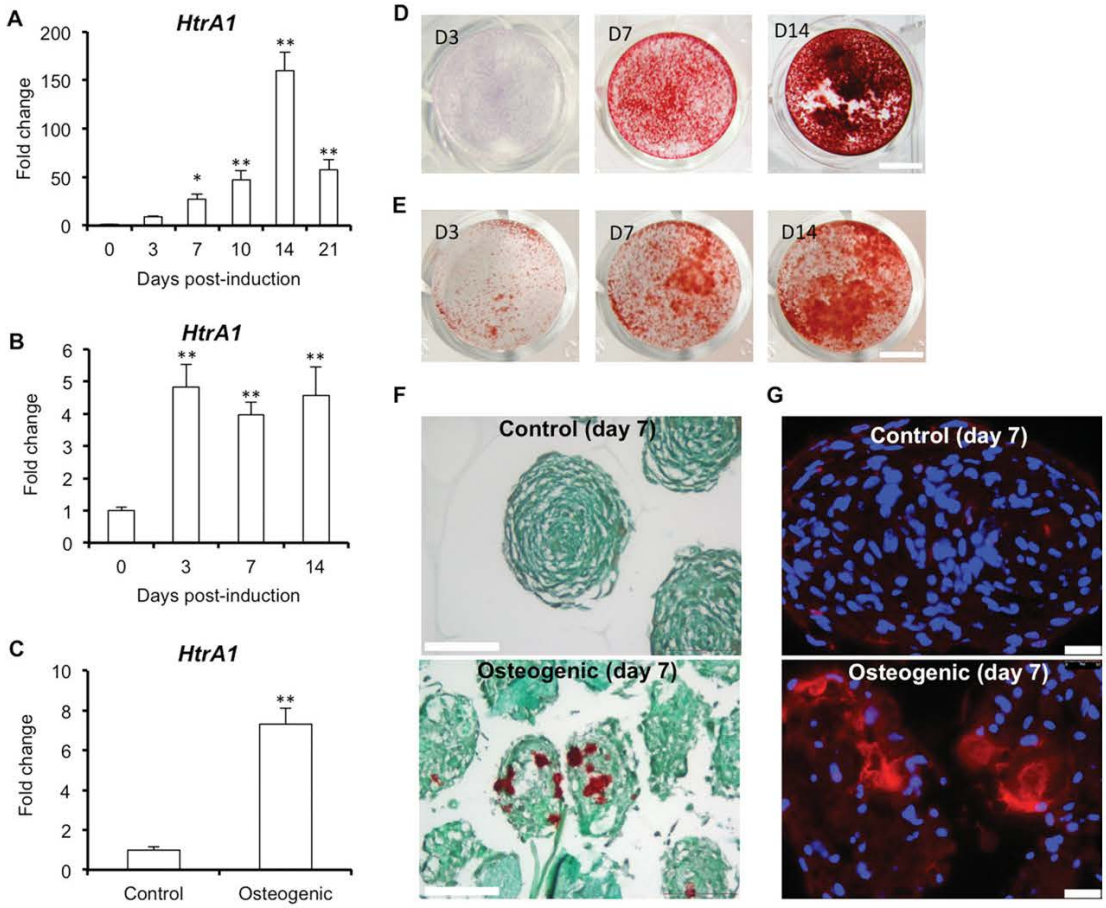

Figure 2. *HtrA1* gene expression is significantly increased in osteogenic mouse embryonic stem cells (mESCs) and mouse adipose-derived stromal cells (mASCs). **(A–C):** *HtrA1* gene expression during osteogenic differentiation of mESCs (A), mASCs (B), and mASC spheroids (day 7) (C) was determined by quantitative polymerase chain reaction and data were normalized to *Mrps12* and expressed as fold change as compared to noninduced controls (Day 0 and control; value 1) using the comparative C_T method. Data are representative of at least two independent experiments performed in triplicate ± SD. *, $p < .05$; **, $p < .01$ as determined by one-way analysis of variance. **(D, E):** Representative images of Alizarin red-stained mESCs (D) and mASCs (E) at various time points following osteogenic induction. Scale bar = 5 mm. **(F):** Representative images of Alizarin red and fast green-stained paraffin wax sections of mASC spheroids incubated without (control) or with osteogenic media (osteogenic) for 7 days. Scale bar = 100 μm. **(G):** Representative immunofluorescence images of HTRA1 (red) and 4,6-diamidino-2-phenylindole (blue) in paraffin wax sections of osteogenic mASC spheroids incubated without (control) or with osteogenic media (osteogenic) for 7 days. Scale bar = 25 μm. Abbreviation: HTRA1, high-temperature requirement protease A1.

either *HTRA1* siRNA or control siRNA were induced to undergo adipogenic differentiation and adipogenic gene expression measured by qRT-PCR (Fig. 3G) and triglyceride accumulation visualized by oil red O staining (Fig. 3H). As anticipated, silencing of the *HTRA1* gene greatly enhanced the number of oil red O-positive cells present with the hBMSC culture and significantly enhanced the expression of specific adipogenic gene markers, peroxisome proliferator-activated receptor gamma 2, and fatty acid binding protein 4, thereby supporting a differential role for HTRA1 in hBMSC lineage commitment.

Recombinant HTRA1 Protein Enhances hBMSC Osteogenesis

As previously mentioned, HTRA1 also exists as a secreted protease and thus may have an extracellular role in the osteogenic differentiation of hBMSCs. We therefore next investigated whether exogenously added recombinant human HTRA1 protein could also influence osteogenic differentiation. hBMSCs undergoing osteogenic differentiation were initially treated every 3 days with either active or inactive HTRA1 for up to 14 days and mineralization determined by Alizarin red staining. Indeed, mineral deposition by differentiating bone-forming cells was greatly enhanced following stimulation with active, but not inactive, HTRA1 (Fig. 4B). Additional studies confirmed that these effects could be reproduced in late-stage (day 10) cultures of osteogenic hBMSCs treated for only 4 days with HTRA1 (Fig. 4C). However, short-term treatment with HTRA1 during the first week of osteogenic differentiation only failed to elicit any noticeable increase in mineralization (Supporting Information Fig. S2), thus implying that the stimulatory actions of HTRA1 were dependent not only on its protease activity but also on the differentiation status of the cells. Further studies using the broad spectrum serine protease inhibitor, AEBSF, confirmed the

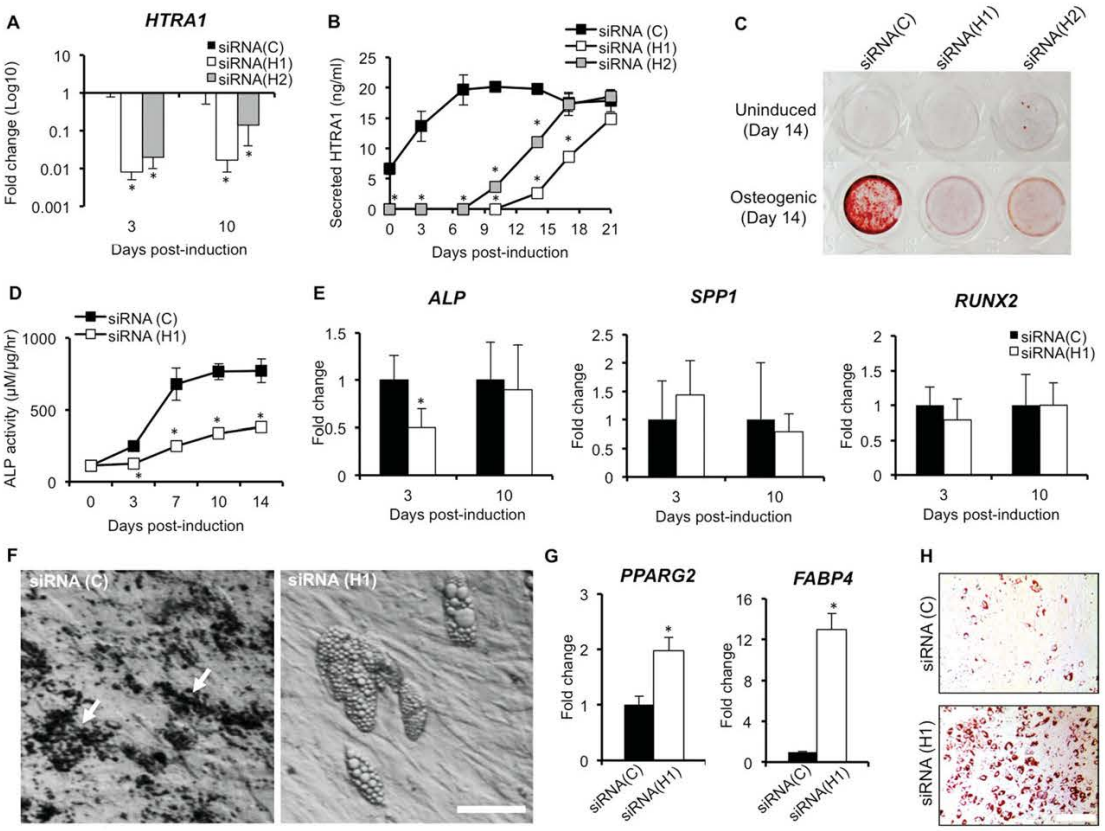

Figure 3. Repression of *HTRA1* gene expression alters lineage commitment of differentiating human bone marrow-derived mesenchymal stem cells (hBMSCs). (**A**): Quantitative polymerase chain reaction analysis of *HTRA1* gene expression in hBMSCs transfected with *HTRA1* siRNAs (siRNA [H1] or [H2]) or control siRNA (siRNA (C)) at 3 and 10 days postosteogenic induction. Data were normalized to beta glucuronidase (*GUSB*) and expressed as fold change (Log10 scale) as compared to cells transfected with control siRNA using the comparative C_T method. *, $p < .01$ as determined by one-way analysis of variance (ANOVA). $n = 3$ separate experiments, ± SD. (**B**): Enzyme-linked immunosorbent assay measurement of secreted HTRA1 from hBMSCs transfected with *HTRA1* siRNAs or control siRNA at various time points postosteogenic induction. *, $p < .01$ as determined by one-way ANOVA. $n = 3$ separate experiments, ± SD. (**C**): Representative images of Alizarin red-stained hBMSCs transfected with *HTRA1* siRNAs or control siRNA at 14 days postosteogenic induction. (**D**): ALP activity in protein lysates from hBMSC transfected with *HTRA1* siRNA or control siRNA at various time points postosteogenic induction. *, $p < .01$ as determined by one-way ANOVA. $n = 3$ separate experiments, ± SD. (**E**): Quantitative polymerase chain reaction analysis of *ALP*, *SPP1*, and *RUNX2* gene expression in hBMSCs transfected with *HTRA1* siRNA or control siRNA at 3 and 10 days postosteogenic induction. Data were normalized to *GUSB* and expressed as fold change as compared to cells transfected with a control siRNA (value 1) using the comparative C_T method. $n = 3$ separate experiments, ± SD. (**F**): Representative phase-contrast micrographs of hBMSCs transfected with control siRNA or *HTRA1* siRNA at 14 days postosteogenic induction. Arrows, mineral deposits. Scale bar = 10 μm. (**G**): Quantitative polymerase chain reaction analysis of *PPARG2* and *FABP4* gene expression in hBMSCs transfected with *HTRA1* siRNA or control siRNA at day 6 postadipogenic induction. Data were normalized to *GUSB* and expressed as fold change as compared to cells transfected with a control siRNA (value 1) using the comparative C_T method. Data are representative of two separate experiments, ± SD. *, $p < .01$ as determined by one-way ANOVA. (**H**): Microscopic images of oil red O-stained hBMSCs transfected with *HTRA1* siRNA or control siRNA at 7 days postadipogenic induction. Scale bar = 20 μm. Images are representative of two separate experiments. Abbreviations: *ALP*, alkaline phosphatase; *FABP4*, fatty acid binding protein 4; HTRA1, high-temperature requirement protease A1; *PPARG2*, peroxisome proliferator-activated receptor gamma 2; *RUNX2*, runt-related transcription factor 2; siRNA, small interfering ribonucleic acid; *SPP1*, secreted phosphoprotein 1.

stimulatory effects of HTRA1 to be dependent on its proteolytic activity (Fig. 4D). Although matrix mineralization was clearly enhanced in differentiating bone-forming cells treated with HTRA1, the expression of several well-known osteogenic markers including *ALP*, *RUNX2*, and *SPP1* remained unaltered at the time point tested (day 10) (Fig. 4E). However, significant increases were observed in the expression levels of *IBSP* and bone morphogenetic protein 5 (*BMP5*). Furthermore, a significant decrease in the expression level of sclerostin (*SOST*) was also observed in cells treated with HTRA1.

IBSP Represents a Novel HTRA1 Substrate During Osteogenic Differentiation of MSCs In Vitro

In this study, we demonstrated that although *IBSP* expression was significantly enhanced in hBMSCs following the addition of HTRA1, IBSP protein was almost completely abolished from the cellular matrix of these cultures, an effect not observed with inactive HTRA1 (Fig. 5A). This was regarded as being specifically due to the HTRA1 protein added due to the fact that collagen Type 1, a proteoglycan not degraded by HTRA1 [20], remained unaffected within the cell matrices

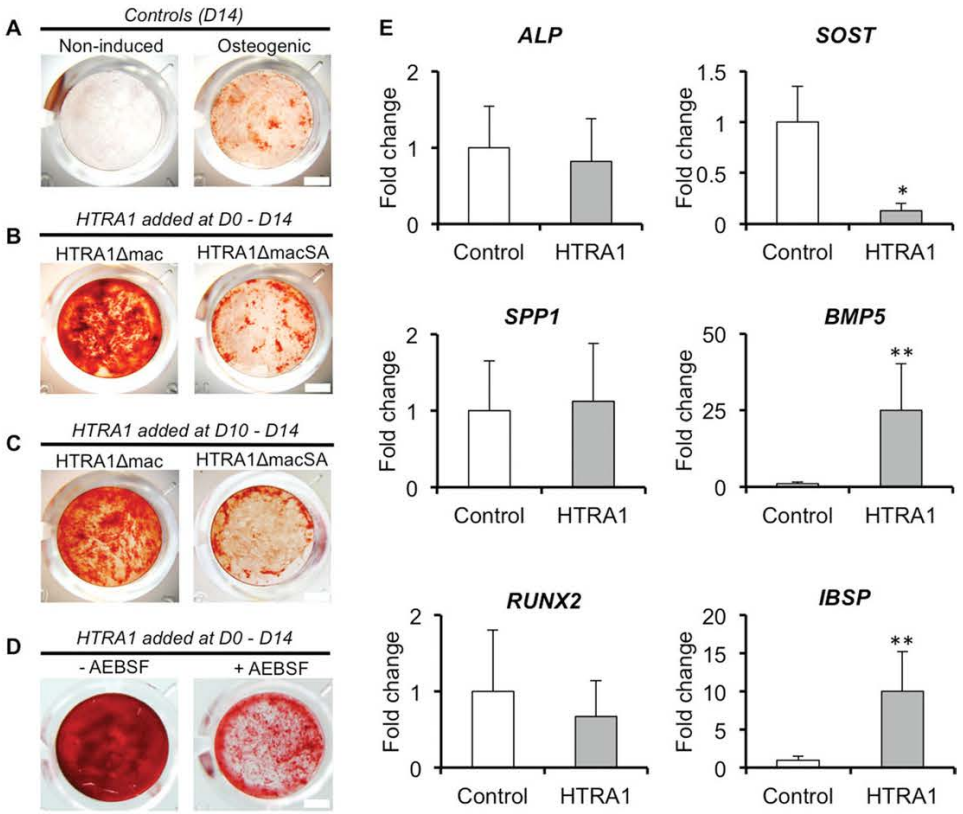

Figure 4. Exogenously added HTRA1 protein enhances human bone marrow-derived mesenchymal stem cell (hBMSC) osteogenic differentiation. **(A–D):** Representative images of Alizarin red-stained day 14 cultures of noninduced hBMSCs (noninduced control) and osteogenic-induced hBMSCs (A), osteogenic-induced hBMSCs previously treated with either proteolytically active (HTRA1Δmac) or inactive (HTRA1ΔmacSA) HTRA1 (5 μg/ml) for 14 days (B) or 4 days (C), and osteogenic-induced hBMSCs previously treated with proteolytically active HTRA1 (5 μg/ml) for 14 days in the presence or absence of AEBSF (20 μg/ml) (D). Data are representative of three independent experiments. Scale bar = 2 mm. **(E):** Quantitative polymerase chain reaction analysis of osteogenic gene expression in hBMSCs treated at day 7 with active HTRA1 (5 μg/ml) and harvested at day 10 postosteogenic induction. Data were normalized to beta glucuronidase and expressed as fold change as compared to untreated cells (value 1) using the comparative C_T method. $n = 3$ separate experiments, ± SD. *, $p < .05$; **, $p < .01$ as determined by Student's t test. Abbreviations: AEBSF, 4-(2-aminoethyl) benzenesulfonyl fluoride hydrochloride; *ALP*, alkaline phosphatase; BMP5, bone morphogenetic protein 5; HTRA1, high-temperature requirement protease A1; IBSP, integrin-binding sialoprotein; RUNX2, runt-related transcription factor 2; SPP1, secreted phosphoprotein 1.

(Supporting Information Fig. S3). The potential for proteolytically active HTRA1 to degrade IBSP was further confirmed by in vitro enzyme assays, where a noticeable reduction in recombinant human IBSP (476 nM) was evident after 8 hours incubation with HTRA1 (45 nM) as determined by Western blot analysis (Fig. 5B). We next used the mASC spheroid culture system to investigate whether endogenous HTRA1 protein could be localized to IBSP directly within differentiating MSCs. Paraffin wax sections of mASCs were stained for HTRA1 and IBSP at various stages of osteogenic differentiation and overlays produced to determine whether HTRA1 could be localized to areas of IBSP protein expression. IBSP was detected within mASC spheroids during the early phase of osteogenesis (day 5), although HTRA1 remained at very low levels and mineral deposition was not detected using Alizarin red staining (Fig. 5C, upper panel and Supporting Information Fig. S4A). By day 9, levels of HTRA1 had greatly increased and it was regularly found colocalized with IBSP in the tissue matrix (Fig. 5C, lower panel). In addition, mineralization of differentiating bone-forming cells within 3D-spheroids was also apparent at this time point as identified by intense Alizarin red staining (Supporting Information Fig. S4B). Sections incubated with isotype-matched IgG antibodies stained negative and served as controls (Supporting Information Fig. S4C).

Localization of HTRA1 and IBSP to Areas of New Bone Formation in Mice

In order to assess the potential involvement of HTRA1 in the reparative process of bone tissue, we used a previously well-established mouse femur osteotomy model (Fig. 6A) [24]. HTRA1 protein was identified in thin paraffin wax bone sections taken from mice at various stages of fracture repair using immunohistochemical staining. At day 7, early osteoid formation was observed within the bone marrow at the osteotomy site and was associated with intense staining for HTRA1 (Fig. 6B). At this time point, HTRA1 was also located within the cells and tissue of the overlying periosteal layer (Supporting Information Fig. S5A). By day 14, the nonmineralized callus had increased greatly in size with numerous HTRA1-positive fibroblast-like cells present throughout the tissue as well as in cells of the newly forming callus (Fig. 6C and Supporting Information Fig. S5B). Large numbers of HTRA1-

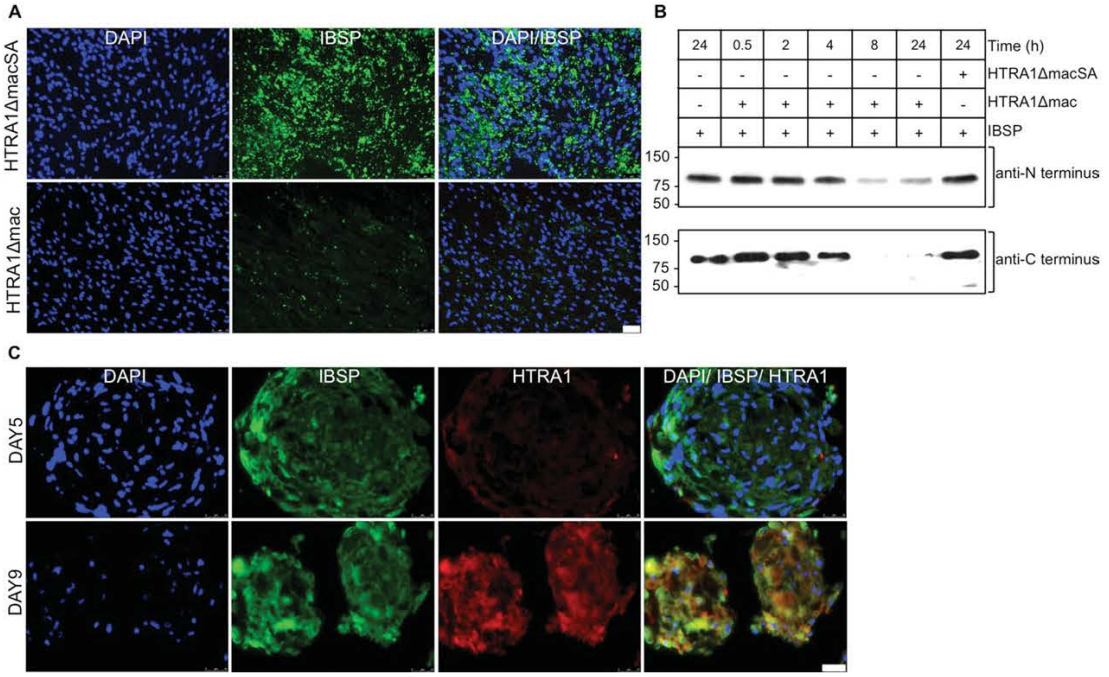

Figure 5. IBSP is an HTRA1 substrate in osteogenic mesenchymal stem cell cultures. (**A**): Representative immunofluorescence micrographs of anti-IBSP (ID1.2) (green) and DAPI (blue)-stained day 14 osteogenic human bone marrow-derived mesenchymal stem cells cultures previously treated for 4 days with 5 μg/ml of either inactive HTRA1 (HTRA1ΔmacSA) or active HTRA1 (HTRA1Δmac). Scale bar = 75 μm. (**B**): Western blot analysis of an in vitro enzyme assay using recombinant human IBSP (476 nM) and HTRA1ΔmacSA (45 nM) or HTRA1Δmac (45 nM), incubated together for up to 24 hours. Equal sample volumes were loaded onto an SDS-PAGE gel and IBSP protein detected using antibodies directed against either the N- or C-terminal regions of human IBSP. (**C**): Representative fluorescence images of anti-IBSP (ID1.2) (green), anti-HTRA1 (red), and DAPI (blue)-stained mouse adipose-derived stromal cell spheroids at 5 and 9 days postosteogenic induction. Scale bar = 25 μm. Data are representative of two independent experiments. Abbreviations: DAPI, 4,6-diamidino-2-phenylindole; HTRA1, high-temperature requirement protease A1; *IBSP*, integrin-binding sialoprotein.

positive chondrocytes were also evident within intact lacunae and represented the early stages of endochondral ossification. By day 28, a substantial proportion of the callus had been replaced by new bone and HTRA1 was now localized to specific areas of active bone formation (Fig. 6D) in association with cuboidal osteoblasts (Supporting Information Fig. S5C). By day 42, the osteotomy gap was almost completely healed (Fig. 6E) and the bone resembled that of a nonoperative control femur (Fig. 6F). In both cases, HTRA1 was almost completely absent, being localized to only a small number of osteocytes within the bone matrix.

Having confirmed that HTRA1 protein was indeed present within actively forming bone tissue, we conducted further investigations to determine whether HTRA1 could also be localized to IBSP within these bone sections, thus providing a potential mode of action for HTRA1 in the context of osteogenesis in vivo. Indeed, colocalization of HTRA1 and IBSP was identified in paraffin wax bone sections from 28-day postoperative mice by double immunofluorescence staining, being confined to areas previously identified as undergoing active regeneration (Fig. 7 and Supporting Information Fig. S6).

Discussion

A complex molecular network of signaling pathways and regulatory factors governs the osteogenesis of multipotent MSCs [17, 18, 27], being reliant on the activation and regulation of a number of key molecular targets including *RUNX2*, *ALP*, *SPP1*, and *IBSP* [28]. Although there have been significant advances in our understanding of the molecular mechanisms involved in controlling osteogenic differentiation, the influence of serine proteases on such processes remains relatively obscure. In this study, we have shown for the first time that the serine protease HTRA1 is a positive regulator of MSC osteogenesis and its presence is required for the efficient mineralization of differentiating bone cells.

The expression of *HTRA1* was upregulated in hBMSCs upon osteogenic induction and was associated with significant increases in the levels of its secreted protein product. Furthermore, HTRA1 production was increased in a time-dependent manner throughout the course of osteogenic differentiation and was closely associated with the appearance of mineralized matrix. Interestingly, expression levels of the closely related HTRA family member, *HTRA3*, were actually downregulated during osteogenesis. This was of particular interest as HTRA1 and HTRA3 are considered to have overlapping functions due to close structural similarities [29]. It may well be therefore that HTRA1 and HTRA3 play differential roles in mediating the osteogenesis of hBMSCs. This pattern of HTRA1 production during osteogenesis of hBMSCs was recapitulated in cultures composed of either mASCs or mESCs, where significant increases in *HtrA1* expression coincided with the appearance of HtrA1 protein and mineralized matrix. Although previous investigations have alluded to the involvement of HTRA1 in mouse osteogenesis [19, 20], our study is the first to report the potential

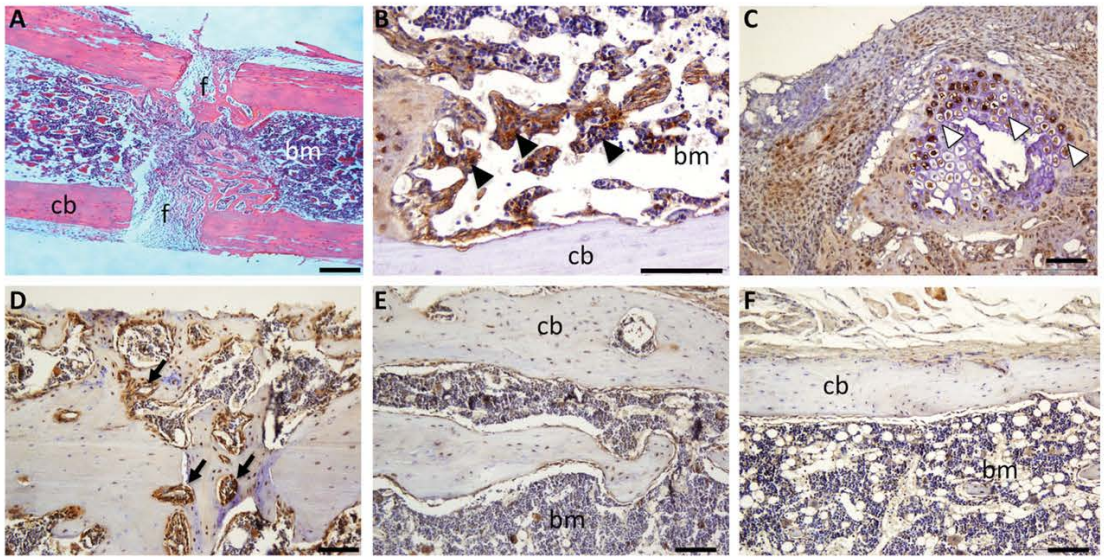

Figure 6. High-temperature requirement protease A1 (HTRA1) protein levels are increased during bone regeneration. (**A**): Representative micrograph of a hematoxylin and eosin-stained paraffin wax section of decalcified mouse femur 7 days following a 0.22 μm osteotomy. Scale bar = 250 μm. **(B–F):** Representative micrographs of anti-HTRA1 (brown)-stained paraffin wax sections of decalcified mouse femora (representative of $n = 3$) at 7 (B), 14 (C), 28 (D), and 42 (E) days following osteotomy. Nonoperative femora served as controls (F). HTRA1 was visualized using horseradish peroxidase-diaminodenzidine and sections counterstained with hematoxylin. HTRA1-positive staining is identified in osteoid (closed arrow heads) at day 7 (B), in chondrocyte lacunae (open arrow heads) and soft tissue, *t*, at day 14 (C), and in sites of active bone regeneration (arrows) at day 28 (D). Scale bar = 100 μm. Abbreviations: bm, bone marrow; cb, cortical bone; f, fracture gap.

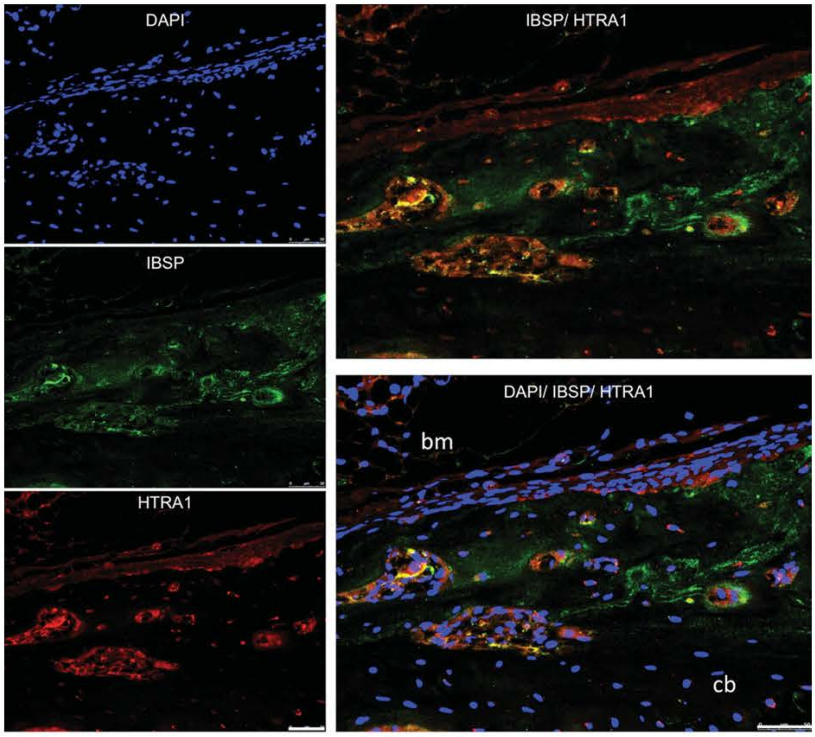

Figure 7. HTRA1 and IBSP colocalize during bone regeneration. Representative immunofluorescence micrographs of paraffin wax sections of decalcified mouse femora at 28 days following osteotomy stained with DAPI (blue), anti-IBSP (ID1.2) (green), and anti-HTRA1 (red). Scale bar = 50 μm. Abbreviations: bm, bone marrow; cb, cortical bone; DAPI, 4,6-diamidino-2-phenylindole; HTRA1, high-temperature requirement protease A1; IBSP, integrin-binding sialoprotein.

role of HTRA1 in human osteogenesis. Based on earlier reports of HTRA1 imparting a negative influence over mineral deposition by murine 2T3 osteoblasts [20], initial expectations were for HTRA1 to inhibit osteogenesis of hBMSCs and thus prevent mineralization of differentiating human bone-forming cells. On the contrary, we found that siRNA-induced loss of HTRA1 function in hBMSCs, effectively suppressed the stimulatory effects of osteogenic culture medium on *ALP* expression and intracellular ALP protein activity by hBMSCs as well as the formation of a mineralized matrix. Although *ALP* expression levels were compromised in cells lacking *HTRA1*, some of the key regulatory factors involved in osteogenesis, including *RUNX2* and *SPP1*, remained intact. It is possible therefore that HTRA1 mediates its effects through specific pathways, independent of these particular elements. In addition to its effects on osteogenesis, *HTRA1* silencing had a profound effect on hBMSC adipogenesis as evidenced by increases in adipogenic gene expression and oil droplet formation. Such observations would suggest that HTRA1 may in fact represent a decisive factor in determining stem cell lineage commitment and that its involvement in stem cell differentiation go somewhat beyond it simply being a mediator of osteoblast formation. Further investigations into the role of HTRA1 in other differentiation pathways, such as chondrogenesis, myogenesis, or even tenogenesis, would therefore represent a logical progression of these studies and may hold particular relevance with regards to the involvement of HTRA1 in musculoskeletal development as has previously been inferred [19].

Based on the fact that HTRA1 is a secreted serine protease, we next directed our attention to the possible influence of HTRA1 on hBMSC osteogenesis by way of its extracellular effects. A specific role for HTRA1 in the osteogenesis of hBMSCs and mineralization of differentiating bone-forming cells was confirmed in studies using both proteolytically active and inactive recombinant forms of human HTRA1 as well the broad spectrum serine protease inhibitor AEBSF. An increase in mineralized matrix formation was observed in cells treated with active HTRA1 only, and was dependent on HTRA1 being present during the initiation phase of mineralization, as short duration treatments prior to the onset of mineralization proved ineffective. This would therefore infer that the stimulatory effects of exogenously added HTRA1 protein on hBMSC osteogenesis and mineralization of differentiating bone-forming cells may be reliant on its ability to regulate factors present within the actively mineralizing ECM. In addition to its ability to affect ECM mineral content, HTRA1 also induced a significant upregulation in the expression of several positive regulators of mineralization, including *BMP5* and *IBSP* [30, 31], although a large proportion of well-known osteogenic genes such as *RUNX2*, *ALP*, and *SPP1* remained unaffected. In addition, the expression level of a potent negative-regulator of mineral formation, *SOST* [32, 33], was markedly downregulated in hBMSCs treated with HTRA1 and may thus represent an additional mechanism by which mineral deposition is enhanced in differentiating bone-forming cells. It is possible, therefore, that the effects of HTRA1 protein on hBMSC mineralization may be mediated indirectly through its ability to modulate the production of both activators and inhibitors of osteogenic differentiation and/or mineralization. These results are in stark contrast to the findings presented in a previous report by Hadfield et al. [20], where HTRA1 was shown to impart a negative influence over mineralized matrix formation by mouse 2T3 osteoblasts. One possible explanation may lie within the fact that 2T3 cells are derived from transgenic mice overexpressing the simian virus 40 (SV40) T antigen and as such are immortalized [34]. The fact that *HTRA1* gene expression is known to be significantly affected in SV40 transformed cells [35] would imply that modifications of the osteogenic status of these cells brought about by changes in HTRA1 expression and activity may not be truly representative of nonimmortalized, primary cells. Further studies aimed at determining the effects of *HtrA1* gene silencing or exogenously added recombinant HTRA1 on primary mASC osteogenesis may help to clarify this point.

Of the osteogenic genes that were regulated by HTRA1, *IBSP* held particular relevance to this study due to the fact that its ability to regulate mineral deposition has previously been reported to be dependent on the actions of serine proteases [15]. Attention was therefore focused on IBSP and its potential involvement in mediating the effects of HTRA1 on both osteogenesis of MSCs and mineralization of differentiating bone-forming cells. IBSP belongs to the family of SIBLING proteins which also includes osteopontin, dentin matrix protein 1, dentin siaolophosphoprotein, and matrix extracellular phosphoglycoprotein [36]. IBSP, along with other SIBLING proteins, is found almost exclusively in bone and dentin and is a major constituent of the mineralizing matrix during new bone formation [37–39]. The primary biological function of IBSP is unclear, although it has been reported to be involved in the initiation of matrix mineralization through the nucleation of hydroxyapatite crystals [40, 41]. Furthermore, it has been proposed that IBSP is required to undergo fragmentation, possibly through the actions of serine proteases, in order to allow for efficient matrix mineralization [15, 42, 43]. In this report, we were able to demonstrate colocalization of HTRA1 and IBSP in osteo-induced mASC spheroid cultures, thus confirming the potential for endogenous HTRA1 to interact with IBSP under osteogenic culture conditions. Additional immunofluorescence analyses of hBMSCs treated with exogenous HTRA1 revealed that this interaction most likely resulted in the digestion and subsequent removal of IBSP protein from the mineralizing matrix. These results would therefore suggest that the stimulatory effects of secreted HTRA1 protein on matrix mineralization in vitro are mediated, at least in part, through its proteolytic actions on IBSP within the ECM. The potential for HTRA1-induced IBSP proteolysis was further confirmed by Western blot analysis where proteolytically active HTRA1 effectively digested recombinant human IBSP protein at equivalent concentrations to those used in the cell culture studies. However, despite us using two different antibodies raised against either the N- or C-terminal regions of IBSP, we were unable to detect any HTRA1 digest fragments. This was somewhat unexpected, as findings from previous studies suggest that IBSP fragmentation plays an important role in its function as an instigator of mineral nodule formation [15]. This is based on the assumption that IBSP facilitates mineralization predominantly through its ability to bind and nucleate hydroxyapatite, although evidence exists to suggest that both intact and fragmented IBSP can also inhibit hydroxyapatite-seeded crystal growth [44]. It is possible therefore that HTRA1 contributes to osteogenesis through the controlled turnover of IBSP within the mineralizing ECM. This is further supported by the observation that *IBSP* gene expression is upregulated by exogenous HTRA1 at the expense of its protein product and may thus constitute a novel feedback mechanism through which HTRA1 regulates matrix mineralization.

The osteogenic differentiation of BMSCs toward mature bone-forming osteoblasts is a critical step in the development and repair of bone tissue. In this study, we used a previously well-established mouse osteotomy model to investigate the expression of HTRA1 protein during bone healing. Immunohistochemical analysis identified high levels of HTRA1 protein within areas of active bone formation at various stages of bone repair although no positive staining was observed in tissue sections from intact bone, thus confirming it to be primarily involved in de novo bone formation. Furthermore, strong positive staining for HTRA1 was also evident in callus tissue

harboring large numbers of chondrocytes and is thus suggestive of its role in both chondrogenesis and endochondral ossification. Such findings could be of significant importance to fracture healing and possibly even cartilage formation, and as such, warrant further investigation. Immunofluorescence analysis of these sections revealed a close association of HTRA1 with IBSP in areas considered to be undergoing active bone regeneration. This lends support to the theory that HTRA1 regulates both osteogenesis of MSCs and mineralization of differentiating bone-forming cells through its interactions with IBSP, although it does not exclude the possibility that HTRA1 mediates its actions through the proteolytic processing of other SIBLING members [45–48].

Summary

The findings from this study therefore implicate HTRA1 as a positive regulator of both osteogenesis of MSCs and mineralization of differentiating bone-forming cells, possibly at the expense of adipogenic differentiation. Based on these properties, HTRA1 may be deemed as a key factor in determining the outcome of diseases such as age-related osteoporosis, where impaired BMSC osteogenesis and upregulated adipogenesis is believed to be a major contributor to the underlying pathology [24, 49].

Acknowledgments

This study was supported in part by the Swiss National Science Foundation Grant 31003A-134935; CABMM Start-up Grant; Forschungskredit of the University of Zurich; Novartis Foundation, formerly Ciba-Geigy-Jubilee-Foundation; and Uniscientia Foundation.

Disclosure of Potential Conflicts of Interest

The authors indicate no potential conflicts of interest.

References

1 Clausen T, Southan C, Ehrmann M. The HtrA family of proteases: Implications for protein composition and cell fate. Mol Cell 2002;10: 443–455.
2 Clausen T, Kaiser M, Huber R et al. HTRA proteases: Regulated proteolysis in protein quality control. Nat Rev Mol Cell Biol 2011;12: 152–162.
3 Vande Walle L, Lamkanfi M, Vandenabeele P. The mitochondrial serine protease HtrA2/Omi: An overview. Cell Death Diff 2008;15: 453–460.
4 Zurawa-Janicka D, Skorko-Glonek J, Lipinska B. HtrA proteins as targets in therapy of cancer and other diseases. Expert Opin Ther Targets 2010;14:665–679.
5 Chien J, Staub J, Hu SI et al. A candidate tumor suppressor HtrA1 is downregulated in ovarian cancer. Oncogene 2004;23:1636–1644.
6 Baldi A, De Luca A, Morini M et al. The HtrA1 serine protease is down-regulated during human melanoma progression and represses growth of metastatic melanoma cells. Oncogene 2002;21:6684–6688.
7 Hu SI, Carozza M, Klein M et al. Human HtrA, an evolutionarily conserved serine protease identified as a differentially expressed gene product in osteoarthritic cartilage. J Biol Chem 1998;273: 34406–34412.
8 Wu J, Liu W, Bemis A et al. Comparative proteomic characterization of articular cartilage tissue from normal donors and patients with osteoarthritis. Arthritis Rheum 2007;56:3675–3684.
9 Grau S, Richards PJ, Kerr B et al. The role of human HtrA1 in arthritic disease. J Biol Chem 2006;281:6124–6129.
10 Tsuchiya A, Yano M, Tocharus J et al. Expression of mouse HtrA1 serine protease in normal bone and cartilage and its upregulation in joint cartilage damaged by experimental arthritis. Bone 2005;37: 323–336.
11 Zhu W, Robey PG, Boskey AL. The regulatory role of matrix proteins in mineralization of bone. In: Marcus R, Feldman D, Nelson DA et al. Osteoporosis 3rd ed. Elsevier Academic Press, 2007; Chapter 9: 191–240.
12 Kundu AK, Putnam AJ. Vitronectin and collagen I differentially regulate osteogenesis in mesenchymal stem cells. Biochem Biophys Res Commun 2006;347:347–357.
13 Huang CH, Chen MH, Young TH et al. Interactive effects of mechanical stretching and extracellular matrix proteins on initiating osteogenic differentiation of human mesenchymal stem cells. J Cell Biochem 2009;108:1263–1273.
14 Klees RF, Salasznyk RM, Kingsley K et al. Laminin-5 induces osteogenic gene expression in human mesenchymal stem cells through an ERK-dependent pathway. Mol Biol Cell 2005;16:881–890.
15 Huffman NT, Keightley JA, Chaoying C et al. Association of specific proteolytic processing of bone sialoprotein and bone acidic glycoprotein-75 with mineralization within biomineralization foci. J Biol Chem 2007;282:26002–26013.
16 Bruder SP, Fink DJ, Caplan AI. Mesenchymal stem cells in bone development, bone repair, and skeletal regeneration therapy. J Cell Biochem 1994;56:283–294.
17 Marie PJ. Transcription factors controlling osteoblastogenesis. Arch Biochem Biophys 2008;473:98–105.
18 Komori T. Regulation of bone development and maintenance by Runx2. Front Biosci 2008;13:898–903.
19 Oka C, Tsujimoto R, Kajikawa M et al. HtrA1 serine protease inhibits signaling mediated by Tgfbeta family proteins. Development 2004; 131:1041–1053.
20 Hadfield KD, Rock CF, Inkson CA et al. HtrA1 inhibits mineral deposition by osteoblasts: Requirement for the protease and PDZ domains. J Biol Chem 2008;283:5928–5938.
21 Mirsaidi A, Kleinhans KN, Rimann M et al. Telomere length, telomerase activity and osteogenic differentiation are maintained in adipose-derived stromal cells from senile osteoporotic SAMP6 mice. J Tissue Eng Regen Med 2012;6:378–390.
22 Casanova EA, Shakhova O, Patel SS et al. Pramel7 mediates LIF/STAT3-dependent self-renewal in embryonic stem cells. Stem Cells 2011;29:474–485.
23 Hooper M, Hardy K, Handyside A et al. HPRT-deficient (Lesch-Nyhan) mouse embryos derived from germline colonization by cultured cells. Nature 1987;326:292–295.
24 Egermann M, Heil P, Tami A et al. Influence of defective bone marrow osteogenesis on fracture repair in an experimental model of senile osteoporosis. J Orthop Res 2010;28:798–804.
25 Kelm JM, Moritz W, Schmidt D et al. In vitro vascularization of human connective microtissues. In: Hauser H, Fussenegger M, eds. Tissue Engineering. Series: Methods in Molecular Medicine. 2nd ed. Humana Press, 2007:162–164.
26 Grau S, Baldi A, Bussani R et al. Implications of the serine protease HtrA1 in amyloid precursor protein processing and Alzheimer's disease. Proc Natl Acad Sci USA 2005;102:6021–6026.
27 Deng ZL, Sharff KA, Tang N et al. Regulation of osteogenic differentiation during skeletal development. Front Biosci 2008;13:2001–2021.
28 Nishimura R, Hata K, Ikeda F et al. Signal transduction and transcriptional regulation during mesenchymal cell differentiation. J Bone Miner Metab 2008;26:203–212.
29 Tocharus J, Tsuchiya A, Kajikawa M et al. Developmentally regulated expression of mouse HtrA3 and its role as an inhibitor of TGF-beta signaling. Dev Growth Differ 2004;46:257–274.
30 Mailhot G, Yang M, Mason-Savas A et al. BMP-5 expression increases during chondrocyte differentiation in vivo and in vitro and promotes proliferation and cartilage matrix synthesis in primary chondrocyte cultures. J Cell Physiol 2008;214:56–64.
31 Gordon JA, Tye CE, Sampaio AV et al. Bone sialoprotein expression enhances osteoblast differentiation and matrix mineralization in vitro. Bone 2007;41:462–473.
32 ten Dijke P, Krause C, de Gorter DJ et al. Osteocyte-derived sclerostin inhibits bone formation: Its role in bone morphogenetic protein and Wnt signaling. J Bone Joint Surg Am 2008;90(suppl 1):31–35.

33 Krause C, Korchynskyi O, de Rooij K et al. Distinct modes of inhibition by sclerostin on bone morphogenetic protein and Wnt signaling pathways. J Biol Chem 2010;285:41614–41626.
34 Ghosh-Choudhury N, Windle JJ, Koop BA et al. Immortalized murine osteoblasts derived from BMP 2-T-antigen expressing transgenic mice. Endocrinology 1996;137:331–339.
35 Zumbrunn J, Trueb B. Primary structure of a putative serine protease specific for IGF-binding proteins. FEBS Lett 1996;398:187–192.
36 Qin C, Baba O, Butler WT. Post-translational modifications of sibling proteins and their roles in osteogenesis and dentinogenesis. Crit Rev Oral Biol Med 2004;15:126–136.
37 Fisher LW, Whitson SW, Avioli LV et al. Matrix sialoprotein of developing bone. J Biol Chem 1983;258:12723–12727.
38 Chen JK, Shapiro HS, Wrana JL et al. Localization of bone sialoprotein (BSP) expression to sites of mineralized tissue formation in fetal rat tissues by in situ hybridization. Matrix 1991;11:133–143.
39 Bianco P, Fisher LW, Young MF et al. Expression of bone sialoprotein (BSP) in developing human tissues. Calcif Tissue Int 1991;49:421–426.
40 Hunter GK, Goldberg HA. Nucleation of hydroxyapatite by bone sialoprotein. Proc Natl Acad Sci USA 1993;90:8562–8565.
41 Tye CE, Rattray KR, Warner KJ et al. Delineation of the hydroxyapatite-nucleating domains of bone sialoprotein. J Biol Chem 2003;278:7949–7955.
42 Kobayashi D, Takita H, Mizuno M et al. Time-dependent expression of bone sialoprotein fragments in osteogenesis induced by bone morphogenetic protein. J Biochem 1996;119:475–481.
43 Gorski JP, Huffman NT, Cui C et al. Potential role of proprotein convertase SKI-1 in the mineralization of primary bone. Cells Tissues Organs 2009;189:25–32.
44 Stubbs JT 3rd, Mintz KP, Eanes ED et al. Characterization of native and recombinant bone sialoprotein: Delineation of the mineral-binding and cell adhesion domains and structural analysis of the RGD domain. J Bone Miner Res 1997;12:1210–1222.
45 Nagata T, Bellows CG, Kasugai S et al. Biosynthesis of bone proteins [SPP-1 (secreted phosphoprotein-1, osteopontin), Bsp (bone sialoprotein) and sparc (osteonectin)] in association with mineralized-tissue formation by fetal-rat calvarial cells in culture. Biochem J 1991;274:513–520.
46 Tsuchiya S, Simmer JP, Hu JC et al. Astacin proteases cleave dentin sialophosphoprotein (DSPP) to generate dentin phosphoprotein (DPP). J Bone Miner Res 2011;26:220–228.
47 Steiglitz BM, Ayala M, Narayanan K et al. Bone morphogenetic protein-1/tolloid-like proteinases process dentin matrix protein-1. J Biol Chem 2004;279:980–986.
48 Guo R, Rowe PS, Liu S et al. Inhibition of MEPE cleavage by Phex. Biochem Biophys Res Commun 2002;297:38–45.
49 Rodriguez JP, Garat S, Gajardo H et al. Abnormal osteogenesis in osteoporotic patients is reflected by altered mesenchymal stem cells dynamics. J Cell Biochem 1999;75:414–423.


See www.StemCells.com for supporting information available online.

THE JOURNAL OF BIOLOGICAL CHEMISTRY VOL. 287, NO. 25, pp. 21335–21345, June 15, 2012

Detrimental Role for Human High Temperature Requirement Serine Protease A1 (HTRA1) in the Pathogenesis of Intervertebral Disc (IVD) Degeneration*[S]

Received for publication, January 24, 2012, and in revised form, April 30, 2012 Published, JBC Papers in Press, May 3, 2012, DOI 10.1074/jbc.M112.341032

André N. Tiaden[‡1], Marina Klawitter[‡§1,2], Vanda Lux[¶], Ali Mirsaidi[‡‖3], Gregor Bahrenberg[‡‖2], Stephan Glanz[‡‖2], Lilian Quero[§4], Thomas Liebscher[**], Karin Wuertz[§‖‡‡4], Michael Ehrmann[¶], and Peter J. Richards[‡‖5]

From the [‡]Bone and Stem Cell Research Group and the [§]Spine Research Group, Center for Applied Biotechnology and Molecular Medicine, University of Zurich, 8057 Zurich, Switzerland, the [¶]Centre for Medical Biotechnology, Faculty of Biology and Geography, University Duisburg-Essen, 45117 Essen, Germany, the [‖]Institute of Physiology and Zurich Center for Integrative Human Physiology (ZIHP), University of Zurich, 8057 Zurich, Switzerland, the [**]Department of Spinal Surgery, SRH Klinikum Karlsbad-Langensteinbach, 76307 Karlsbad, Germany, and the [‡‡]AOSpine Research Network, 8600 Duebendorf, Switzerland

Background: HTRA1 has been associated with intervertebral disc (IVD) degeneration although its role is unknown.
Results: HTRA1 up-regulated matrix metalloproteinase (MMP) production by IVD cells via the generation of fibronectin fragments.
Conclusion: HTRA1 plays a detrimental role in the pathogenesis of IVD degeneration.
Significance: HTRA1 may represent a novel therapeutic target for the treatment of spinal disc degeneration.

Human HTRA1 is a highly conserved secreted serine protease that degrades numerous extracellular matrix proteins. We have previously identified HTRA1 as being up-regulated in osteoarthritic patients and as having the potential to regulate matrix metalloproteinase (MMP) expression in synovial fibroblasts through the generation of fibronectin fragments. In the present report, we have extended these studies and investigated the role of HTRA1 in the pathogenesis of intervertebral disc (IVD) degeneration. *HTRA1* mRNA expression was significantly elevated in degenerated disc tissue and was associated with increased protein levels. However, these increases did not correlate with the appearance of rs11200638 single nucleotide polymorphism in the promoter region of the *HTRA1* gene, as has previously been suggested. Recombinant HTRA1 induced MMP production in IVD cell cultures through a mechanism critically dependent on MEK but independent of IL-1β signaling. The use of a catalytically inactive mutant confirmed these effects to be primarily due to HTRA1 serine protease activity. HTRA1-induced fibronectin proteolysis resulted in the generation of various sized fragments, which when added to IVD cells in culture, caused a significant increase in MMP expression. Furthermore, one of these fragments was identified as being the amino-terminal fibrin- and heparin-binding domain and was also found to be increased within HTRA1-treated IVD cell cultures as well as in disc tissue from patients with IVD degeneration. Our results therefore support a scenario in which HTRA1 promotes IVD degeneration through the proteolytic cleavage of fibronectin and subsequent activation of resident disc cells.

Degeneration of the intervertebral disc (IVD)[6] is now regarded as one of the major causes of lower back pain, which is a highly prevalent, debilitating, and costly disorder (1, 2). The pathogenesis of degeneration is a highly complex and poorly understood process with many different genetic, biological, and mechanical influences playing key roles in the breakdown of extracellular matrix (ECM) components (3). The predominant means by which ECM is degraded is thought to be due to the proteolytic actions of matrix metalloproteinases (MMPs) and aggrecanases (ADAMTS). A number of MMPs, including MMP-1, -3, -7, -9, and -13, as well as ADAMTS-4, have been shown to increase in the IVD during disc degeneration and are responsible for the breakdown of several matrix components, the most notable being aggrecan and collagen (4–7). Both MMPs and their inhibitors (TIMP-1, -2, and -3) have been localized to the resident chondrocyte-like cells of the nucleus pulposus and inner fibrosus compartments of the IVD (4), thus implicating these cells in disease pathogenesis. The secretion of MMPs by human IVD cells is mediated in part through the stimulatory effects of various pro-inflammatory cytokines, the most prominent of which is IL-1β (8). In addition, fibronectin peptide fragments of the ECM have also been shown to induce MMP production by IVD cells (9) and are potent instigators of experimental disc degeneration (10). Moreover, fibronectin fragments have been shown to accumulate in the IVD during

* This work was supported by a grant from the Center for Applied Biotechnology and Molecular Medicine Start-up Grant/Mäxi Foundation.
[S] This article contains supplemental Table 1 and Figs. 1–4.
[1] Both authors contributed equally to this work.
[2] Supported by grants from the Swiss National Science Foundation.
[3] Supported by grants from the Stiftung Osteoporose Schweiz and Forschungskredit UZH, University of Zurich.
[4] Supported by grants from AOSpine. We thank Dr. Jurgen Klasen (University Hospital Balgrist, University of Zurich, Zurich, Switzerland) for providing fresh human disc biopsies used for all cell culture experiments.
[5] To whom correspondence should be addressed: Center for Applied Biotechnology and Molecular Medicine, University of Zürich, Winterthurerstrasse 190, Zürich 8057, Switzerland. Tel.: 41-44-635-3801; Fax: 41-44-635-6840; E-mail: peter.richards@cabmm.uzh.ch.

[6] The abbreviations used are: IVD, intervertebral disc; ECM, extracellular matrix; SNP, single nucleotide polymorphism; MMP, matrix metalloproteinase; IL-1RA, IL-1 receptor antagonist; ANOVA, analysis of variance; qRT-PCR, quantitative RT-PCR.

degeneration (11), although the proteases responsible for their formation remain elusive.

Human HTRA1 (high temperature requirement serine protease A1) belongs to a well defined family of serine proteases originally identified in bacteria (12). Although primarily regarded as a key regulator of tumor development and subsequent malignancies (13–15), a growing body of evidence now exists to suggest that HTRA1 may also play a central role in determining the outcome of various musculoskeletal disease pathologies, including Duchenne muscular dystrophy (16), osteoarthritis (17–19), and rheumatoid arthritis (19, 20). It has recently been shown in a Japanese population study that a single nucleotide polymorphism (SNP) located within the HTRA1 promoter is associated with spinal disc degeneration, where increases in spinal disc narrowing were observed in patients without the G allele (AA) as compared with those bearing at least one G allele (GG + GA) (21). It would therefore appear that HTRA1 may also play a role in disc pathology, although its influence on disease and its mechanism of action have not yet been elucidated.

Observations from our own studies examining the role of HTRA1 in osteoarthritis imply that HTRA1 may actually have a detrimental effect on the pathogenesis of musculoskeletal disease. Elevated levels of HTRA1 protein were measured in the synovial fluid from osteoarthritic patients, and primary synovial fibroblasts isolated from diseased patients were identified as being a major source of HTRA1 (19). The addition of proteolytically active HTRA1 to fibroblast cultures resulted in marked up-regulation of various MMPs, including MMP-1 and MMP-3, both of which have been implicated in cartilage and joint destruction in arthritic patients. Further experiments confirmed that the stimulatory effects of HTRA1 on MMP expression were protease-dependent and were related to the formation of fibronectin fragments due to extracellular degradation. Such observations are therefore strongly suggestive of a central role for HTRA1 in joint degeneration through its proteolytic actions on ECM components and thus may also be indicative of its role in other disease pathologies, such as disc degeneration.

In the current study, we used IVD tissue and cell samples from surgical patients in order to further investigate the potential involvement of HTRA1 in IVD degeneration. Our findings implicate HTRA1 as a key factor in the underlying pathology associated with IVD degeneration. HTRA1 may therefore represent a novel target for the development of more effective therapeutic strategies to treat this debilitating condition.

EXPERIMENTAL PROCEDURES

Materials—Human fibronectin and rabbit IgG were purchased from R & D Systems (Abingdon, UK). IL-1 receptor antagonist (IL-1RA) was obtained from Abcam (Cambridge, UK), and MEK1/2 inhibitors PD98059 and U0126 were from Sigma-Aldrich (Buchs, Switzerland). Monoclonal antibodies against the fibronectin carboxyl-terminal heparin-binding domain (Mab1935) and the amino-terminal fibrin- and heparin-binding domain (Mab1936) were from Chemicon International. A polyclonal anti-HTRA1 antibody was generated as described previously (19). All anti-IgG horseradish peroxidase (HRP)-conjugated, fluorescence-conjugated secondary antibodies and normal serum were from Jackson ImmunoResearch (Suffolk, UK). DAPI was purchased from Sigma-Aldrich. Collagenase NB4 was purchased from Serva/Promega (Duebendorf, Switzerland), and dispase II was from Roche Applied Science (Rotkreuz, Switzerland).

Tissue Harvesting—IVD tissue and/or blood was obtained from a total of 39 patients undergoing spinal surgery for symptomatic degenerative disc disease, disc herniation, or spinal trauma following informed consent in accordance with the local ethical guidelines (carried out at the SRH Clinic Karlsbad-Langensteinbach, Karlsbad, Germany). The degree of IVD degeneration in patients was assessed prior to surgical intervention by magnetic resonance imaging (MRI) using a four-level grading system based on Pfirrmann's classification of disc degeneration (22). Degeneration grades were assigned as follows: grade 1, non-degenerated (normal disc height); grade 2, mild degeneration (slight decrease in disc height); grade 3, moderate degeneration (moderate decrease in disc height); grade 4, severe degeneration (collapsed disc space).

Isolation and Culture of IVD Cells—Human IVD cells were isolated from the discs of a total of 14 patients undergoing spinal surgery for disc herniation (carried out at Balgrist University Hospital, Zürich, Switzerland) as described previously (23). Briefly, IVD tissue was enzymatically digested (0.2% collagenase NB4, 0.3% dispase II) for 4–8 h, and cells were thereafter cultured in growth medium consisting of DMEM/F-12 supplemented with 10% FCS, penicillin (50 units/ml), streptomycin (50 μg/ml), and amphotericin B (25 μg/ml) and incubated at 37 °C with 5% CO_2 and used at passages 2–3.

Recombinant Human HTRA1—Purified recombinant His-tagged HTRA1 in which the amino-terminal mac25 homology domain was absent (termed HTRA1Δmac) was produced in *Escherichia coli* and purified using Ni^{2+}-NTA chromatography as described previously (19, 24). The enzymatically inactive mutated form of HTRA1Δmac, termed HTRA1ΔmacSA, was generated through conversion of residue serine 328 to alanine by mutagenesis.

Stimulation of IVD Cells with Recombinant HTRA1—IVD cells were cultured in 6-well plates at 3.5×10^5 cells/well and serum starved for 2 h prior to stimulation. Cells were incubated in medium alone or in medium supplemented with either HTRA1Δmac (5 μg/ml) or HTRA1ΔmacSA (5 μg/ml) for up to 24 h. Concentrations used were based on previous observations using human synovial fibroblasts (19). After this time, RNA and culture supernatants were harvested for further analysis. In the case of inhibition studies, IVD cells were preincubated with either PD98059 (10 μM), U0126 (10 μM), or IL-1RA (250 ng/ml) for 2 h prior to stimulation.

Quantitative RT-PCR (qRT-PCR)—Total RNA was isolated from either intact IVD tissue or cells and purified using TRIzol reagent (Invitrogen AG, Basel, Switzerland) according to the manufacturer's instructions. RNA (0.5 μg) was reverse transcribed to cDNA using Superscript II (Invitrogen AG) and random hexanucleotide primers (Promega AG, Dübendorf, Switzerland). Quantification of mRNA expression was performed with TaqMan Gene Expression Assays (Applied Biosystems, Rotkreuz, Switzerland) (supplemental Table 1) using the StepOnePlus real-time PCR system (Applied Biosystems), and

values were normalized to *GAPDH* mRNA levels and presented as -fold change according to the $2^{-\Delta\Delta}C_T$ method. In cases where individual patients ($n = 36$) were compared for expression levels of *HTRA1* and *FN* mRNA in IVD tissue, data were normalized to *TBP* and presented as $2^{-\Delta}C_T$. Each 10-μl reaction consisted of 1× TaqMan fast universal PCR master mix (Applied Biosystems), 1× TaqMan gene expression assay, and 10 ng of cDNA (based upon initial RNA concentrations). All reactions were performed in triplicate in fast optical 96-well reaction plates (Applied Biosystems) at 95 °C for 20 s and 40 cycles of 95 °C for 1 s and 60 °C for 20 s.

SNP Analysis—A total of 35 patients were genotyped using a TaqMan SNP genotyping assay specific for the SNP, rs11200638, according to the manufacturer's instructions (Applied Biosystems). Patients were grouped according to their individual genotypes, and association studies were performed in order to determine the influence of the rs11200638 (A) risk allele on susceptibility to IVD degeneration. The influence of rs11200638 on *HTRA1* expression in IVD tissue was also assessed in patients from whom both RNA and DNA samples were obtained ($n = 32$).

Western Blot Analysis of Patient IVD Tissue—Patient IVD samples ($n = 12$) were selected based on degeneration grade. Protein was extracted using CelLytic M (Sigma-Aldrich) containing a protease inhibitor mixture (Sigma-Aldrich), and protein amounts were determined initially by a Bio-Rad protein assay (Bio-Rad, Reinach, Switzerland). Protein samples were boiled for 5 min in loading buffer (50 mM Tris-HCl, pH 6.8, 2% SDS, 10% glycerol, 100 mM DTT, 0.002% bromphenol blue), and equal amounts of protein were loaded onto 12% SDS-polyacrylamide gels. Further corrections to the loading volumes were made following densitometric analysis of Coomassie Blue-stained gels, thus allowing for accurate comparisons to be made between individual patient samples. Protein was then electroblotted onto PVDF membranes using the Trans-Blot Turbo blotting system (Bio-Rad) and incubated in 5% skim milk, 50 mM Tris-HCl, pH 7.6, 150 mM NaCl, 0.1% Tween 20 (TBST) for 1 h at room temperature. Membranes were then incubated for 1 h at room temperature with either rabbit anti-human HTRA1 (1:2000) or mouse anti-fibronectin amino-terminal fibrin- and heparin-binding domain (Mab1936) (1 μg/ml). After washing in TBST three times for 5 min each, membranes were incubated with a HRP-conjugated anti-mouse or anti-rabbit IgG (1:10,000) for 1 h at room temperature. Following a further washing step, peroxidase activity was detected using SuperSignal West Pico Chemiluminescent Substrate (Thermo Scientific, Lausanne, Switzerland).

Immunofluorescence Microscopy—Unfixed frozen IVD tissue sections were air-dried for 20 min, blocked with normal goat serum (1:10), and incubated with polyclonal anti-HTRA1 (1:50) or control rabbit IgG (2 μg/ml) in phosphate-buffered saline (PBS), pH 7.3, 1% BSA for 16 h at 4 °C. Tissue samples containing HTRA1 were then identified using goat anti-rabbit-Cy3 (1:400). Sections were mounted in Mowiol/DABCO (1,4-diazabicyclo[2.2.2]octane) (Sigma-Aldrich) containing DAPI (0.5 g/ml), and images were captured using the Leica DMI6000B automated inverted research microscope system (Leica Microsystems).

Quantification of Secreted MMP-3—MMP-3 protein levels in culture supernatants were determined using an MMP-3-specific ELISA kit according to the manufacturer's instructions (R & D Systems).

Proteolytic Enzyme Assays—Degradation of fibronectin by HTRA1Δmac was determined using methods described previously (19). Briefly, HTRA1Δmac and recombinant human fibronectin, in an equimolar ratio, were incubated together in Tris-buffered saline (TBS), pH 8.5, for 16 h at 37 °C. In some reactions, HTRA1Δmac was replaced by proteolytically inactive HTRA1ΔmacSA. Fibronectin, HTRA1Δmac, and HTRA1ΔmacSA were also incubated separately under the same conditions and served as controls. In order to assess whether HTRA1Δmac could also generate fibronectin fragments in IVD cell cultures, supernatants (20 ml) were harvested from cells treated with HTRA1Δmac (5 μg/ml) or HTRA1ΔmacSA (5 μg/ml) for 24 h and concentrated using Amicon Ultra-15, 10,000 molecular weight cut-off filter units (Millipore). Fibronectin fragments were analyzed on 4–15% Mini-PROTEAN TGX Precast gels (Bio-Rad) by Coomassie Blue staining and immunoblotting using either mouse anti-fibronectin carboxyl-terminal heparin-binding domain (Mab1935) (1 μg/ml) or mouse-anti-fibronectin amino-terminal fibrin- and heparin-binding domain (Mab1936) (1 μg/ml) as described above. The EnzCheck elastase kit (Molecular Probes, Basel, Switzerland) was used to confirm the proteolytic activity of recombinant HTRA1 proteins according to the manufacturer's protocol.

Effect of Fibronectin Fragments on MMP Expression—Equimolar concentrations of fibronectin (20 μg) and HTRA1Δmac (5 μg) were incubated under the conditions described above. Control reactions were also performed and included TBS, pH 8.5, alone or in combination with either fibronectin or HTRA1Δmac. Samples were then diluted into equilibration buffer containing TBS, pH 7.6, with 20 mM imidazole and incubated with 50 μl of pre-equilibrated HisPur Ni^{2+}-NTA resin (Qiagen, Hombrechtikon, Switzerland) in spin columns (Thermo Scientific) for 1 h at 4 °C. Columns were then centrifuged for 5 min at 1600 rpm, and the affinity column flow-through fraction was collected, dialyzed in TBS for 4 h at 4 °C using Slide-A-Lyzer MINI dialysis devices (3500 molecular weight cut-off) (Thermo Scientific), and then incubated with IVD cells for up to 24 h, after which time MMP expression was evaluated by qRT-PCR.

Statistical Analysis—All statistical analyses were carried out using SPSS19.0 (SPSS Inc., Chicago, IL). Parametric analysis of normally distributed data were performed using the two-tailed unpaired Student's t test or one-way analysis of variance (ANOVA) followed by Tukey's post hoc tests for multiple-group comparisons. Pearson's correlation coefficient was used to evaluate the relationship between the expression levels of selected genes in patient tissue samples. The χ^2 test was used to compare allele frequencies in patients with or without IVD degeneration (1 degree of freedom). In all cases, a p value of <0.05 was considered statistically significant.

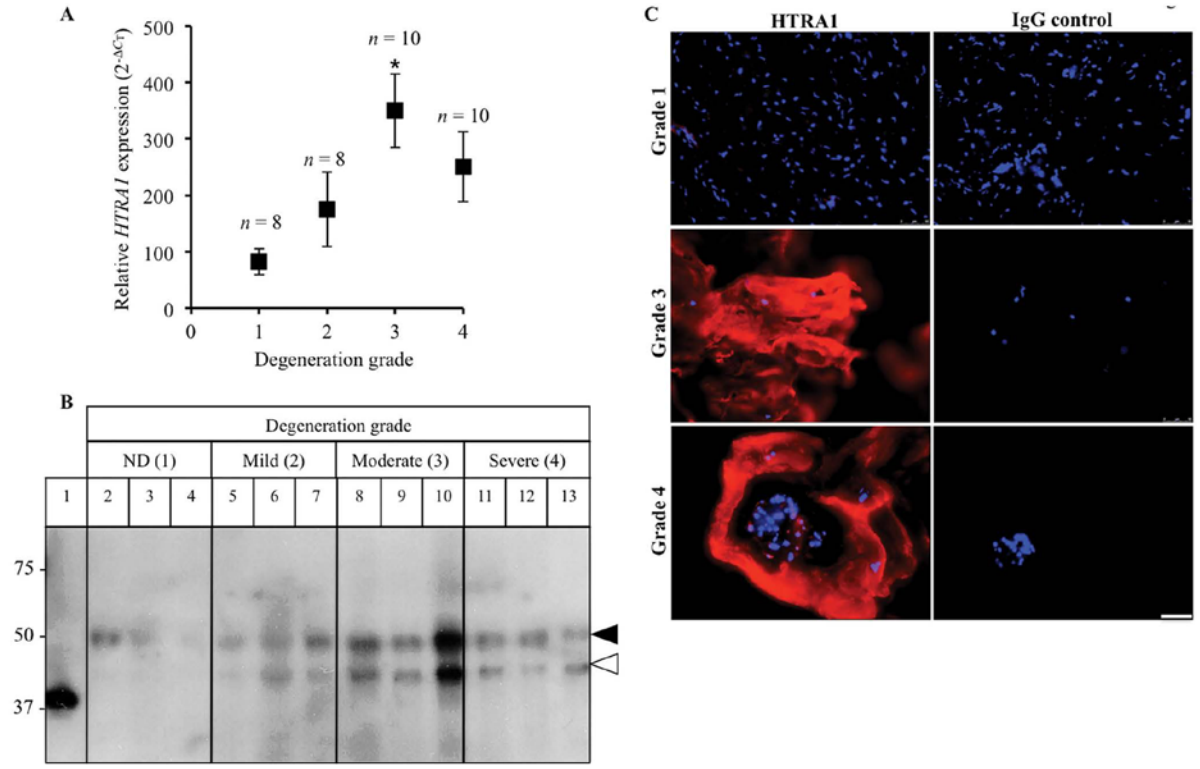

FIGURE 1. **Detection of HTRA1 in human IVD tissue.** *A*, *HTRA1* mRNA levels in intact IVD tissue samples from patients ($n = 36$) with varying degrees of IVD degeneration were determined by qRT-PCR and presented as $2^{-\Delta}C_T$. *, $p < 0.05$, as determined by one-way ANOVA *Error bars*, S.E. *B*, protein extracts from patient IVD tissues ($n = 12$) were loaded onto a 12% SDS-polyacrylamide gel, and immunoblotting was performed using a polyclonal antibody specific for HTRA1. *Lane 1*, *HTRA1Δmac* (4 ng); *lanes 2–4*, non-degenerated (*ND*) discs; *lanes 5–7*, mildly degenerated discs; *lanes 8–10*, moderately degenerated discs; *lanes 11–13*, severely degenerated discs. *Closed arrowhead*, 50-kDa HTRA1; *open arrowhead*, 42-kDa HTRA1. *C*, representative images of HTRA1 protein within frozen IVD tissue sections as identified by immunofluorescence staining. HTRA1 was detected using a Cy3-labeled secondary antibody (*red*), and nuclei were labeled with DAPI (*blue*). The specificity of staining was confirmed through the use of a nonspecific rabbit IgG control (*IgG*). Grade 1 represents a normal, non-degenerated IVD, whereas grades 3 and 4 signify moderate and severe degeneration, respectively. *Scale bar*, 50 μm.

RESULTS

We have previously demonstrated that HTRA1 plays a central role in the regulation of MMP expression in synovial fibroblasts from arthritic patients and that its stimulatory effects may be linked to the generation of fibronectin fragments (19). In the present report, we further investigated this property of HTRA1 in IVD cell cultures and aimed to establish its potential role in IVD degeneration.

Identification of HTRA1 in Patient Tissue—HTRA1 mRNA levels within IVD tissue samples from patients with varying degrees of disc degeneration were normalized to *TBP* and presented as $2^{-\Delta}C_T$. Expression levels significantly correlated ($r = 0.375$; $p = 0.024$) with patient degeneration grade and were found to be markedly increased in patients with severity scores of 3 (4-fold; $p = 0.015$) and 4 (3-fold; $p = 0.2$) as compared with control patients (Fig. 1*A*). Western blot analysis of IVD protein samples using a polyclonal antibody against HTRA1 identified two main species of HTRA1 protein migrating at ~50 kDa (*closed arrowhead*) and ~42 kDa (*open arrowhead*), which most likely represented the full-length and processed forms of HTRA1, respectively (Fig. 1*B* and supplemental Fig. 1) (25). The 50-kDa HTRA1 was found at varying levels in the majority samples tested, whereas the 42-kDa form of HTRA1 was identified in degenerated IVD protein samples only and was noticeably increased in the more severely affected discs. HTRA1 protein was also identified within both the cells and ECM of frozen IVD tissue sections, as determined by immunofluorescence staining, and levels were found to be increased in the more severely affected patients as compared with the control trauma patients (Fig. 1*C*).

Analysis of Patient rs11200638 SNP Genotype—In light of the recent evidence linking the rs11200638 SNP (G>A) in the *HTRA1* gene promoter and spinal disc degeneration in Japanese women (21), we investigated whether the rs11200638 risk allele frequency between patient groups used in the current study was associated with susceptibility to IVD degeneration. DNA from a total of 35 patients was subjected to SNP genotyping using the TaqMan SNP genotyping assay specific for rs11200638 SNP. Contrary to previous expectations, we were unable to demonstrate any significant differences in SNP allele frequencies between control patients without disc degeneration (25%) and patients with degeneration grades of 2 (14.3%; $p = 0.4$), 3 (15%; $p = 0.37$), or 4 (15%; $p = 0.37$) (Table 1). We also performed a comparative analysis of *HTRA1* expression levels in IVD tissue from 32 patients of known genotype. However, no significant associations could be made between

TABLE 1
rs11200638 SNP Genotyping of European patients with and without IVD degeneration

Genotype	Degeneration grade				*n*	Relative *HTRA1* expression[a]	*p* value[b]
	1 ($n = 8$)	2 ($n = 7$)	3 ($n = 10$)	4 ($n = 10$)			
GG	5	5	7	7	23	204.1 ± 35.6	
GA	2	2	3	3	8	307 ± 87.3	0.20
AA	1	0	0	0	1	14.9	
GA + AA	3	2	3	3	9	274.5 ± 83.5	0.37
G allele	12	12	17	17			
A allele[c]	4 (25%)	2 (14.3%) $p = 0.4$[d]	3 (15%) $p = 0.37$[d]	3 (15%) $p = 0.37$[d]			

[a] Comparisons were made between *HTRA1* expression levels ± S.E. in IVD tissue and genotype frequency in patients where both RNA and DNA samples were available ($n = 32$).
[b] Student's *t* test was used to compare *HTRA1* expression levels between patients carrying the risk allele (GA/AA) and those homozygous for the wild type allele (GG).
[c] Percentages refer to risk allele (A) frequency.
[d] The χ^2 test was used to evaluate the significance of differences in risk allele (A) frequency between patients with IVD degeneration (grades 2–4) and control patients without IVD degeneration (grade 1) ($n = 35$).

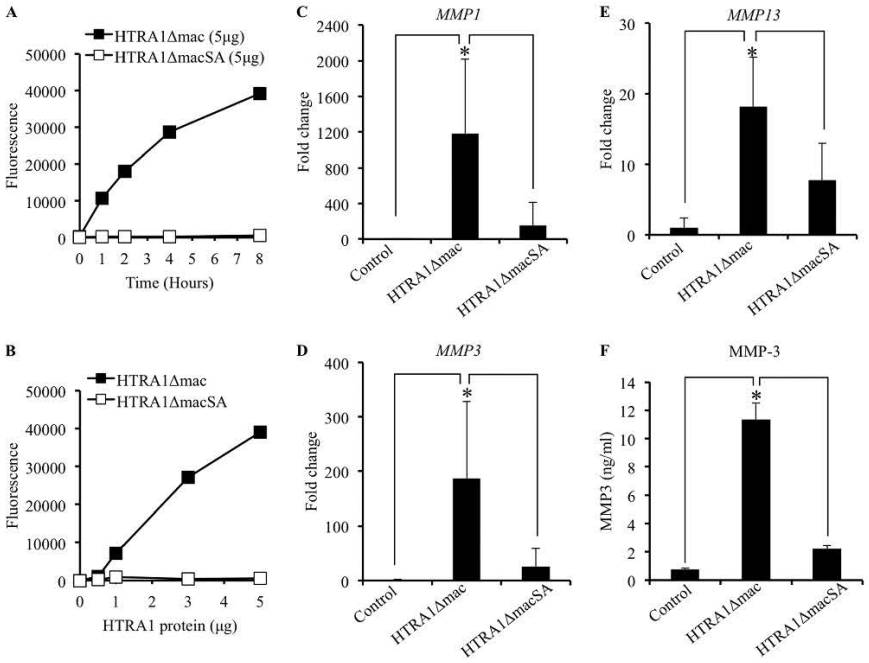

FIGURE 2. **Regulation of MMP expression in IVD cells by recombinant HTRA1.** *A* and *B*, recombinant HTRA1 proteolytic activity was determined using soluble bovine BODIPY FL-labeled DQ-elastin (100 μg/ml) as a substrate. Digestion of the DQ-elastin yielded fluorescent fragments detectable at 530 nm by a fluorescence microplate reader. The amount of DQ-elastin digestion was measured at selected time points (0, 1, 2, 4, and 8 h) using a defined amount of HTRA1 (5 μg) (*A*) or was determined after incubation for 8 h with varying amounts of HTRA1 (0, 0.5, 1, 3, and 5 μg) (*B*). *C–E*, the effects of recombinant HTRA1 (5 μg/ml) on MMP expression levels in IVD cells after a 24-h incubation period were determined by qRT-PCR, and the -fold change as compared with untreated controls was determined using the $2^{-\Delta\Delta C_T}$ method ($n = 4–6$ patients). *F*, a specific MMP-3 ELISA was used to investigate the effects of recombinant HTRA1 on MMP protein secretion in supernatants obtained from IVD cells. Shown are results of triplicate determinations ± S.D. (*error bars*). *, $p < 0.01$, as determined by one-way ANOVA.

HTRA1 expression levels and the rs11200638 genotype (Table 1).

Effect of Recombinant HTRA1 on MMP Production by IVD Cells—In order to investigate how HTRA1 may contribute to IVD degeneration, we generated both proteolytically active and inactive recombinant forms of HTRA1 lacking the amino-terminal mac25 homology domain as described previously (19). The protease activity of the active protein, termed HTRA1Δmac, was confirmed by its ability to cleave purified bovine elastin and was dependent on both incubation time (Fig. 2*A*) and protein amount (Fig. 2*B*). No such activity was observed with the proteolytically inactive form of HTRA1 (HTRA1ΔmacSA) in which serine 328, part of the serine protease catalytic triad domain, had been substituted for alanine. The effects of these recombinant proteins on MMP production by cultured IVD cells were then investigated. Cells were incubated for up to 24 h with either HTRA1Δmac (5 μg/ml) or HTRA1ΔmacSA (5 μg/ml), and the -fold change in mRNA expression levels of *MMP1*, *MMP3*, and *MMP13* was determined by qRT-PCR. HTRA1Δmac induced a significant increase in the expression levels of MMPs tested as compared with untreated cells and cells treated with the proteolytically inactive HTRA1ΔmacSA (Fig. 2, *C–E*). In addition, HTRA1Δmac also enhanced the expression of *ADAMTS4* (aggrecanase-1), although no increase was observed in *MMP2* (gelatinase A) expression, and *ACAN* (aggrecan) expression was actually reduced (supplemental Fig. 2). MMP expression was also up-regulated in HTRA1ΔmacSA-treated cells,

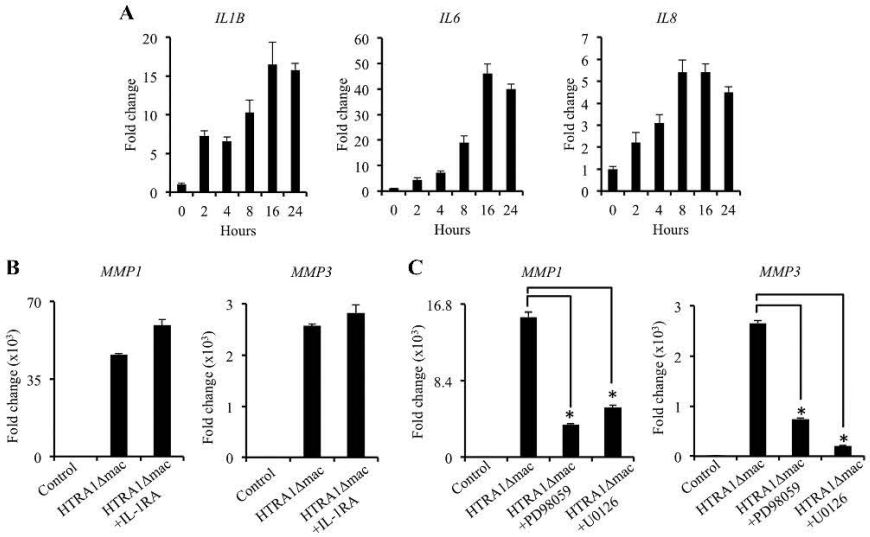

FIGURE 3. **Down-regulation of HTRA1-induced MMP expression in IVD cells by MEK inhibition.** *A*, *IL1B*, *IL6*, and *IL8* mRNA expression levels were measured in IVD cell cultures by qRT-PCR in response to HTRA1Δmac (5 μg/ml) stimulation over the course of 24 h, and the -fold change as compared with untreated cells was determined using the $2^{-\Delta\Delta}C_T$ method. *B*, the influence of IL-1β inhibition on HTRA1-induced *MMP1* and *MMP3* expression by IVD cells was evaluated by qRT-PCR after a 24-h incubation with HTRA1Δmac (5 μg/ml) in combination with the IL-1RA (250 ng/ml), and the -fold change as compared with untreated controls was determined using the $2^{-\Delta\Delta}C_T$ method. *C*, the effects of MEK inhibitors PD98059 (10 μM) and U0126 (10 μM) on HTRA1-induced *MMP1* and *MMP3* expression by IVD cells were evaluated by qRT-PCR after a 24-h incubation, and the -fold change as compared with untreated controls was determined using the $2^{-\Delta\Delta}C_T$ method. In each case, data are representative of at least two separate experiments performed using IVD cells isolated from a total of $n = 5$ patients. Shown are results of triplicate determinations ± S.D. (*error bars*). *, $p < 0.01$, as determined by one-way ANOVA.

although expression levels were over 3–7-fold less than those observed in cells incubated with HTRA1Δmac and were not deemed statistically significant as compared with untreated control cells (*MMP1*, $p = 0.19$; *MMP3*, $p = 0.41$; *MMP13*, $p = 0.41$). Clearly, therefore, HTRA1-induced MMP expression in IVD cells is primarily a protease-dependent phenomenon, although it would appear that other routes of activation may also exist. In addition to its stimulatory effects on MMP mRNA expression, HTRA1Δmac also enhanced MMP protein production, as evidenced by results obtained from the MMP-3 ELISA (Fig. 2*F*). Low levels of secreted MMP-3 were detected in the supernatants of untreated cells (0.76 ng/ml ± 0.04) but became significantly elevated following stimulation with HTRA1Δmac (11.33 ng/ml ± 0.68; $p < 0.001$). As with our previous findings, these stimulatory effects of HTRA1 were significantly diminished following inactivation of its protease activity, although levels remained elevated as compared with untreated cells (2.23 ± 0.13 ng/ml; $p = 0.089$).

Influence of MEK and IL-1β Inhibition on HTRA1-induced MMP Production—Of the known instigators of MMP expression by IVD cells, IL-1β is considered to be the most potent and, as such, is centrally involved in both IVD cell activation and IVD degeneration (8). Furthermore, IL-1β has previously been shown to play a central role in mediating MMP production by fibronectin fragments in cultures of bovine articular cartilage (26). We therefore investigated if the expression of IL-1β, along with several other cytokines, including IL-6 and IL-8, was up-regulated in IVD cells by HTRA1Δmac and whether this had any influence on the induction of MMP expression by HTRA1Δmac. Indeed, expression levels of the cytokines tested were up-regulated in IVD cells stimulated with HTRA1Δmac (5 μg/ml) in a time-dependent manner (Fig. 3*A*). However, additional studies focusing on the inhibition of IL-1β signaling using the IL-1RA (250 ng/ml) failed to demonstrate any significant alterations in the ability of HTRA1 to induce MMP expression in IVD cells (Fig. 3*B* and supplemental Fig. 3). This would suggest that HTRA1 does not mediate its stimulatory effects through IL-1β production, although we cannot exclude the possibility that other cytokines may be involved.

We have previously demonstrated that MMP expression by human synovial fibroblasts is up-regulated in response to HTRA1 stimulation and that this was at least partly dependent on the generation of fibronectin fragments (19). Furthermore, fibronectin fragments were recently confirmed as being potent inducers of MMP expression in IVD cells, mediating their effects through activation of the MEK pathway (27). We therefore investigated whether inhibition of MEK could influence the actions of HTRA1 on IVD MMP expression. Indeed, inclusion of either of the specific MEK inhibitors PD98059 (10 μM) or U0126 (10 μM) 2 h prior to treatment with HTRA1Δmac (5 μg/ml) significantly abrogated its stimulatory effects on the expression of *MMP1* and *MMP3* (Fig. 3*C*), thereby supporting the theory that fibronectin fragments may represent one possible route through which HTRA1 mediates its stimulatory effects on IVD cells.

Effect of Fibronectin Fragments on MMP Expression by IVD Cells—Based on the above results, we further investigated the potential involvement of fibronectin fragments in mediating the actions of HTRA1 on IVD cells. We observed a noticeable increase in the level of a 27–29-kDa fibronectin fragment containing the amino-terminal fibrin- and heparin-binding domain in the supernatants from IVD cell cultures previously treated with HTRA1Δmac (5 μg/ml) as compared with cells incubated in medium alone or with the inactive

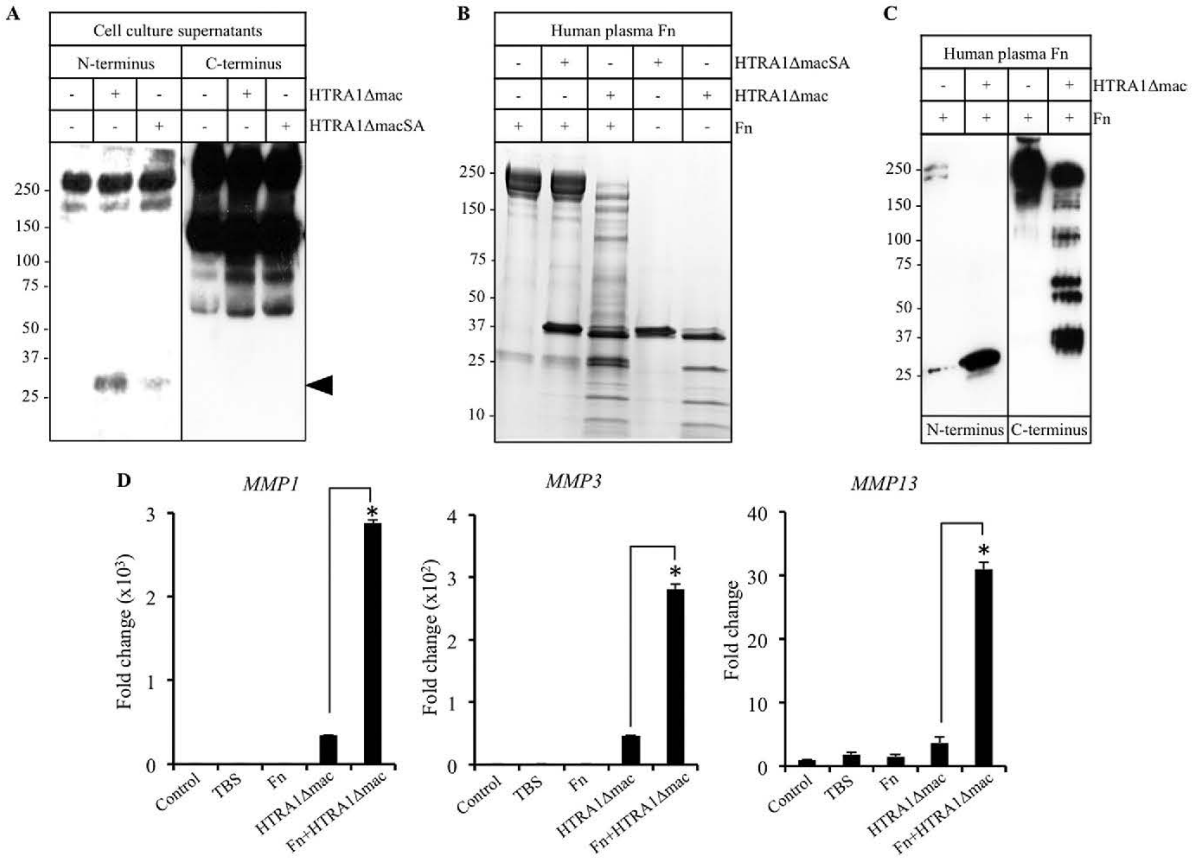

FIGURE 4. **Stimulation of IVD cells with HTRA1-generated fibronectin fragments.** *A*, concentrated protein supernatants (15 μg) from IVD cells treated for 24 h without or with HTRA1Δmac (5 μg/ml) or HTRA1ΔmacSA (5 μg/ml) were subjected to immunoblotting using antibody Mab1935 specific for the fibronectin carboxyl-terminal heparin-binding domain (*C terminus*) or Mab1936 specific for the fibronectin amino-terminal fibrin- and heparin-binding domain (*N terminus*). Fibronectin fragments containing the amino-terminal fibrin- and heparin-binding domain are identified by the *closed arrowhead*. *B*, purified human plasma-derived fibronectin (*Fn*) was incubated with HTRA1Δmac or HTRA1ΔmacSA at equimolar concentrations in TBS, pH 8.5, for 16 h at 37 °C, and samples were loaded onto a 4–15% gradient gel and stained with Coomassie Blue. Fibronectin and recombinant HTRA1 alone were also loaded and served as controls. *C*, an equimolar concentration of human plasma-derived fibronectin and HTRA1Δmac were incubated for 16 h, and fibronectin fragments were visualized by Western blot analysis using the antibodies described in *A*. *D*, equimolar concentrations of fibronectin (20 μg) and HTRA1Δmac (5 μg) were incubated for 16 h, and fibronectin fragments were purified by affinity chromatography. IVD cells were incubated with purified HTRA1-digested fibronectin (*Fn+HTRA1Δmac*) for 24 h, and expression levels of *MMP1*, *MMP3*, and *MMP13* mRNA were determined by qRT-PCR and the -fold change as compared with untreated controls was determined using the $2^{-\Delta\Delta}C_T$ method. Additional cultures were incubated with either affinity-purified Tris-buffered saline, pH 7.6 (*TBS*), fibronectin (*Fn*), or HTRA1 (*HTRA1Δmac*) or left untreated (*Control*). Data are representative of two separate experiments performed using IVD cells from two patients. Shown are results of triplicate determinations ± S.D. *, $p < 0.01$, as determined by one-way ANOVA.

HTRA1ΔmacSA (5 μg/ml) (Fig. 4*A* and supplemental Fig. 4*A*). Interestingly, increases in fibronectin fragments containing the carboxyl-terminal heparin-binding domain were evident in both HTRA1Δmac- and HTRA1ΔmacSA-treated cell cultures as compared with untreated controls. Further analyses confirmed that HTRA1Δmac, but not HTRA1ΔmacSA, could digest equimolar concentrations of human plasma-derived fibronectin after a 16-h incubation period, resulting in various sized fragments being generated, as determined by SDS-PAGE (Fig. 4*B*). The appearance of HTRA1Δmac as several bands is due to its autoproteolytic activity, as described previously (19), an effect not observed with HTRA1ΔmacSA. Western blot analysis of the products generated from HTRA1Δmac-induced fibronectin proteolysis revealed the presence of numerous fragments containing the carboxyl-terminal heparin-binding domain as well as the 27–29-kDa fragment containing the amino-terminal fibrin- and heparin-binding domain previously identified in the supernatants from HTRA1Δmac-treated IVD cells (Fig. 4*C*). We next investigated whether the fibronectin fragments generated by HTRA1 were also capable of activating IVD cells. Following an overnight incubation of human plasma-derived fibronectin with HTRA1Δmac (equimolar concentration), digested and undigested fibronectin was purified by affinity chromatography using Ni^{2+}-NTA to remove the majority of His-tagged HTRA1Δmac (supplemental Fig. 4*B*) and then incubated for up to 24 h with IVD cells. The expression levels of *MMP1*, *MMP3*, and *MMP13* (Fig. 4*D*) were all significantly increased in IVD cells incubated with the purified mixture of fibronectin fragments. By comparison, MMP expression in control cultures stimulated with the affinity column flow-through fraction from HTRA1Δmac samples in the absence of fibronectin was 6–9-fold less ($p < 0.01$), thus confirming that fibronectin fragments were the predominant cause of IVD cell activation.

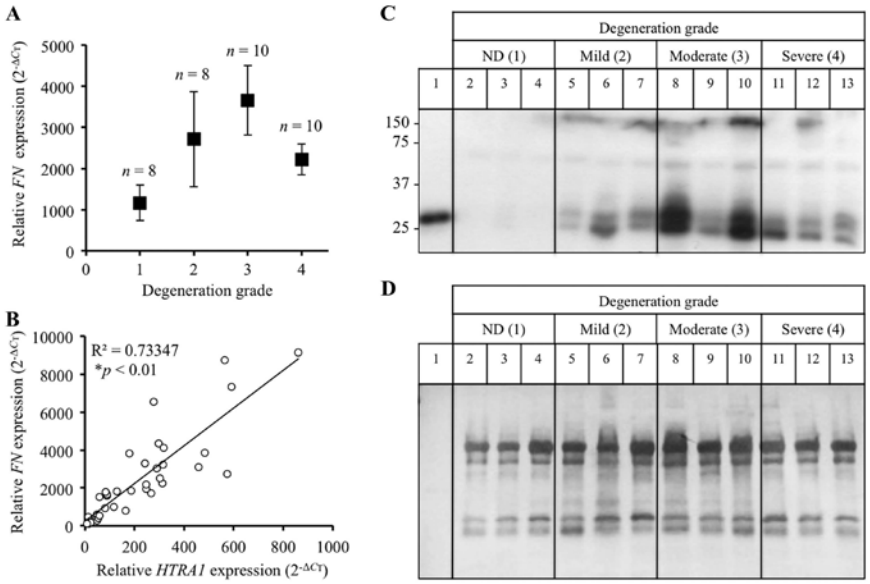

FIGURE 5. **Detection of fibronectin fragments in degenerated IVD tissue.** *A*, fibronectin (*FN*) mRNA levels in intact IVD tissue samples from patients ($n = 36$) with varying degrees of IVD degeneration were determined by qRT-PCR and presented as $2^{-\Delta}C_T \pm$ S.E. (*error bars*). *B*, correlation study between *FN* and *HTRA1* mRNA levels ($2^{-\Delta}C_T$) in patient IVD tissue samples ($n = 36$). R^2, square of correlation coefficient; $p < 0.01$ as determined from Pearson's correlation coefficient. *C*, protein extracts from patient IVD tissues ($n = 12$) were loaded onto a 12% SDS-polyacrylamide gel, and immunoblotting was performed using a monoclonal antibody (Mab1936) specific for the amino-terminal fibrin- and heparin-binding domain. *D*, the PVDF membrane used in *C* was stained with Coomassie Blue in order to confirm equal protein loading. *Lane 1*, HTRA1-digested human plasma-derived fibronectin; *lanes 2–4*, non-degenerated (*ND*) discs; *lanes 5–7*, mildly degenerated discs; *lanes 8–10*, moderately degenerated discs; *lanes 11–13*, severely degenerated discs.

Association of Fibronectin Fragments with Disc Degeneration—Both fibronectin and fibronectin fragments are known to increase with increasing disc degeneration and are thus considered to be an integral part of the underlying pathology (11). In the present study, fibronectin mRNA levels within IVD tissue samples from patients with varying degrees of disc degeneration were normalized to *TBP* and presented as $2^{-\Delta}C_T$. Fibronectin expression levels within patient disc tissue samples were indeed elevated in response to increases in degeneration grade (Fig. 5*A*) and correlated significantly with *HTRA1* mRNA expression levels ($r = 0.856$; $p < 0.01$) (Fig. 5*B*). Furthermore, Western blot analysis of IVD protein samples revealed an increase in fibronectin fragments containing the amino-terminal fibrin- and heparin-binding domain (Fig. 5*C*) in degenerated discs. Moreover, the majority of amino-terminal fragments identified were found to be of a similar size (27–29 kDa) to the fragment identified within samples of HTRA1-digested human fibronectin (*lane 1*). Membranes were counterstained with Coomassie Blue to confirm equal protein loading (Fig. 5*D*).

DISCUSSION

In the current study, we have identified HTRA1 mRNA and protein in the IVDs of human subjects and demonstrated an association between expression levels and severity of IVD degeneration. HTRA1 has previously been linked with disc degeneration following the association of a single nucleotide polymorphism, rs11200638, in the *HTRA1* gene and loss of disc height in postmenopausal Japanese women (21). In the present study, we were unable to show any significant association between the frequency of the risk allele (A) of SNP rs11200638 and IVD degeneration in a small European surgical patient population ($n = 35$). Furthermore, we found no evidence to suggest that the A allele of SNP rs11200638 has any significant influence on *HTRA1* expression levels in IVD tissue. This is supported by findings from studies investigating the role of HTRA1 in age-related macular degeneration, where, although closely associated with disease risk, rs11200638 alone was unable to significantly alter *HTRA1* expression (28, 29). It was subsequently reported that the additional disruption of the adjacent gene, *LOC387715*, was necessary in order for rs11200638 to have a positive influence on *HTRA1* expression (28).

We have previously shown that HTRA1 has the potential to stimulate MMP production by human synovial fibroblasts, thus implicating it in the pathogenesis of arthritis (19). As in the joints of arthritic patients, MMPs play a central role in orchestrating ECM breakdown in discs of patients with IVD degeneration (4–7). Therefore, we next investigated whether HTRA1 could also influence MMP production in human IVD cells. Consistent with our earlier findings with human synovial fibroblasts, recombinant HTRA1 was able to induce the expression of *MMP1*, *MMP3*, and *MMP13* mRNA, as well as MMP-3 protein, in short term IVD cell cultures. In addition, we also observed a significant increase in *ADAMTS4* expression in IVD cells stimulated with HTRA1. As with MMP-1, -3, and -13, ADAMTS-4 is also up-regulated in degenerated discs (4) and may therefore represent an additional route through which HTRA1 could influence ECM breakdown. These stimulatory effects were found to be primarily reliant on HTRA1 protease activity as evidenced by the fact that the proteolytically inactive form of HTRA1 (HTRA1ΔmacSA) was unable to significantly enhance MMP production. Neverthe-

less, increases in MMP production were apparent in cultures treated with HTRA1ΔmacSA and may be indicative of an additional, and as yet unidentified, protease-independent mechanism through which HTRA1 mediates its stimulatory effects. It is possible that further studies utilizing other mutant forms of HTRA1 may further assist in trying to decipher the exact cause of these stimulatory effects.

Degradation of the ECM within degenerated IVDs can give rise to fibronectin fragments of various sizes, which themselves are capable of activating resident disc cells to produce matrix-degrading proteases in a MEK-dependent manner (9, 27). Furthermore, the stimulatory properties of certain fibronectin fragment species on cellular MMP production are known to be mediated through the actions of IL-1β (26). In the current report, we demonstrated that the stimulatory effects of HTRA1 on MMP production by IVD cells were indeed MEK-dependent. Moreover, despite the fact HTRA1 induced the expression of *IL1B*, along with several other cytokines, inhibition of IL-1β signaling through the use of the IL-1RA failed to have any significant impact on HTRA1-induced MMP expression in IVD cells. On closer examination, it was revealed that IVD cell cultures and purified human plasma-derived fibronectin incubated with HTRA1Δmac both consisted of increased levels of a fibronectin fragment containing the 27–29-kDa amino-terminal fibrin- and heparin-binding domain. Furthermore, MMP expression was enhanced in IVD cells following stimulation with the proteolytic products of HTRA1-digested human plasma-derived fibronectin. Considering this, together with the additional observation that HTRA1-induced MMP expression was also dependent on MEK activity, we conclude that the stimulatory effects of HTRA1 on MMP production by IVD cells are mediated, at least in part, through the generation of fibronectin fragments. Interestingly, increases in fibronectin fragments containing the carboxyl-terminal heparin-binding domain, were also evident in the culture supernatants of cells treated with the HTRA1ΔmacSA. The fact that HTRA1ΔmacSA was proteolytically inactive and only able to generate fibronectin fragments in the presence of cells would suggest that these effects were most likely mediated through the stimulated secretion of other active proteases. This may therefore offer some explanation as to why MMP production by IVD cells was enhanced with HTRA1ΔmacSA, although the mechanism of action still remains to be determined. Furthermore, the observation that levels of the 27–29-kDa fibronectin fragment containing the amino-terminal fibrin- and heparin-binding domain were elevated predominantly in cell cultures treated with HTRA1Δmac would further imply that these fragment species are of particular relevance with regard to IVD cell activation.

Increased production of fibronectin by resident IVD cells has been observed within degenerated disc tissue samples and is considered to be central to the ongoing reparative and remodeling processes associated with IVD degeneration (30, 31). In the present study, we observed a marked increase in fibronectin expression in IVD tissue from patients with moderate to severe disc degeneration, which correlated significantly with changes in *HTRA1* expression levels. At present, it is not known whether fibronectin and HTRA1 share common regulatory pathways,

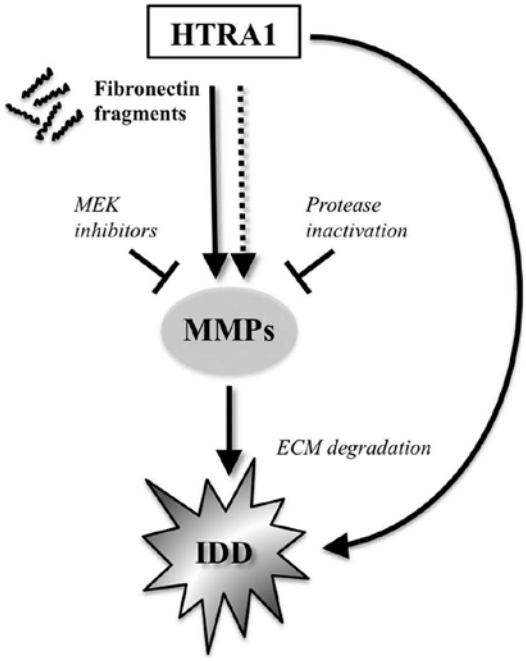

FIGURE 6. **A theoretical model for the role of HTRA1 in IVD degeneration.** Based on our findings, we propose that HTRA1 accumulates in IVD tissue undergoing degeneration and stimulates MMP production by resident cells in a predominantly protease-dependent manner, via activation of the MEK pathway. Furthermore, we suggest that the stimulatory effects of HTRA1 on IVD cells are mediated indirectly through its ability to generate fibronectin fragments, although other routes of cellular activation cannot be ruled out. *IDD*, intervertebral disc degeneration.

although it would appear that both of their expression patterns are dependent on factors intrinsic to the degenerative process. Given the fact that HTRA1-generated fibronectin fragments serve as potent inducers of MMP production, overexpression of fibronectin and *HTRA1* within IVDs is likely to have a significant influence on the development of disc degeneration. This is supported by our finding that small molecular mass fragments (27–29 kDa) containing the amino-terminal fibrin- and heparin-binding domain of fibronectin could also be identified within degenerated disc samples. The involvement of such fragments in disc degeneration has already been alluded to in a recent report by Anderson *et al.* (32), where a single fibronectin fragment with an estimated size of 25 kDa was detected in degenerated discs by immunoblotting with the same monoclonal antibody as used in the current study. It is possible, therefore, that HTRA1 protease activity may in fact be one of the main causative agents responsible for generating such fibronectin fragments within degenerated discs.

Taken together, these findings led us to propose a working model for the biological role of HTRA1 in IVD degeneration (Fig. 6). In addition to its already well characterized ability to directly degrade ECM proteins known to be present within IVDs (19, 20, 33–35), HTRA1 may also further modulate ECM breakdown indirectly through fibronectin fragment production and subsequent up-regulation of MMPs by resident disc cells. Clearly, further investigations are required in order to identify which particular fragments are responsible for the activation of

IVD cells *in vitro* and to clarify the involvement of fibronectin fragments in IVD degeneration. Furthermore, additional studies are needed to fully evaluate the potential stimulatory effects of other soluble mediators (*e.g.* cytokines) released by IVD cells following incubation with HTRA1. Moreover, examination of the possible interplay between inflammatory mediators and fibronectin fragments in the regulation of Toll-like receptor signaling pathways in IVD cells may also lend further insight into how HTRA1 contributes to the catabolic response in IVD degeneration (36). These results therefore encourage the design of specific HTRA1 inhibitors for the treatment of patients with disc degeneration, an endeavor that will no doubt be facilitated by information gleaned from the recently solved crystal structure of HTRA1 (37).

REFERENCES

1. Peterson, C. K., Bolton, J. E., and Wood, A. R. (2000) A cross-sectional study correlating lumbar spine degeneration with disability and pain. *Spine* **25,** 218–223
2. Luoma, K., Riihimäki, H., Luukkonen, R., Raininko, R., Viikari-Juntura, E., and Lamminen A. (2000) Low back pain in relation to lumbar disc degeneration. *Spine* **25,** 487–492
3. Freemont, A. J., Watkins, A., Le Maitre, C., Jeziorska, M., and Hoyland, J. A. (2002) Current understanding of cellular and molecular events in intervertebral disc degeneration. Implications for therapy. *J. Pathol.* **196,** 374–379
4. Le Maitre, C. L., Freemont, A. J., and Hoyland, J. A. (2004) Localization of degradative enzymes and their inhibitors in the degenerate human intervertebral disc. *J. Pathol.* **204,** 47–54
5. Le Maitre, C. L., Freemont, A. J., and Hoyland, J. A. (2006) Human disc degeneration is associated with increased MMP 7 expression. *Biotech. Histochem.* **81,** 125–131
6. Roberts, S., Caterson, B., Menage, J., Evans, E. H., Jaffray, D. C., and Eisenstein, S. M. (2000) Matrix metalloproteinases and aggrecanase. Their role in disorders of the human intervertebral disc. *Spine* **25,** 3005–3013
7. Bachmeier, B. E., Nerlich, A., Mittermaier, N., Weiler, C., Lumenta, C., Wuertz, K., and Boos, N. (2009) Matrix metalloproteinase expression levels suggest distinct enzyme roles during lumbar disc herniation and degeneration. *Eur. Spine J.* **18,** 1573–1586
8. Millward-Sadler, S. J., Costello, P. W., Freemont, A. J., and Hoyland, J. A. (2009) Regulation of catabolic gene expression in normal and degenerate human intervertebral disc cells. Implications for the pathogenesis of intervertebral disc degeneration. *Arthritis Res. Ther.* **11,** R65
9. Anderson, D. G., Li, X., and Balian, G. (2005) A fibronectin fragment alters the metabolism by rabbit intervertebral disc cells *in vitro*. *Spine* **30,** 1242–1246
10. Greg Anderson, D., Li, X., Tannoury, T., Beck, G., and Balian, G. (2003) A fibronectin fragment stimulates intervertebral disc degeneration *in vivo*. *Spine* **28,** 2338–2345
11. Oegema, T. R., Jr., Johnson, S. L., Aguiar, D. J., and Ogilvie, J. W. (2000) Fibronectin and its fragments increase with degeneration in the human intervertebral disc. *Spine* **25,** 2742–2747
12. Clausen, T., Kaiser, M., Huber, R., and Ehrmann, M. (2011) HTRA proteases. Regulated proteolysis in protein quality control. *Nat. Rev. Mol. Cell Biol.* **12,** 152–162
13. Shridhar, V., Sen, A., Chien, J., Staub, J., Avula, R., Kovats, S., Lee, J., Lillie, J., and Smith, D. I. (2002) Identification of underexpressed genes in early and late stage primary ovarian tumors by suppression subtraction hybridization. *Cancer Res.* **62,** 262–270
14. Chien, J., Staub, J., Hu, S. I., Erickson-Johnson, M. R., Couch, F. J., Smith, D. I., Crowl, R. M., Kaufmann, S. H., and Shridhar, V. (2004) A candidate tumor suppressor HtrA1 is down-regulated in ovarian cancer. *Oncogene* **23,** 1636–1644
15. Baldi, A., De Luca, A., Morini, M., Battista, T., Felsani, A., Baldi, F., Catricalà, C., Amantea, A., Noonan, D. M., Albini, A., Natali, P. G., Lombardi, D., and Paggi, M. G. (2002) The HtrA1 serine protease is down-regulated during human melanoma progression and represses growth of metastatic melanoma cells. *Oncogene* **21,** 6684–6688
16. Bakay, M., Zhao, P., Chen, J., and Hoffman, E. P. (2002) A Web-accessible complete transcriptome of normal human and DMD muscle. *Neuromuscul. Disord.* **12,** S125–S141
17. Hu, S. I., Carozza, M., Klein, M., Nantermet, P., Luk, D., and Crowl, R. M. (1998) Human HtrA, an evolutionarily conserved serine protease identified as a differentially expressed gene product in osteoarthritic cartilage. *J. Biol. Chem.* **273,** 34406–34412
18. Wu, J., Liu, W., Bemis, A., Wang, E., Qiu, Y., Morris, E. A., Flannery, C. R., and Yang, Z. (2007) Comparative proteomic characterization of articular cartilage tissue from normal donors and patients with osteoarthritis. *Arthritis Rheum.* **56,** 3675–3684
19. Grau, S., Richards, P. J., Kerr, B., Hughes, C., Caterson, B., Williams, A. S., Junker, U., Jones, S. A., Clausen, T., and Ehrmann, M. (2006) The role of human HtrA1 in arthritic disease. *J. Biol. Chem.* **281,** 6124–6129
20. Tsuchiya, A., Yano, M., Tocharus, J., Kojima, H., Fukumoto, M., Kawaichi, M., and Oka, C. (2005) Expression of mouse HtrA1 serine protease in normal bone and cartilage and its up-regulation in joint cartilage damaged by experimental arthritis. *Bone* **37,** 323–336
21. Urano, T., Narusawa, K., Kobayashi, S., Shiraki, M., Horie-Inoue, K., Sasaki, N., Hosoi, T., Ouchi, Y., Nakamura, T., and Inoue, S. (2010) Association of HTRA1 promoter polymorphism with spinal disc degeneration in Japanese women. *J. Bone Miner. Metab.* **28,** 220–226
22. Pfirrmann, C. W., Metzdorf, A., Zanetti, M., Hodler, J., and Boos, N. (2001) Magnetic resonance classification of lumbar intervertebral disc degeneration. *Spine* **26,** 1873–1878
23. Wuertz, K., Urban, J. P., Klasen, J., Ignatius, A., Wilke, H. J., Claes, L., and Neidlinger-Wilke, C. (2007) Influence of extracellular osmolarity and mechanical stimulation on gene expression of intervertebral disc cells. *J. Orthop. Res.* **25,** 1513–1522
24. Grau, S., Baldi, A., Bussani, R., Tian, X., Stefanescu, R., Przybylski, M., Richards, P., Jones, S. A., Shridhar, V., Clausen, T., and Ehrmann, M. (2005) Implications of the serine protease HtrA1 in amyloid precursor protein processing. *Proc. Natl. Acad. Sci. U.S.A.* **102,** 6021–6026
25. Nie, G., Li, Y., and Salamonsen, L. A. (2005) Serine protease HtrA1 is developmentally regulated in trophoblast and uterine decidual cells during placental formation in the mouse. *Dev. Dyn.* **233,** 1102–1109
26. Yasuda, T., and Poole, A. R. (2002) A fibronectin fragment induces type II collagen degradation by collagenase through an interleukin-1-mediated pathway. *Arthritis Rheum.* **46,** 138–148
27. Xia, M., and Zhu, Y. (2011) Fibronectin fragment activation of ERK increasing integrin α and β subunit expression to degenerate nucleus pulposus cells. *J. Orthop. Res.* **29,** 556–561
28. Yang, Z., Tong, Z., Chen, Y., Zeng, J., Lu, F., Sun, X., Zhao, C., Wang, K., Davey, L., Chen, H., London, N., Muramatsu, D., Salasar, F., Carmona, R., Kasuga, D., Wang, X., Bedell, M., Dixie, M., Zhao, P., Yang, R., Gibbs, D., Liu, X., Li, Y., Li, C., Li, Y., Campochiaro, B., Constantine, R., Zack, D. J., Campochiaro, P., Fu, Y., Li, D. Y., Katsanis, N., and Zhang, K. (2010) Genetic and functional dissection of HTRA1 and LOC387715 in age-related macular degeneration. *PLoS Genet.* **6,** e1000836
29. Kanda, A., Chen, W., Othman, M., Branham, K. E., Brooks, M., Khanna, R., He, S., Lyons, R., Abecasis, G. R., and Swaroop, A. (2007) A variant of mitochondrial protein LOC387715/ARMS2, not HTRA1, is strongly associated with age-related macular degeneration. *Proc. Natl. Acad. Sci. U.S.A.* **104,** 16227–16232
30. Nerlich, A. G., Bachmeier, B. E., and Boos, N. (2005) Expression of fibronectin and TGF-β1 mRNA and protein suggest altered regulation of extracellular matrix in degenerated disc tissue. *Eur. Spine J.* **14,** 17–26
31. Gruber, H. E., Hoelscher, G. L., Ingram, J. A., Bethea, S., Zinchenko, N., and Hanley, E. N. Jr. (2011) Variations in aggrecan localization and gene expression patterns characterize increasing stages of human intervertebral disk degeneration. *Exp. Mol. Pathol.* **91,** 534–539
32. Anderson, D. G., Markova, D., Adams, S. L., Pacifici, M., An, H. S., and Zhang, Y. (2010) Fibronectin splicing variants in human intervertebral disc and association with disc degeneration. *Spine* **35,** 1581–1588
33. Tocharus, J., Tsuchiya, A., Kajikawa, M., Ueta, Y., Oka, C., and Kawaichi,

M. (2004) Developmentally regulated expression of mouse HtrA3 and its role as an inhibitor of TGF-β signaling. *Dev. Growth Differ.* **46**, 257–274
34. Hadfield, K. D., Rock, C. F., Inkson, C. A., Dallas, S. L., Sudre, L., Wallis, G. A., Boot-Handford, R. P., and Canfield, A. E. (2008) HtrA1 inhibits mineral deposition by osteoblasts. Requirement for the protease and PDZ domains. *J. Biol. Chem.* **283**, 5928–5938
35. Chamberland, A., Wang, E., Jones, A. R., Collins-Racie, L. A., LaVallie, E. R., Huang, Y., Liu, L., Morris, E. A., Flannery, C. R., and Yang, Z. (2009) Identification of a novel HtrA1-susceptible cleavage site in human aggrecan. Evidence for the involvement of HtrA1 in aggrecan proteolysis *in vivo*. *J. Biol. Chem.* **284**, 27352–27359
36. Su, S. L., Tsai, C. D., Lee, C. H., Salter, D. M., and Lee, H. S. (2005) Expression and regulation of Toll-like receptor 2 by IL-1β and fibronectin fragments in human articular chondrocytes. *Osteoarthr. Cartil.* **13**, 879–886
37. Truebestein, L., Tennstaedt, A., Mönig, T., Krojer, T., Canellas, F., Kaiser, M., Clausen, T., and Ehrmann, M. (2011) Substrate-induced remodeling of the active site regulates human HTRA1 activity. *Nat. Struct. Mol. Biol.* **18**, 386–388

*Title Page

Assessment of the Matrix Degenerative Effects of MMP-3, ADAMTS-4 and HTRA1 injected into a bovine Intervertebral Disc Organ Culture Model

Tina Furtwängler[1], Samantha C.W. Chan[1] PhD, Gregor Bahrenberg[2,3],

Peter J. Richards[2,3] PhD, Benjamin Gantenbein-Ritter[1*] PhD

[1] *Institute for Surgical Technology and Biomechanics, University of Bern, Switzerland*

[2] *Bone and Stem Cell Research Group, Center for Applied Biotechnology and Molecular Medicine (CABMM), University of Zurich, Switzerland*

[3] *Zurich Center for Integrative Human Physiology (ZIHP), University of Zurich, Switzerland*

*Corresponding Author
Benjamin Gantenbein-Ritter
University of Bern, Medical Faculty
Institute for Surgical Technology and Biomechanics
Tissue & Organ Mechanobiology
Stauffacherstrasse 78
3014 Bern
Switzerland
Tel: + 41 031 631 5926
Fax: + 41 031 631 5960
E-mail: benjamin.gantenbein@istb.unibe.ch

Acknowledgements We thank Elena Calandriello for assistance with histological assays.

*Structured Abstract (300 words)

Enzyme-Mediated Intervertebral Disc Degeneration Model

Abstract

Study design. *In vitro* study to develop an intervertebral disc degeneration (IDD) organ culture model, using coccygeal bovine intervertebral discs (IVDs) and injection of proteolytic enzymes MMP-3, ADAMTS-4 and HTRA1.

Objective. This study aimed to develop an *in-vitro* model of enzyme-mediated IDD to mimic the clinical outcome in humans for investigation of therapeutic treatment options.

Summary of Background Data. Bovine IVDs are comparable to human IVDs in terms of cell composition and biomechanical behavior. Researchers injected papain and trypsin into them to create an IDD model with a degenerated nucleus pulposus (NP) area. They achieved macroscopic cavities as well as a loss of glycosaminoglycans (GAGs). However, none of these enzymes are clinically relevant.

Methods. Bovine IVDs were harvested maintaining the endplates. Active forms of MMP-3, ADAMTS-4 and HTRA1 were injected at a dose of 10µg/ml each. Phosphate buffered saline (PBS) was injected as a control. Discs were cultured for 8 days and loaded diurnally (day 1 to day 4 with ~0.4 MPa for 16 h) and left under free swelling condition from day 4 to day 8 to avoid expected artifacts due to dehydration of the NP. Outcome parameters included disc height, metabolic cell activity, DNA content, glycosaminoglycan (GAG) content, total collagen content, relative gene expression and histological investigation.

Results. The mean metabolic cell activity was significantly lower in the NP area of discs injected with ADAMTS-4 compared to the day 0 control discs. Disc height was decreased following injection with HTRA1, and was significantly correlated with changes in GAG/DNA of the NP tissue. Total collagen content tended to be lower in groups injected with ADAMTS4 and MMP-3.

Conclusions. MMP-3, ADAMTS-4 and HTRA1 neither provoked visible matrix degradation nor major shifts in gene expression. However, cell activity was significantly reduced and HTRA1 induced loss of disc height which positively correlated with changes in GAG/DNA content. The use of higher doses of these enzymes or a combination thereof may therefore be necessary to induce disc degeneration.

*Key Points (3-5 main points of the article)

Keypoints

- Injection of ADAMTS-4 resulted in significantly reduced metabolic cell activity in the NP area after 8 days of diurnally loaded organ culture compared to the day 0 control group (p=0.0433).
- The change in disc height due to HTRA1injection positively correlated with the change in GAG/DNA of the NP tissue ($r_{spearman} = 1.0$, $p = 0.0167$).
- Total collagen content measured indirectly by hydroxy (HO)-proline content was not significantly reduced but tended to be lower in groups injected with ADAMTS-4 and MMP-3.
- GAG/ HO ratio was generally higher in NP (11.32 ± 2.30, PBS control) and lower in AF tissue (3.45 ± 0.63). No significant changes were found among treatment groups.
- Relative gene expression of anabolic and catabolic genes did not show any significant changes after 8 days of organ culture.
- Histology of sagittal sections revealed no significant reductions in proteoglycan content nor collagen content (Masson trichrome, picrosirius red, safranin o/fast green staining)

*Mini Abstract (50 words)

Miniabstract

Three enzymes, MMP-3, ADAMTS-4 and HTRA1 were injected into bovine *in vitro* organ culture for 8 days. Metabolic cell activity was significantly reduced in discs injected with ADAMTS-4. No significant changes were observed in tissue gene expression, collagen content or morphology although HTRA1 did induce a loss in disc height which positively correlated with changes in GAG/DNA content.

*Manuscript Text (must include page numbers)

Introduction

Low back pain (LBP), a common musculoskeletal disorder[1-3] with a lifetime-prevalence of up to 84%[4] causes an enormous economic burden due to activity limitation and work absence.[5] Lumbar intervertebral disc degeneration (IDD) is highly associated with non-specific LBP.[6] It is a multi-causal condition due to aging,[7,8] genetic components,[9-11] obesity[12] and carrying out identical work or posture almost all day.[13] Biomechanical studies showed that complex loading like asymmetric compression of the intervertebral disc (IVD) has detrimental effects.[14,15] One major characteristic of IDD is a predominance of catabolic enzymes over the main anabolic components, namely type-II collagen and aggrecan. The proteolytic endopeptidase MMP-3 could be found to induce loss of proteoglycans (PGs) in the aging IVD of mice.[16] Higher levels of MMP-3 were found in human degenerated discs, which suggested that MMP-3 may be involved in IDD.[17] ADAMTS-4, a metalloproteinase, which cleaves aggrecan,[18] is expressed in herniated disc regions, accompanied with a decrease in PGs.[19] Higher degeneration levels could be correlated with higher amount of ADAMTS-4 in NP and AF[20] thus, it plays a major role in IDD.[21] Furthermore, mRNA and protein levels of the serine proteinase HTRA1 were shown to be elevated in patients with severe IDD.[22] It provoked a significant increase in MMP-1,-3, -13 and ADAMTS-4 and a decrease in aggrecan.

Current treatment options for IDD in the field of tissue engineering aim to repair or to regenerate the NP by injecting biomaterials[23,24] seeded with cells[25] and preconditioned with growth-factors.[26,27] Before testing them *in vivo* it is necessary to test them *in vitro* in an animal organ culture model that exhibits similar cell types, extracellular matrix (ECM) components, biochemical and biomechanical behavior and a degenerated NP area that allows injection of some biomaterial combined with an intact AF. Existing models of IDD using bovine explants generate cavities by injection of papain and trypsin.[28-30] However, these previously tested enzymes are very general proteases and cleave multiple peptide bindings

and are not very specific to the problem of human IDD. Thus, there is a general lack of knowledge whether more clinical relevant enzymes, such as ADAMTS-4, MMP-3 or HTRA1 would cause a degenerative pattern to a disc tissue if injected into a healthy IVD.

The aim of this study was to develop an animal organ culture model of enzyme-driven intervertebral disc degeneration that can be used to mimic the clinical outcome of human IDD. Studies were carried out to determine the effects of a single injection of MMP-3, ADAMTS-4 or HTRA1, in bovine coccygeal IVDs cultured for 8 days under diurnal loading. Typical features of IDD observed in this system included decreases in metabolic cell activity, DNA, glycosaminoglycans (GAG) and collagen content as well as an up-regulation in the expression of endogenous catabolic genes and a down-regulation in the expression of anabolic genes.

Materials and Methods

Disc harvest and injection of selected enzymes. The preparation of intact IVD for organ culture followed our previously established protocol.[31] Fresh bovine tails aged between 6 and 9 months obtained from a local abattoir were dissected within 4 hours after slaughter. Five to six coccygeal bovine IVDs could be harvested per tail. Muscles and tendons were removed and the IVD was cut 1-2 mm towards the vertebra by hammering on top using a custom-made industrial blade holder. Hyaline cartilage of the growth plate on the cutting side was removed until only the bony endplate was exposed. Discs were washed with a jet lavage system (Zimmer inc., Münsingen, Switzerland) with sterile lactated Ringer's solution for 30 seconds on each site and an angle of about 60° to allow better diffusion.[32] In four discs either active enzymes or phosphate buffered saline (PBS) as a control has been injected using a 1ml syringe (BD Luer Lock ™, Franklin Lakes NJ, USA) with a sterile 22-G needle. For MMP-3 (SRP7783, Sigma-Aldrich, Buchs, Switzerland) injections a Hamilton syringe (#1710, 100ml

volume; Hamilton, Bonaduz, Switzerland) was used. The aim was to inject as much volume as possible to compensate for the differences in disc size. The most distal IVD with the smallest diameter was used as day 0 control. The enzyme concentrations used were chosen based on the following findings from other researchers. Ishiguro *et al.* detected a MMP-3 concentration of 11.7 µg/ml in the synovial fluid of osteoarthritis patients.[33]A plasma concentration of ADAMTS-4 of 100.2 ± 31.6 ng/ml could be found in patients with acute coronary syndrome.[34] Tiaden *et al.* incubated human IVD cells from herniated IVDs for 24 h in medium supplemented with recombinant HTRA1 at a concentration of 5 µg/ml to investigate the role of HTRA1 in IVD degeneration.[22]Purified recombinant active HTRA1 (HTRA1Δmac) was produced in *Escherichia coli* and purified using metal-affinity chromatography as previously described.[35] There were five repeats run (N = 5), each with a freshly harvested bovine tail and the following group assignment for every tail: Group 1: Injection of MMP-3 (10µg/ml) (Sigma-Aldrich, Buchs, Switzerland), Group 2: Injection of ADAMTS-4 (10µg/ml) (R&D systems, Oxon, UK), Group 3: Injection of HTRA1 (10µg/ml), Group 4: Injection of PBS (Control), Group 5: day 0 fresh Control.

Organ culture, loading equipment and loading regime. The injected discs were placed in culture chambers, which were specifically designed for a novel type of two degree of freedom bioreactor.[32] The chambers consisted of two cylindrical glass parts, the upper one enclosing the lower one. They are tightly connected to blocks made of polyoxymethylene which carry serrated titanium plates that are in direct contact with the discs. The chambers were fixed with a bar construction and filled with High Glucose Dulbecco's Modified Eagle Medium (HG-DMEM) (Gibco, Invitrogen, Basel, Switzerland) containing 4.5 g/l D-glucose, L-Glutamin, 0.11 g/l pyruvate, 100 U/ml streptomycin and 100 µg/ml penicillin, 5% fetal calf serum (FCS) and 0.1% amphotericin β (all from Sigma-Aldrich, Buchs, Switzerland). The chambers were

placed in the incubator at 37°C and 5% CO_2. Medium was replaced every two days. For the first 24 h, the discs were not loaded to avoid pressing out the enzyme after injection. From day 1 to day 4 three diurnally loading cycles (with ~0.4MPa for 16h and no load for 8h) have been applied. For loading plastic boxes filled with lead beads and a total weight of 4kg have been used. No load has been applied the remaining four cycles until day 8 to avoid expected artifacts due to dehydration of the NP. The aim was to detect only the effects of enzyme injection.

Disc height. The disc height was measured using an analogue caliper, which has been placed along the midline of the disc for measurement.

Metabolic cell activity. Metabolic cell activity was measured using the resazurin sodium salt metabolic cell activity assay (Sigma-Aldrich, Buchs, Switzerland). NP and AF tissue of all experimental groups were incubated in 500µl of resazurin solution (50µM in HG-DMEM containing 5%FCS) for 5 hours at 37°C. Fluorescence was measured at an excitation wavelength of 547nm and emission wavelength of 582nm using a spectramax M5 microplate reader (Molecular Devices, Sunnyvale, United States).

Determination of GAG, DNA and Hydroxy (HO)-Proline content. Dried tissue samples were digested for approximately 16 hours at 60°C using 125µg/ml papain from *Papaya latex* (Sigma-Aldrich, Buchs, Switzerland). For GAG content determination 1,9 dimethylmethylene blue (DMMB) at pH 1.5 and chondroitin sulfate (Sigma-Aldrich) for the standard curve has been used. Absorbance was measured at 595 nm immediately. The quantity of DNA was determined using Bisbenzimide (Hoechst 33258 dye). Standards were prepared from calf

thymus (Sigma-Aldrich). The plate was read at excitation wavelength of 350 nm and emission wavelength of 450 nm.

For determination of HO-proline a colorimetric quantitative assay was used. Color reaction and standards were prepared in duplicates using saturated NaCl, Chloramin T (Sigma-Aldrich) and 4-Dimethylamino-benzaldehyd (DABA) solution (Fluka, Sigma-Aldrich, Switzerland). Absorbance was read at 560nm. All assays were read using a spectramax M5 microplate reader (Molecular Devices, Sunnyvale, United States).

Real-time polymerase chain reaction (PCR). NP and AF tissue was pulverized under liquid nitrogen and total RNA was isolated using TRI REAGENT® (Molecular Research Center, Cincinnati, MA, USA), GenElute miniprep kit (Sigma-Aldrich, Buchs, Switzerland) and DNase I (Sigma-Aldrich). To synthesize cDNA by reverse transcription the iScript kit from Bio-Rad was used. cDNA was diluted with 80µl of 1X tris-ethylenediaminetetraacetic acid (EDTA)-buffer. A mastermix containing forward and reverse primers of the bovine species of selected anabolic and catabolic genes and iQ™ SYBR® Green Supermix (Bio-Rad, Cressier, Switzerland) was used. Real-time PCR was conducted on a real-time PCR detection system (iQ5 cycler, Bio-Rad) using the following amplification routine: denaturation 95°C for 3 min, 50 amplification cycles: 95°C for 10s, 57°C for 40s, followed by melting curve analysis. As reference ribosomal 18S has been used. Oligonucleotide primers (all from Microsynth, Balgach, CH) have been designed with Primer Beacon Designer™ Software (Premier Biosoft Inc., Palo Alto, CA, USA) using nucleotide sequences taken from the GenBank database. The primers are listed in Table 1. The cycle number at which increase in fluorescence and therefore in cDNA appears exponential was measured by setting the threshold to 55 relative fluorescence units (RFUs). The relative gene expression ($2^{-\Delta\Delta Ct}$) was determined by comparing either ΔC_t of day 0 samples with ΔC_t of the enzyme injected discs of day 8.

Histological evaluation. Discs cut into halves were fixed in 4% formalin for 2 days. Samples were dehydrated and infiltrated and finally embedded in methyl methacrylate (MMA). Samples were sectioned into slides of 6µm thickness using a microtome (Microm International, Waldorf, Germany). Slides were stained with Masson's Trichrome stain[36], Safranin O/ Fast green and picrosirius stain. The stained slides were mounted in Eukitt™ (Sigma) and photographed using the bright field modus of the Nikon Eclipse 800 microscope.

Statistics. Mean values ± the standard error of the mean (SEM) were calculated. Prism 6, GraphPad Software, Inc., v6.0b has been used for statistical analysis. For statistical analysis, the non-parametric Kruskal-Wallis-test was used and Dunn's test for *post-hoc* pairwise comparisons. Spearman's rank correlation coefficient was used to compare changes in disk height and GAG/DNA content. A significance value of $p < 0.05$ was specified.

Results

Disc height versus GAG content

The change in disc height due to HTRA1injection positively correlated with the change in GAG/DNA of the NP tissue ($r_{spearman} = 1.0$, $p = 0.0167$, Figure 1). These results suggest that HTRA1 may contribute to decreases in disc height under pathological conditions and may subsequently provoke additional features of IDD.

Metabolic cell activity. Metabolic cell activity was expressed as relative fluorescent units (RFUs) and normalized to the dry weight of the tissue. A significantly lower metabolic cell activity was observed in the ADAMTS-4 injected group as compared to the Control group at

day 0 (p = 0.0433, Figure 2). ADAMTS-4 was therefore assumed to be a suitable enzyme to mimic IDD in the described experimental setup. In general, metabolic cell activity was higher for day 0 samples than for day 8 samples (Figure 2). This difference was also statistically significant in the AF for the pairing of MMP-3 versus d0 (p = 0.0079) and HTRA1 versus d0 (p = 0.0394).

DNA, GAG and HO-Proline content. The mean DNA content in the NP tissue was higher for the day 0 group than the four groups cultured for 8 days (Figure 3). Discs injected with HTRA1 and the PBS Control group showed the lowest values, although were not significantly reduced. The values in AF tissue were similar in all groups. None of the groups showed significantly different DNA content. The mean change in GAG content normalized to DNA is shown in Figure 4. The mean GAG content tended to be higher after culture in NP tissue in all groups. The values for NP tissue were highest for the PBS control, followed by HTRA1, ADAMTS-4 and MMP-3. The HO-proline content tended to be decreased in ADAMTS-4 and MMP-3 (Figure 5). However, no significant differences were attained between treatment groups, also with respect to GAG/HO-Proline ratio (Figure 6).

Relative gene expression. Comparison of groups injected with enzymes to the PBS control group revealed a higher expression of anabolic genes, i.e. *ACAN* and type-II collagen in the NP and AF of enzyme-injected discs (Figure 7). Interestingly, gene expression of the two catabolic enzymes ADAMTS-4 and MMP-13 was found to be up-regulated by about 10,000 times in the NP and these were found down-regulated in the annulus fibrosus tissue relative to PBS control. Expression levels of RNA of inhibitors of metalloproteinases, TIMP-1 and TIMP-3 remained unchanged from level of the PBS control and day 0 control (day 0 data not shown). MMP-3 did not show major deviations from the baseline (Figure 7).

Histological evaluation. No striking differences in stained components could be observed in any of the cultured samples at day 0 to day 8 (Figure 8). Injection of ECM degenerating enzymes did not lead to the expected pattern of disc degeneration, and did not induce any major structural changes at the cellular level (data not shown). However, a decrease in proteoglycans was noted in the nucleus pulposus area following treatment with ADAMTS-4 (Figure 8).

Discussion

IVD Organ Culture Study

The aim of this study was to develop an *in vitro* bovine organ culture model of IDD by injecting a subset of catabolic proteases with the intention of mimicking the clinical outcome of human IDD. Here, we focused on three selected enzymes representing two out of four major classes of proteases, i.e. MMP-3, ADAMTS-4 (both belonging to the family of MMPs) and HTRA1 (a representative of the serine proteases, Figure 9).[37]

Decrease of disc height due to a loss in GAG content is a typical feature of IDD.[38,39] In this study, the change in disc height of the group injected with HTRA1 in fact showed positive correlation to the change in GAG content, which leads to the assumption that HTRA1 could have degenerative potential, which is supported by previous findings from studies carried out by the authors where HTRA1 was demonstrated as being upregulated in degenerated IVDs from human patients.[22].

The effect of external loading is an important feature of the study design to consider. The human IVD is exposed to certain loads, such as static or dynamic axial compression and torsion. Complex loading, for example bending combined with compression, as well as overload or immobilization[40] can result in disc damage. However, there is a physiological

load ranging from 0.1MPa to ~2 MPa[41] in which dynamic compression facilitates nutrition and waste exchange.[42] This means that IVDs require a certain physiological amount of load both *in vivo* and *in vitro*. The load of 0.4 MPa applied diurnally for three cycles in this study is comparable to the load applied in other studies but is still far from the range that is thought to cause degeneration. A study which investigated the influence of targeted trypsin injection and 16 hours compression loading on magnetic resonance (MR) parameters, mechanical and biomechanical parameters of bovine disc segment showed that only loading had a significant effect on the MR parameters and biochemical composition in terms of IDD whereas trypsin had a larger effect on the mechanical properties.[43] However, the detrimental role of the loading pattern should be investigated in further studies.

In the current study, the metabolic cell activity in NP tissue was significantly lower in discs injected with ADAMTS-4 compared to d0 control. This result suggested that injection of ADAMTS-4 at a concentration of 10µg/ml may lower the cell proliferation and viability in the described experimental setup and therefore may represent a suitable tool for an *in vitro* animal IDD model. Certainly, reduced cell viability has previously been reported in whole bovine or rabbit IVD organ cultures cultured under degenerative conditions.[44-46] The bovine coccygeal IVD is considered to be the most appropriate tissue to mimic the conditions in the human IVD and as such, has been used several times for characterization and investigation of an organ culture model.[45,47-52] However, studies that focus on simulation of IDD using bovine discs are rare. To the authors' knowledge, the present study is the first to use injections of recombinant human MMP-3, ADAMTS-4 and HTRA1 to develop an enzyme-based disc degeneration model using the bovine IVD. The current study can be compared with other organ culture models using more catabolic proteolytic enzymes like papain and trypsin. Several studies using those enzymes either with or without load revealed more explicit results in terms of detection of macroscopic cavities after injection. Compressive mechanical loading

even accelerated loss of proteoglycans, water content and mechanical properties in much shorter incubation times (around 24-48h).[28,43,53] A short overview of current studies using trypsin and/or papain (a cysteine protease, Figure 9) to simulate IDD is given in Table 2. Trypsin and papain being non-specific in terms of peptide recognition sites and also being responsible for major GAG loss over a short period of time, however, does not attack cell viability of remaining cells,[29,53] which is surprising but also interesting for the application of testing hydrogels for the IVD repair.[30] Comparing papain with trypsin, trypsin has to be considered less standardized since it represents a mixture of at least three trypsins and thus, is difficult to dose or compare between different products and batches. Furthermore, comparing the macroscopic changes of the investigated three clinically relevant enzymes with the cysteine-dependent proteinase papain there was no real cavity visible using sagittal cuts. Thus, papain produces a highly consistent and reproducible space for injection of biomaterials and seems to act specifically on GAG-rich tissue (Figure 10).[28,29]

Molecular structure and catabolic actions of the three investigated enzymes

MMPs are endopeptidases that play an essential role in various physiological and pathological processes such as angiogenesis, morphogenesis,[54] tissue repair, tumor metastasis, tumor invasion, and inflammatory diseases. MMPs are a family of zinc-containing and zinc dependent enzymes that have the ability to breakdown connective tissue by hydrolyzing components of the ECM.[55] This is important in the process of tissue resorption and the release of biologically active molecules. Most of the MMPs are composed of a propeptide domain that contains a cysteine switch motif with a sulfhydryl group,[56] a catalytic domain, which contains three conserved histidines, which ligate the active site Zn^{2+}, a proline-rich linker region and a hemopexin-like C-terminal domain (Figure 9). Most MMPs are secreted as inactive pro-enzymes (zymogens). The cysteine thiol and zinc ion interaction keeps proMMPs

in a latent state. This linkage must be disrupted to activate the enzyme.[57] The exact in vivo mechanism of activation of proMMPs is not yet known. Further, all MMPs (except MMP-23) have a signal peptide to function in the extracellular space.[58] In our, study we made sure that all enzymes were already in the activated state as we obtained them from the manufacturers to exclude uncertainty from activation procedure using mercury-containing compounds, such as 4-Amino-Phenyl-Mercuric Acetate (APMA).

The ADAMTS (A disintegrin and metalloproteinase with thrombospondin motifs) family belongs to the superfamily of metalloproteinases and includes 19 members. ADAMTS-4 (synonym aggrecanase-1) is a secreted multidomain metalloproteinase (Figure 9),[59] which cleaves aggrecan at four sites within the chondroitin-sulfate rich region of the aggrecan core protein. The prodomain is essential for proper folding. It impedes substrate access by its proximity to the catalytic pocket and its excision is a prerequisite for ADAMTS-4 activity (Figure 9).[60] The catalytic domain contains the active site, the catalytic zinc essential for hydrolysis and two calcium-binding sites. The active site has a dynamic nature with two different conformations depending on the presence of a ligand. Concerning the disintegrin-like domain (Dis) up to now there is no evidence that it binds integrin but very likely it also regulates the enzyme activity. The ancillary domains are the central thrombospondin domain (TS), the cysteine-rich domain (CysR) and the spacer domain (Figure 9).[60]

In humans, the high temperature requirement (HTRA) serine protease family consists of four members termed HTRA1, -2, -3 and -4.[61]In addition to its involvement in tumor suppression, HTRA1 may also play a role in cartilage, joint and IVD degeneration due to its ability to upregulate MMP expression through the generation of fibronectin fragments. [22,62] It has also been speculated that HTRA1 may influence the development and maintenance of other musculoskeletal tissues including muscle and bone.[63,64]

Inhibition of MMPs

The catalytic activity of MMPs is regulated at four points: First, at the level of transcription and thus the gene expression. Secondly, growth factors and cytokines play a role. It could be shown that TNF-α and to an even higher extend IL-1β up-regulates MMP-3, -9 and -13. [65]The third point for regulation is the pro-enzyme activation through the interaction with ECM components.[54] *In vivo* they are activated by tissue or plasma proteinases. *In vitro* e.g. mercurial compounds such as APMA) are used to activate the enzymes. A fourth aspect is the inactivation of enzymes, which means inhibition by endogenous inhibitors. Such inhibitors are called Tissue Inhibitors of Metalloproteinases (TIMPs). There are currently four known TIMPs (TIMP-1, TIMP-2, TIMP-3 and TIMP-4) in humans, which bind tightly to the catalytic side of most metalloproteinases in a 1:1 stoichiometry. TIMP-1 and TIMP-2 are able to inhibit all MMPs. In particular, TIMP-1 forms a complex with the catalytic domain of MMP-3. However, the gene expression level of our study indicated no change during the culture time fort he TIMPs but a strong upregulation of mRNA of MMP-13 and ADAMTS-4 (Figure 7).

Doses of enzymes detected in human pathological state

Which doses of exogenous enzymes are meaningful to induce disc degeneration in an organ culture model? Here, we relied on evidence of osteoarthritic research. Examples for the concentration of MMP-3 in the blood serum level of patients suffering from anti-neutrophil cytoplasmic antibodies-associated vasculitis or oral lichen planus ranged from 21.6 to 99.6 ng/ml. The secreted MMP-3 level in the supernatants from IVD cells treated with HTRA1 was even lower. Nevertheless, later MMP-3 concentration selection based on the findings of Nemoto *et al.*[17]who found concentrations of 0.57 µg/ml/mg wet weight MMP-3 released in the medium of human IVD explant culture and Ishiguro *et al.*[33]detected concentration of 11.7

µg/ml in synovial fluid of osteoarthritic patients. Only very few information could be found on typical concentrations of ADAMTS-4. From patients with acute coronary syndrome a concentration of 100.2ng/ml ± 31.6 ADAMTS-4 was measured in the plasma.[34] The decision for the final test concentration of HTRA1 was mainly based on the work of Tiaden *et al.*[22] who incubated human IVD cells from herniated IVDs for 24 hours in medium supplemented with recombinant HTRA1 at a concentration of 5µg/ml to investigate the role of HTRA1 in IVD degeneration. The results described herein, lead to the conclusion that none of the investigated enzymes at this dosage, are capable of inducing profound changes in the disc ECM. Consequently, we may have to consider increased doses, and/or combinations of these selected enzymes in future studies. However, we also injected a 100 µg of HTRA1 (~ 100-1,000 times more than physiologically measured in synovial fluid) under free-swelling to exclude artifacts from loading. However, even with this high concentration and in the absence of loading, we could not detect any striking changes happening to the ECM (data not shown).

Conclusion

It was the aim of this study to assess the degenerative effects of matrix degrading enzymes but also to comprise their clinical relevance. Although, clinical relevant MMP-3, ADAMTS-4 and HTRA1 showed some promising effects, the use of higher doses of these enzymes or a combination thereof may be necessary to induce disc degeneration. Considering the balance between costs per unit or per µg of enzyme, it is a consequence that the proteinases papain or trypsin are much more catabolic (Figure 10) and much cheaper per i.U. cysteine. Therefore, higher concentrations of papain and trypsin can be applied easily for a disc degeneration model and make them more appealing than the injection of excess MMP-3, ADAMTS-4 or HTRA1 although not mimicking the clinical situation.

*References (cited in order of appearance)

References

1. Ricci JA, Stewart WF, Chee E, et al. Back pain exacerbations and lost productive time costs in United States workers. *Spine (Phila Pa 1976)* 2006; 31:3052-60.

2. Stewart WF, Ricci JA, Chee E, et al. Lost productive time and costs due to diabetes and diabetic neuropathic pain in the US workforce. *J Occup Environ Med* 2007; 49:672-9.

3. Strine TW, Hootman JM. US national prevalence and correlates of low back and neck pain among adults. *Arthritis Rheum* 2007; 57:656-65.

4. Cassidy JD, Carroll LJ, Côté P. The Saskatchewan health and back pain survey. The prevalence of low back pain and related disability in Saskatchewan adults. *Spine (Phila Pa 1976)* 1998; 23:1860-6; discussion 1867.

5. Maniadakis N, Gray A. The economic burden of back pain in the UK. *Pain* 2000; 84:95-103.

6. Livshits G, Popham M, Malkin I, et al. Lumbar disc degeneration and genetic factors are the main risk factors for low back pain in women: the UK Twin Spine Study. *Ann Rheum Dis* 2011; 70:1740-5.

7. Boos N, Weissbach S, Rohrbach H, et al. Classification of age-related changes in lumbar intervertebral discs: 2002 Volvo Award in basic science. *Spine (Phila Pa 1976)* 2002; 27:2631-44.

8. Miller JA, Schmatz C, Schultz AB. Lumbar disc degeneration: correlation with age, sex, and spine level in 600 autopsy specimens *Spine* 1988; 13:173-178.

9. Battié MC, Videman T, Gibbons LE, et al. 1995 Volvo Award in clinical sciences. Determinants of lumbar disc degeneration. A study relating lifetime exposures and magnetic resonance imaging findings in identical twins. *Spine (Phila Pa 1976)* 1995; 20:2601-12.

10. Kalichman L, Hunter DJ. The genetics of intervertebral disc degeneration. Associated genes. *Joint Bone Spine* 2008; 75:388-96.
11. Battié MC, Videman T, Levalahti E, et al. Heritability of low back pain and the role of disc degeneration. *Pain* 2007; 131:272-80.
12. Biglarian A, Seifi B, Bakhshi E, et al. Low back pain prevalence and associated factors in Iranian population: findings from the national health survey. *Pain Res Treat* 2012; 2012:653060.
13. Li JY, Wang S, He LH, et al. Risk factors of low back pain among the Chinese occupational population: a case-control study. *Biomed Environ Sci* 2012; 25:421-9.
14. Walter BA, Korecki CL, Purmessur D, et al. Complex loading affects intervertebral disc mechanics and biology. *Osteoarthritis Cartilage* 2011; 19:1011-8.
15. Le Maitre CL, Pockert A, Buttle DJ, et al. Matrix synthesis and degradation in human intervertebral disc degeneration. *Biochem Soc Trans* 2007; 35:652-5.
16. Fujita K, Ando T, Ohba T, et al. Age-related expression of MCP-1 and MMP-3 in mouse intervertebral disc in relation to TWEAK and TNF-α stimulation. *J Orthop Res* 2012; 30:599-605.
17. Nemoto O, Yamagishi M, Yamada H, et al. Matrix metalloproteinase-3 production by human degenerated intervertebral disc. *J Spinal Disord* 1997; 10:493-8.
18. Tortorella MD, Pratta M, Liu RQ, et al. Sites of aggrecan cleavage by recombinant human aggrecanase-1 (ADAMTS-4). *J Biol Chem* 2000; 275:18566-73.
19. Hatano E, Fujita T, Ueda Y, et al. Expression of ADAMTS-4 (aggrecanase-1) and possible involvement in regression of lumbar disc herniation. *Spine (Phila Pa 1976)* 2006; 31:1426-32.

20. Patel KP, Sandy JD, Akeda K, et al. Aggrecanases and aggrecanase-generated fragments in the human intervertebral disc at early and advanced stages of disc degeneration. *Spine* 2007; 32:2596-603.

21. Le Maitre CL, Freemont AJ, Hoyland JA. Localization of degradative enzymes and their inhibitors in the degenerate human intervertebral disc. *J Pathol* 2004; 204:47-54.

22. Tiaden AN, Klawitter M, Lux V, et al. A detrimental role for human high temperature requirement serine protease A1 (HTRA1) in the pathogenesis of intervertebral disc (IVD) degeneration. *J Biol Chem* 2012; 287:21335-45.

23. Yao NZ, Zhang ZM, Jin DD. In vivo experimental study of lumbar nucleus replacement with pectin/polyvinyl alcohol composite hydrogel. *Zhonghua Wai Ke Za Zhi* 2010; 48:784-7.

24. Chen YC, Su WY, Yang SH, et al. In situ forming hydrogels composed of oxidized high molecular weight hyaluronic acid and gelatin for nucleus pulposus regeneration. *Acta Biomater* 2012; 9:5181-93.

25. Mauth C, Bono E, Haas S, et al. Cell-seeded polyurethane-fibrin structures--a possible system for intervertebral disc regeneration. *Eur Cell Mater* 2009; 18:27-38; discussion 38-9.

26. Chan SC, Gantenbein-Ritter B. Intervertebral disc regeneration or repair with biomaterials and stem cell therapy--feasible or fiction? *Swiss Med Wkly* 2012; 142:w13598.

27. Ehlicke F, Freimark D, Heil B, et al. Intervertebral disc regeneration: Influence of growth factors on differentiation of human mesenchymal stem cells (hMSC). *Int J Artif Organs* 2010; 33:244-52.

28. Roberts S, Menage J, Sivan S, et al. Bovine explant model of degeneration of the intervertebral disc. *BMC Musculoskelet Disord* 2008; 9:24.

[redacted]

33. Ishiguro N, Ito T, Ito H, et al. Relationship of matrix metalloproteinases and their inhibitors to cartilage proteoglycan and collagen turnover: analyses of synovial fluid from patients with osteoarthritis. *Arthritis Rheum* 1999; 42:129-36.

34. Zha Y, Chen Y, Xu F, et al. Elevated level of ADAMTS4 in plasma and peripheral monocytes from patients with acute coronary syndrome. *Clin Res Cardiol* 2010; 99:781-6.

[redacted]

36. Bancroft JD, Stevens A, Turner DR. *Theory and practice of histological techniques,* Churchill Livingstone Edinburgh, 1982.

37. Horn F. *Biochemie des Menschen: das Lehrbuch für das Medizinstudium: 1200 Abbildungen,* Georg Thieme Verlag, 2009.

38. Korecki CL, MacLean JJ, Iatridis JC. Dynamic compression effects on intervertebral disc mechanics and biology. *Spine (Phila Pa 1976)* 2008; 33:1403-9.

39. Korecki CL, Kuo CK, Tuan RS, et al. Intervertebral disc cell response to dynamic compression is age and frequency dependent. *J Orthop Res* 2009; 27:800-6.

40. Stokes IA, Iatridis JC. Mechanical conditions that accelerate intervertebral disc degeneration: overload versus immobilization. *Spine* 2004; 29:2724-32.

41. Wilke HJ, Neef P, Caimi M, et al. New in vivo measurements of pressures in the intervertebral disc in daily life. *Spine (Phila Pa 1976)* 1999; 24:755-62.

42. Le Maitre CL, Fotheringham AP, Freemont AJ, et al. Development of an in vitro model to test the efficacy of novel therapies for IVD degeneration. *J Tissue Eng Regen Med* 2009; 3:461-9.

43. Mwale F, Demers CN, Michalek AJ, et al. Evaluation of quantitative magnetic resonance imaging, biochemical and mechanical properties of trypsin-treated intervertebral discs under physiological compression loading. *J Magn Reson Imaging* 2008; 27:563-73.

44. Korecki CL, MacLean JJ, Iatridis JC. Characterization of an in vitro intervertebral disc organ culture system. *Eur Spine J* 2007; 16:1029-37.

45. Demers CN, Antoniou J, Mwale F. Value and limitations of using the bovine tail as a model for the human lumbar spine *Spine* 2004; 29:2793-9.

46. Haschtmann D, Stoyanov JV, Ettinger L, et al. Establishment of a novel intervertebral disc/endplate culture model: analysis of an ex vivo in vitro whole-organ rabbit culture system. *Spine* 2006; 31:2918-25.

47. Showalter BL, Beckstein JC, Martin JT, et al. Comparison of Animal Discs Used in Disc Research to Human Lumbar Disc: Torsion Mechanics and Collagen Content. *Spine (Phila Pa 1976)* 2012; 37:E900-7.

48. Holm S, Nachemson A. Variations in the nutrition of the canine intervertebral disc induced by motion. *Spine (Phila Pa 1976)* 1983; 8:866-74.

49. Beckstein JC, Sen S, Schaer TP, et al. Comparison of animal discs used in disc research to human lumbar disc: axial compression mechanics and glycosaminoglycan content. *Spine (Phila Pa 1976)* 2008; 33:E166-73.

50. Oshima H, Ishihara H, Urban JP, et al. The use of coccygeal discs to study intervertebral disc metabolism. *J Orthop Res* 1993; 11:332-8.

51. Handa T, Ishihara H, Ohshima H, et al. Effects of hydrostatic pressure on matrix synthesis and matrix metalloproteinase production in the human lumbar intervertebral disc. *Spine (Phila Pa 1976)* 1997; 22:1085-91.

52. Minogue BM, Richardson SM, Zeef LA, et al. Transcriptional profiling of bovine intervertebral disc cells: implications for identification of normal and degenerate human intervertebral disc cell phenotypes. *Arthritis Res Ther* 2010; 12:R22.

53. Jim B, Steffen T, Moir J, et al. Development of an intact intervertebral disc organ culture system in which degeneration can be induced as a prelude to studying repair potential. *Eur Spine J* 2011; 20:1244-54.

54. Nagase H, Woessner JF. Matrix metalloproteinases *The Journal of Biological Chemistry* 1999; 274:21491-21494.

55. Visse R, Nagase H. Matrix metalloproteinases and tissue inhibitors of metalloproteinases: structure, function, and biochemistry. *Circ Res* 2003; 92:827-39.

56. Hiller O, Lichte A, Oberpichler A, et al. Matrix metalloproteinases collagenase-2, macrophage elastase, collagenase-3, and membrane type 1-matrix metalloproteinase impair clotting by degradation of fibrinogen and factor XII. *J Biol Chem* 2000; 275:33008-13.

57. Van Wart HE, Birkedal-Hansen H. The cysteine switch: a principle of regulation of metalloproteinase activity with potential applicability to the entire matrix metalloproteinase gene family. *Proc Natl Acad Sci U S A* 1990; 87:5578-82.

58. Parks WC, Mecham RP. *Matrix metalloproteinases,* Academic Press New York:, 1998.

59. Gendron C, Kashiwagi M, Lim NH, et al. Proteolytic activities of human ADAMTS-5: comparative studies with ADAMTS-4. *J Biol Chem* 2007; 282:18294-306.

60. Stanton H, Melrose J, Little CB, et al. Proteoglycan degradation by the ADAMTS family of proteinases. *Biochim Biophys Acta* 2011; 1812:1616-29.

61. Clausen T, Kaiser M, Huber R, et al. HTRA proteases: regulated proteolysis in protein quality control. *Nat Rev Mol Cell Biol* 2011; 12:152-62.

62. Grau S, Richards PJ, Kerr B, et al. The role of human HtrA1 in arthritic disease. *J Biol Chem* 2006; 281:6124-9.

63. Tiaden AN, Breiden M, Mirsaidi A, et al. Human serine protease HTRA1 positively regulates osteogenesis of human bone marrow-derived mesenchymal stem cells and mineralization of differentiating bone-forming cells through the modulation of extracellular matrix protein. *Stem Cells* 2012; 30:2271-82.

64. Tiaden AN, Richards PJ. The Emerging Roles of HTRA1 in Musculoskeletal Disease. *Am J Pathol* 2013:182(5):1482-8

65. Millward-Sadler SJ, Costello PW, Freemont AJ, et al. Regulation of catabolic gene expression in normal and degenerate human intervertebral disc cells: implications for the pathogenesis of intervertebral disc degeneration. *Arthritis Res Ther* 2009; 11:R65.

List of Tables

Table 1: Bovine specific primers (*Bos taurus*) for real time RT-PCR using the SYBR green system. All PCR reactions were run in 2-step protocol (95° for 15s and 57°C for 40s) for 50 cycles.

Gene	*Common gene name*	*Primer for*	*Primer rev*
Bt_18S	Bovine reference gene	ACG GAC AGG ATT GAC AGA TTG	CCA GAG TCT CGT TCG TTA TCG
Bt_Col1A2	Collagen1 A2	GCC TCG CTC ACC AAC TTC	AGT AAC CAC TGC TCC ATT CTG
Bt_Col 2	Collagen 2	CGG GTG AAC GTG GAG AGA CA	GTC CAG GGT TGC CAT TGG AG
Bt_ACAN	Aggrecan core protein	GGC ATC GTG TTC CAT TAC AG	ACT CGT CCT TGT CTC CAT AG
Bt_IL1b	Interleukin 1 beta	AGTGCCATCCTTCTGTCA	CATTGCCTTCTCCGCTATT
Bt_IL-6	Interleukin 6 (interferon, beta 2)	GACTACTTCTGACCACTC	ATTCTTCTCACATATCTCC TT
Bt_VCAN	Versican	CTGGAGAAGATTGTGTTG	GTGTAGGTGAGATGGTAA
Bt TIMP-1	Tissue inhibitor of metalloproteinases_1	CAACTCCGATGTCGTCAT	TCTCATAACGCTGGTATAA GG
Bt TIMP-2	Tissue inhibitor of metalloproteinases_2	TTGGAGGAAAGAAGGAGTA	CACGATGAAGTCACAGAG
Bt TIMP-3	Tissue inhibitor of metalloproteinases_3	CAGCAGATAGACTCAAGGT	GACACAGACAGACACAGT
Bt_MMP3	Matrix metalloproteinase 3	CTT CCG ATT CTG CTG TTG CTA TG	ATG GTG TCT TCC TTG TCC CTT G
Bt_MMP13	Matrix metalloproteinase 13	TCC TGG CTG GCT TCC TCT TC	CCT CGG ACA AGT CTT CAG AAT CTC
Bt-ADAMTS-4	A disintegrin and metalloproteinase with thrombospondin motifs-4	TCC TGG CTG GCT TCC TCT TC	CCT CGG ACA AGT CTT CAG AAT CTC

Table 2: Recent studies using Trypsin and/or Papain for organ culture model.

Reference	*Injected Enzyme*	*Load*	*Duration*	*Main Results*
Jim et al.[53]	**Trypsin**: 2.5g/50µl PBS	No	4 weeks	60% Loss of proteoglycans after 7 days
Roberts et al.[28]	**Papain**: 20mg/ml **Trypsin**: 1,5,10,20 mg/ml	No	2 weeks	Discs were macro- and microscopically fragmented, severe metachromasia, macroscopic cavities and 20% loss of proteoglycans after 2 weeks.
Chan et al.[29]	**Papain**: 3,15,30,60,150 U/ml	No	10 days	Macroscopic cavity for 30U/ml and higher GAGs completely lost for 15U/ml and higher (less than 10% left in NP area), drop in compressive and rotational stiffness, loss of water content for 60U/ml and higher
Mwale *et al.*[43]	**Trypsin**: 5 mg	Yes, 1 Hz, 16 h	16 hours	Effect of loading was greater on MR parameters and biochemical composition typical for IDD Trypsin had larger effect on mechanical properties

Figure Legends

Figure 1. Change in disc height compared to change in GAG content in NP tissue of bovine disc explants injected with HTRA1 at day 0 and after 8 days of diurnal loaded organ culture. A significant positive correlation could be detected using Spearman correlation test and including the measurements of the first main experiment ($r_{spearman}$=1.0, p=0.0167, N = 5).

Figure 2. Mean metabolic cell activity in RFU/ µg dry weight (mean ± SEM, N = 5) of bovine IVD explants at day 0 and after 8 days of diurnal loaded organ culture. Significant differences could be found in NP: ADAMTS-4 vs. d0 (P = 0.0433) and AF: MMP-3 vs. d0 (P =0.0079) and HTRA1 vs. d0 (P = 0.0394), * = $P < 0.05$, ** $0.001<P < 0.01$.

Figure 3. Mean DNA content/ dry weight of bovine IVD organ culture with injected enzymes (mean ± SEM, N = 5) at day 0 and after 8 days of culture. Although the value for day 0 Control group in NP tissue is higher than in all cultured groups, no significant differences amongst the five groups could be found.

Figure 4. Mean GAG/DNA ratio of bovine IVD organ culture with injected enzymes (mean ± SEM, N = 5) at day 0 and after 8 days of culture.

Figure 5. HO-Proline content per dry weight tissue bovine IVD organ culture with injected enzymes (mean ± SEM, N = 5) at day 0 and after 8 days of culture, NP: nucleus pulposus, AF: annulus fibrosus.

Figure 6. GAG / HO-Proline ratio of bovine IVD organ culture with injected enzymes (mean ± SEM, N = 5) at day 0 and after 8 days of culture. * = $P < 0.05$.

Figure 7. Relative gene expression ($2^{-\Delta\Delta Ct}$ method) in NP and AF tissue of bovine IVD organ culture with injected enzymes relative to PBS control after 8 days of culture (N = 5, mean ± SEM).

Figure 8. Histological sagittal sections of bovine IVD organ culture with injected enzymes on day 0 and after 8 days of culture. Left column: Masson's trichrome, middle column: Pircosirius red, right column: Safranin O/Fast Green.

Figure 9. 1. Overview of classification families of proteases according to Horn (2009)[37] 2. General domain arrangement of vertebrate MMPs after Nagase *et al.* (1999)[54] and Parks *et al.* (1998).[58]

Figure 10. Macroscopic sagittal view of bovine coccygeal IVDs cut with a a guillotine-like cutter tool after 8 days of organ culture injected either with phosphate buffered saline (PBS) control or with one of three catabolic enzymes MMP-3, ADAMTS-4 and HTRA1 (concentration of ~1 µg/ disc) compared to the cysteine-dependent proteinase papain with 30 U/disc.[29] The arrow denotes the cavity, created after 48h of incubation with 30 U of injected papain.

Figure 1
Click here to download high resolution image

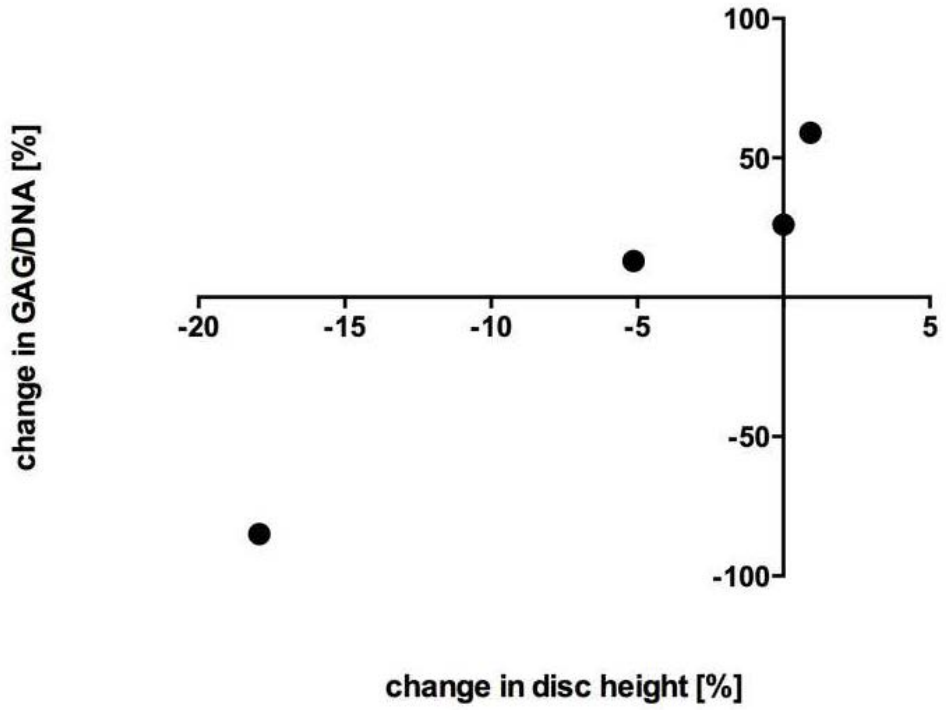

Figure 2
Click here to download high resolution image

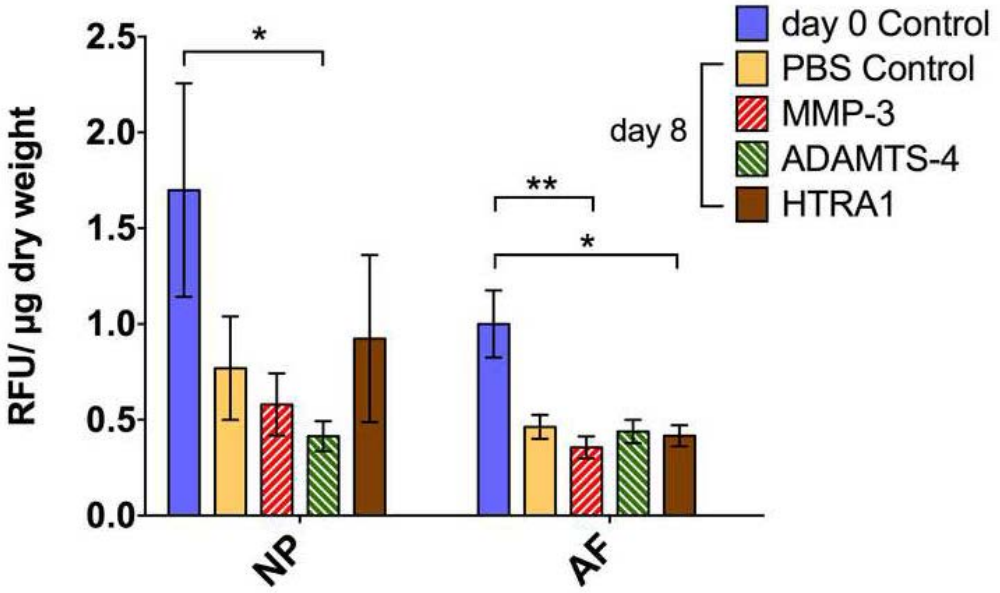

Figure 3
Click here to download high resolution image

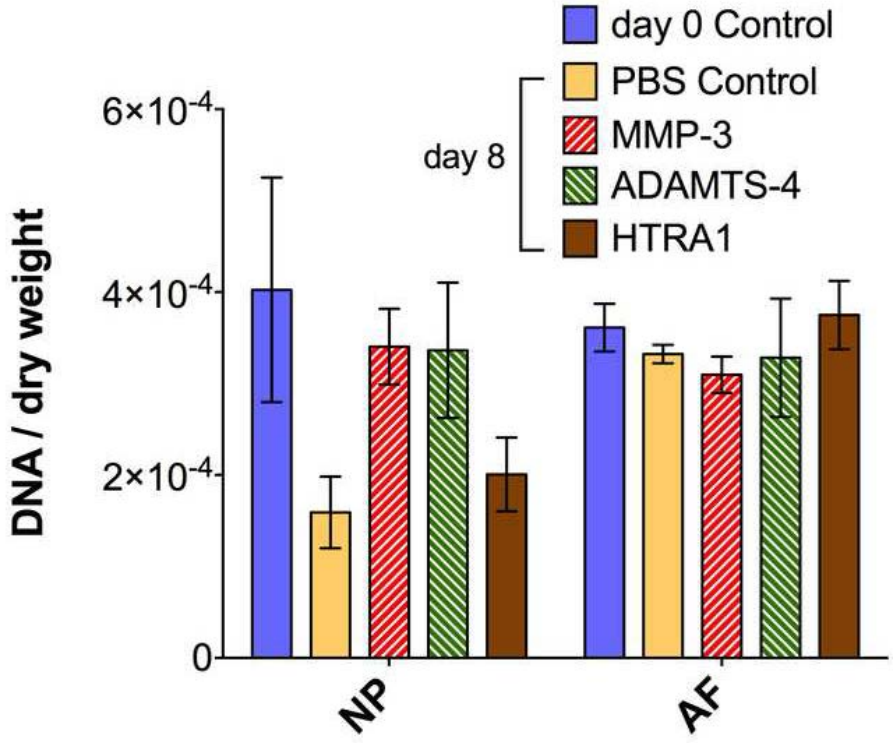

Figure 4
Click here to download high resolution image

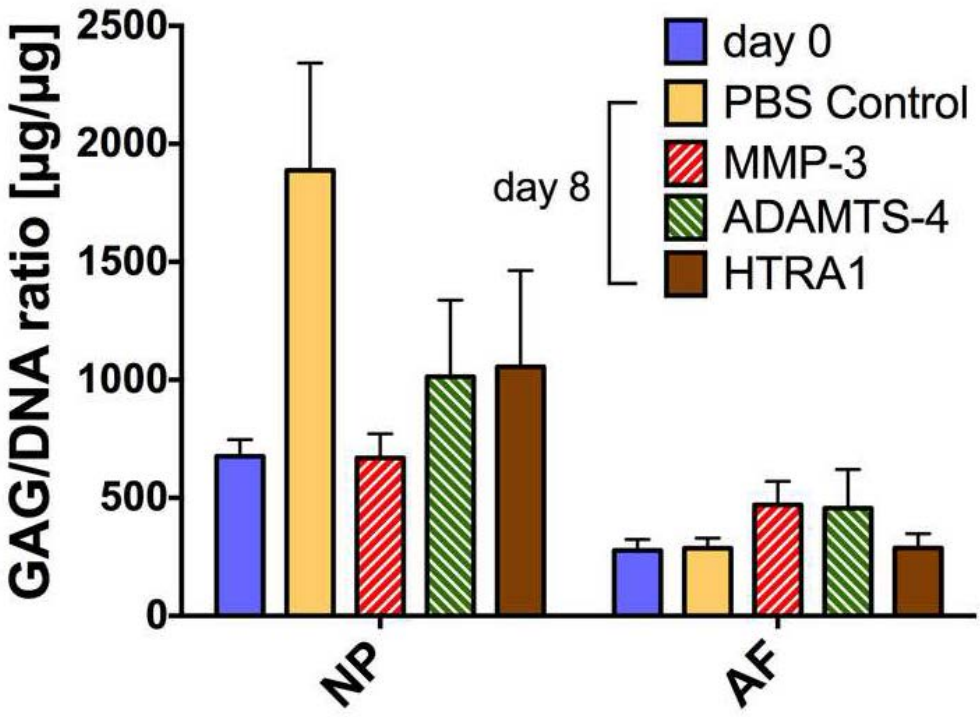

Figure 5
Click here to download high resolution image

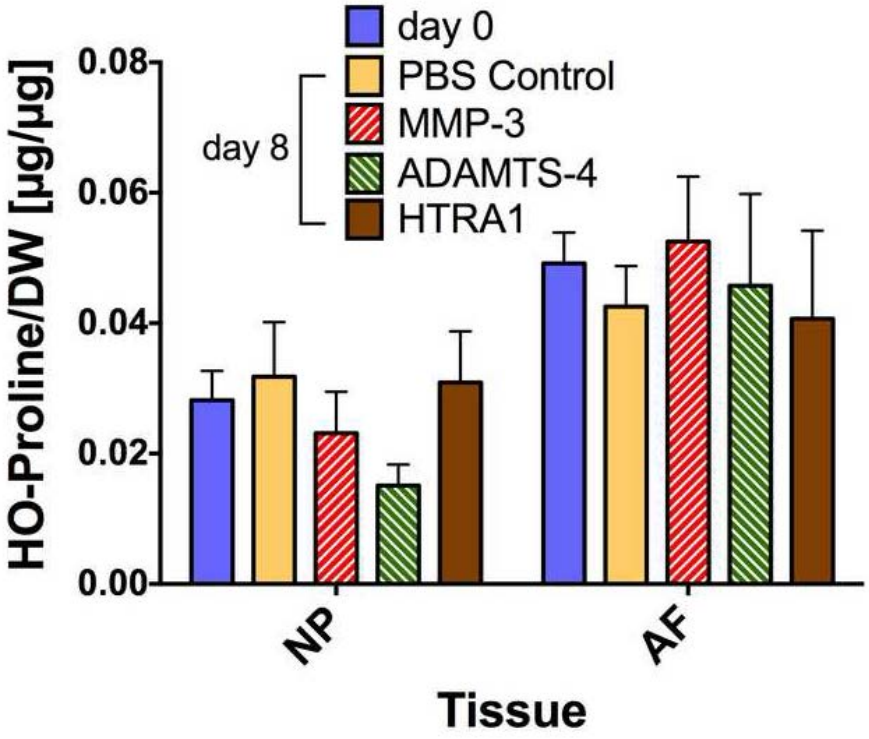

Figure 6
Click here to download high resolution image

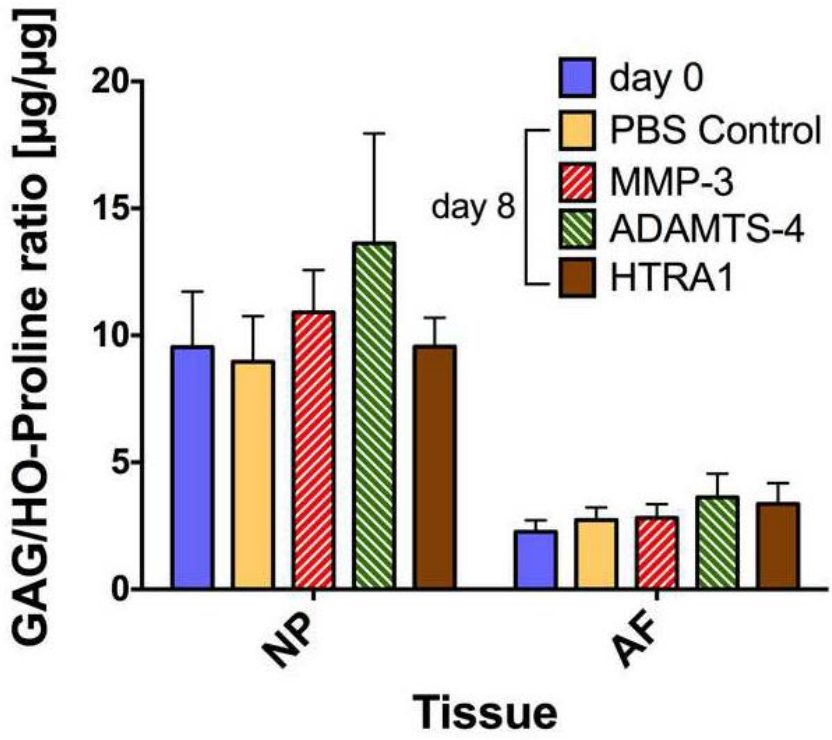

Figures 7
Click here to download high resolution image

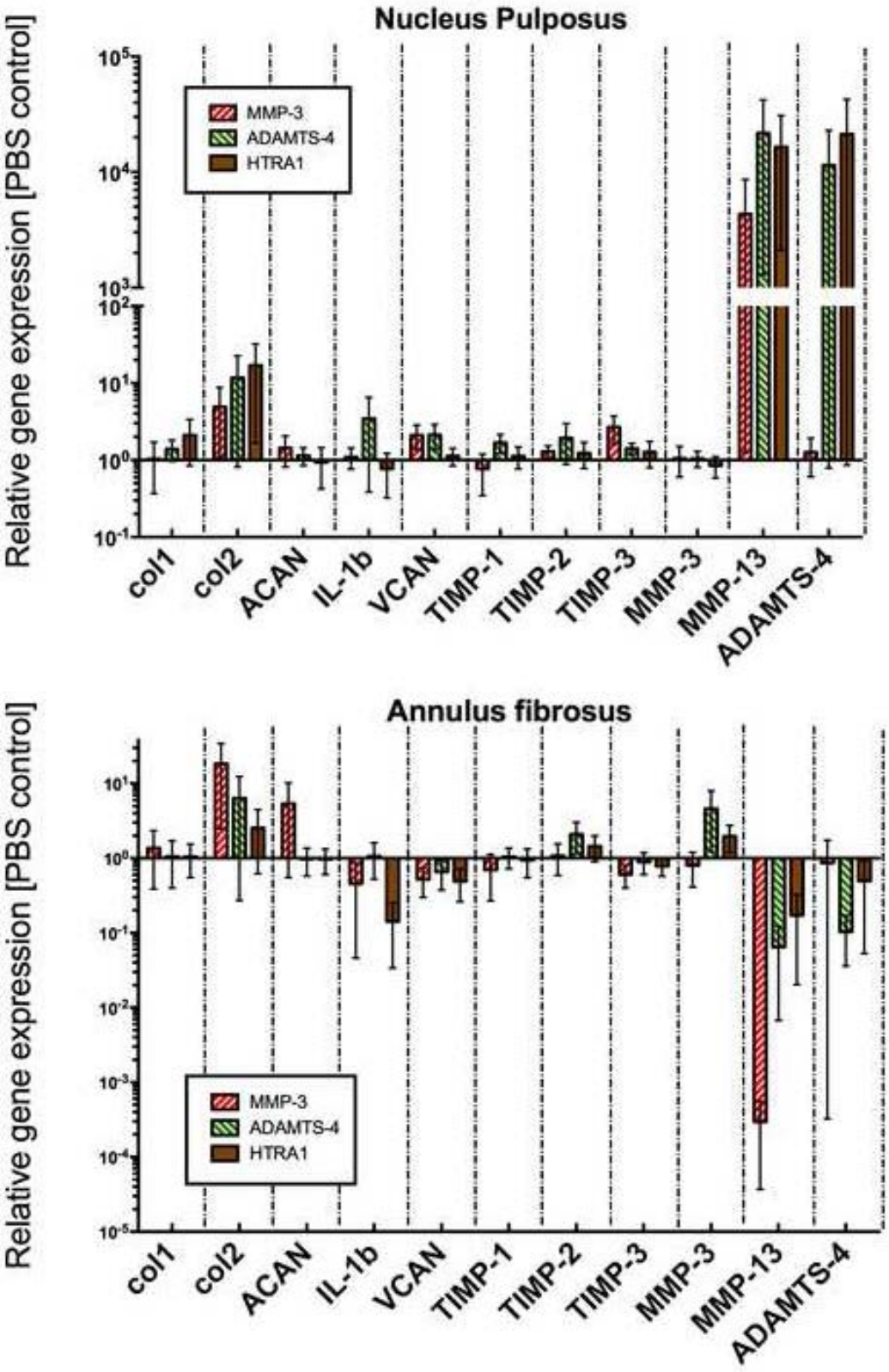

Figure 8
Click here to download high resolution image

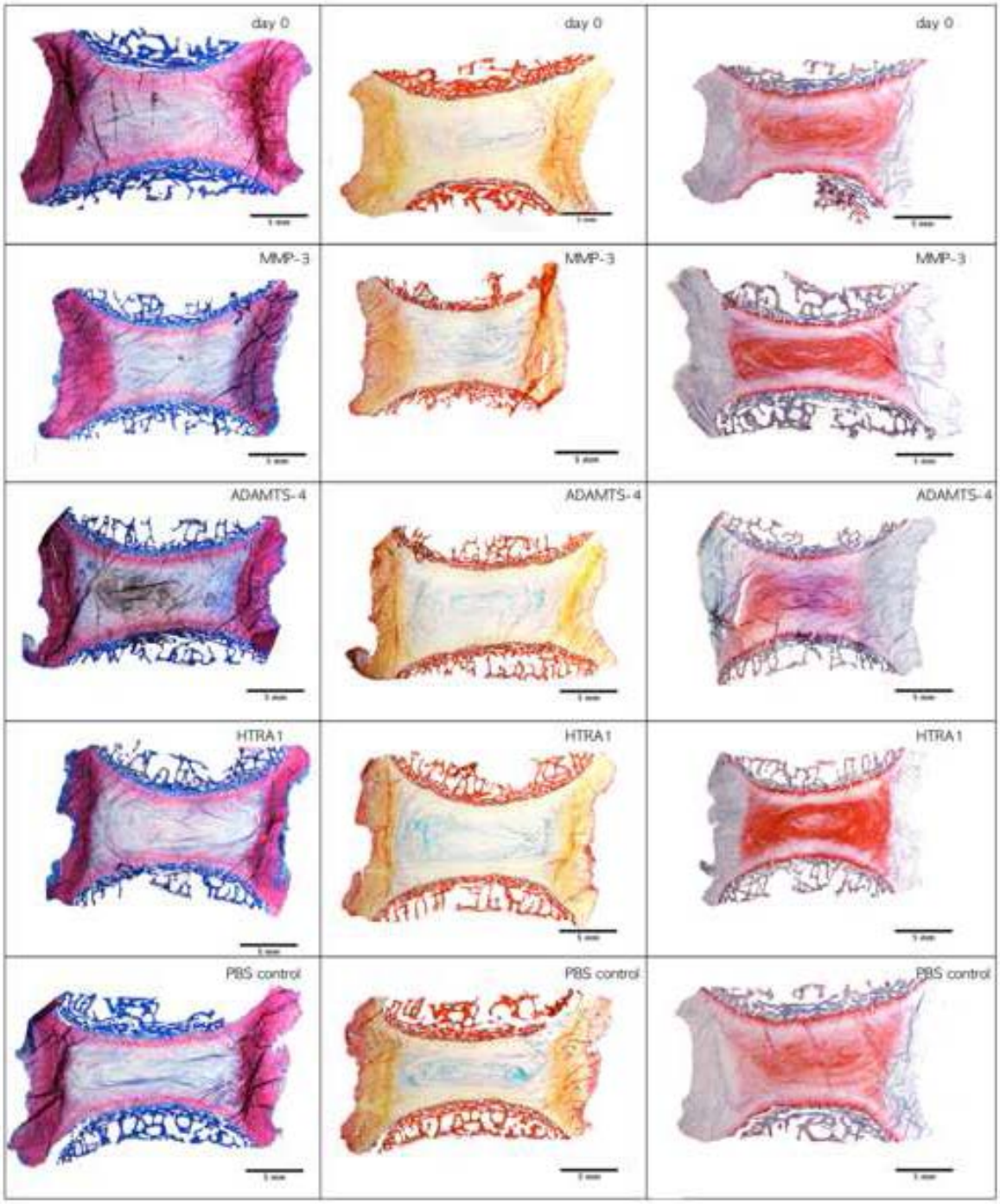

Figure 9
Click here to download high resolution image

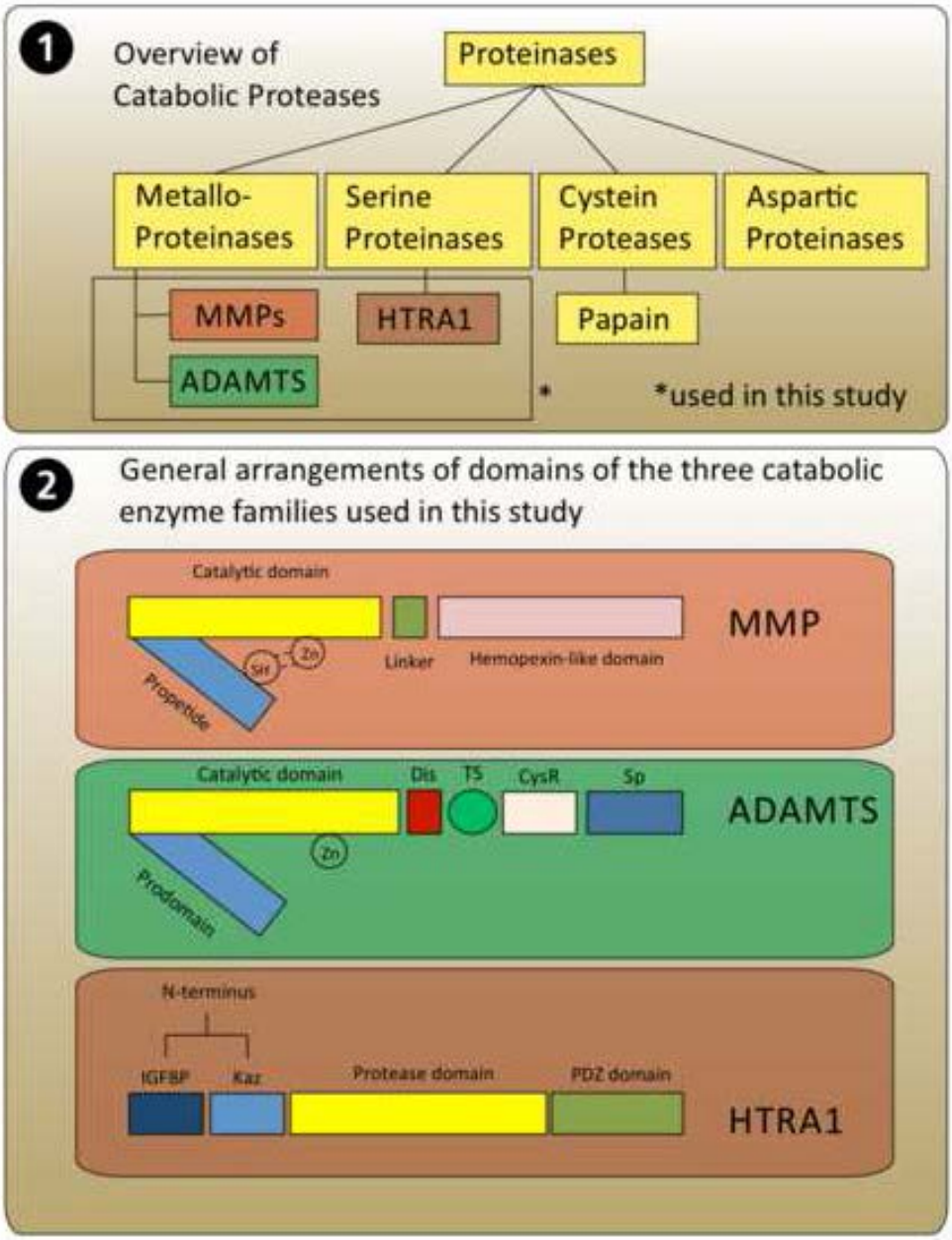

Abbreviations:

CysR: Cysteine-rich domain
Dis: disintegrin-like domain
IGFBP: Insulin-like growth factor binding protein
Kaz: Kazal-like module
PDZ: postsynaptic density of 95kDa
SH: SulfHydrl group
Sp: Spacer domain
TS: thrombospondin domain
Zn: Zinc (active site)

Figure 10
Click here to download high resolution image

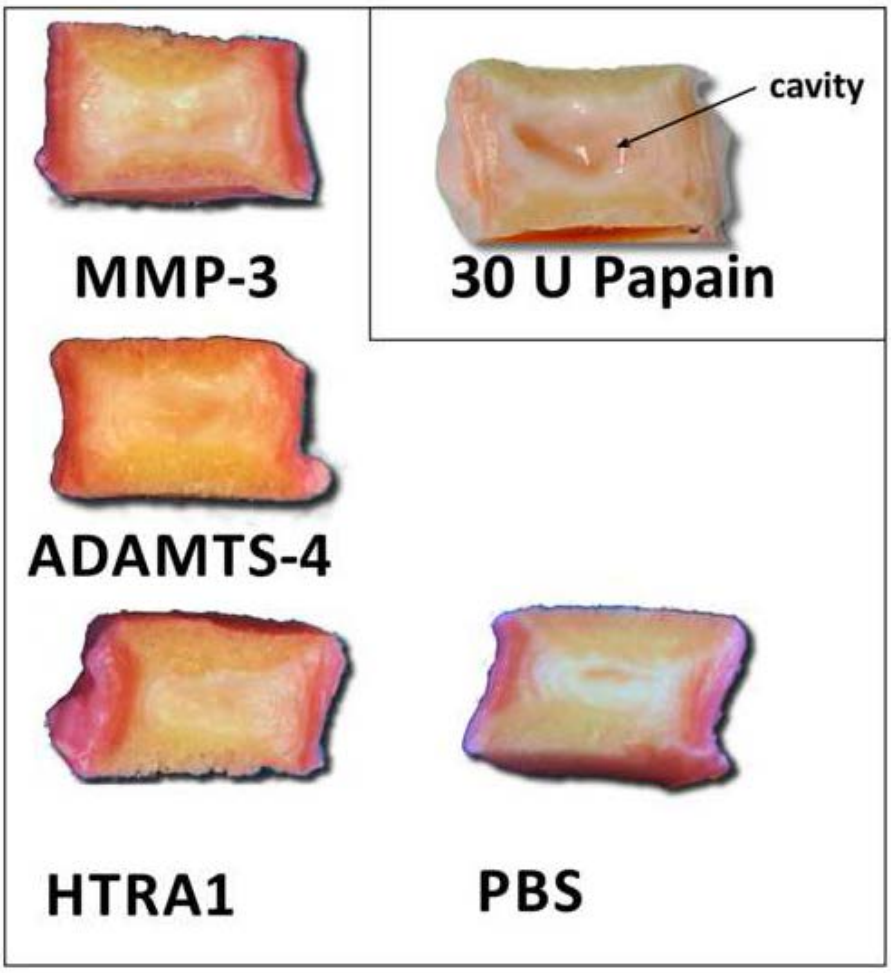

4 Unpublished data

As described by Tennstaedt et al (2012), recombinant HTRA1 protein was overexpressed and purified from bacteria [112]. To confirm the purity of the final protein, 4 µg of each protein was loaded on a SDS-PAGE gel and stained with Coomassie Blue (Fig. 8). A total of 4 µg of BSA was also used as a loading control.

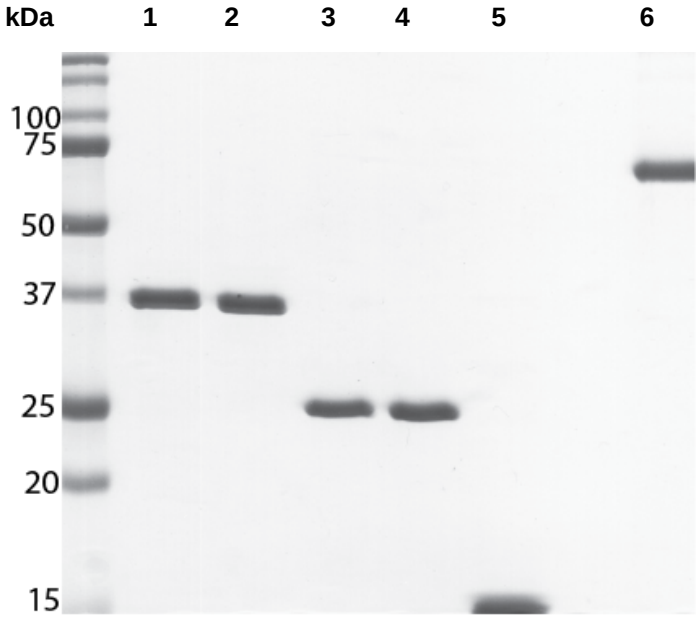

Figure 8: Coomassie Clue stained SDS-PAGE of 4µg protein per lane. 1 = ΔMac; 2 = ΔMacSA; 3 = ΔMac/ΔPDZ; 4 = ΔMacSA/ΔPDZ; 5 = ΔMac/Δprotease; 6 = BSA (loading control).

As purified recombinant protein was to be subsequently used under sterile cell culture conditions, LPS content had to be in a range suitable for cell culture systems. Hence, a LPS test was performed for all constructs purified before they were used in cell culture (Pierce LAL Chromogenic Endotoxin Quantitation Kit, Thermo Scientific). Figure 9 shows a representative measurement of the LPS content of three recombinant HTRA1 constructs, as well as of the αLG4-5 construct (Fig. 18). Since the FDA's guideline allows a maximum endotoxin level of up to 0.25 EU/ml, all samples tested are applicable for cell culture usage [176]. Conclusively, the recombinant proteins tested can even be considered endotoxin-free, as the detection limit of the assay used lies in the range of approximately 0.05 EU/ml.

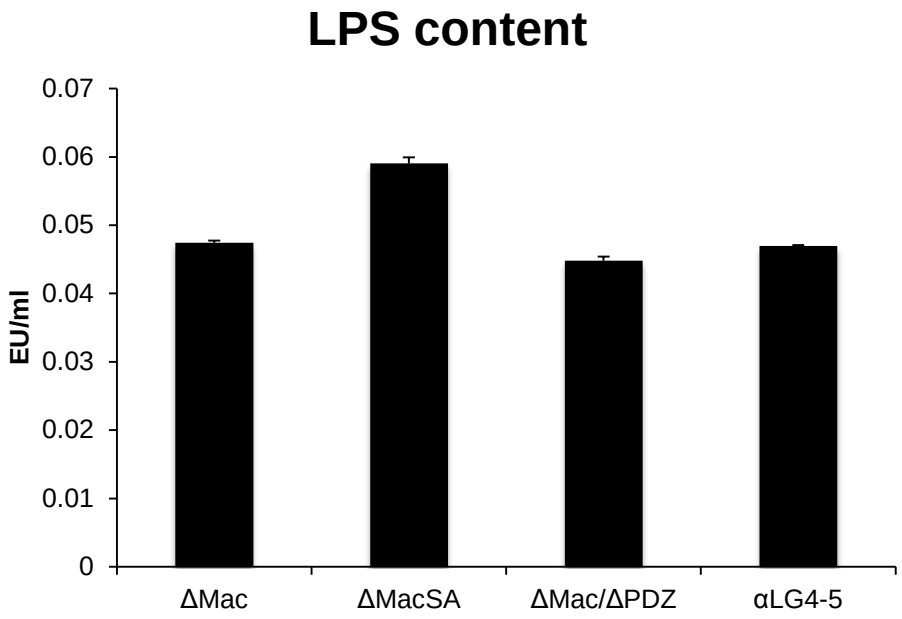

Figure 9: Representation of the LPS-content of the recombinant protein samples used in cell culture.

In a next step, recombinant HTRA1 and HTRA3 protein constructs were used in a proteolytic assay set up (c.f. [177]) to determine their protease activity towards BODIPY-FL-labeled DQ elastin conjugate using the EnzChek Elastase Assay Kit [177] (Fig. 10 and 11). All constructs carrying an active proteolytic domain showed a time-dependent increase in fluorescence, thereby indicating cleavage of the elastin substrate. At the same time, all inactive constructs exhibited almost no cleavage of elastin at all (Fig. 10).

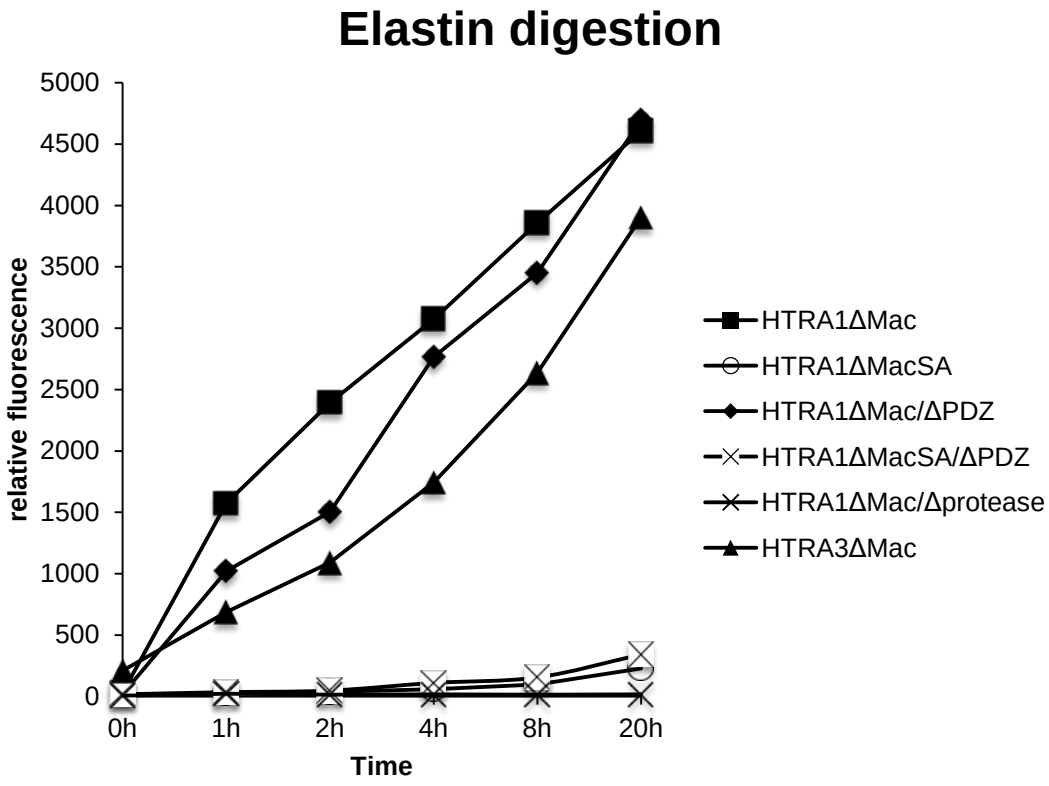

Figure 10: Time course of the protease activity assay with different recombinant HTRA1 and HTRA3 constructs.

In the same set up, HTRA1, HTRA3 and trypsin were incubated with BODIPY-FL-labeled DQ elastin conjugate in the absence or presence of a specific HTRA1 antibody (10 µg/ml, antibody kindly provided by Novartis). It was shown that the presence of the antibody resulted in a significant decrease of HTRA1 activity ($p<0.001$ after 4 h), while HTRA3 ($p=0.24$ after 4 h) and trypsin ($p=0.05$) activity remained unaltered or was even slightly increased (Fig. 11).

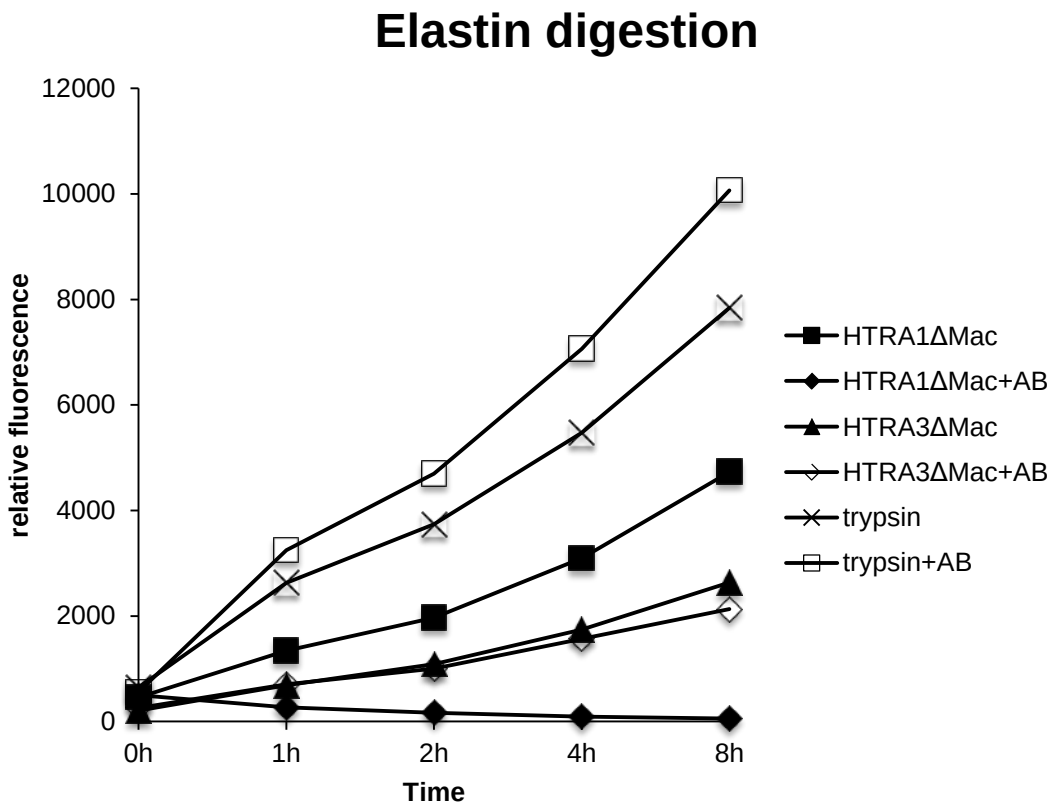

Figure 11: Time course of the protease activity assay with recombinant HTRA1, HTRA3 and trypsin protein, with and without anti HTRA1 antibody (10 µg/ml).

To clarify the oligomeric status of different recombinant HTRA1 constructs, a Blue-Native-PAGE gel was performed (Fig. 12). While the HTRA1ΔMac protein constructs under denatured conditions showed only one distinct band, native conditions revealed at least five different species of oligomeric states for this construct. The same was true for the ΔMac/ΔPDZ domain of HTRA1. At the same time, the ΔMac/Δprotease domain showed only one band at the predicted size of approximately 18kDa.

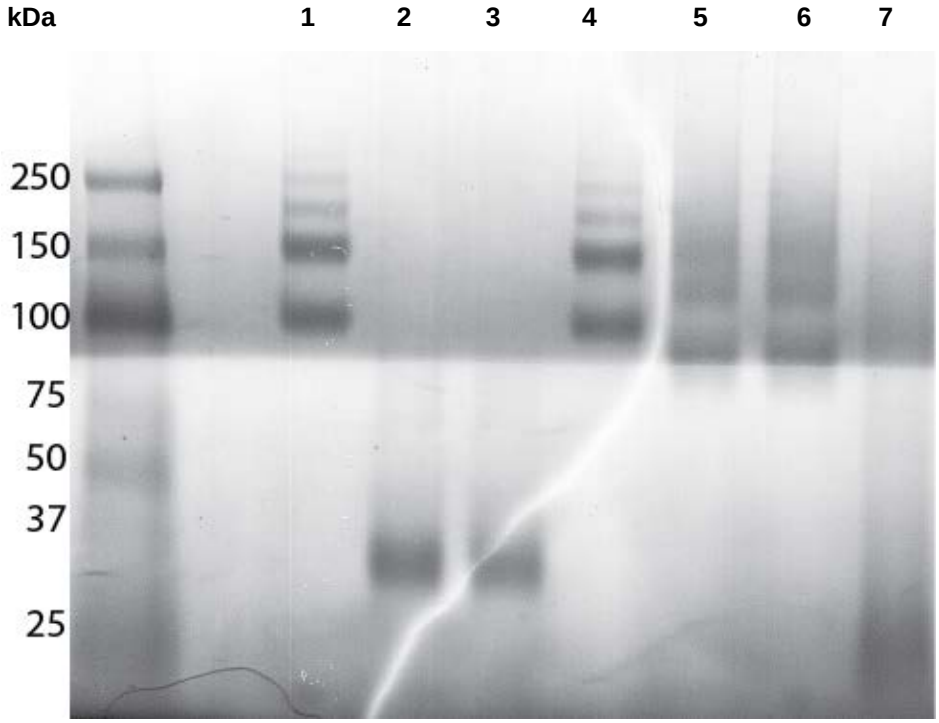

Figure 12: Coomassie Blue stained Blue-Native-PAGE gel of the different HTRA1 recombinant constructs. 1 = HTRA1ΔMac; 2 = HTRA1ΔMac + 0.1% SDS (Sodium dodecyl sulfate); 3 = HTRA1ΔMac + 1% SDS; 4 = HTRA1ΔMacSA; 5 = HTRA1ΔMac/ΔPDZ; 6 = HTRA1ΔMacSA/ΔPDZ; 7 = HTRA1ΔMac/Δprotease.

Figure 13 shows the result of a WST-1 assay performed with cells that were undifferentiated, differentiated and untreated, or differentiated and treated with recombinant active HTRA1ΔMac. No significant differences were observed, which serves as proof that the seen effects of HTRA1 not due to a decrease in cell proliferation and survival.

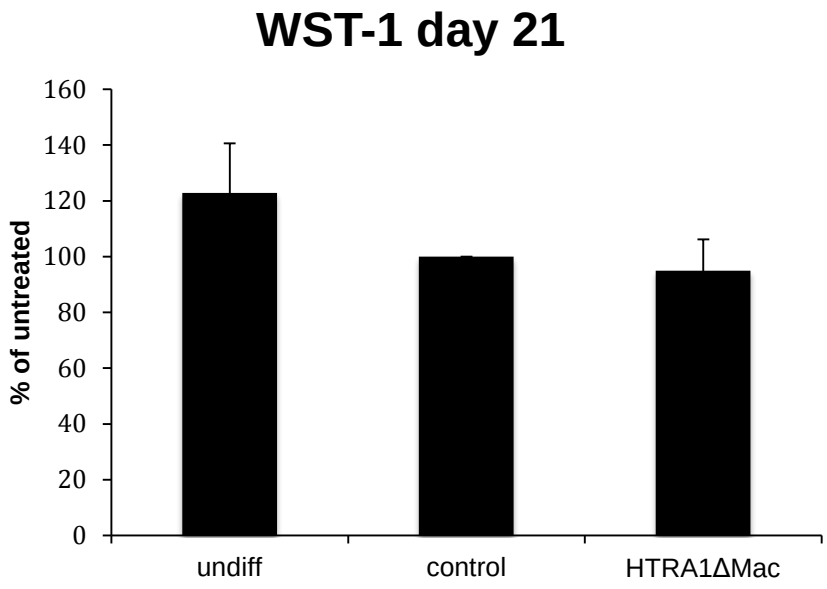

Figure 13: WST-1 assay of cells treated with or without recombinant HTRA1 protein and heparin for 21 days.

Furthermore, a first known cleavage substrate of HTRA1 was tested with the recombinant protein produced within this thesis. The digestion of the substrate fibronectin (FN) was evaluated when incubated over night with HTRA1ΔMac at 37°C (molar ratio of 2:1) (Fig. 14). It was found that HTRA1 could cleave fibronectin in this *in vitro* set up.

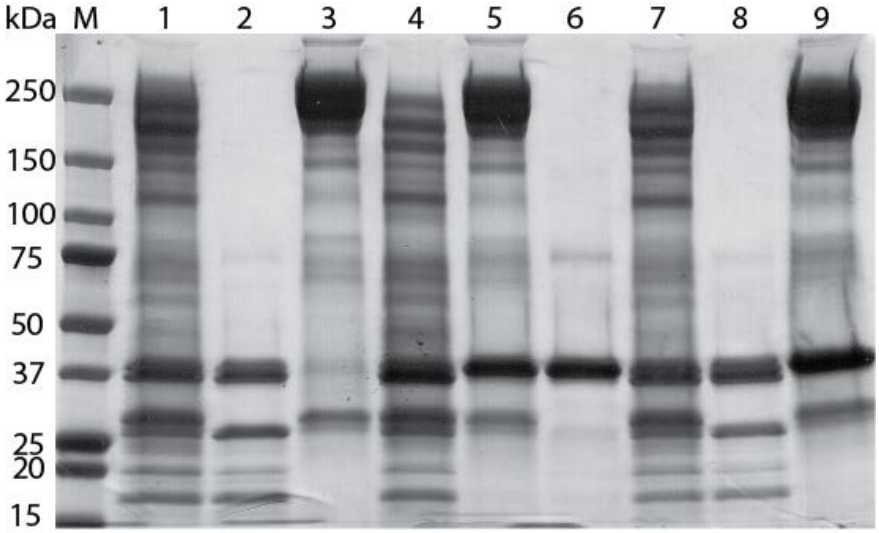

Figure 14: Coomassie Blue stained gradient SDS-PAGE gel of the fibronectin digestion by HTRA1ΔMac and HTRA1ΔMacSA. 1 = 5 µg HTRA1ΔMac and 10 µg FN; 2 = 5 µg HTRA1ΔMac; 3 = 10 µg FN; 4 = 5 µg HTRA1ΔMac of old batch and 10 µg FN; 5 = 5 µg HTRA1ΔMacSA and 10 µg FN; 6 = 5 µg HTRA1ΔMacSA; 7 = 5 µg retained HTRA1ΔMacSA from 50 kDA cutoff Amicon and 10 µg FN; 8 = 5 µg retained HTRA1ΔMac from 50 kDA cutoff Amicon; 9 = 5 µg retained HTRA1ΔMacSA from 50 kDA cutoff Amicon.

Similarly, the stability of recombinant HTRA1ΔMac under different conditions was evaluated. For this, 3 µg of the recombinant protein was loaded on a SDS-PAGE gel either freshly, or subsequent to an overnight incubation at 37°C with or without $CaCl_2$ (5 mM) (Fig. 15). It was found that HTRA1 was partially degraded when incubated over night at 37°C, and the presence of $CaCl_2$ increased this effect. The same observation holds true with the activity of HTRA1 towards FN.

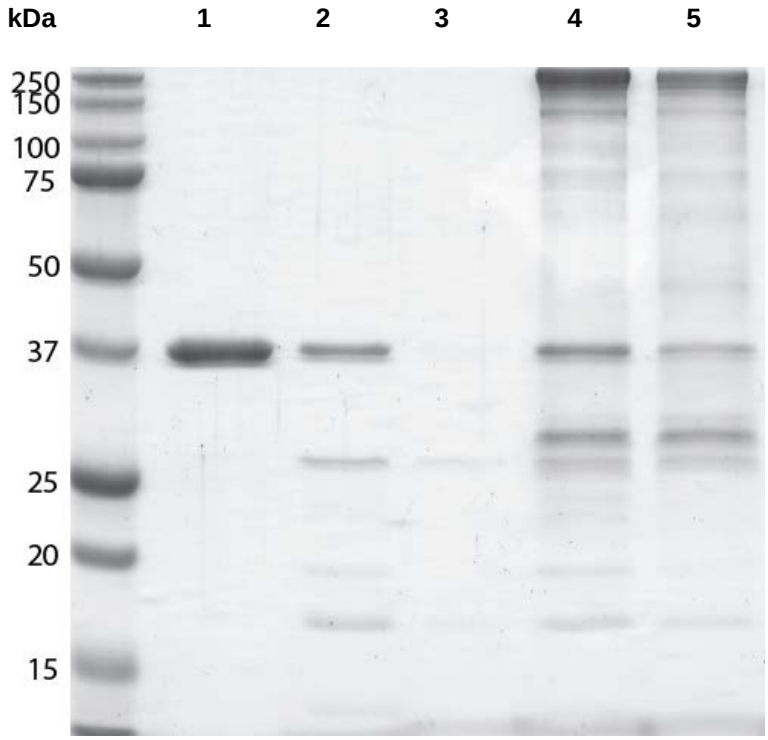

Figure 15: Coomassie Blue stained SDS-PAGE of a stability test of recombinant HTRA1 protein (3 µg per lane) and fibronectin. 1 = HTRA1ΔMac; 2 = HTRA1ΔMac o/n 37°C; 3 = HTRA1ΔMac o/n 37°C + $CaCl_2$ (5 mM); 4 = HTRA1ΔMac + FN; 5 = HTRA1ΔMac + FN + $CaCl_2$.

Next to fibronectin, we looked at the involvement of other cellular surface proteins potentially involved in the adipogenesis. CD105 (endoglin) is one example of a known binding partner of the TGF-β pathway and is therefore another potential candidate for degradation by HTRA1, either actively or passively (e.g. MMPs) [178]. We therefore performed an *in vitro* digestion assay of HTRA1ΔMac and CD105 (molar ratio of 1:5; recombinant CD105 was obtained from R&D Systems) (Fig. 16). Several weakly stained CD105 fragments were observed following HTRA1 treatment as determined by Western blot analysis. Heparin, an agent used to inhibit HTRA1´s binding ability to the cell surface [177] was included in order to look at a potential inhibition or activation towards HTRA1´s proteolytic activity. However, the inclusion of heparin (purchased from SIGMA-ALDRICH) in this reaction had no impact on the proteolytic activity of HTRA1 towards CD105. It therefore appeared that HTRA1 has a minimal proteolytic activity towards CD105.

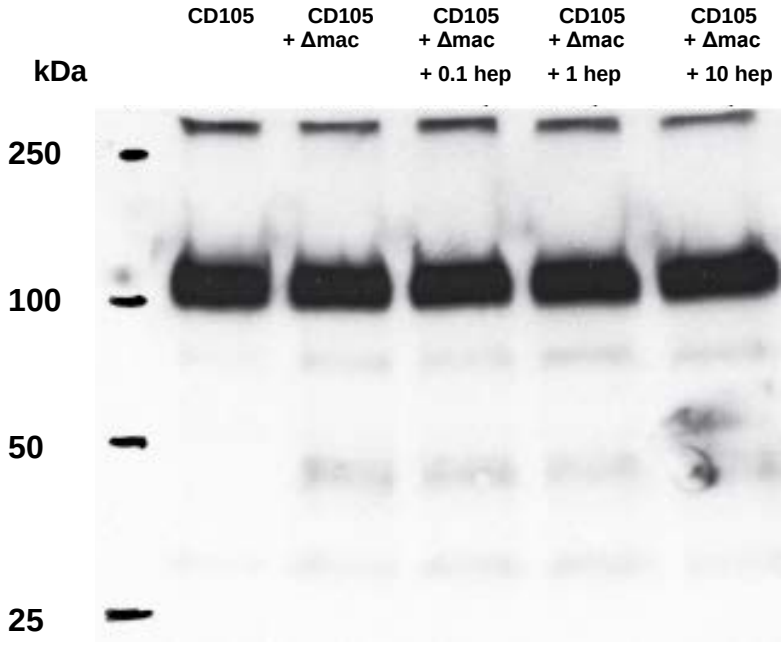

Figure 16: anti CD105-Western blot of the *in vitro* digestion of recombinant CD105 by HTRA1ΔMac. Heparin (hep) was added to the reaction in a concentration range from 0.1 to 10 µg/ml.

In order to further clarify HTRA1's influence on CD105, hMSCs were incubated with HTRA1ΔMac and CD105 staining (PE anti-human CD105, BioLegend) was evaluated by FACS analysis (c.f. [177]) (Fig. 17). However, no significant effects on CD105 surface staining could be observed, thereby confirming HTRA1's lack of proteolytic activity towards CD105.

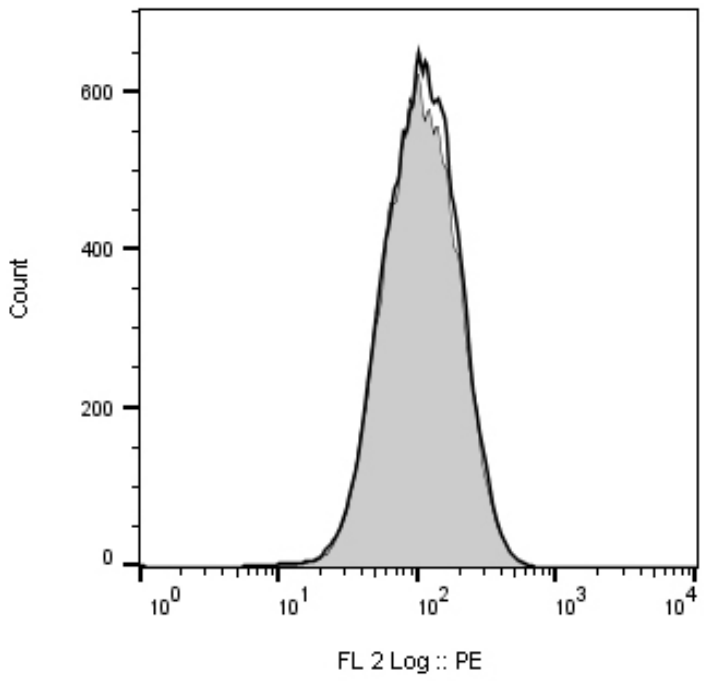

Figure 17: Histogram of hMSCs treated (black line, no fill) or untreated (grey fill) with HTRA1ΔMac prior to the staining of CD105 with a fluorescently labeled antibody [177].

Whilst analysing cell supernatants for additional sources of ECM fragments, we noticed that as compared to undifferentiated hMSCs, the supernatants of adipogenic hMSCs harboured less soluble laminin-α4, which appeared as ~ 45- and 65 kDa-bands following immunoblotting (Fig. 18). Moreover, supernatants harvested from adipogenic hMSCs treated with HTRA1ΔMac, but not with HTRA1ΔMacSA, contained at least two additional laminin-α4 fragments, observed as bands at ~ 42 and 24 kDa. This was considered to be of particular relevance with regards to adipogenic induction based on the findings of a previous study in which laminin-α4 fragments containing the globular regions αLG4-5 were shown to have a negative influence on adipogenesis [179].

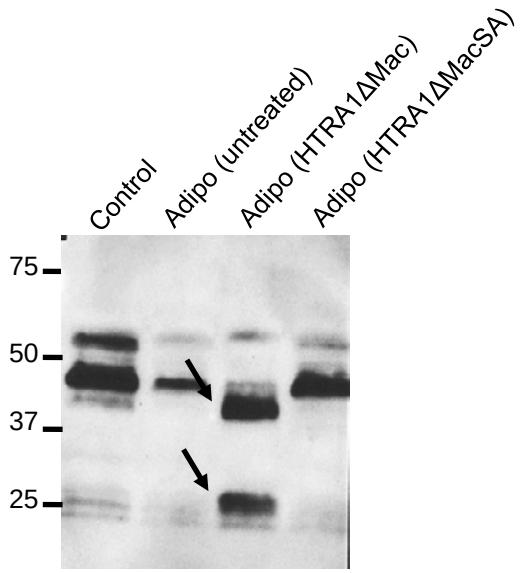

Figure 18: HTRA1 generates reactive ECM fragments. Western blot analysis of native laminin-α4 in concentrated supernatants harvested from undifferentiated hMSCs (control), untreated adipogenic hMSCs, or adipogenic hMSCs treated with recombinant HTRA1ΔMac (45 nM) for 2 days. *Arrows* indicate specific laminin-α4 fragments due to HTRA1ΔMac treatment.

Furthermore, HTRA1ΔMac was able to generate similar sized fragments when incubated with a recombinant form of laminin-α4 (Fig. 19).

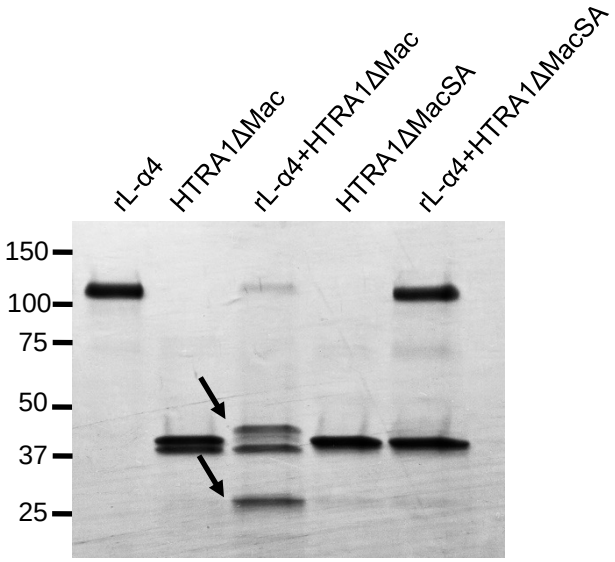

Figure 19: Equimolar concentrations (225 nM) of recombinant laminin-α4 (rL-α4) and recombinant HTRA1 were incubated together overnight at 37°C, and total protein separated by SDS-PAGE and analysed with Coomassie staining. *Arrows* indicate specific laminin-α4 fragments due to HTRA1ΔMac treatment.

In order to gain deeper insights into this specific fragment produced by HTRA1, N-terminal sequencing of the 42 kDa fragment was performed and revealed a cleavage site between V1442 and A1443 within the linker region adjoining globular regions αLG3 and αLG4-5 (Fig. 20), thereby verifying that this fragment is produced specifically by the actions of HTRA1.

(1234-1402) **G3** - PIESSPLFLLHKKGK
NLSKPKASQNKKGGKSKDAPSWD
PV ▼ ALKLPERNTPRNSHCHLSNSP
RAIEH - **G4-5** (1469-1820)

Figure 20: Amino acid sequence of laminin-α4 linkage region between αLG3 and αLG4-5 indicating the HTRA1 cleavage site as determined by N-terminal sequencing (*arrow head*).

Since we hypothesized that the αLG4-5 fragment produced by HTRA1 was reactive towards hMSC adipogenesis, we generated a purified recombinant form of the αLG4-5$^{1443\text{-}1820}$ as shown in figure 21, in order to be able to utilize the fragment in our cell culture system and thereby mimicking a potential downstream effect of HTRA1´s action on the hMSCs.

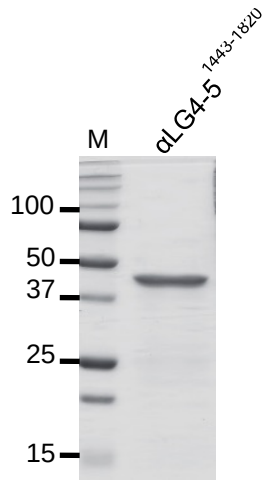

Figure 21: Purified baculovirus generated recombinant αLG4-5$^{1443\text{-}1820}$ fragment (3 μg) separated on a SDS-PAGE gel and visualized by Coomassie blue staining.

After its successful production and purification, the fragment was tested for its effects on oil droplet formation in hMSCs undergoing adipogenesis (Fig. 22). We observed a significant and dose dependent decrease in oil droplet formation in differentiating hMSCs after 18 days of treatment with αLG4-5 at concentrations ranging from 0.25 to 1 μg/ml, thereby confirming the HTRA1-generated laminin-α4 fragments could indeed influence hMSC adipogenesis.

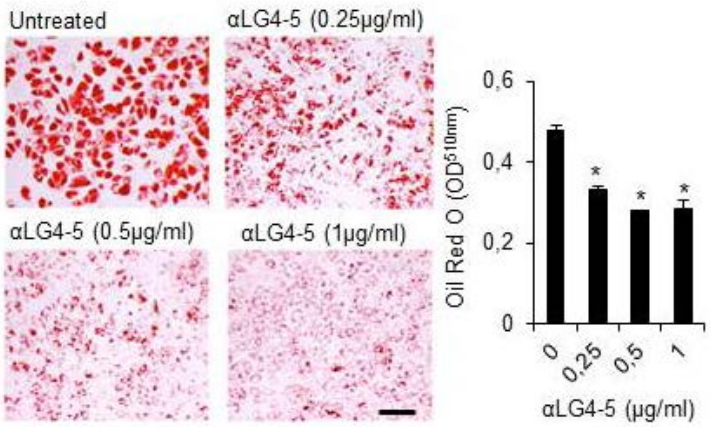

Figure 22: Quantification of Oil Red O staining of hMSCs treated with varying concentrations of recombinant αLG4-5 at day 18 post adipogenic induction. **P* < 0.001 as compared to untreated.

As we could already show that the effects on oil droplet formation of hMSCs were due to HTRA1´s ability to induce MMP secretion [177], we subsequently analyzed the effects of the αLG4-5 treatment on MMP protein secretion (Fig. 23). However, no significant increases in MMP-3 protein production were observed.

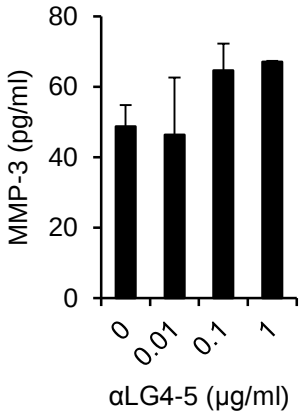

Figure 23: Effect of recombinant αLG4-5 on MMP-3 protein secretion in adipogenic hMSCs at day 14.

By contrast, MMP-13 protein secretion was significantly downregulated in cells treated with αLG4-5 at all concentrations tested (Fig. 24).

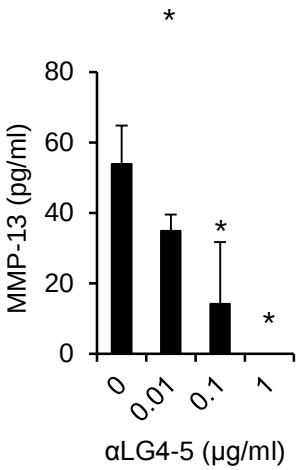

Figure 24: Effect of recombinant αLG4-5 on MMP-13 protein secretion in adipogenic hMSCs at day 14.

Furthermore, when silencing laminin-α4 expression in hMSCs using siRNA, we were able to significantly enhance oil droplet formation in both untreated and HTRA1-treated adipogenic hMSCs (Fig. 25), while the effect of HTRA1 on oil droplet formation was still maintained, but to a lesser degree. Thus, HTRA1´s ability to inhibit oil droplet formation in hMSCs undergoing adipogenesis may partially be reliant on the actions of reactive laminin-α4 fragments. However, this appears to be independent of MMP production by the cells.

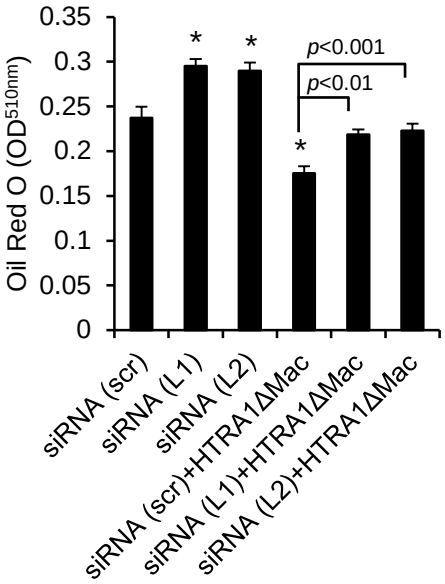

Figure 25: Quantification of Oil Red O staining of hMSCs treated with or without HTRA1 and knockdown of laminin-α4 with two different oligos at day 18 post adipogenic induction. **P* < 0.001 as compared to untreated.

Preparation of recombinant αLG4-5$^{1443-1820}$. Overexpression of human his-tagged αLG4-5$^{1443-1820}$ was performed in SF21 insect cells using the pBacPAK8 Vector system (Clontech Laboratories, Saint-Germain-en-Laye, France) according to the manufacturer's protocol. αLG4-5$^{1443-1820}$ was purified by affinity chromatography using HisTrap FF Crude columns (GE Healthcare, Glattbrug, Switzerland) followed by size exclusion chromatography. Purified protein was subsequently concentrated using Amicon Ultra columns (10kDa size exclusion, Millipore) prior to use.

5 General discussion and perspectives

The ubiquitously expressed trypsin-like serine protease HTRA1 is undoubtedly involved in the regulation of a large number of intracellular and extracellular processes [140, 150, 166, 177, 180-182]. As many of these processes involve cross talk between important signaling pathways (e.g. TGF-β signaling), it is likely that HTRA1 levels must be carefully regulated to allow for the normal functioning of healthy tissue. It is therefore not surprising that HTRA1 can be regarded as having either a beneficial or detrimental role in disease [109]. The work described in this thesis primarily focuses on the role of HTRA1 in the regulation of hMSC adipogenesis. The basis for this study comes from the observation that HTRA1 acts as a positive mediator of hMSC osteogenesis, thus implicating it in bone formation and repair. Interestingly, the differentiation of hMSCs towards osteogenesis and adipogenesis is often regulated in a reciprocal manner [175]. Furthermore, the bones of patients with osteoporosis are characterized by having low bone mass in combination with significantly increased levels of fat marrow [183-185]. This leads to the assumption that a dysfunctional bone marrow tissue favors hMSC adipogenesis over the desired osteogenesis. Indeed, both animal and human studies have repeatedly demonstrated a significant impairment in the capacity of resident bone hMSCs from osteoporotic subjects to undergo osteogenesis, whilst adipogenic capabilities remain intact and in some instances even elevated [186]. In the presented work, we demonstrate that HTRA1 has a strong effect on hMSC lineage commitment, where it acts to suppress adipogenesis [177], whilst promoting osteogenesis [165]. Hence, it could be considered as a potential gatekeeper of multi lineage commitment in hMSCs. However, the question as to which pathways are affected in the facilitation or suppression of either of the two lineage commitments remains open. Still, with regards to hMSC adipogenesis, some important insights are offered by the findings within this thesis, highlighting MAP kinase-dependent upregulation of MMPs as being a possible means through which HTRA1 mediates its suppressive effects [177].

The influence of HTRA1 on ECM turnover has been well described and has been linked to various diseases in which ECM breakdown is a central pathological

feature [107, 129, 146, 148, 156]. This breakdown of tissue material is realized by an upregulation of MMPs which, in turn, is most likely mediated through the actions of reactive fibronectin fragments (Fnf) species, as shown by our own lab in the context of HTRA1´s involvement in joint and IVD degeneration [107, 129]. However, in adipose tissue homeostasis and development, ECM remodeling and reorganization by MMPs is a well-known requirement for adipose-tissue integrity and stem cell adipogenesis [187, 188]. The dysregulation of MMP production may therefore be an underlying cause for several adipose tissue-related diseases and may define adipocyte health in general. Our own findings support this hypothesis, as an increased production of MMP-1, -3 and -13 by adipogenic hMSCs upon stimulation with HTRA1 was found to lead to a loss of several ECM components and ultimately to a decrease in lipid accrual [177]. Thus, HTRA1 is suggested to have a detrimental role in hMSC adipogenesis via the upregulation of MMPs. Surprisingly, these effects were found to be independent of Fnfs, while evidence was found to suggest that MMP-13 itself is responsible for the generation of these fragments in response to HTRA1. We therefore speculate that alternative mechanisms must exist through which HTRA1´s ability to regulate MMP production is mediated by hMSCs.

We were able to gain some insights into the detailed mechanism of how HTRA1´s actions are mediated by manipulating its trypsin-like serine protease domain, as well as its protein-binding PDZ domain. Conclusively, both domains are necessary in order to allow for its inhibitory influence on hMSC adipogenesis via the production of MMPs, the decrease in type IV collagen and laminin, as well as the decrease in lipid uptake. Importantly, it was found that HTRA1 could directly interact with surface bound heparan sulfate (HS) via its PDZ domain. This sequestration of HTRA1 to the cell surface could therefore potentially allow for it to closely interact with HS-containing glycoproteins, i.e. potential substrates. Indeed, evidence is given by the fact that we were able to detect increased levels of soluble syndecan-4 as a result of adipogenic hMSCs being exposed to structurally intact HTRA1. Since syndecans are known to be important regulators of lipid uptake in differentiating adipocytes [189, 190], the release of syndecan-4 from the cell surface may explain the observed inhibition of lipid accrual in adipogenic hMSCs treated with HTRA1. In addition to syndecans, other glycoproteins exist within the ECM of adipocytes which are potential substrates of HTRA1. One

example is nidogen, which was successfully shown to be a substrate of HTRA1 [146] and which represents an important stabilizing element of the adipocyte basal lamina through its binding to type IV collagen and laminin [191]. Thus, nidogen cleavage by HTRA1 and the subsequent stimulatory effects of the fragments may therefore be an alternative route through which HTRA1 mediates its inhibitory effects on adipocyte maturation and development.

Additionally, HTRA1´s ability to both induce MMP production and inhibit hMSC adipogenesis was considered as being dependent on JNK activity and, to a lesser extent, ERK. The interpretation of the involvement of p38 was hampered by the fact that the inhibition of p38 activation resulted in a decreased oil droplet formation in adipogenic hMSCs throughout all treatment conditions. The regulation of MMP expression is primarily through MAP kinase activation [192] and several studies have been able to demonstrate an ERK and JNK involvement in the suppression of hMSC adipogenesis [193-195]. Although unable to ascertain its cause, we were able to identify MAP kinase activation as a central factor in mediating the effects of HTRA1 during hMSC adipogenesis. Furthermore, both the proteolytic activity and PDZ domain are required for efficient MAP kinase activation. Hence, both its binding and its ability to degrade specific substrates are required for HTRA1 to influence MAP kinase activation in hMSCs.

Syndecan-4 shedding may represent one potential means by which HTRA1 could act on MAP kinase activation, whereby the disruption of the syndecan-4 to MAP kinase signaling cascade contributes to an increased JNK activation [196]. Importantly, both MAP kinases and MMPs are known to be central factors in the pathophysiology of adipose tissue, even extending to the development of insulin resistance in obese mice and humans [197-199]. The severity of insulin resistance among obese patients clearly involves adipocyte integrity [200]. Thus, factors negatively influencing adipogenesis of hMSCs and adipocyte function are likely to contribute to and possibly instigate insulin resistance. Therefore, inappropriately high levels of HTRA1 in the adipose tissue of obese individuals can be interpreted as being an indicator of deficiencies and malfunctions in the development of adipocytes within adipose tissue. In line with this, we were able to detect HTRA1 in the visceral fat from obese patients, with levels being greatest at sites of cellular infiltration and crown-like structures. Furthermore, MMP-13 was also localized to the same regions of the fat tissue as HTRA1, thus re-enforcing the concept of

there being a close working relationship between these two proteases. We furthermore suggest macrophages as representing a potential cellular source for HTRA1 in the fat tissue, as they are considered to be the predominant cell type in crown-like structures [37, 201] and are known to be potent inducers of MMPs in adipocytes [202].

Undoubtedly, this thesis only addresses a small part of a wider story, and to understand exactly how HTRA1's ability to manipulate the ECM results in a dysregulation of hMSC differentiation will require more detailed investigations. For instance, the influence of HTRA1 on TGF-β has been well characterized in other cell systems [154, 166], where an upregulation of TGF signaling can be observed due to the lack of attenuation of TGF-β signaling events by HTRA1. Since TGF-β signaling is known to have a central role in the regulation of stem cell differentiation [203, 204], it appears logical that the effect of HTRA1 on adipogenic hMSCs is also partially driven via the TGF-β pathway. Another important aspect is the maturation and activity state of many of the factors involved. Here, the actual enzymatic activity of HTRA1 as well as that of the MMPs is of great importance, as they are known to exist in activate and inactive states both inside and outside of the cell [205, 206]. We cannot rule out the fact that HTRA1´s effects are, to a certain extent, also occurring intracellularly. More importantly however, the impact of protease inhibitors (e.g. serpins, TIMPs) could also be of significant importance. Certainly, gene expression studies, as well as *ex vivo* activity assays of certain enzymes, may be able to shed some light on the potential players regulating HTRA1's impact on the ECM, as well as on the cells themselves. Also, other parts of adipocyte maturation were not addressed within this study. One example is lipolysis, which ensures a constant release of free fatty acids from mature adipocytes [207, 208]. Dependent on whether or not the net inflow exceeds the outflow, the cells accumulate or reduce their overall oil droplet content (c.f. chapter 1.2.1.1). Thus, an increase in lipolysis is a scenario, which could contribute to the effects of HTRA1 on hMSCs undergoing adipogenesis. By analysing protein amounts of the hormone-sensitive lipase (HSL) by Western blot, this part of the fatty acid homeostasis could be addressed rather easily.

As previously mentioned, ECM fragments other than Fnfs might potentially be involved in mediating the effects of HTRA1 on hMSC adipogenesis. During the

course of this study, we confirmed laminin-α4 as being an HTRA1 substrate, identifying several fragments within the supernatants of HTRA1 treated hMSCs (c.f. section 4, figures 18 – 21). In order to further investigate their potential role in regulating adipogenesis, we treated cells with the recombinant laminin-α4 fragment produced by HTRA1, called αLG4-5. We consistently found that αLG4-5 was capable of inhibiting oil droplet formation in the adipogenic hMSCs (section 4, figure 22). However, this process appeared to be independent of MMPs, based on a lack of MMP-3 upregulation, and even a significant decrease in MMP-13 production (section 4, figure 23 + 24). Therefore, it is possible that HTRA1's inhibitory actions towards hMSC lipid accrual may also involve the actions of reactive laminin-α4 fragments, independently of MMP activity. However, we also speculated that MMPs induced by HTRA1 could themselves generate the reactive αLG4-5 fragments, thereby explaining the lack of effects seen with NNGH in preventing loss of lipid droplet accumulation in αLG4-5-treated cells. Thus, the effects seen by the αLG4-5 fragment on adipogenesis could potentially be explained by the diverse implications of the fragments on hMSCs undergoing adipogenesis. As proposed by Yamashita et al [179], the αLG4-5 fragment may modulate FGF-2 signaling directly by binding to syndecans via their heparin-binding region, thereby blocking the actions of FGF resulting in the suppression of adipogenesis [209].

Thus, HTRA1 may represent a master regulator between adipogenesis and osteogenesis, determining, the cellular fate of hMSCs. If indeed the case, this may have far reaching implications for the maintenance of tissue where stem cell commitment plays an important role. One such example is in white adipose tissue (WAT), where inhibition of hMSC adipogenesis by exposure to HTRA1 may be considered detrimental with regards to the maintenance of adipocyte function [210, 211]. Furthermore, increased levels of HTRA1 within adipose tissue may even represent a biomarker for insulin-resistance and possibly an additional diagnostic factor for type 2 diabetes. Moreover, fully functional adipocytes within the WAT are a prerequisite for appropriate insulin sensitivity of the adipose tissue and thereby ultimately have implications for the whole body. A cell with a dysfunctional ECM environment caused by different proteases, may contribute to the loss of insulin sensitivity of the tissue itself. This may be caused by an increase of fatty acids in

the circulation of the body due to a relative low net intake of fatty acids into the fat tissue, thereby disturbing the insulin response pathways [200, 212]. In addition, the cell's ability to affect a proper insulin response may also be influenced by alterations in cell surface receptor availability (e.g. GLUT-4) [213] due to pathological levels of HTRA1. This could be addressed by employing a high fat diet model using *Htra1*$^{-/-}$ knockout mouse model, where the ensuing obese phenotype may be significantly altered as compared to wild type mice, resulting in a slower onset of diabetes type II in these mice. However, this was considered outside the realms of this particular study. It is therefore envisaged that future studies will be required in order to fill the gaps in our knowledge regarding the impact of HTRA1 on adipogenesis *in vivo*. Furthermore, a more detailed understanding of the intracellular responses initiated by the exposure of the hMSCs to HTRA1-generated ECM fragments, in particular laminin-α4, is required in order to identify new possible therapeutic targets. Moreover, it would be interesting to translate the findings from the current study on adipogenesis to the osteogenesis system. Here the reciprocally regulated effects could be studied further, thereby allowing for additional insights into the transition and differentiation between osteogenesis and adipogenesis in more detail. Furthermore, details about time-dependent changes of certain intracellular pathways over the whole time period of the differentiation and HTRA1 treatment procedure would help to further identify potential signaling cascades involved in mediating HTRA1's effects. Certainly, arrays targeting the secretome of cells undergoing differentiation and the ECM composition would help tremendously in providing additional information with regards to the changes occurring during osteo- and adipogenesis in the presence and absence of HTRA1.

In conclusion, our findings highlight HTRA1 as being a central negative regulator of hMSC adipogenesis. The relevance of this is made evident by the fact that the adipose tissue plays an important role in many processes of the human body, being involved in regulating energy homeostasis of the skeletal musculature and other tissues. Importantly, the differential effect of HTRA1 on hMSC adipogenesis and osteogenesis offers novel insights into its potential impact on other diseases such a age-related bone loss, where HTRA1´s capacity to inhibit adipogenesis and

to promote osteogenesis would be considered beneficial in the maintenance of normal bone quality [212, 214].

References

1. Kolios, G. and Y. Moodley, *Introduction to stem cells and regenerative medicine.* Respiration, 2013. **85**(1): p. 3-10.
2. Gurtner, G.C., M.J. Callaghan, and M.T. Longaker, *Progress and potential for regenerative medicine.* Annu Rev Med, 2007. **58**: p. 299-312.
3. Nombela-Arrieta, C., J. Ritz, and L.E. Silberstein, *The elusive nature and function of mesenchymal stem cells.* Nat Rev Mol Cell Biol, 2011. **12**(2): p. 126-31.
4. Bubela, T., et al., *Is belief larger than fact: expectations, optimism and reality for translational stem cell research.* BMC Med, 2012. **10**: p. 133.
5. Tuch, B.E., *Stem cells--a clinical update.* Aust Fam Physician, 2006. **35**(9): p. 719-21.
6. Totey, S., et al., *Adult stem cells: a clinical update.* J Stem Cells, 2009. **4**(2): p. 105-21.
7. Kfoury, Y. and D.T. Scadden, *Mesenchymal Cell Contributions to the Stem Cell Niche.* Cell Stem Cell, 2015. **16**(3): p. 239-253.
8. Li, L. and T. Xie, *Stem cell niche: structure and function.* Annu Rev Cell Dev Biol, 2005. **21**: p. 605-31.
9. Gardner, R.L., *Stem cells: potency, plasticity and public perception.* J Anat, 2002. **200**(Pt 3): p. 277-82.
10. Conway, A. and D.V. Schaffer, *Biophysical regulation of stem cell behavior within the niche.* Stem Cell Res Ther, 2012. **3**(6): p. 50.
11. Yue, B., *Biology of the extracellular matrix: an overview.* J Glaucoma, 2014. **23**(8 Suppl 1): p. S20-3.
12. Theocharis, A.D., et al., *Cell-matrix interactions: focus on proteoglycan-proteinase interplay and pharmacological targeting in cancer.* Febs j, 2014. **281**(22): p. 5023-42.
13. Paiva, K.B. and J.M. Granjeiro, *Bone tissue remodeling and development: focus on matrix metalloproteinase functions.* Arch Biochem Biophys, 2014. **561**: p. 74-87.
14. Keely, P.J., *Proteolytic remodeling of the ECM and the geometric control of stem cell fate.* Dev Cell, 2013. **25**(4): p. 325-6.
15. Thomson, J.A., et al., *Embryonic stem cell lines derived from human blastocysts.* Science, 1998. **282**(5391): p. 1145-7.
16. Takahashi, K., et al., *Induction of pluripotent stem cells from adult human fibroblasts by defined factors.* Cell, 2007. **131**(5): p. 861-72.
17. Wu, D.C., A.S. Boyd, and K.J. Wood, *Embryonic stem cell transplantation: potential applicability in cell replacement therapy and regenerative medicine.* Front Biosci, 2007. **12**: p. 4525-35.
18. Majo, F., et al., *Oligopotent stem cells are distributed throughout the mammalian ocular surface.* Nature, 2008. **456**(7219): p. 250-4.
19. Berendsen, A.D. and B.R. Olsen, *Regulation of adipogenesis and osteogenesis in mesenchymal stem cells by vascular endothelial growth factor A.* J Intern Med, 2015.
20. Ben-Tabou de-Leon, S. and E.H. Davidson, *Gene regulation: gene control network in development.* Annu Rev Biophys Biomol Struct, 2007. **36**: p. 191.

21. Christophersen, N.S. and K. Helin, *Epigenetic control of embryonic stem cell fate.* J Exp Med, 2010. **207**(11): p. 2287-95.
22. Guenther, M.G. and R.A. Young, *Transcription. Repressive transcription.* Science, 2010. **329**(5988): p. 150-1.
23. Jopling, C., S. Boue, and J.C. Izpisua Belmonte, *Dedifferentiation, transdifferentiation and reprogramming: three routes to regeneration.* Nat Rev Mol Cell Biol, 2011. **12**(2): p. 79-89.
24. Morrison, S.J. and J. Kimble, *Asymmetric and symmetric stem-cell divisions in development and cancer.* Nature, 2006. **441**(7097): p. 1068-74.
25. Tyndall, A., et al., *Autologous haematopoietic stem cell transplants for autoimmune disease--feasibility and transplant-related mortality. Autoimmune Disease and Lymphoma Working Parties of the European Group for Blood and Marrow Transplantation, the European League Against Rheumatism and the International Stem Cell Project for Autoimmune Disease.* Bone Marrow Transplant, 1999. **24**(7): p. 729-34.
26. Gratwohl, A., et al., *Hematopoietic stem cell transplantation: a global perspective.* JAMA, 2010. **303**(16): p. 1617-24.
27. Fridriksdottir, A.J., O.W. Petersen, and L. Ronnov-Jessen, *Mammary gland stem cells: current status and future challenges.* Int J Dev Biol, 2011. **55**(7-9): p. 719-29.
28. Visvader, J.E. and J. Stingl, *Mammary stem cells and the differentiation hierarchy: current status and perspectives.* Genes Dev, 2014. **28**(11): p. 1143-58.
29. Barker, N., *Adult intestinal stem cells: critical drivers of epithelial homeostasis and regeneration.* Nat Rev Mol Cell Biol, 2014. **15**(1): p. 19-33.
30. Slorach, E.M., F.C. Campbell, and J.R. Dorin, *A mouse model of intestinal stem cell function and regeneration.* J Cell Sci, 1999. **112 Pt 18**: p. 3029-38.
31. Kershaw, E.E. and J.S. Flier, *Adipose tissue as an endocrine organ.* J Clin Endocrinol Metab, 2004. **89**(6): p. 2548-56.
32. Frayn, K.N., P. Arner, and H. Yki-Jarvinen, *Fatty acid metabolism in adipose tissue, muscle and liver in health and disease.* Essays Biochem, 2006. **42**: p. 89-103.
33. Ali, A.T., et al., *Adipocyte and adipogenesis.* Eur J Cell Biol, 2013. **92**(6-7): p. 229-36.
34. Dimitriadis, G., et al., *Insulin effects in muscle and adipose tissue.* Diabetes Res Clin Pract, 2011. **93 Suppl 1**: p. S52-9.
35. Frayn, K.N., et al., *Integrative physiology of human adipose tissue.* Int J Obes Relat Metab Disord, 2003. **27**(8): p. 875-88.
36. Surmi, B.K. and A.H. Hasty, *Macrophage infiltration into adipose tissue: initiation, propagation and remodeling.* Future Lipidol, 2008. **3**(5): p. 545-556.
37. Cinti, S., et al., *Adipocyte death defines macrophage localization and function in adipose tissue of obese mice and humans.* J Lipid Res, 2005. **46**(11): p. 2347-55.
38. Nakamura, M.T., B.E. Yudell, and J.J. Loor, *Regulation of energy metabolism by long-chain fatty acids.* Prog Lipid Res, 2014. **53**: p. 124-44.
39. Lobo, S., et al., *Fatty acid metabolism in adipocytes: functional analysis of fatty acid transport proteins 1 and 4.* J Lipid Res, 2007. **48**(3): p. 609-20.

40. Mashek, D.G. and R.A. Coleman, *Cellular fatty acid uptake: the contribution of metabolism.* Curr Opin Lipidol, 2006. **17**(3): p. 274-8.
41. Shiojima, I. and K. Walsh, *Regulation of cardiac growth and coronary angiogenesis by the Akt/PKB signaling pathway.* Genes Dev, 2006. **20**(24): p. 3347-65.
42. Carobbio, S., B. Rosen, and A. Vidal-Puig, *Adipogenesis: new insights into brown adipose tissue differentiation.* J Mol Endocrinol, 2013. **51**(3): p. T75-85.
43. Nicholls, D.G., V.S. Bernson, and G.M. Heaton, *The identification of the component in the inner membrane of brown adipose tissue mitochondria responsible for regulating energy dissipation.* Experientia Suppl, 1978. **32**: p. 89-93.
44. Saely, C.H., K. Geiger, and H. Drexel, *Brown versus white adipose tissue: a mini-review.* Gerontology, 2012. **58**(1): p. 15-23.
45. Lidell, M.E., M.J. Betz, and S. Enerback, *Brown adipose tissue and its therapeutic potential.* J Intern Med, 2014. **276**(4): p. 364-77.
46. Bluher, M. and C.S. Mantzoros, *From leptin to other adipokines in health and disease: facts and expectations at the beginning of the 21st century.* Metabolism, 2015. **64**(1): p. 131-45.
47. Nakamura, K., J.J. Fuster, and K. Walsh, *Adipokines: a link between obesity and cardiovascular disease.* J Cardiol, 2014. **63**(4): p. 250-9.
48. Ouchi, N., et al., *Adipokines in inflammation and metabolic disease.* Nat Rev Immunol, 2011. **11**(2): p. 85-97.
49. Grahame Hardie, D., *AMP-activated protein kinase: a key regulator of energy balance with many roles in human disease.* J Intern Med, 2014. **276**(6): p. 543-59.
50. Chen, M., et al., *Adiponectin regulates ACTH secretion and the HPAA in an AMPK-dependent manner in pituitary corticotroph cells.* Mol Cell Endocrinol, 2014. **383**(1-2): p. 118-25.
51. Conde, J., et al., *Adipokines: biofactors from white adipose tissue. A complex hub among inflammation, metabolism, and immunity.* Biofactors, 2011. **37**(6): p. 413-20.
52. Bliddal, H., A.R. Leeds, and R. Christensen, *Osteoarthritis, obesity and weight loss: evidence, hypotheses and horizons - a scoping review.* Obes Rev, 2014. **15**(7): p. 578-86.
53. Haslam, D.W. and W.P. James, *Obesity.* Lancet, 2005. **366**(9492): p. 1197-209.
54. Gray, D.S. and K. Fujioka, *Use of relative weight and Body Mass Index for the determination of adiposity.* J Clin Epidemiol, 1991. **44**(6): p. 545-50.
55. Lavie, C.J., R.V. Milani, and H.O. Ventura, *Obesity and cardiovascular disease: risk factor, paradox, and impact of weight loss.* J Am Coll Cardiol, 2009. **53**(21): p. 1925-32.
56. Pradhan, A., *Obesity, metabolic syndrome, and type 2 diabetes: inflammatory basis of glucose metabolic disorders.* Nutr Rev, 2007. **65**(12 Pt 2): p. S152-6.
57. Kaneto, H., D. Kawamori, and T.A. Matsuoka, *[Insulin resistance in pancreatic beta-cells: possible implication in beta-cell glucose toxicity].* Nihon Rinsho, 2006. **64 Suppl 9**: p. 203-11.

58. Lu, P., et al., *Extracellular matrix degradation and remodeling in development and disease.* Cold Spring Harbor perspectives in biology, 2011. **3**(12).
59. Frantz, C., K.M. Stewart, and V.M. Weaver, *The extracellular matrix at a glance.* J Cell Sci, 2010. **123**(Pt 24): p. 4195-200.
60. Mauney, J., B.R. Olsen, and V. Volloch, *Matrix remodeling as stem cell recruitment event: a novel in vitro model for homing of human bone marrow stromal cells to the site of injury shows crucial role of extracellular collagen matrix.* Matrix Biol, 2010. **29**(8): p. 657-63.
61. Streuli, C., *Extracellular matrix remodelling and cellular differentiation.* Current opinion in cell biology, 1999. **11**(5): p. 634-40.
62. Iozzo, R.V., *Matrix proteoglycans: from molecular design to cellular function.* Annu Rev Biochem, 1998. **67**: p. 609-52.
63. Kim, S.H., J. Turnbull, and S. Guimond, *Extracellular matrix and cell signalling: the dynamic cooperation of integrin, proteoglycan and growth factor receptor.* J Endocrinol, 2011. **209**(2): p. 139-51.
64. Lin, X., *Functions of heparan sulfate proteoglycans in cell signaling during development.* Development, 2004. **131**(24): p. 6009-21.
65. Peach, R.J., et al., *Identification of hyaluronic acid binding sites in the extracellular domain of CD44.* J Cell Biol, 1993. **122**(1): p. 257-64.
66. Fraser, J.R., T.C. Laurent, and U.B. Laurent, *Hyaluronan: its nature, distribution, functions and turnover.* J Intern Med, 1997. **242**(1): p. 27-33.
67. Chattopadhyay, S. and R.T. Raines, *Review collagen-based biomaterials for wound healing.* Biopolymers, 2014. **101**(8): p. 821-33.
68. Robinson, T.F., et al., *Structure and function of connective tissue in cardiac muscle: collagen types I and III in endomysial struts and pericellular fibers.* Scanning Microsc, 1988. **2**(2): p. 1005-15.
69. van Dijk, F.S., et al., *Osteogenesis Imperfecta: A Review with Clinical Examples.* Mol Syndromol, 2011. **2**(1): p. 1-20.
70. Jobling, R., et al., *The collagenopathies: review of clinical phenotypes and molecular correlations.* Curr Rheumatol Rep, 2014. **16**(1): p. 394.
71. Muiznieks, L.D., A.S. Weiss, and F.W. Keeley, *Structural disorder and dynamics of elastin.* Biochem Cell Biol, 2010. **88**(2): p. 239-50.
72. Pankov, R. and K.M. Yamada, *Fibronectin at a glance.* J Cell Sci, 2002. **115**(Pt 20): p. 3861-3.
73. Aumailley, M., et al., *A simplified laminin nomenclature.* Matrix Biol, 2005. **24**(5): p. 326-32.
74. Colognato, H. and P.D. Yurchenco, *Form and function: the laminin family of heterotrimers.* Dev Dyn, 2000. **218**(2): p. 213-34.
75. Horejs, C.M., et al., *Biologically-active laminin-111 fragment that modulates the epithelial-to-mesenchymal transition in embryonic stem cells.* Proc Natl Acad Sci U S A, 2014. **111**(16): p. 5908-13.
76. Hu, P. and B.H. Luo, *Integrin bi-directional signaling across the plasma membrane.* J Cell Physiol, 2013. **228**(2): p. 306-12.
77. Delaine-Smith, R.M. and G.C. Reilly, *The effects of mechanical loading on mesenchymal stem cell differentiation and matrix production.* Vitam Horm, 2011. **87**: p. 417-80.
78. Hynes, R.O., *Integrins: bidirectional, allosteric signaling machines.* Cell, 2002. **110**(6): p. 673-87.

79. Elosegui-Artola, A., et al., *Rigidity sensing and adaptation through regulation of integrin types.* Nat Mater, 2014. **13**(6): p. 631-7.
80. Shattil, S.J., C. Kim, and M.H. Ginsberg, *The final steps of integrin activation: the end game.* Nat Rev Mol Cell Biol, 2010. **11**(4): p. 288-300.
81. Carey, D.J., *Syndecans: multifunctional cell-surface co-receptors.* Biochem J, 1997. **327 (Pt 1)**: p. 1-16.
82. Choi, S., et al., *Transmembrane domain-induced oligomerization is crucial for the functions of syndecan-2 and syndecan-4.* J Biol Chem, 2005. **280**(52): p. 42573-9.
83. Zhang, Y., et al., *Targeting of heparanase-modified syndecan-1 by prosecretory mitogen lacritin requires conserved core GAGAL plus heparan and chondroitin sulfate as a novel hybrid binding site that enhances selectivity.* J Biol Chem, 2013. **288**(17): p. 12090-101.
84. Echtermeyer, F., et al., *Syndecan-4 regulates ADAMTS-5 activation and cartilage breakdown in osteoarthritis.* Nat Med, 2009. **15**(9): p. 1072-6.
85. Clark, P., *Protease-mediated ectodomain shedding.* Thorax, 2014. **69**(7): p. 682-4.
86. Weber, S. and P. Saftig, *Ectodomain shedding and ADAMs in development.* Development, 2012. **139**(20): p. 3693-709.
87. Gattazzo, F., A. Urciuolo, and P. Bonaldo, *Extracellular matrix: a dynamic microenvironment for stem cell niche.* Biochim Biophys Acta, 2014. **1840**(8): p. 2506-19.
88. Bodle, J.C., A.D. Hanson, and E.G. Loboa, *Adipose-derived stem cells in functional bone tissue engineering: lessons from bone mechanobiology.* Tissue Eng Part B Rev, 2011. **17**(3): p. 195-211.
89. Vigetti, D., et al., *Epigenetics in extracellular matrix remodeling and hyaluronan metabolism.* FEBS J, 2014. **281**(22): p. 4980-92.
90. Kessenbrock, K., C.Y. Wang, and Z. Werb, *Matrix metalloproteinases in stem cell regulation and cancer.* Matrix Biol, 2015.
91. Shitomi, Y., et al., *ADAM10 controls collagen signaling and cell migration on collagen by shedding the ectodomain of discoidin domain receptor 1 (DDR1).* Mol Biol Cell, 2015. **26**(4): p. 659-73.
92. Sonoda, K. and K. Kato, *A disintegrin and metalloproteinase 9 is involved in ectodomain shedding of receptor-binding cancer antigen expressed on SiSo cells.* Biomed Res Int, 2014. **2014**: p. 482396.
93. Langjahr, P., et al., *Metalloproteinase-dependent TLR2 ectodomain shedding is involved in soluble toll-like receptor 2 (sTLR2) production.* PLoS One, 2014. **9**(12): p. e104624.
94. Vandooren, J., P.E. Van den Steen, and G. Opdenakker, *Biochemistry and molecular biology of gelatinase B or matrix metalloproteinase-9 (MMP-9): the next decade.* Crit Rev Biochem Mol Biol, 2013. **48**(3): p. 222-72.
95. Nissinen, L. and V.M. Kahari, *Matrix metalloproteinases in inflammation.* Biochim Biophys Acta, 2014. **1840**(8): p. 2571-80.
96. Albrechtsen, R., et al., *ADAM12 redistributes and activates MMP-14, resulting in gelatin degradation, reduced apoptosis and increased tumor growth.* J Cell Sci, 2013. **126**(Pt 20): p. 4707-20.
97. Hou, S., et al., *The secreted serine protease xHtrA1 stimulates long-range FGF signaling in the early Xenopus embryo.* Dev Cell, 2007. **13**(2): p. 226-41.

98. Acosta, H., et al., *The serpin PN1 is a feedback regulator of FGF signaling in germ layer and primary axis formation.* Development, 2015. **142**(6): p. 1146-58.
99. Haq, S.K., et al., *Protease inhibitors: a panacea?* J Biochem Mol Toxicol, 2010. **24**(4): p. 270-7.
100. Frochaux, V., et al., *Alpha-1-antitrypsin: a novel human high temperature requirement protease A1 (HTRA1) substrate in human placental tissue.* PLoS One, 2014. **9**(10): p. e109483.
101. Huntington, J.A., R.J. Read, and R.W. Carrell, *Structure of a serpin-protease complex shows inhibition by deformation.* Nature, 2000. **407**(6806): p. 923-6.
102. Clausen, T., C. Southan, and M. Ehrmann, *The HtrA family of proteases: implications for protein composition and cell fate.* Mol Cell, 2002. **10**(3): p. 443-55.
103. Skorko-Glonek, J., et al., *HtrA protease family as therapeutic targets.* Curr Pharm Des, 2012.
104. De Luca, A., et al., *Distribution of the serine protease HtrA1 in normal human tissues.* J Histochem Cytochem, 2003. **51**(10): p. 1279-84.
105. Zurawa-Janicka, D., J. Narkiewicz, and B. Lipinska, *[Characterization of the HtrA family of proteins].* Postepy Biochem, 2007. **53**(1): p. 27-36.
106. Pallen, M.J. and B.W. Wren, *The HtrA family of serine proteases.* Mol Microbiol, 1997. **26**(2): p. 209-21.
107. Grau, S., et al., *The role of human HtrA1 in arthritic disease.* The Journal of biological chemistry, 2006. **281**(10): p. 6124-9.
108. Baldi, A., et al., *The HtrA1 serine protease is down-regulated during human melanoma progression and represses growth of metastatic melanoma cells.* Oncogene, 2002. **21**(43): p. 6684-8.
109. Tiaden, A.N. and P.J. Richards, *The emerging roles of HTRA1 in musculoskeletal disease.* Am J Pathol, 2013. **182**(5): p. 1482-8.
110. Eigenbrot, C., et al., *Structural and functional analysis of HtrA1 and its subdomains.* Structure, 2012. **20**(6): p. 1040-50.
111. Truebestein, L., et al., *Substrate-induced remodeling of the active site regulates human HTRA1 activity.* Nat Struct Mol Biol, 2011. **18**(3): p. 386-8.
112. Tennstaedt, A., et al., *Human high temperature requirement serine protease A1 (HTRA1) degrades tau protein aggregates.* J Biol Chem, 2012. **287**(25): p. 20931-41.
113. Hou, J., D.R. Clemmons, and S. Smeekens, *Expression and characterization of a serine protease that preferentially cleaves insulin-like growth factor binding protein-5.* J Cell Biochem, 2005. **94**(3): p. 470-84.
114. Oka, C., et al., *HtrA1 serine protease inhibits signaling mediated by Tgfbeta family proteins.* Development, 2004. **131**(5): p. 1041-53.
115. Schlott, B., et al., *Interaction of Kazal-type inhibitor domains with serine proteinases: biochemical and structural studies.* J Mol Biol, 2002. **318**(2): p. 533-46.
116. Rawlings, N.D., D.P. Tolle, and A.J. Barrett, *Evolutionary families of peptidase inhibitors.* Biochem J, 2004. **378**(Pt 3): p. 705-16.
117. Clausen, T., et al., *HTRA proteases: regulated proteolysis in protein quality control.* Nat Rev Mol Cell Biol, 2011. **12**(3): p. 152-62.
118. Hedstrom, L., *Serine protease mechanism and specificity.* Chem Rev, 2002. **102**(12): p. 4501-24.

119. Lee, H.J. and J.J. Zheng, *PDZ domains and their binding partners: structure, specificity, and modification.* Cell Commun Signal, 2010. **8**: p. 8.
120. Ye, F. and M. Zhang, *Structures and target recognition modes of PDZ domains: recurring themes and emerging pictures.* Biochem J, 2013. **455**(1): p. 1-14.
121. Hui, S., X. Xing, and G.D. Bader, *Predicting PDZ domain mediated protein interactions from structure.* BMC Bioinformatics, 2013. **14**: p. 27.
122. Murwantoko, et al., *Binding of proteins to the PDZ domain regulates proteolytic activity of HtrA1 serine protease.* Biochem J, 2004. **381**(Pt 3): p. 895-904.
123. Kim, D.Y. and K.K. Kim, *Structure and function of HtrA family proteins, the key players in protein quality control.* J Biochem Mol Biol, 2005. **38**(3): p. 266-74.
124. Canfield, A.E., et al., *HtrA1: a novel regulator of physiological and pathological matrix mineralization?* Biochem Soc Trans, 2007. **35**(Pt 4): p. 669-71.
125. Kim, S. and R.T. Sauer, *Cage assembly of DegP protease is not required for substrate-dependent regulation of proteolytic activity or high-temperature cell survival.* Proc Natl Acad Sci U S A, 2012. **109**(19): p. 7263-8.
126. Hansen, G. and R. Hilgenfeld, *Architecture and regulation of HtrA-family proteins involved in protein quality control and stress response.* Cell Mol Life Sci, 2013. **70**(5): p. 761-75.
127. Sawa, J., et al., *Molecular transformers in the cell: lessons learned from the DegP protease-chaperone.* Curr Opin Struct Biol, 2010. **20**(2): p. 253-8.
128. Chien, J., et al., *Serine protease HtrA1 associates with microtubules and inhibits cell migration.* Mol Cell Biol, 2009. **29**(15): p. 4177-87.
129. Tiaden, A.N., et al., *Detrimental role for human high temperature requirement serine protease A1 (HTRA1) in the pathogenesis of intervertebral disc (IVD) degeneration.* J Biol Chem, 2012. **287**(25): p. 21335-45.
130. Lipinska, B., M. Zylicz, and C. Georgopoulos, *The HtrA (DegP) protein, essential for Escherichia coli survival at high temperatures, is an endopeptidase.* J Bacteriol, 1990. **172**(4): p. 1791-7.
131. Zong, L., et al., *Changes in the level of serum high-temperature requirement A1 (HtrA1) during pregnancy and its relationship to preeclampsia.* Hypertens Pregnancy, 2012. **31**(4): p. 389-97.
132. Nie, G., et al., *Distinct expression and localization of serine protease HtrA1 in human endometrium and first-trimester placenta.* Dev Dyn, 2006. **235**(12): p. 3448-55.
133. Hasan, M.Z., et al., *Abnormal development of placenta in HtrA1-deficient mice.* Dev Biol, 2015. **397**(1): p. 89-102.
134. Chen, H.W., et al., *Identification of cross-reactive epitopes on the conserved 47-kilodalton antigen of Orientia tsutsugamushi and human serine protease.* Infect Immun, 2009. **77**(6): p. 2311-9.
135. Chien, J., X. He, and V. Shridhar, *Identification of tubulins as substrates of serine protease HtrA1 by mixture-based oriented peptide library screening.* Journal of cellular biochemistry, 2009. **107**(2): p. 253-63.

136. Campioni, M., et al., *The serine protease HtrA1 specifically interacts and degrades the tuberous sclerosis complex 2 protein.* Mol Cancer Res, 2010. **8**(9): p. 1248-60.
137. Bao, W., et al., *HtrA1 resensitizes multidrug-resistant hepatocellular carcinoma cells by targeting XIAP.* Biomed Pharmacother, 2015. **70**: p. 97-102.
138. He, X., et al., *HtrA1 sensitizes ovarian cancer cells to cisplatin-induced cytotoxicity by targeting XIAP for degradation.* Int J Cancer, 2012. **130**(5): p. 1029-35.
139. Xia, J., et al., *Elevated serine protease HtrA1 inhibits cell proliferation, reduces invasion, and induces apoptosis in esophageal squamous cell carcinoma by blocking the nuclear factor-kappaB signaling pathway.* Tumour Biol, 2013. **34**(1): p. 317-28.
140. Skorko-Glonek, J., et al., *HtrA protease family as therapeutic targets.* Curr Pharm Des, 2013. **19**(6): p. 977-1009.
141. Zurawa-Janicka, D., J. Skorko-Glonek, and B. Lipinska, *HtrA proteins as targets in therapy of cancer and other diseases.* Expert Opin Ther Targets, 2010. **14**(7): p. 665-79.
142. Chien, J., et al., *HtrA serine proteases as potential therapeutic targets in cancer.* Curr Cancer Drug Targets, 2009. **9**(4): p. 451-68.
143. An, E., et al., *Identification of novel substrates for the serine protease HTRA1 in the human RPE secretome.* Invest Ophthalmol Vis Sci, 2010. **51**(7): p. 3379-86.
144. Chamberland, A., et al., *Identification of a novel HtrA1-susceptible cleavage site in human aggrecan: evidence for the involvement of HtrA1 in aggrecan proteolysis in vivo.* J Biol Chem, 2009. **284**(40): p. 27352-9.
145. Polur, I., et al., *Role of HTRA1, a serine protease, in the progression of articular cartilage degeneration.* Histol Histopathol, 2010. **25**(5): p. 599-608.
146. Vierkotten, S., P.S. Muether, and S. Fauser, *Overexpression of HTRA1 leads to ultrastructural changes in the elastic layer of Bruch's membrane via cleavage of extracellular matrix components.* PLoS One, 2011. **6**(8): p. e22959.
147. Massague, J., *TGFbeta signalling in context.* Nat Rev Mol Cell Biol, 2012. **13**(10): p. 616-30.
148. Beaufort, N., et al., *Cerebral small vessel disease-related protease HtrA1 processes latent TGF-beta binding protein 1 and facilitates TGF-beta signaling.* Proc Natl Acad Sci U S A, 2014. **111**(46): p. 16496-501.
149. Jacobo, S.M. and A. Kazlauskas, *Focus on molecules: HtrA1 and neovascular AMD.* Exp Eye Res, 2012. **94**(1): p. 4-5.
150. Fu, Y., *A functional approach to examine the role of HTRA1 versus ARMS2 in AMD.* Invest Ophthalmol Vis Sci, 2014. **55**(10): p. 6524.
151. Dewan, A., et al., *HTRA1 promoter polymorphism in wet age-related macular degeneration.* Science, 2006. **314**(5801): p. 989-92.
152. Esposito, V., et al., *Analysis of HtrA1 serine protease expression in human lung cancer.* Anticancer Res, 2006. **26**(5a): p. 3455-9.
153. He, X., et al., *Downregulation of HtrA1 promotes resistance to anoikis and peritoneal dissemination of ovarian cancer cells.* Cancer research, 2010. **70**(8): p. 3109-18.

154. Liu, J., F. Dong, and J. Hoh, *Loss of HtrA1-induced attenuation of TGF-beta signaling in fibroblasts might not be the main mechanism of CARASIL pathogenesis.* Proc Natl Acad Sci U S A, 2015.
155. Cai, B., et al., *A frameshift mutation in HTRA1 expands CARASIL syndrome and peripheral small arterial disease to the Chinese population.* Neurol Sci, 2015.
156. Grau, S., et al., *Implications of the serine protease HtrA1 in amyloid precursor protein processing.* Proc Natl Acad Sci U S A, 2005. **102**(17): p. 6021-6.
157. Turunen, M., et al., *No association between high temperature requirement 1 (HTRA1) gene polymorphisms and Alzheimer's disease.* Neurobiol Aging, 2011. **32**(3): p. 547 e7-9.
158. Erener, S., et al., *ARTD1 deletion causes increased hepatic lipid accumulation in mice fed a high-fat diet and impairs adipocyte function and differentiation.* FASEB J, 2012. **26**(6): p. 2631-8.
159. Hou, Y., et al., *The inhibitory effect of IFN-gamma on protease HTRA1 expression in rheumatoid arthritis.* J Immunol, 2014. **193**(1): p. 130-8.
160. Hou, Y., et al., *Lipopolysaccharide increases the incidence of collagen-induced arthritis in mice through induction of protease HTRA-1 expression.* Arthritis Rheum, 2013. **65**(11): p. 2835-46.
161. Bakay, M., et al., *A web-accessible complete transcriptome of normal human and DMD muscle.* Neuromuscul Disord, 2002. **12 Suppl 1**: p. S125-41.
162. Tsuchiya, A., et al., *Expression of mouse HtrA1 serine protease in normal bone and cartilage and its upregulation in joint cartilage damaged by experimental arthritis.* Bone, 2005. **37**(3): p. 323-36.
163. Graham, J.R., et al., *Serine protease HTRA1 antagonizes transforming growth factor-beta signaling by cleaving its receptors and loss of HTRA1 in vivo enhances bone formation.* PLoS One, 2013. **8**(9): p. e74094.
164. Hadfield, K.D., et al., *HtrA1 inhibits mineral deposition by osteoblasts: requirement for the protease and PDZ domains.* J Biol Chem, 2008. **283**(9): p. 5928-38.
165. Tiaden, A.N., et al., *Human serine protease HTRA1 positively regulates osteogenesis of human bone marrow-derived mesenchymal stem cells and mineralization of differentiating bone-forming cells through the modulation of extracellular matrix protein.* Stem Cells, 2012. **30**(10): p. 2271-82.
166. Li, R. and Q. Zhang, *HtrA1 may regulate the osteogenic differentiation of human periodontal ligament cells by TGF-beta1.* J Mol Histol, 2015. **46**(2): p. 137-44.
167. Choy, L., J. Skillington, and R. Derynck, *Roles of autocrine TGF-beta receptor and Smad signaling in adipocyte differentiation.* J Cell Biol, 2000. **149**(3): p. 667-82.
168. Lowe, C.E., S. O'Rahilly, and J.J. Rochford, *Adipogenesis at a glance.* J Cell Sci, 2011. **124**(Pt 16): p. 2681-6.
169. Mauney, J. and V. Volloch, *Adult human bone marrow stromal cells regulate expression of their MMPs and TIMPs in differentiation type-specific manner.* Matrix Biol, 2010. **29**(1): p. 3-8.
170. Chun, T.H., *Peri-adipocyte ECM remodeling in obesity and adipose tissue fibrosis.* Adipocyte, 2012. **1**(2): p. 89-95.

171. Supanji, et al., *HtrA1 is induced by oxidative stress and enhances cell senescence through p38 MAPK pathway.* Exp Eye Res, 2013. **112**: p. 79-92.
172. Kim, J. and J. Ko, *A novel PPARgamma2 modulator sLZIP controls the balance between adipogenesis and osteogenesis during mesenchymal stem cell differentiation.* Cell Death Differ, 2014. **21**(10): p. 1642-55.
173. Chen, Q., et al., *An osteopontin-integrin interaction plays a critical role in directing adipogenesis and osteogenesis by mesenchymal stem cells.* Stem Cells, 2014. **32**(2): p. 327-37.
174. Kawai, M. and C.J. Rosen, *PPARgamma: a circadian transcription factor in adipogenesis and osteogenesis.* Nat Rev Endocrinol, 2010. **6**(11): p. 629-36.
175. James, A.W., *Review of Signaling Pathways Governing MSC Osteogenic and Adipogenic Differentiation.* Scientifica (Cairo), 2013. **2013**: p. 684736.
176. DEPT. OF HEALTH, E., AND, W.P.H. SERVICE, and F.A.D. ADMINISTRATION, *Bacterial Endotoxins/Pyrogens.* 1985.
177. Tiaden, A., et al., *HTRA1 inhibits adipogenic differentiation of human mesenchymal stem cells via MAP kinase-mediated MMP upregulation.* manuscript in preparation, 2015.
178. Nachtigal, P., et al., *The role of endoglin in atherosclerosis.* Atherosclerosis, 2012. **224**(1): p. 4-11.
179. Yamashita, H., et al., *Cryptic fragment alpha4 LG4-5 derived from laminin alpha4 chain inhibits de novo adipogenesis by modulating the effect of fibroblast growth factor-2.* Dev Growth Differ, 2008. **50**(2): p. 97-107.
180. Stanhope, T.J., et al., *Expression of Protease HtrA1 Is Increased at the Site of Ectopic Pregnancy.* Obstet Gynecol, 2014. **123 Suppl 1**: p. 32s-3s.
181. Zhang, L., et al., *High temperature requirement factor A1 (HTRA1) gene regulates angiogenesis through transforming growth factor-beta family member growth differentiation factor 6.* J Biol Chem, 2012. **287**(2): p. 1520-6.
182. Jiang, J., et al., *Overexpression of HTRA1 leads to down-regulation of fibronectin and functional changes in RF/6A cells and HUVECs.* PLoS One, 2012. **7**(10): p. e46115.
183. Hardouin, P., V. Pansini, and B. Cortet, *Bone marrow fat.* Joint Bone Spine, 2014. **81**(4): p. 313-9.
184. Pei, L. and P. Tontonoz, *Fat's loss is bone's gain.* J Clin Invest, 2004. **113**(6): p. 805-6.
185. Kawai, M., F.J. de Paula, and C.J. Rosen, *New insights into osteoporosis: the bone-fat connection.* J Intern Med, 2012. **272**(4): p. 317-29.
186. Rodriguez, J.P., et al., *Mesenchymal stem cells from osteoporotic patients produce a type I collagen-deficient extracellular matrix favoring adipogenic differentiation.* J Cell Biochem, 2000. **79**(4): p. 557-65.
187. Maquoi, E., et al., *Modulation of adipose tissue expression of murine matrix metalloproteinases and their tissue inhibitors with obesity.* Diabetes, 2002. **51**(4): p. 1093-101.
188. Chavey, C., et al., *Matrix metalloproteinases are differentially expressed in adipose tissue during obesity and modulate adipocyte differentiation.* J Biol Chem, 2003. **278**(14): p. 11888-96.

189. Wilsie, L.C., et al., *Cell surface heparan sulfate proteoglycans contribute to intracellular lipid accumulation in adipocytes.* Lipids Health Dis, 2005. **4**: p. 2.
190. Kasza, I., et al., *Syndecan-1 is required to maintain intradermal fat and prevent cold stress.* PLoS Genet, 2014. **10**(8): p. e1004514.
191. Yurchenco, P.D., *Basement membranes: cell scaffoldings and signaling platforms.* Cold Spring Harb Perspect Biol, 2011. **3**(2).
192. Reuben, P.M. and H.S. Cheung, *Regulation of matrix metalloproteinase (MMP) gene expression by protein kinases.* Front Biosci, 2006. **11**: p. 1199-215.
193. Tominaga, S., et al., *Negative regulation of adipogenesis from human mesenchymal stem cells by Jun N-terminal kinase.* Biochem Biophys Res Commun, 2005. **326**(2): p. 499-504.
194. Chiu, L.H., et al., *Diverse effects of type II collagen on osteogenic and adipogenic differentiation of mesenchymal stem cells.* J Cell Physiol, 2012. **227**(6): p. 2412-20.
195. Fu, L., et al., *Stimulation of osteogenic differentiation and inhibition of adipogenic differentiation in bone marrow stromal cells by alendronate via ERK and JNK activation.* Bone, 2008. **43**(1): p. 40-7.
196. Saoncella, S., et al., *Syndecan-4 regulates ATF-2 transcriptional activity in a Rac1-dependent manner.* J Biol Chem, 2004. **279**(45): p. 47172-6.
197. Bost, F., et al., *The role of MAPKs in adipocyte differentiation and obesity.* Biochimie, 2005. **87**(1): p. 51-6.
198. Unoki, H., et al., *Increased matrix metalloproteinase-3 mRNA expression in visceral fat in mice implanted with cultured preadipocytes.* Biochem Biophys Res Commun, 2006. **350**(2): p. 392-8.
199. Meissburger, B., et al., *Adipogenesis and insulin sensitivity in obesity are regulated by retinoid-related orphan receptor gamma.* EMBO Mol Med, 2011. **3**(11): p. 637-51.
200. Guilherme, A., et al., *Adipocyte dysfunctions linking obesity to insulin resistance and type 2 diabetes.* Nat Rev Mol Cell Biol, 2008. **9**(5): p. 367-77.
201. Murano, I., et al., *Dead adipocytes, detected as crown-like structures, are prevalent in visceral fat depots of genetically obese mice.* J Lipid Res, 2008. **49**(7): p. 1562-8.
202. Gao, D. and C. Bing, *Macrophage-induced expression and release of matrix metalloproteinase 1 and 3 by human preadipocytes is mediated by IL-1beta via activation of MAPK signaling.* J Cell Physiol, 2011. **226**(11): p. 2869-80.
203. Moses, H.L. and R. Serra, *Regulation of differentiation by TGF-beta.* Curr Opin Genet Dev, 1996. **6**(5): p. 581-6.
204. Fei, T. and Y.G. Chen, *Regulation of embryonic stem cell self-renewal and differentiation by TGF-beta family signaling.* Sci China Life Sci, 2010. **53**(4): p. 497-503.
205. Murphy, G., et al., *Mechanisms for pro matrix metalloproteinase activation.* APMIS, 1999. **107**(1): p. 38-44.
206. Visse, R. and H. Nagase, *Matrix metalloproteinases and tissue inhibitors of metalloproteinases: structure, function, and biochemistry.* Circ Res, 2003. **92**(8): p. 827-39.

207. Bezaire, V. and D. Langin, *Regulation of adipose tissue lipolysis revisited.* Proc Nutr Soc, 2009. **68**(4): p. 350-60.
208. Nielsen, T.S., et al., *Dissecting adipose tissue lipolysis: molecular regulation and implications for metabolic disease.* J Mol Endocrinol, 2014. **52**(3): p. R199-222.
209. Kakudo, N., A. Shimotsuma, and K. Kusumoto, *Fibroblast growth factor-2 stimulates adipogenic differentiation of human adipose-derived stem cells.* Biochem Biophys Res Commun, 2007. **359**(2): p. 239-44.
210. Wernstedt Asterholm, I., et al., *Adipocyte inflammation is essential for healthy adipose tissue expansion and remodeling.* Cell Metab, 2014. **20**(1): p. 103-18.
211. Richard, A.J., et al., *Naringenin inhibits adipogenesis and reduces insulin sensitivity and adiponectin expression in adipocytes.* Evid Based Complement Alternat Med, 2013. **2013**: p. 549750.
212. Lv, S., et al., *Correlation of obesity and osteoporosis: Effect of free fatty acids on bone marrow-derived mesenchymal stem cell differentiation.* Exp Ther Med, 2010. **1**(4): p. 603-610.
213. Gustafson, B., et al., *Insulin resistance and impaired adipogenesis.* Trends Endocrinol Metab, 2015. **26**(4): p. 193-200.
214. Rosen, C.J. and M.L. Bouxsein, *Mechanisms of disease: is osteoporosis the obesity of bone?* Nat Clin Pract Rheumatol, 2006. **2**(1): p. 35-43.

CURRICULUM VITAE

GREGOR BAHRENBERG

Address: Langstrasse 118
8004 Zürich
Switzerland

Telephone: +41763368867
E-mail: gregor.bahrenberg@cabmm.uzh.ch

Date of birth: 21 July 1986
Nationality: German

WORK EXPERIENCE

Since 10/2013:	Board member, scientific collaborator and treasurer of the think tank "NeoHumanitas" (http://www.neohumanitas.org/?lang=en)
Since 09/2011:	Doctoral studies at the Life Science Zürich Graduate School of ETH and UZH Zürich, Institute for Applied Biotechnology and Molecular Medicine (CABMM), Bone and Stem Cell Research Group, PD Dr. Peter Richards PhD thesis title: "The Role of HtrA1 in adipose-derived stromal cell (ASC) lineage commitment"
10/2010 – 03/2011:	Diploma thesis at the Max-Planck-Institute for Molecular Physiology in Dortmund Department of Prof. Dr. Roger S. Goody, Group of Dr. Stefan Raunser Diploma thesis title: "Biochemical and structural analysis of the ABC-transporter BSEP from *Thermococcus sibiricus* and *Pyrococcus horikoshii*"
05/2009 – 06/2009:	Institute of Medical Microbiology and Hospital Hygiene at the University of Düsseldorf Department of Prof. Dr. Klaus Pfeffer, Group of Dr. Stefanie Scheu Supportive work on "Visualization of IFNbeta production by plasmacytoid versus conventional dendritic cells under specific stimulation conditions"

UNIVERSITY STUDIES

Since 09/2011:	Doctoral studies at the Life Science Zürich Graduate School of ETH and UZH Zürich
10/2006 – 03/2011:	Studies of Biology at the Heinrich-Heine University Düsseldorf

LIST OF PUBLICATIONS

1.
HTRA1 inhibits adipogenic differentiation of human mesenchymal stem cells via MAP kinase-mediated MMP upregulation.
Tiaden AN*, **Bahrenberg G***, Mirsaidi A, Glanz S, Blueher M, Ehrmann M, Richards PJ.
*authors contributed equally
manuscript submitted to *Proc Natl Acad Sci USA (July 2015)*
2.
Use of biomimetic microtissue spheroids and specific growth factor supplementation to improve tenocyte differentiation and adaptation to a collagen-based scaffold *in vitro*.
Theiss F, Mirsaidi A, Mhanna R, Glanz S, **Bahrenberg G**, Tiaden AN, Richards PJ.
manuscript under review *Biomaterials (July 2015)*
3.
Human serine protease HTRA1 positively regulates osteogenesis of human bone marrow-derived mesenchymal stem cells and mineralization of differentiating bone-forming cells through the modulation of extracellular matrix protein.
Tiaden AN, Breiden M, Mirsaidi A, Weber FA, **Bahrenberg G**, Glanz S, Cinelli P, Ehrmann M, Richards PJ.
Stem Cells. 2012 Oct;30(10):2271-82. doi: 10.1002/stem.1190.
4.
Detrimental role for human high temperature requirement serine protease A1 (HTRA1) in the pathogenesis of intervertebral disc (IVD) degeneration.
Tiaden AN, Klawitter M, Lux V, Mirsaidi A, **Bahrenberg G**, Glanz S, Quero L, Liebscher T, Wuertz K, Ehrmann M, Richards PJ.
J Biol Chem. 2012 Jun 15;287(25):21335-45. doi: 10.1074/jbc.M112.341032. Epub 2012 May 3
5.
Assessment of the Matrix Degenerative Effects of MMP-3, ADAMTS-4 and HTRA1 injected into a bovine Intervertebral Disc Organ Culture Model
Furtwängler T, Chan SC, **Bahrenberg G**, Richards PJ, Gantenbein-Ritter B
Spine (Phila Pa 1976). 2013 Oct 15;38(22):E1377-87. doi: 10.1097/BRS.0b013e31829ffde8

COMPUTER SKILLS

Office:	Comprehensive knowledge Advanced education in MS Excel "Large data sets" certificate by eduQua
Adobe:	Comprehensive knowledge in Adobe Photoshop and Illustrator

ADVANCED EDUCATION

Participation in the international conference "Nanomedicine" 2012, held by the MERH centre Zurich (Medizin – Ethik – Recht Helvetiae Kompetenzzentrum),

Participation in the symposium "autopsy and religion" 2012, held by the MERH centre Zurich

Participation in the graduate study course "Ethics and good scientific practice for life scientists" 2013, held by Dr. Anna Deplazes Zemp, Institute of Biomedical Ethics, University of Zurich

Participation in the symposium "Contemporary Issues in Biomedical Ethics" 2012, held by Dr. Jeffrey Kahns, John Hopkins University

COMMUNITY SERVICES

07/2004 – 02/2010:	Caretaker of a youth group at the St. Bonifatius local church community in Dortmund
04/2003 – 12/2006:	Volunteer at "Gasthaus Dortmund", a soup kitchen for homeless people
05/2003:	Volunteer at the "AWO-Behindertenwerkstätten Dortmund", a daycare centre for handicapped people

SCHOOL EDUCATION

08/1997 – 06/2006:	Mallinckrodt-Gymnasium in Dortmund Allgemeine Hochschulreife (German qualification for university entrance)
08/1993 – 06/1997:	Elementary School in Dortmund

LANGUAGES

German:	Native speaker	
English:	02/2010 – 06/2010:	Language study travel in Australia and New Zealand
	11/2010:	International English Language Testing System exam (IELTS)

Zürich, July 8th 2015

Acknowledgements

I would like to express my acknowledgements to all the people who helped and supported me through the past four years, especially to all my PhD committee members involved. A big thanks to PD Dr. Peter J. Richards for choosing me for this project and for all the discussions, ideas and support. Thanks to Prof. Dr. François Verrey for being the responsible faculty member and for all the challenging questions towards the project which pushed us even further. Also thanks to Prof. Dr. Beat Thöny who was always willing to give advice and inspiring input. Last but not least I would like to thank Prof. Dr. Michael Ehrmann, without whom this project wouldn´t have been possible in the first place.

„Ich müsste mich eigentlich im Minuten-Takt bei Gott bedanken."

- Jürgen Klopp